3. Objetives

The general objective of this work was to study the possibility of using the Advanced Oxidation Processes (AOPs) based on ozone in the treatment of low biodegradable and/or toxic compounds, which cannot be treated by a conventional biological treatment.

Nitroaromatics and chlorophenols constitute a threat to human health and produce a public concern, thus several of them have been listed among the 130 priority pollutants given by the US EPA in the Federal Clean Water Act (CWA), e.g. nitrobenzene and 2,4-dichlorophenol (EPA, 2002), which have been chosen as model compounds. Recently, the US EPA has also included them in a reduced list of drinking water contaminants to be investigated in the period 2001-2005 (Hayward, 1999).

As it has been mentioned in the introduction, the high cost derived from the use of an AOP can make attractive the possibility of coupling that AOP with a biological treatment. In case of low biodegradable compounds, the oxidation of organic compounds by an AOP usually produces oxygenated organic products and low molecular weight acids that are more biodegradable. With toxic compounds, the AOP would be extended until the point that no inhibition due to toxicity was observed.

Few articles have been found in the literature regarding the treatment of NB and DCP by means of AOPs based on ozone. In the group of AOPs Engineering ("Grup de Qualitat" of Generalitat de Catalunya) of the Department of Chemical Engineering at the University of Barcelona an experimental installation suitable for this purpose is available. Thus, it has been considered convenient to study the effect on the degradation and biodegradability enhancement of NB and DCP aqueous solutions by means of the following processes: single ozonation, ozonation combined with hydrogen peroxide (O_3/H_2O_2) and UV radiation (O_3/UV), ozonation combined with both hydrogen peroxide and UV radiation (O_3/UV/H_2O_2) and ozonation combined with UV light and iron salts (O_3/UV/Fe).

The necessary analytical techniques were tuned to achieve the main objectives, which can be summarized as follows:

- Effect on the removal and mineralization rate of the studied compounds by each of the following processes:

    a) **Single ozonation:** The variables subject of study are: ozone production, pH, initial concentration of the pollutant and the presence of radical scavengers. Besides

this, the stoichiometric coefficients for the reaction of ozone with NB and DCP are to be estimated.

b) Ozonation combined with hydrogen peroxide: To study the effect of the addition of hydrogen peroxide at different concentrations to single ozonation, trying to establish an optimum hydrogen peroxide dose in the case of NB solutions.

c) Ozonation combined with UV radiation: To check the possible synergistic effect of the combination of ozone with UV radiation and the use of UVA light (emitting in the range 300-420 nm) instead of UV light (254 nm).

d) Ozonation combined with UV radiation and hydrogen peroxide: To investigate the effect of the addition of hydrogen peroxide at the UV-enhanced ozonation.

e) Ozonation combined with UV radiation and iron salts: To study the influence of Fe(III) concentration, the use of Fe(II) ion instead of Fe(III), to check the possible scavenging effect of chloride ions, and the use of UVA instead of UV light.

- To explore the effect of these AOPs on the biodegradability of NB and DCP aqueous solutions. BOD/COD and BOD/TOC ratios will used as biodegradability indicators.

- To study the biodegradation of a DCP solution after being ozonated according to the biodegradability study in aerobic reactors.

- To identify the main intermediates produced in the oxidation of these solutions, trying to relate the present intermediates with changes in the biodegradability of the solutions.

- To model the sequential ozonation and biological oxidation of a waste water, focusing on the potential impact of residual ozone on the performance of the biological reactor.

To achieve the experimental objectives, the following variables will be followed throughout the treatment time:

- Concentration of the target compounds
- pH
- Concentration of ozone in the residual gas
- Concentration of dissolved ozone
- Total organic carbon (TOC)
- Chemical oxygen demand (COD)
- Biological oxygen demand (BOD)

4. Materials and methods

4.1. Experimental set-up

4.1.1. Advanced Oxidation Processes – Pilot Plant

a) Experimental set up

All the Advanced Oxidation Processes were carried out in a 21-L pilot plant (Figure 4.1). It consists of a contacting-tank (# 1) made of PVC, where the gas-liquid mixture enters into by its lower part, allowing the gas to perform an additional route throughout the tank, increasing the contacting zone (Figure 4.2).

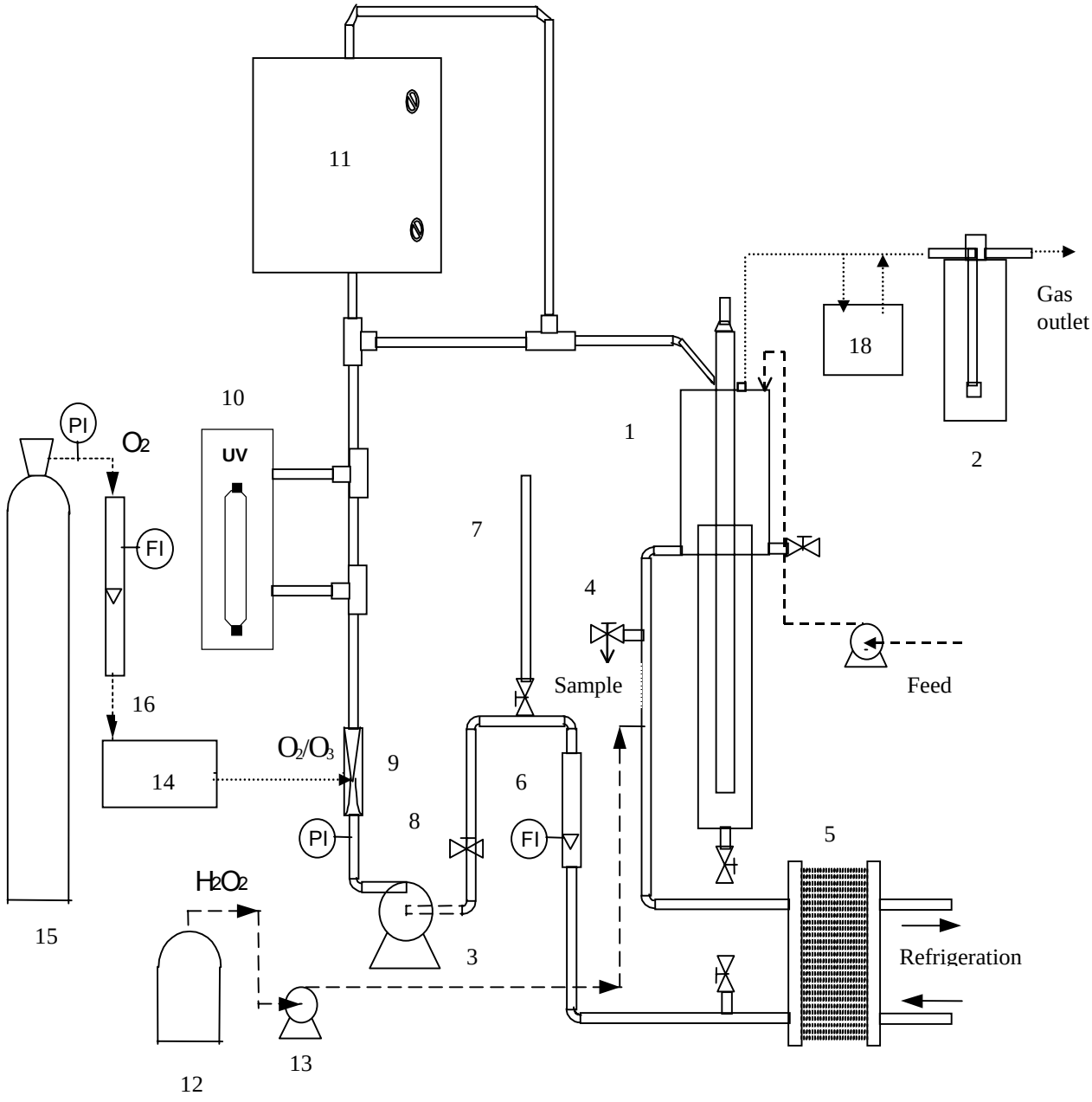

Figure 4.1. Scheme of the experimental set up

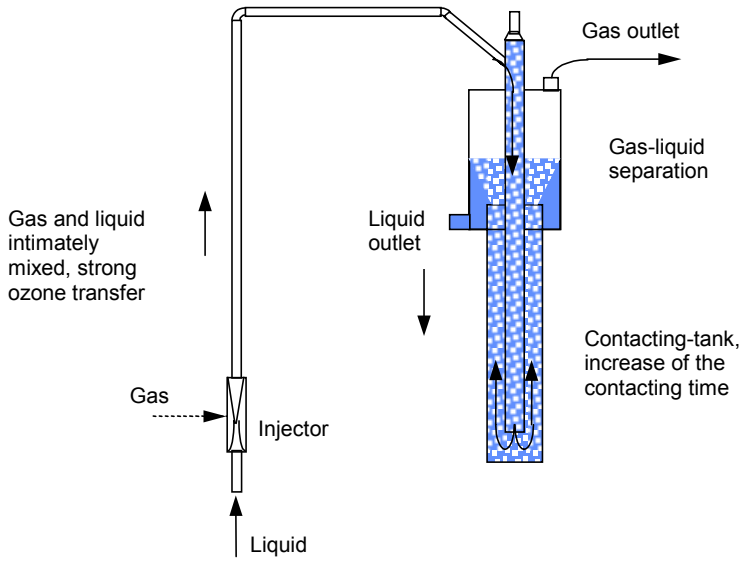

Figure 4.2. Detail of the experimental set up – Contacting-tank

The gas-liquid mixture enters into the vessel by its upper part, goes down through the central tube and rises through the tank, separating finally in the upper part of the contact chamber, where a cylindrical wall creates a liquid chamber where there are no gas bubbles. In the upper part, a gas outlet brings the residual ozone to the gas exhaust trap (called “killer”, # 2).

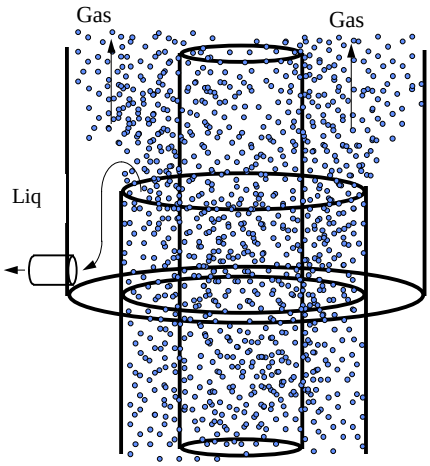

Figure 4.3. Gas-liquid separator

A side outlet communicates with the recirculation of the liquid to a centrifugal stainless steel pump (# 3, nominal power 0.37 kW). In this line it can be seen:

- Sample withdrawal (# 4)
- Heat exchanger (# 5)
- Liquid flow-meter (# 6)
- Pipe purge (# 7)
- Flow adjusting valve (# 8)

After the pump it is located the contacting point between the gas and the liquid (# 9). Different contacting systems can be found. In the present case a chlorine-type venturi injector was chosen, made of PVC and designed to introduce up to 1000 $g.h^{-1}$ of chlorine (ca. 400 $L.h^{-1}$ at 100 kPa and 0ºC). This is one of the most effective mass transfer systems, where the high turbulence created and the intimate mixture in the contacting zone succeed in producing in a small space a quick transfer of ozone from the gas to the liquid phase.

Behind the injection three routes are possible: one, to the contacting-vessel; two, to the UV lamp; and three, to the UVA photoreactor. The UV lamp (# 10), UV705 Trojan Technologies Inc., is a 26-W nominal power monochromatic lamp, emitting at 253.7 nm. The UVA photoreactor (# 11) consists of a cylindrical pyrex 2-L reactor, surrounded by eight 15-W Philips black light fluorescent tubes. These irradiate the solution with UV light in the range 300 - 420 nm, with a maximum centered at 360 nm.

In the experiments where hydrogen peroxide was dosified, this was fed from a bottle (# 12) with a 3% (weight) H_2O_2 solution by means of a peristaltic pump (# 13, ISM 829).

Ozone was generated by a SANDER 301.19 ozonizer (# 14), fed by pure oxygen (99% purity, # 15), with a maximum production of ozone from oxygen of 30 $g.h^{-1}$ at the normal working flow (400 $L.h^{-1}$, flow-meter # 16), resulting a mixture of oxygen and ozone stream, which is injected to the system by means of the venturi (# 9). The ozone not consumed (residual ozone) goes out from the system to be measured on line in a SANDER QuantOzon ozone-in-gas-phase measurer (0 – 20 $g.m^{-3}$, # 17) , before being reduced to oxygen in a KI solution (# 2), avoiding the emission of ozone to the atmosphere.

A recent picture of the experimental device is shown in Figure 4.4. and in Figure 4.5 it can also be seen the ozonizer and the ozone measurer.

Figure 4.4. Reactor, UV and UVA photoreactor

Figure 4.5. Installation, ozonizer and ozone measurer.

b) Experimental procedure

The procedure followed in the experiments carried out in the pilot plant was as follows:

- Preparate the initial pollutant solution and solutions used in the analyses of dissolved ozone, in those experiments where this analysis was carried out.
- Add KI to the ozone killer.
- Calibrate of the pH meter.
- Charge the reactor with the solution to be treated, 21-23 L.
- Switch on the refrigeration system on the plant and the ozonizer.
- Switch on the centrifugal pump and set it for a recirculation rate of 230 $L.h^{-1}$.
- Switch on the air extraction system.
- Open the oxygen bottle to the system and set flow rate to 400 $L.h^{-1}$.
- Switch on the corresponding lamps (UV or UVA), in those experiments where light was used.
- Switch on the ozonizer (the intensity was increased gradually until the desired value) and the residual ozone measurer.
- When the intensity reaches the desired value, switch on the timer clock.
- Switch on the H_2O_2-dosifying pump, in those experiments where this reactant was dosified.
- Withdraw of samples at different time intervals to be analyzed later by HPLC, pH, dissolved ozone, TOC, COD and BOD. Residual ozone was on line measured.
- When the last sample was withdrawn, switch off the lamps and the dosifying pumps, where used.
- Decrease the ozonizer intensity gradually until 0. Oxygen goes on passing through the installation to avoid accumulation of ozone in the system.
- Close the oxygen bottle, switch off the extraction system and the centrifugal pump.
- Empty out and cleaning of the reactor.

4.1.2. Bioassay - Biological reactors

a) Experimental set up

The bioassay was performed on 1.5-L reactors. Magnetic stirring was used to maintain biomass suspended. Air was fed through a diffuser. The study was carried out in semi-continuous stirred tank reactors. That is, once a hydraulic retention time (HRT) was fixed, the calculated volume was taken out of the reactor and the same volume fed each day (or each 12 hours) to the reactor. In Figure 4.6, both reactors used in the bioassay are shown.

Figure 4.6. Biological reactors used in the bioassay

b) Experimental procedure.

The procedure followed in the start-up of the reactors and the daily practice performed with them is the following:

1. Acclimated-to-phenol reactor

   The biomass of this reactor was first acclimated to phenol, as this compound has a chemical structure similar to the possible intermediates produced in the ozonation

of a 2,4-dichlorophenol solution. The start-up of this reactor consisted of the following steps:

- The reactor was initially charged with the following mixture:
  - 400 mL of biomass from a municipal waste water treatment plant (Gavà, Barcelona)
  - 250 mL of a 100-ppm phenol solution
  - 850 mL of municipal waste water
  - macronutrients (3 mL of NH_4Cl solution, 3 mL of $CaCl_2$ solution, 3 mL of $FeCl_3$ solution, 3 mL of $MgSO_4$ solution and 9 mL of phosphate buffer solution)

  A HRT of 10 days was fixed. The corresponding volume to be taken out from the reactor and fed with fresh solution daily was:

$$q = \frac{V}{HRT} = \frac{1500\ mL}{10\ days} = 150\ mL/day$$

  Analyses carried out every day were: pH, TSS (total suspended solids) and DOC (dissolved organic carbon).

- After one cycle (10 days), the reactor was fed with only 100-ppm phenol solution (instead of mixture municipal waste water / phenol solution). That is, ca. 1100 mL of the solution was taken out from the reactor and the corresponding volume of 100-ppm phenol solution (with the needed macronutrients) was fed to the reactor. Initial seeding was 1.5 $g.L^{-1}$. A HRT of 1.5 days was fixed, so the daily volume to be fed was 1 L. Daily analyses carried out were pH, TSS and DOC.

- After 7 cycles (11 days), the reactor was considered to be acclimated to the phenol solution. Then the pre-treated solution was fed, by mixing it with the 100-ppm phenol solution in different percentages (from 20% pre-ozonated solution / 80% phenol solution up to 100% pre-ozonated solution) and at different HRTs (from 10 days up to 12 hours).

- Daily procedure with the reactor was as follows:
  - Stop the magnetic stirring and the feeding of air to allow the biomass to settle down.
  - Take out the corresponding volume of solution (q = 1500 mL/HRT).

- Feed the reactor with fresh solution of the corresponding phenol/pre-ozonated solution/macronutrients mixture, previously neutralized at pH 7.
- Perform pH, TSS, TVSS (total volatile suspended solids) and DOC analyses.

- When HRT = 12 hours, this procedure was done twice a day.

Note: the effluent from the pre-treatment step was left for at least 24 h. before feeding the biological reactor to prevent the presence of residual ozone.

2. Non-acclimated reactor.

This reactor was fed with 1.5 $g.L^{-1}$ of activated sludge coming from a waste water treatment plant and municipal waste water. The start-up and daily procedure of this reactor consisted of the following steps:

- The reactor was initially charged with the following mixture:
  - 400 mL of biomass from a municipal waste water treatment plant (Gavà, Barcelona)
  - 1100 mL of municipal waste water
  - macronutrients (3 mL of NH_4Cl solution, 3 mL of $CaCl_2$ solution, 3 mL of $FeCl_3$ solution, 3 mL of $MgSO_4$ solution and 9 mL of phosphate buffer solution)

  A hydraulic retention time (HRT) of 10 days was fixed. The corresponding volume to be taken out from the reactor and fed daily with fresh solution was, then, 150 $mL.day^{-1}$. Analyses carried out every day were: pH, TSS and DOC.

- After few days, the pre-treated solution was started to be fed. Ca. 1100 mL of the solution was taken out from the reactor and the corresponding volume of a mixture with 20% pre-ozonated solution / 80% municipal waste water was fed to the reactor. A HRT of 10 days was fixed, so the daily volume of new solution to be fed was 150 mL. Daily analyses carried out were pH, TSS, TVSS and DOC.

- The percentage of pre-treated solution was gradually increased, from 20% pre-ozonated solution / 80% municipal waste water up to 100% pre-ozonated solution, and HRTs was progressively reduced as well from 10 days to 12 hours.

- Daily procedure with the reactor was as follows:
  - Stop the magnetic stirring and the feeding of air to allow the biomass to settle down.
  - Take out the corresponding volume of solution (q = 1500 mL/HRT).
  - Feed the reactor with fresh solution of the corresponding municipal waste water /pre-ozonated solution, previously neutralized at pH 7.
  - Perform pH, TSS, TVSS (total volatile suspended solids) and DOC analyses.
  - When HRT = 12 hours, this procedure was done twice a day.

Note: the effluent from the pre-treatment step was left for at least 24 h. before feeding the biological reactor to prevent the presence of residual ozone.

4.2. Reagents

Reagents used in the experimental part have been the following:

- Nitrobenzene, $C_6H_5NO_2$ (98%, PROBUS)
- 2,4-Dichlorophenol, $C_6H_4Cl_2O$ (>98%, MERCK)
- Oxygen, O_2 N40 (AIR LIQUIDE) or C40 (CARBUROS METÁLICOS)
- Hydrogen peroxide, H_2O_2 (33%, PROBUS)
- Iron(III) chloride 6-hydrate, $FeCl_3 \cdot 6H_2O$ (98%, PROBUS)
- Iron(III) sulfate $Fe_2(SO_4)_3$ (GR for analyses, MERCK)
- Iron(II) sulfate 7-hydrate, $Fe_2SO_4 \cdot 7H_2O$ (98%, PANREAC)
- Potassium iodide, KI (99.5%, MERCK)
- Phosphoric acid, H_3PO_4 (85%, PROBUS)
- Acetonitrile (99.8%, isocratic grade for HPLC, MERCK)
- Borax, $Na_2B_4O_7 \cdot 10H_2O$ (GR for analyses, MERCK)
- Uranyl nitrate 6-hydrate, $UO_2(NO_3)_2 \cdot 6H_2O$ (98%, PANREAC)
- Oxalic acid dihydrate, $C_2H_2O_4 \cdot 2H_2O$ (99.5%, PANREAC)
- Potassium hydrogen phthalate, $C_8H_4O_4HK$ (99.9%, PROBUS)
- Potassium permanganate, $KMnO_4$ (99%, PROBUS)
- Potassium dichromate, $K_2Cr_2O_7$ (99%, PROBUS)
- Sulfuric acid, H_2SO_4 (95-98%, MERCK)
- Silver sulfate, Ag_2SO_4 (99%, PROBUS)
- Mercury sulfate, $HgSO_4$ (98%, PROBUS)

- Sodium dihydrogen phosphate hydrate, $NaH_2PO_4 \cdot H_2O$ (purissimum-CODEX, PANREAC)
- Potassium hydroxide, KOH (extra-pure, MERCK)
- Ammonium chloride, NH_4Cl (purissimum-CODEX, PANREAC)
- Calcium chloride, $CaCl_2$ (95%, PANREAC)
- Magnesium sulfate, $MgSO_4$ (purissimum-CODEX, PANREAC)
- Sodium hydroxide, NaOH (>97%, MERCK)
- Potassium indigotrisulfonate (75%, ALDRICH)
- Millipore water (Milli-Q Millipore system, with a 18 $M\Omega.cm^{-1}$ resistivity)

4.3. Analytical methods.

4.3.1. Actinometry.

This is a common method to determine the intensity of a radiation source. In the present case, the actinometric system used is the photochemical decomposition of oxalic acid in presence of uranyl nitrate (Volman and Seed, 1964; Heidt et al., 1979; Esplugas and Vicente, 1983). The decomposition reaction of oxalic acid, in a pH range of between 3 and 7, and a conversion of oxalic acid lower than 20% is the following:

$$(UO_2)^{2+} + H_2C_2O_4 \xrightarrow{h\nu} (UO_2)^{2+} + CO_2 + CO + H_2O \qquad [4.1]$$

By the knowledge of the actinometer and the lamp characteristics, the radiation intensity can be calculated. This method will be deeper explained in section 5.

4.3.2. pH.

The pH measurements were carried out with a Crison GLP-22 pH-meter, calibrated with two buffer solutions of pH 4 and 7. The analysis was not performed on line, but after each sample withdrawal.

4.3.3. High Performance Liquid Chromatography (HPLC)

To study the degradation of nitrobenzene and 2,4-dichlorophenol, it is necessary to determine its concentration during time. The selected method has been the high performance liquid chromatography in reverse phase.

The liquid chromatograph used consists of :

- Waters degasser.
- Controller Waters 600.
- Autosampler Waters 717.
- Oven for columns and temperature controller Waters
- Photodiode array detector Waters 996.
- Millenium software.

The column used presented the following characteristics:

- Packing: SPHERISORB ODS2
- Particle size: 5 μm
- Length: 25 cm
- Inner diameter: 0.46 cm.

The mobile phase used was a mixture acetonitrile:water:phosphoric acid (40:60:0.5%), isocratically delivered (constant composition and flow rate) by a pump at a flow rate of 1 $mL.min^{-1}$. The wavelength of the UV detector was selected from the absorption spectra of nitrobenzene and 2,4-dichlorophenol (see Figure 4.7 and 4.8). Maximum absorption of nitrobenzene and 2,4-dichlorophenol were found to be 267.3 and 280 nm, respectively. Injected volume of each sample was 10 μL. Temperature was set at 25ºC. Under these conditions, retention time for nitrobenzene and 2,4-dichlorophenol were 14.8 and 15.5 min, respectively. Integration was performed from the peaks area and the calibration was done by means of nitrobenzene and 2,4-dichlorophenol standards.

4.3.4. Total Organic Carbon (TOC)

To determine the quantity of organically bound carbon, the organic molecules must be broken down to single carbon units and converted to a single molecular form that can be measured quantitatively. TOC methods utilize heat and oxygen, ultraviolet irradiation, chemical oxidants, or combinations of these oxidants to convert organic carbon to carbon dioxide (CO_2).

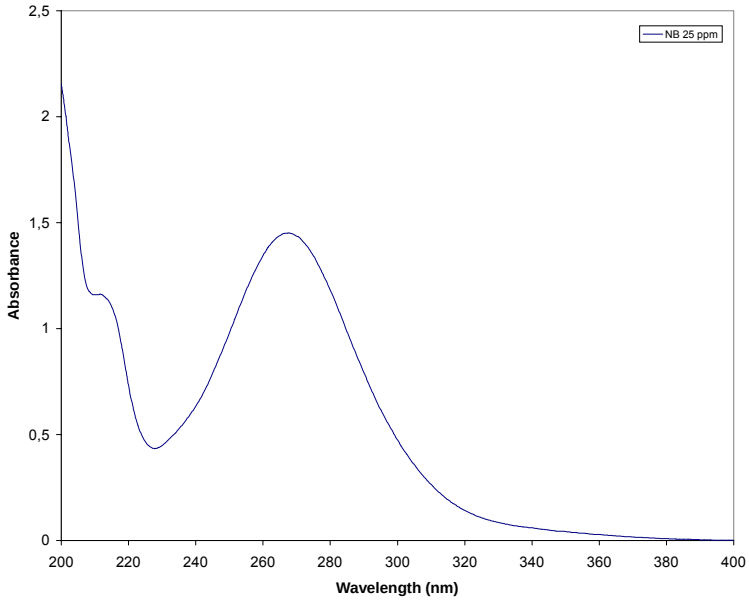

Figure 4.7. Nitrobenzene absorption spectrum

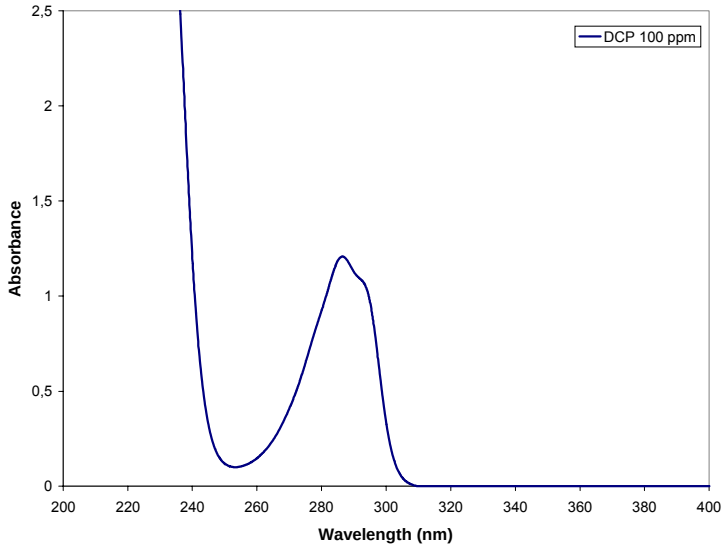

Figure 4.8. Absorption spectrum of 2,4-Dichlorophenol.

In the present case, TOC has been determined by the combustion method and analyzing the resultant CO_2 with a Dohrmann DC-190 TOC analyzer. The system consists of a combustion tube filled with platinum catalyst, through which passes an oxygen flow of 200 $cm^3.min^{-1}$ (99.999% purity) Temperature of reaction zone is maintained at 680ºC.

Samples are introduced into the combustion chamber by means of an automatic sampler, the water is vaporized and the organic matter is completely oxidized to CO_2 and water by catalytic oxidation. The gas stream carries away the CO_2 produced through a condenser and into a gas/liquid separator to remove most of the water formed. Remaining

water can be removed by a dehumificator, which operates at a temperature in the range of between 0-10ºC. The dry gas containing the CO_2 passes through a scrubber to separate halogens and finally reaches a nondispersive infrared analizer (NDIR) to determine the amount of total carbon (TC). In the present case, TC is equivalent to TOC as the amount of inorganic carbon (IC) is negligible (samples are acidified at pH lower than 3 and aireated with oxygen).

The fraction of organic carbon that passes through a 0.45 μm-pore-diameter filter is called dissolved organic carbon (DOC).

The standard solution used to calibrate the TOC equipment is a solution of potassium hydrogen phthalate containing 100 mg $C.L^{-1}$. Injected volume of sample was 200 μL. Theoretical TOC values of 100 ppm of nitrobenzene and 2,4-dichlorophenol are 58.5 and 44.2 mg $C.L^{-1}$, respectively.

4.3.5. Chemical Oxygen Demand (COD)

The Chemical Oxygen Demand (COD) is used as a measure of the oxygen equivalent of the organic matter content of a sample that is susceptible to oxidation by a strong chemical oxidant, dichromate in acidic medium in the present case.

Chemical oxygen demand has been determined by the Standard Methods 5220 D: closed reflux, colorimetric method (Standard Methods, 1985). This analysis consists of heating to an elevated temperature (150°C) a known sample volume with an excess of potassium dichromate in presence of acid (H_2SO_4) for a period of two hours in sealed glass tubes. During this time the organic matter is oxidized and dichromate (yellow) is replaced by the chromic ion (green) [4.2]. Silver sulfate (Ag_2SO_4) is added as catalyst for the oxidation of certain classes of organic compounds.

$$Cr_2O_7^{2-} + 14\,H^+ + 6\,e \rightleftarrows 2\,Cr^{3+} + 7\,H_2O \qquad [4.2]$$

The method is completed by colorimetric determination of the amount of chrome produced. This can be done rapidly and easily by using an spectrophotometer. It is an exact method used in many laboratories nowadays.

The presence of chlorides in the solution can interfere the COD determination, as chlorides can be oxidized by the dichromate [4.3]:

$$6\,Cl^- + Cr_2O_7^{2-} + 14\,H^+ \rightarrow 3\,Cl_2 + 2\,Cr^{3+} + 7\,H_2O \qquad [4.3]$$

This interference can be avoided by adding a solution of mercury sulfate ($HgSO_4$) to the mixture, as the mercury ion combines with the chlorine ion to form mercury chloride ($HgCl_2$). A ratio 10:1 of sulfate:chloride is recommended (Ramalho, 1991).

Nitrite (NO_2^-) exerts a COD of 1.1 mg O_2.mg NO_2^-, what could be important in the case of nitrobenzene experiments analysis. As concentrations of NO_2^- has found to be lower than 1-2 mg $NO_2^-.L^{-1}$, this interference is considered insignificant.

For the COD test two solutions are to be prepared:

- Digestion solution (0.2 N $K_2Cr_2O_7$), prepared by adding to about 500 mL distilled water: 10.216 g $K_2Cr_2O_7$, primary standard grade, previously dried at 103ºC for 2h, 167 mL of concentrated H_2SO_4, and 33.3 g of $HgSO_4$. Dissolve, cool to room temperature, and dilute to 1000 mL.

- Catalyst solution, prepared by adding Ag_2SO_4 to concentrated sulfuric acid at the rate of 5.5 g $Ag_2SO.kg^{-1}$ H_2SO_4 . Let stand 1 to 2 days to dissolve Ag_2SO_4.

In standard tubes of 10 mL, the following amounts of each solution are added: 2.5 mL of the sample, 1.5 mL of the digestion solution and 3.5 mL of the catalyst solution. Tightly cap tubes and invert each several times to mix completely. Place the ampules in a block digester to 150ºC and reflux for 2 hours. Afterwards, cool to room temperature and then measure the absorbency by spectrophotometry at a wavelength of 585 nm.

To establish the relation between the absorbency and the COD, calibration is needed. The calibration curve was done for the photometer (LF 2400, Windaus Labortechnik) by using five standards from potassium hydrogen phthalate (KHP) solution with COD equivalents from 20 to 900 mg$O_2.L^{-1}$ (KHP has a theoretical COD of 1.176 mg $O_2.mg^{-1}$).

For nitrobenzene, if the following oxidation reaction is established [4.4]:

$$C_6H_5NO_2 + \frac{31}{4}O_2 \rightarrow 6\,CO_2 + \frac{5}{2}H_2O + NO_3 \qquad [4.4]$$

for a 100-ppm solution, a maximum theoretical COD value of 202 mg $O_2.L^{-1}$ is obtained, and a 0.50 mg NB.mg^{-1} O_2 ratio. In the case of 2,4-dichlorophenol, a ratio of 0.85 mg

DCP.mg^{-1} O_2 has been established (Adams et al., 1997), so the theoretical COD value of a 100-ppm DCP solution is 118 mg O_2.L^{-1}.

4.3.6. Biochemical Oxygen Demand (BOD)

The Biochemical Oxygen Demand (BOD) is related to the amount of biodegradable organic matter in a water sample. During oxidative degradation of organic matter, aerobic microorganisms which perform it consume oxygen present in water as dissolved gas. BOD is expressed as weight of oxygen consumed per unit volume of water during a defined period of time at a defined temperature, e.g. mg O_2.L^{-1} (or ppm) during 5 days at 20ºC. To complete biological oxidation at 20ºC a period of time between 21 and 28 days is required. This parameter is one of the most widely used for organic pollutants applied to both waste water and surface water. In the present case it has been followed the respirometric method (Standard Methods, 5210 D). Respirometric methods provide direct measurement of the oxygen consumed by microorganisms from an air or oxygen-enriched environment in a closed vessel under conditions of constant temperature and agitation. Samples with a BOD lower than 800-900 ppm do not need dilution. The supply of oxygen is continuous and made easy by stirring.

BOD has been performed by means of an Oxitop system (VELP Scientifica). It is a manometric respirometer, which relates the oxygen uptake to the change in pressure caused by oxygen consumption while maintaining a constant volume. The reaction-vessels content is mixed by magnetic stirring. Carbon dioxide produced is removed by suspending a strongly alkaline agent (NaOH) within the closed reaction chamber. A steady reduction of gas pressure is obtained, which can be metered by suitable manometers (Oxitop membranes).

General procedure for the BOD test can be summarized as follow:

a) Preparation of the buffer solution and the supplementary nutrients

Buffer and nutrients solutions used in the test are to be prepared as follows:

- Phosphate buffer solution, 1.5 N: Dissolve 207 g sodium dihydrogen phosphate, $NaH_2PO_4 \cdot H_2O$ in water. Neutralize to pH 7.2 with 6N KOH and dilute to 1 L.
- Ammonium chloride solution, 0.71N: Dissolve 38.2 g NH_4Cl in water. Neutralize to pH 7 with KOH. Dilute to 1 L.
- Magnesium sulfate solution, 0.41N*:* Dissolve 101 g $MgSO_4.7H_2O$ in water and dilute to 1 L.

- Ferric chloride solution, 0.018N*:* Dissolve 4.84 g $FeCl_3.6H_2O$ in 1 L water.
- Calcium chloride solution, 0.25N*:* Dissolve 27.7 g $CaCl_2$ in 1 L water.
- Potassium hydroxide solution, 6N: Dissolve 336 g KOH in about 700 mL water and dilute to 1 L.
- Glucose-glutamic acid solution: Dry reagent-grade glucose and reagent-grade glutamic acid at 103°C for 1 h. Add 15.0 g glucose and 15.0 g glutamic acid to distilled water and dilute to 1 L. Neutralize to pH 7 using 6N potassium hydroxide.

b) Preparation of the seeding microorganisms

Microorganisms that are used in the BOD test are non-acclimated organisms. The preparation of these consists of taking a volume of activated sludge bacteria solution operating at the sewage works of Gavà (Barcelona, Spain), centrifuge it and take the desired volume from the supernatant. If the bacteria were stored in the refrigerator they should be pulled out and let to reach temperature of 20±5°C.

c) Preparation of the testing bottles

Depending on the range of BOD value, the total volume of solution used in the test changes. The range of BOD and the correlated volume needed are shown in table 4.1.

Table 4.1. Ranges of BOD and the correlated total volume of sample.

Expected value of BOD (mg $O_2.L^{-1}$)	Total sample volume (mL)	Multiplication factor
0-40	432	1
0-80	365	2
0-200	250	5
0-400	164	10
0-800	97	20
0-2000	43.5	50
0-4000	22.7	100

In the present case, BOD values were lower than 40 mg $O_2.L^{-1}$, so the total volume of the sample was fixed at 432 mL. Each volume was filled with the following amounts of each solution: 425 mL of sample, 2.595 mL of buffer solution, 0.865 mL of NH_4Cl, $MgSO_4$ and $CaCl_2$ solutions, and 0.650 mL of biomass (this amount was fixed by the guidelines

given by the Standard Methods, 5210 D). For each BOD test, a "blank bottle" has to be arranged, containing the bacteria, buffer and nutrient solutions and Millipore water. Samples, previously aerated, are allowed to reach 20ºC in the refrigerator, then 2 NaOH tablets are added in a quiver and the bottles are sealed with the Oxitop membrane, reset the zero and kept in the incubator thermostatically controlled at a 20 ± 1 °C with agitation for up to 21 days.

The value of n-days BOD is calculated by using the formula:

$$BOD_n = (BOD_S - BOD_B) \, x \, N \qquad [4.5]$$

Where:

BOD_S = BOD of the sample measured after n days

BOD_B = BOD of the blank measured after n days

N = multiplication factor

The performance of this method was previously tested with the glucose-glutamic acid standard, with a satisfactory result.

4.3.7. Concentration of ozone in the gas phase.

The ozone in the gas phase is measured with the UV absorption method. The ozone flows through the gas measuring cell, through which a UV-beam is leaded. Between 200 and 300 nm ozone has a broad absorption band, which is known as Hartley-band. At 253.7 nm the absorption coefficient of ozone has a maximum. The relation between absorption of light and ozone concentration is defined by the Lambert-Beer law:

$$C = \frac{\log\left(\frac{H_o}{H_c}\right)}{d.\varepsilon} \qquad [4.6]$$

where: C = ozone concentration ($g.m^{-3}$)

H_o = light intensity without ozone

H_C = light intensity with ozone

d = length of the gas measuring cell (mm)

ε = extinction coefficient (6.3)

From the absorption of light, the ozone concentration can be calculated directly. The apparatus used is a Sander QuantOzon "1", that operates in the range 0 – 20 $g.m^{-3}$.

4.3.8. Ozone measurement in the aqueous phase.

For the determination of ozone concentrations in water, the indigo-trisulfonate method (Bader and Hoigné, 1981, 1982; Standard Methods 4500-O_3 B, 1985; Masschelein et al., 1998) has been used. It is based on the principle that in acidic solution potassium indigo-trisulfonate ($C_{16}H_7N_2O_{11}S_3K_3$) is discolored by aqueous ozone and the degree of discoloration is compared to a blank solution of the dye. The decrease in absorbance is linear with increasing ozone concentration. The proportionality constant at 600 nm, maximum absorbance of the indigo solution, is 0.42 ± 0.01 $L.cm^{-1}.mg^{-1}$. The range of application of this method is 0.05 to 0.6 mg $O_3.L^{-1}$. This method is quantitative, selective, and simple.

Hydrogen peroxide decolorize the indigo reagent very slowly. H_2O_2 does not interfere if ozone is measured in less than 6 hours after adding reagents. Fe(III) does not interfere.

Preparation of the reagents was done as follows:

- *Indigo stock solution*: Add about 500 mL distilled water and 1 mL conc. phosphoric acid to a 1-L volumetric flask. With stirring, add 770 mg potassium indigo trisulfonate. Fill to mark with distilled water. A 1:100 dilution exhibits an absorbance of 0.20 ± 0.010 cm^{-1} at 600 nm. This stock solution is stable for about 4 months when stored in the dark. Discard when absorbance of a 1:100 dilution falls below 0.16 cm^{-1}.

- *Working solution*: This solution is made up immediately before use by dilution of 25 mL of the stock solution to 250 mL containing 2.5 g. of analytical grade NaH_2PO_4 and 1.75 mL of analytical grade H_3PO_4.

5 mL of working solution are introduced into each of two 50 mL volumetric flasks. One is filled with ozone-free water (e.g. millipore water) and the other with 10 mL of the sample and completed with millipore water. The difference in absorption of light at 600 nm between blank and sample is measured. The measurement is to be done as soon as possible but in all instances within 4 hours when stored in the dark. Add sample so that completely decolorized zones are eliminated quickly by gently shaking, but no ozone degassing occurs. The concentration is dissolved ozone is determined as follows:

$$C_{o_3}\ (mg.L^{-1}) = \frac{\Delta A \cdot V_T}{f \cdot b \cdot V} \qquad [4.7]$$

where ΔA is the difference in absorbance between sample and blank, V_T is the total volume (50 mL), b is the path length of cell (1 cm), V is the volume of sample added (10 mL) and f is the proportionality constant (0.42 cm^{-1}). The error of this method is ca. 5%.

4.3.9. Total suspended solids (TSS)

Suspended solid refer to non-filterable matter suspended in water and waste water. Solids may affect water or effluent quality adversely in a number of ways. Analyses are important in the control of biological and physical waste water treatment processes and for assessing compliance with regulatory agency waste water effluent limitations. "Total solids" is the term applied to the material residue left in the vessel after evaporation of a sample and its subsequent drying in an oven at a defined temperature. Total solids includes "total suspended solids", the portion of total solids retained by a filter (of 2.0 μm (or smaller) nominal pore size), and "total dissolved solids", the portion that passes through the filter.

In the analysis of TSS (Standard Methods 2540 D, 1985), a well-mixed sample is filtered through a weighed standard glass-fiber filter and the residue retained on the filter is dried to a constant weight at 103 to 105ºC. The increase in weight of the filter represents the total suspended solids.

Firstly, the glass-fiber filter disks are to be prepared. For it:

- Insert the disk with wrinkled side up in the filtration apparatus, apply vacuum and wash disk with three successive 200-mL portions of Millipore water.
- Dry the filter in an oven at 103 to 105ºC for 1 hour. If volatile solids are to be measured, ignite at 550ºC for 15 min in a muffle furnace.
- Cool in desiccator to balance temperature and weight. Store in desiccator until needed.

For sample analysis:

- Assemble filtering apparatus and filter and begin suction.
- Add 10 mL of the sample onto the glass-fiber filter.
- Wash with three successive 10-mL volumes of Millipore water, allowing complete drainage between washings, and continue suction for about 3 min after filtration is complete.
- Carefully remove filter from filtration apparatus.

- Dry for 1 hour at 103 to 105ºC in an oven, cool in a desiccator to balance temperature and weight.

TSS are calculated as follows:

$$\text{mg TSS.L}^{-1} = \frac{(A - B)\,x\,1000}{\text{sample volume, mL}} \qquad [4.8]$$

where: A = weight of filter + dried residue, mg
B = weight of filter, mg.

4.3.10. Total volatile suspended solids (TVSS)

The residue from the previous test is ignited to constant weight at 550ºC (Standard Methods 2540 E, 1985). The remaining solids represent the fixed total, dissolved, or suspended solids while the weight lost on ignition is the volatile solids. The determination is useful in control of waste water treatment plant operation because it offers a rough approximation of the amount of organic matter present in the solid fraction of waste water, activated sludge, and industrial wastes.

The procedure follows the previous one. Once the glass-fiber filter has been placed at 103 to 105ºC for 1 hour, cooled to room temperature and weighted, the residue is ignited to constant weight in a muffle furnace at a temperature of 550ºC for 15 minutes. Have furnace up to temperature before inserting the sample. Let the filter cool to room temperature. Weigh the disk as soon as it has cooled to room temperature. The TVSS is calculated as the lost of weight (equation 4.9):

$$\text{mg TVSS.L}^{-1} = \frac{(A - C)\,x\,1000}{\text{sample volume, mL}} \qquad [4.9]$$

where: A = weight of residue + filter before ignition, mg
C = weight of residue + filter after ignition, mg.

5. Experimental results - Discussion

5.1. Actinometry.

Before carrying out the experiments where the ultraviolet radiation takes part, experiments based on the photochemical decomposition of oxalic acid in presence of uranyl ion (Volman and Seed, 1964; Heidt et al., 1979; Esplugas and Vicente, 1983) were performed to determine the amount of radiation emitted by the lamps and transferred into the reactor. The mechanism of this reaction is very complex, being reaction products CO, CO_2, HCOOH, U^{4+} and H_2O. Nevertheless, for a pH range of between 3 and 7, and oxalic acid conversions lower than 20%, the reaction that takes place is [5.1]:

$$UO_2^{2+} + C_2O_4H_2 \rightarrow UO_2^{2+} + CO + CO_2 + H_2O \qquad [5.1]$$

5.1.1. Mathematical model.

The intensive reaction rate is defined by [5.2]:

$$r_R = -\sum_{\lambda} \Phi_\lambda \cdot \mu_\lambda \cdot q_\lambda \qquad [5.2]$$

being Φ the quantum yield, μ_λ the uranyl absorption for each wavelength and q_λ the modulus of the radiation density flux vector at the wavelength λ, which can be determined by the geometric parameters of the reactor and a proper emission model for the lamp.

As the uranyl is not consumed in the reaction, the absorbance remains constant and the kinetics is order zero with respect to the concentration of reactants and first order with respect to the absorbed radiation.

By introducing the mass balance in equation [5.2] and integrating,

$$n^0_{ox} - n_{ox} = R_{ox} \cdot t = -\int_V \sum_{\lambda} \Phi_\lambda \cdot \mu_\lambda \cdot q_\lambda \cdot t \cdot dV \qquad [5.3]$$

The absorbed photon flow at a wavelength λ is given by the expression [5.4]:

$$W_{abs,\lambda} = \int_V \mu_\lambda \cdot q_\lambda \cdot dV \qquad [5.4]$$

By substituting [5.3] in [5.4], [5.5] is obtained:

$$n^0_{ox} - n_{ox} = -\sum_{\lambda} \Phi_\lambda \cdot W_{abs,\lambda} \cdot t \qquad [5.5]$$

As the lamp emits mainly in a unique wavelength, equation [5.5] can be simplified as:

$$n^0_{ox} - n_{ox} = -\Phi_\lambda \cdot W_{abs,\lambda} \cdot t \qquad [5.6]$$

The value of Φ_λ at a λ in the range of between 250-262 nm is 0.6 mol.Einstein^{-1}.

5.1.2. Experimental method.

A 0.05 mol.L^{-1} oxalic acid and 0.01 mol.L^{-1} uranyl nitrate solution is prepared. Samples are withdrawn at intervals of between 2-3 minutes and titrated with a 0.1 N $KMnO_4$ solution. Two actinometries were carried out and results are presented below:

- **Actinometry 1.**

Time (min.)	n_{H2C2O4} (mol)	$n^0_{H2C2O4} - n_{H2C2O4}$ (mol)
0	0.1453	0
2	0.1444	$9x10^{-4}$
4	0.1429	$2.4x10^{-3}$
6	0.1406	$4.65x10^{-3}$
8	0.1391	$6.15x10^{-3}$
10	0.1373	$8x10^{-3}$
12	0.1358	$9.5x10^{-3}$
14	0.1343	$1.11x10^{-2}$
16	0.1335	$1.176x10^{-2}$

- **Actinometry 2.**

Time (min.)	n_{H2C2O4} (mol)	$n^0_{H2C2O4} - n_{H2C2O4}$ (mol)
0	0.1380	0
3	0.1373	$7.5x10^{-4}$
6	0.1343	$3.74x10^{-3}$
9	0.1309	$7.11x10^{-3}$
12	0.1279	$1.01x10^{-2}$
15	0.1261	$1.2x10^{-2}$
18	0.1231	$1.5x10^{-2}$
21	0.1205	$1.76x10^{-2}$
24	0.1178	$2.02x10^{-2}$

Results of both actinometries are presented in Graph 5.1, where the pertinent linear fittings have been performed.

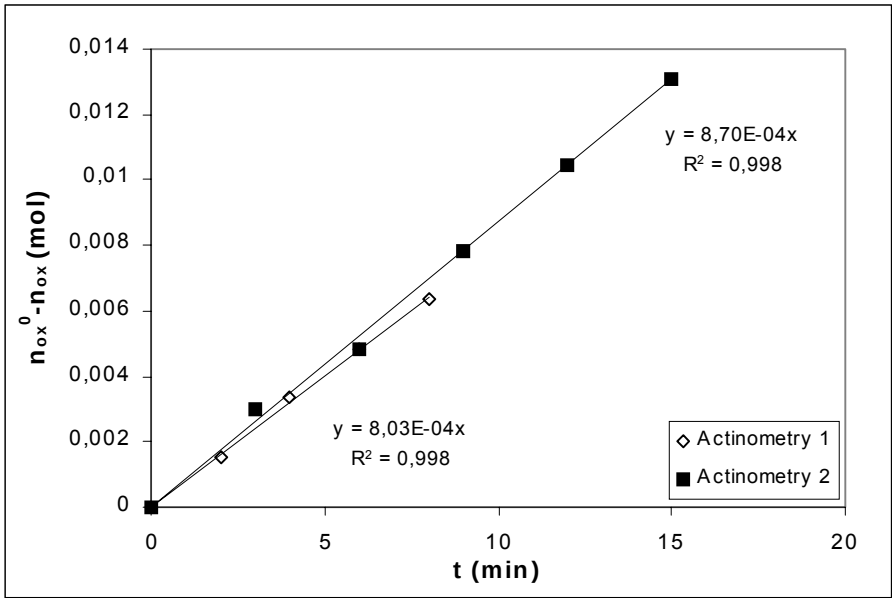

Graph 5.1. Comparison of actinometries 1 and 2.

5.1.3. Actinometry results.

The slope of the graph is equal to:

slope = $\Phi_\lambda * W_{abs,\lambda}$

With the value of Φ_λ, $W_{abs,\lambda}$ is obtained:

a) Actinometry 1, with a 95% confidence level

$W_{abs,\lambda}$ = 24.17 μEinstein.s^{-1} ≈ 11.5 W

b) Actinometry 2, with a 95% confidence level

$W_{abs,\lambda}$ = 23.08 μEinstein.s^{-1} ≈ 11 W

According to the actinometry results, the photon flow entering the reactor at a wavelength of 253.7 nm is, in average, 23.7 μEinstein.s^{-1} (1 Einstein = 1 mol photon).

NITROBENZENE (NB)

5.2. Previous experiments with nitrobenzene – Stripping with oxygen.

One preliminary experiment was performed to determine the possible contribution of an oxygen stripping to the degradation of nitrobenzene (NB). In this experiment, pure oxygen was bubbled through a ca.100-ppm NB solution during 90 minutes. Results are presented in Appendix A1.1, Table NB-S. As it can be observed, the diminution of the NB concentration is insignificant, taking into account the experimental and HPLC analysis error. Thus, the disappearance of NB due to volatilization will be considered negligible. Any degree of NB removal by means of the AOPs will be produced by the action of these combinations without contribution of the stripping.

5.3. Single ozonation of NB.

In the first set of experiments carried out with NB, the effect of single ozonation on the degradation and biodegradability of NB aqueous solutions was studied. The influence of ozone production, pH, initial NB concentration and scavengers on the degradation of NB was tested, as well as the effect of single ozonation on the biodegradability of these solutions. Moreover, the stoichiometric coefficient of the reaction between ozone and NB was determined. Results are shown on section Appendix 1.2, Tables NB-O1 to NB-O15. In the following graphs, most of results will be plotted versus the *absorbed* ozone dose. Mass transfer of ozone from the gaseous to the aqueous phase can be a limiting factor, causing a part of applied ozone to be lost in the off-gas. The *absorbed* ozone dose is thus more informative because it indicates the amount of dissolved ozone available for oxidation. The absorbed ozone dose was calculated by subtracting the concentration of ozone in the off-gas from the inlet concentration.

5.3.1. Influence of the ozone production

To study the effect of the amount of fed ozone, aqueous solutions of ca. 100 ppm (in the range 90-100 ppm (0.73-0.81 mmol.L^{-1} NB)) where treated by single ozonation changing the production of ozone from 4.1 g.h^{-1} (11.5 g.m^{-3}) to 14.6 g.h^{-1} (41 g.m^{-3}). The pH was allowed to progress freely and temperature was 18-20ºC. Results are shown in section A1.2, Tables NB-O1 to NB-O4.

The evolution of the normalized NB concentration during time is shown in Graph 5.2. It can be observed that the slope of the curve C/C_0 vs. time at initial time increases with the ozone production, diminishing the time of treatment needed to achieve a desired degree of removal, thus increasing the conversion at a given time. For example, after 40 minutes of treatment, conversions are 55%, 76%, 85% and 96% for ozone production of 4.1, 7.4, 11.1 and 14.6 $g.h^{-1}$, respectively. An increase in the ozone production may enhance the absorption rate as the driving force grows, increasing then the oxidation rate. It has been found that the NB removal rate increases linearly with the production (correlation coefficient $r^2 = 0.97$, see Table 5.1).

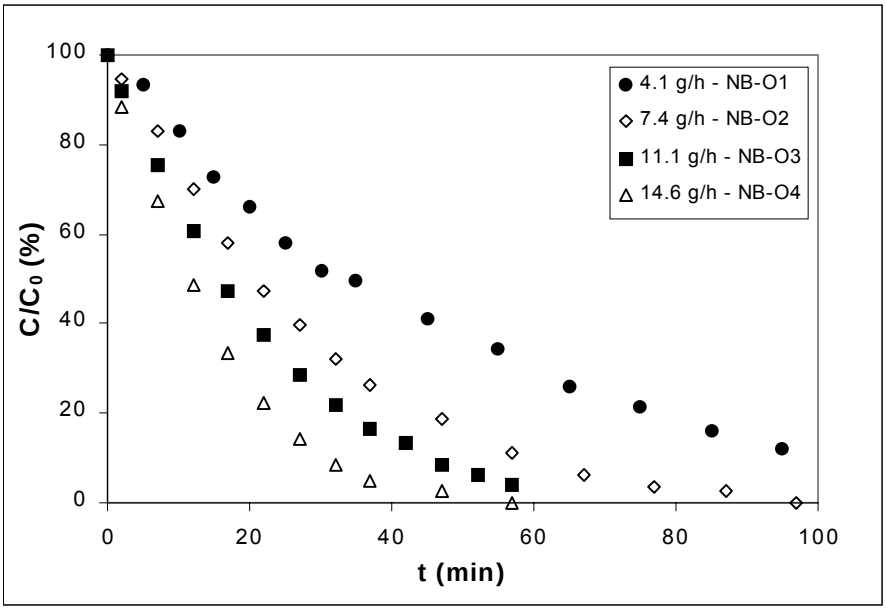

Graph 5.2. Effect of the ozone production on NB ozonation – Normalized concentration.

Table 5.1. Effect of the ozone production on the initial NB removal rate

Ozone production ($g.h^{-1}$)	NB removal rate ($mg.min^{-1}$)
4.1	36.6
7.4	51.1
11.1	61.8
14.6	78.4

Ozonation rates are lower than those found for 2,4-dichlorophenol (see section 5.12). The nitro group deactivates the electrophilic aromatic substitution reactions, a way through which ozone reacts with aromatic compounds (Bailey, 1958), deriving in lower ozonation rates.

Nevertheless, if the amount of DCP removed is plotted versus the absorbed ozone dose (see Graph 5.3), this amount increases only slightly with the ozone production. This

fact may suggest that mass transfer is lightly controlling the process, but mostly chemical reaction may be controlling.

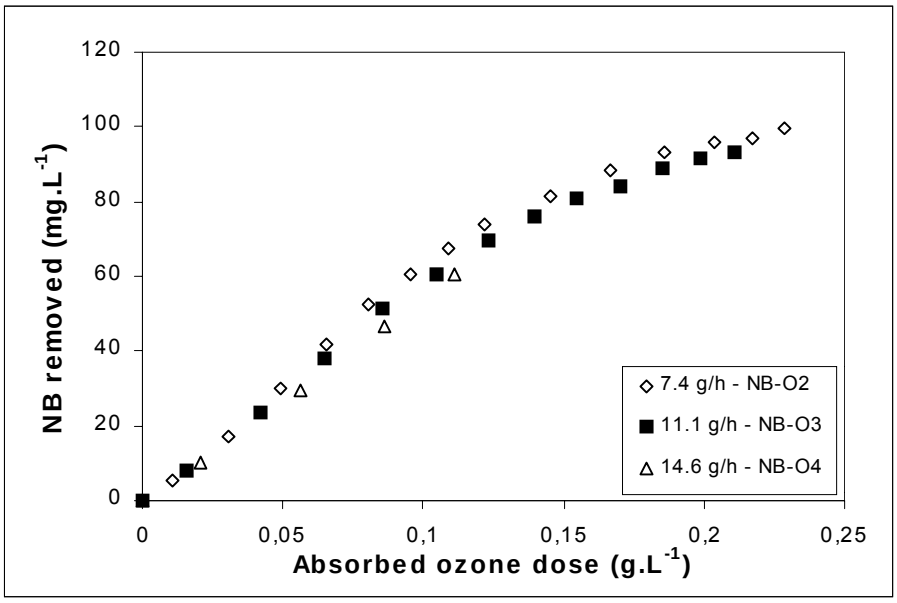

Graph 5.3. Influence of the ozone production on NB ozonation – Amount of NB removed vs. absorbed ozone dose

Another point of interest is the evolution of the concentration of ozone in the residual gas during time (Graph 5.4). The shape of the curves would suggest the presence of "plateaus" where the concentration of ozone would remain constant. This behavior was observed by Beltrán et al. (1998a) as well. It can be seen that the first plateau is produced when a 60-70% initial NB removal has been achieved. From this point it seems that a change in the reactivity of NB with ozone is produced, maybe due to the higher reactive nature of some of the present intermediates. The second plateau is produced when almost all initial NB disappears. Residual ozone increases with the ozone production because, if chemical reaction is mostly controlling the process, the same dose of ozone is absorbed, i.e. more non-reacted ozone is leaving the system.

An useful parameter to estimate the amount of required ozone is the *stoichiometric coefficient* of the reaction of NB with ozone, that is, moles of ozone consumed per mol of NB removed. This value can be calculated from data presented in Graph 5.3, amount of NB removed and ozone consumed (as the absorbed ozone dose multiplied by the volume of treated solution, 21 L). This coefficient has to be calculated at initial time, as afterwards intermediates are produced and will affect this value. It has to be pointed out that this value is only an estimation, as the experimental device used in this experimentation is not

the proper one and this work has not been carried out in high excess of NB to assure the total consumption of ozone practically at an instantaneous rate by NB and not by the intermediates products formed. Graph 5.5 present the stoichiometric coefficient for the experiments NB-O2 and NB-O3. The stoichiometric coefficient has been found to be ca. 4 mol O_3 consumed per mol of NB removed in the range of production tested. A similar value was found in a previous research (Caprio et al., 1984).

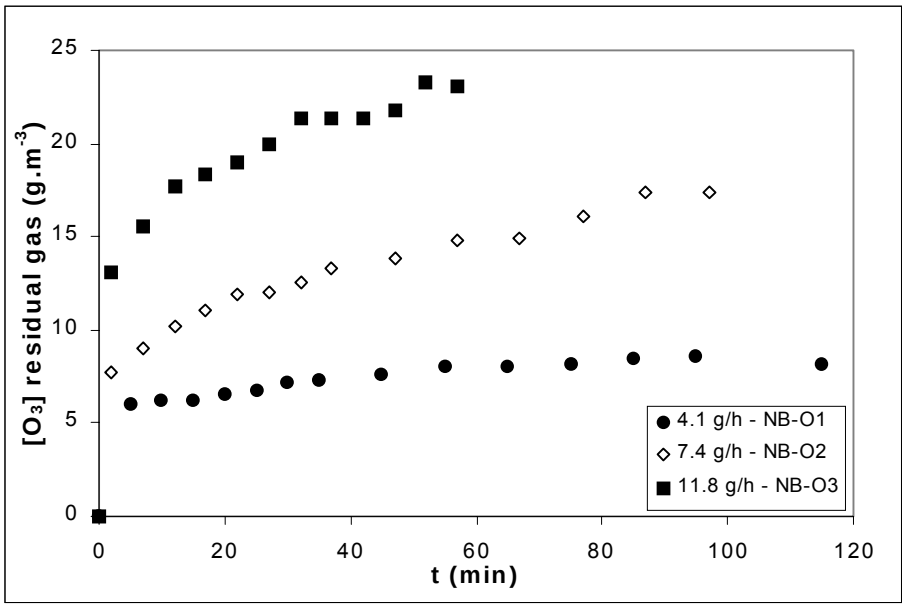

Graph 5.4. Influence of the ozone production on NB ozonation – Residual ozone.

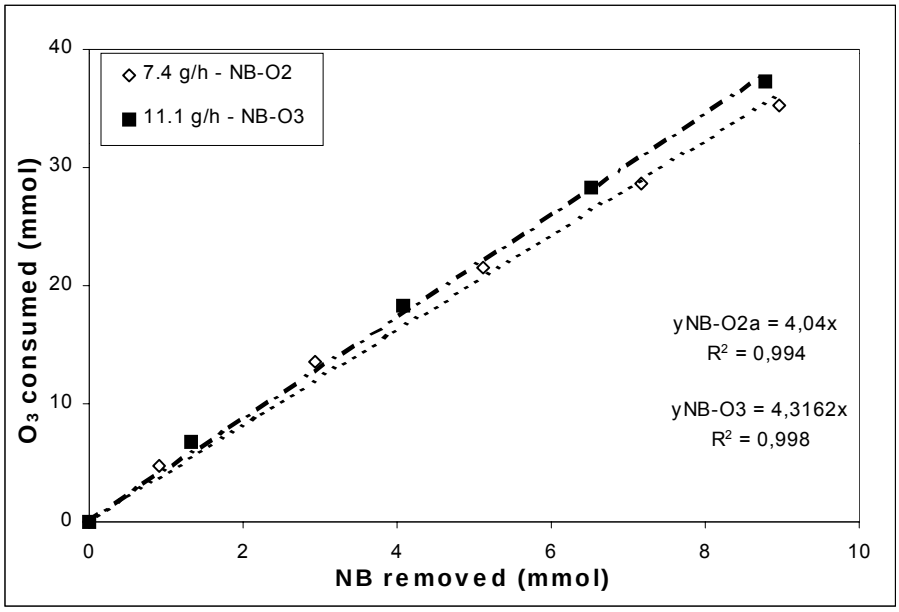

Graph 5.5. Stoichiometric coefficient for the reaction of NB with ozone

5.3.2. Effect of pH.

As it has already been mentioned, pH is one of the most important variables in the ozonation processes, due to the catalytic action of hydroxyl ions on the ozone decomposition (Staehelin and Hoigné, 1985):

$$O_3 + OH^- \rightarrow O_2^{\bullet} + HO_2^{\bullet} \qquad (k = 70\ M^{-1}.s^{-1}) \qquad [2.4]$$

To study the influence of pH in the ozonation of NB, aqueous NB solutions of ca. 100 ppm initial concentration (in the range 95-105 ppm (0.77-0.85 mmol.L^{-1})) were treated by maintaining the pH of the medium at the following values:

- pH = 3, by means of H_3PO_4. It was not buffered: as observed in previous experiments, ozonation processes evolve to pH 3.
- pH = 6.8, by means of the buffer 0.025 mmol.L^{-1} KH_2PO_4 - 0.025 mmol.L^{-1} Na_2HPO_4
- pH = 9, by means of 0.01 mmol.L^{-1} $Na_2B_4O_7$ (borax).

The temperature of the experiments was 18-20ºC and the ozone production was set at 7.4 g.h^{-1}. Results are shown in section A1.2, Tables NB-O2a and NB-O5 to NB-O7. As it has been observed in Graph 5.6, the concentration of ozone in the residual gas decreases when increasing pH, confirming that more ozone is being decomposed by the action of hydroxyl ions.

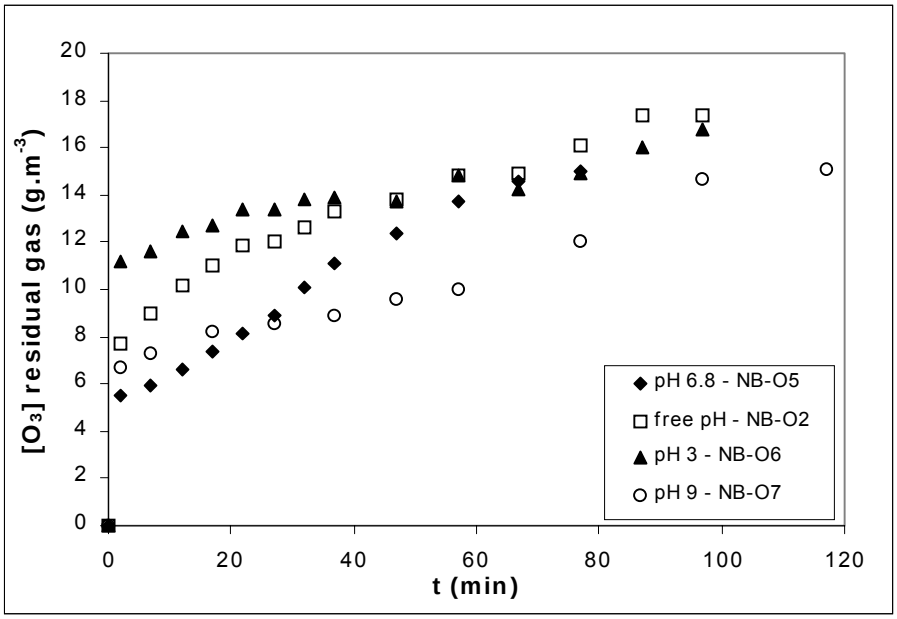

Graph 5.6. Effect of pH on the ozonation of NB – Residual ozone

Graph 5.7 presents the evolution of the normalized NB concentration during time at different pHs in the range 3 to 9. Best results have been obtained at neutral pH. Slightly lower disappearance rates have been achieved by the experiments carried out at free pH and pH 3. However, at pH 9 the reaction seems to be partially inhibited. Since nitroaromatic hydrocarbons are non-dissociating compounds, the rate constant of their direct reaction with ozone is independent of pH. As differences observed in this graph between pH 3 and 9 are rather small, this behavior would suggest then, that the direct pathway of ozone action is the main responsible of the NB degradation. Nevertheless, in the literature (Beltran et al., 1998a) has been found that works carried out at lower ozone productions (0.15 $g.h^{-1}$) showed marked differences between experiments performed at pH 2 and 7: NB conversions at a given time were found to be 30% at pH 2 and 60% at pH 7. Other works (Glaze et al., 1987) point out as well that the decomposition of nitroaromatic compounds in aqueous solution takes place mainly through radical pathway.

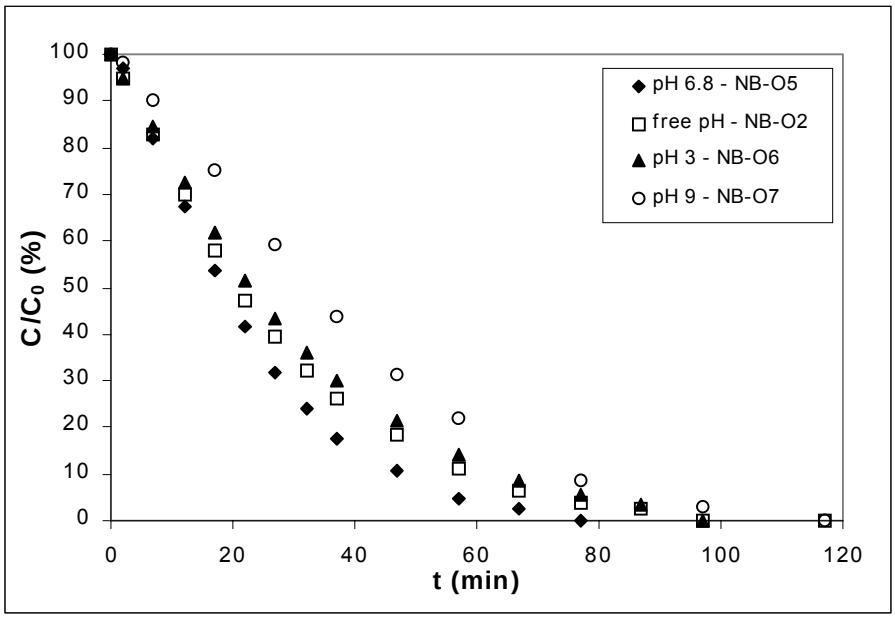

Graph 5.7. Effect of pH on the ozonation of NB – Normalized concentration

Nevertheless, as it has been shown in Graph 5.6, as pH increases more ozone is decomposed into hydroxyl radicals. Why this higher production of hydroxyl radicals is not translated into a higher disappearance rate at pH 9? This could be explained by the withdrawing character of the nitro group, which depletes the aromatic ring of electron density. The mechanism of the OH· radical on aromatic compounds is analogous to an electrophilic substitution, and this kind of substitution is retarded by electron-accepting substituents (Lipczynska-Kochany, 1991). Beltrán et al. (1998a) observed the inhibition of

the removal rate of NB at pH 12. They attributed this inhibition at the dissociation of hydroxyl radicals into the oxygen anion radical through the equilibrium:

$$OH^{\bullet} \rightleftarrows O^{\bullet} + H^{+} \qquad [5.6]$$

whose pKa is 11.9.

5.3.3. Influence of the initial concentration.

To study the effect of this variable, aqueous NB solutions of different initial concentrations (in the range 100-250 ppm, higher concentrations are not possible due to foaming problems) were treated by single ozonation, at room temperature (18-20ºC) and with the same ozone production (7.4 $g.h^{-1}$), allowing pH to evolve freely. Results are shown in section A1.2, Tables NB-O2, NB-O8 and NB-O9.

The decrease of the NB concentration as NB removed vs. the treatment time is presented in Graph 5.8. As it can be observed, during the initial stage of treatment the disappearance rate of NB is independent of the initial concentration and equal to ca. 55 $mg.min^{-1}$ (27 $mmol.h^{-1}$). It can also be seen that, for a given reaction time, an increase in the initial concentration leads to a smaller conversion, although the disappearance rate is higher. Thus, e.g. after 60 minutes of treatment conversions are 90%, 58% and 50% for initial concentrations 100, 223 and 250 ppm, respectively.

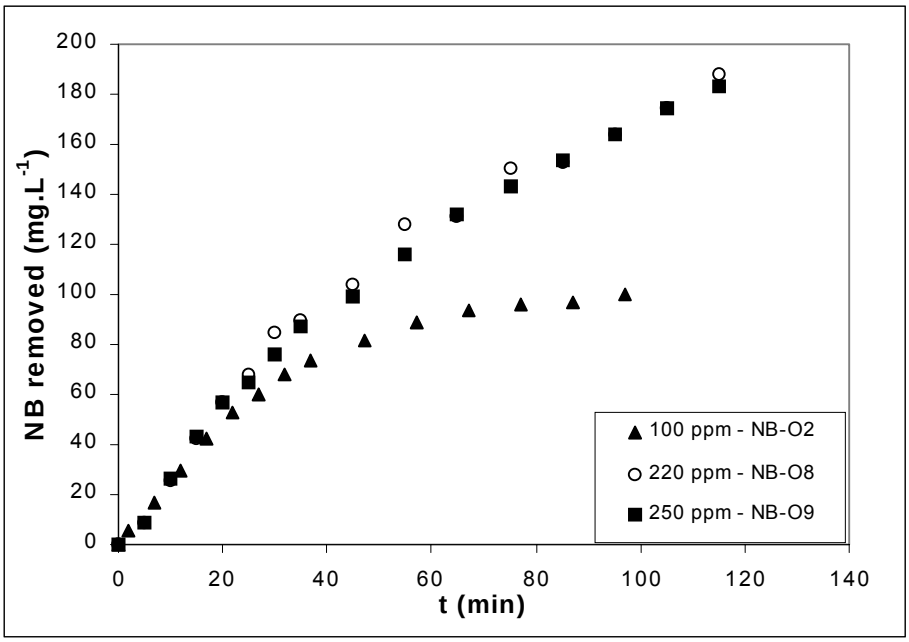

Graph 5.8. Influence of the initial concentration on NB ozonation – NB removed vs. time of treatment

When the amount of NB removed is plotted versus the absorbed ozone dose (Graph 5.9) it can be observed that the disappearance rate is practically non-dependent of the initial NB concentration. The stoichiometric coefficient has been estimated to be ca. 4 mol of ozone per mol of NB removed.

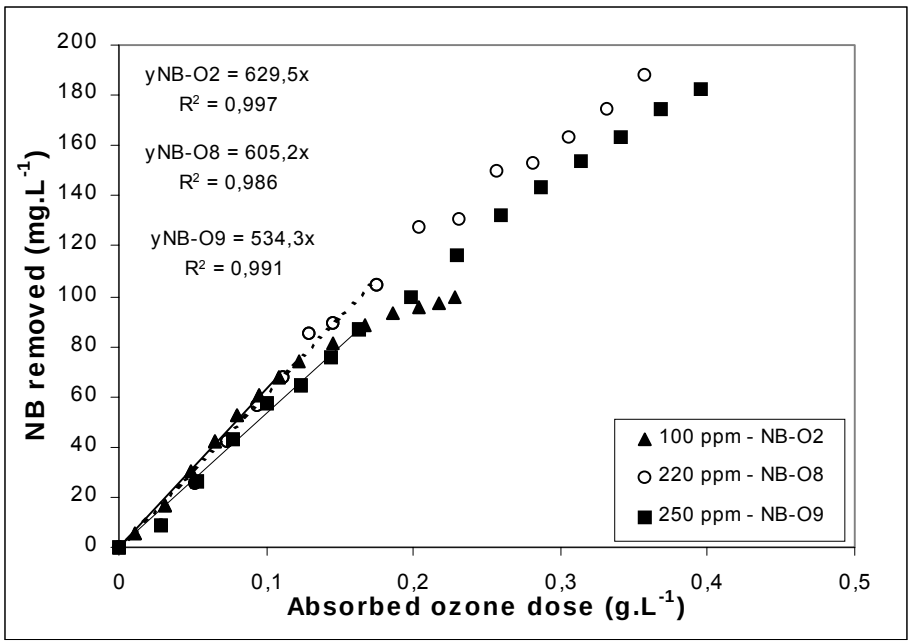

Graph 5.9. Influence of the initial concentration on NB ozonation – NB removed vs. absorbed ozone dose

An interesting aspect would be measurement of dissolved ozone. In our case, those measurements were not performed, but the published literature (Beltrán et al., 1998a) reports the presence of dissolved ozone in higher amount as higher is the initial NB concentration. This fact suggests that the reaction takes place in the liquid phase, thus being a slow reaction. This behavior does not mean that high oxidation rates cannot be achieved. The presence of certain substances or phenolic intermediates, like nitrophenols (which have been identified among the intermediates), can promote the decomposition of ozone increasing the generation of free radicals (Staehelin and Hoigné, 1985).

The ozonation of NB seems to follow a pseudo-first order kinetics at initial time. By fitting the logarithm of the normalized concentration to a straight line (see Graph 5.10), pseudo-first order kinetic constants for the experiments NB-O2, NB-O8 and NB-O9 have been estimated and presented in Table 5.2. The value of this kinetic constant is reduced to half when the initial NB concentration is doubled. Kinetic constants have been found to be in the order of magnitude of values reported in the literature (Baozhen and Jun, 1988).

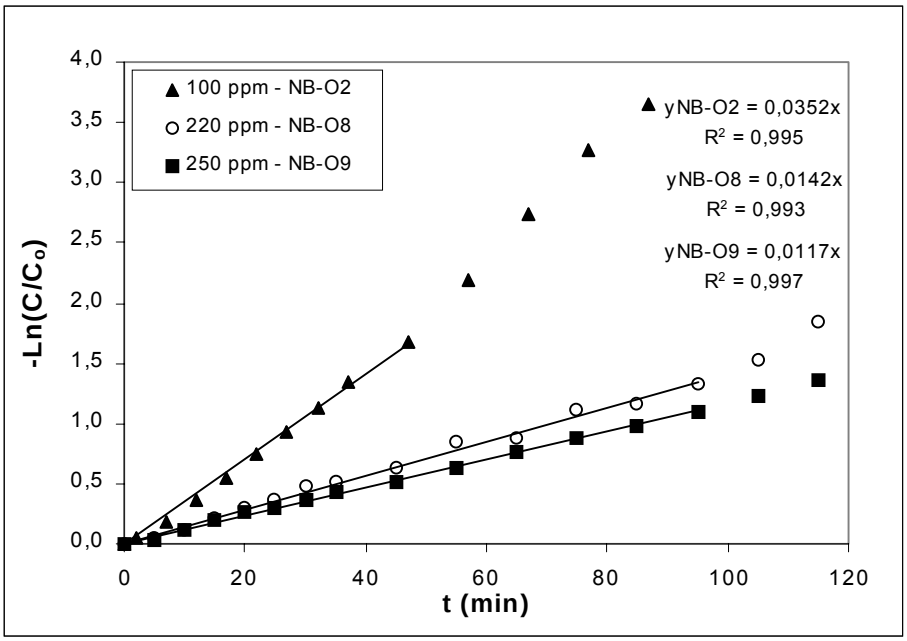

Graph 5.10. Influence of the initial concentration on NB ozonation - Estimation of the pseudo-first order kinetic constants

Table 5.2. Pseudo-first order kinetic constants as a function of the initial NB concentration

Experiment	Initial NB conc. (mg.L^{-1})	k (min^{-1})
NB-O2a	100	0.0352
NB-O8	223	0.0142
NB-O9	246	0.0117

With regard to the concentration of ozone in the residual gas (Graph 5.11) it can be observed that the amount of residual ozone decreases when the initial NB concentration is increased, as the amount of non-reacted ozone is smaller.

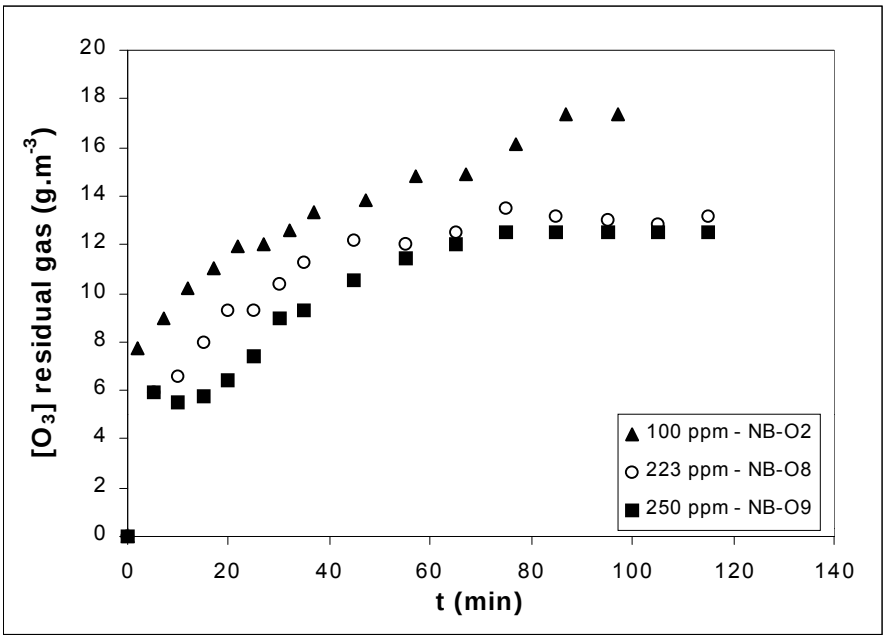

Graph 5.11. Influence of the initial concentration on NB ozonation – Residual ozone

5.3.4. Influence of hydroxyl radical scavengers: carbonates and t-BuOH

As it has been commented before, the literature points out that the radical pathway is the main responsible of the NB degradation by ozone. To check this, one experiment at pH 10 was performed in presence of carbonate and bicarbonate ions (0.025 mol.L^{-1}) as hydroxyl radical scavengers. Kinetic constants of hydroxyl radicals with HCO_3^- and CO_3^{2-} are $8.5.10^6$ $M^{-1}.s^{-1}$ and $3.9.10^8$ $M^{-1}.s^{-1}$, respectively (Acero and Gunten, 2000).

$$HCO_3^- + OH^\bullet \rightarrow HCO_3^\bullet + OH^- \quad \Uparrow\Downarrow \quad CO_3^{\bullet-} + H^+ \qquad [2.15]$$

$$CO_3^{2-} + OH^\bullet \rightarrow CO_3^{\bullet-} + OH^- \qquad [2.13]$$

This experiment (see section A1.2, Table NB-O11) is compared with results obtained by single ozonation of NB at a similar pH (9, experiment NB-O7). Graph 5.12 show comparison of the evolution of the normalized concentration. As it can be observed, a significant inhibitory effect is produced, as radicals react preferably with carbonates than with NB. At pH 9 NB is completely removed in less than two hours. After this time in presence of carbonates the conversion of NB is 70%. The important diminution of the disappearance rate in presence of carbonates confirms the noteworthy contribution of the radical pathway in the mechanism of ozonation of this compound. This result is important

in practical cases because natural waters contain carbonates that would retard the ozonation rate.

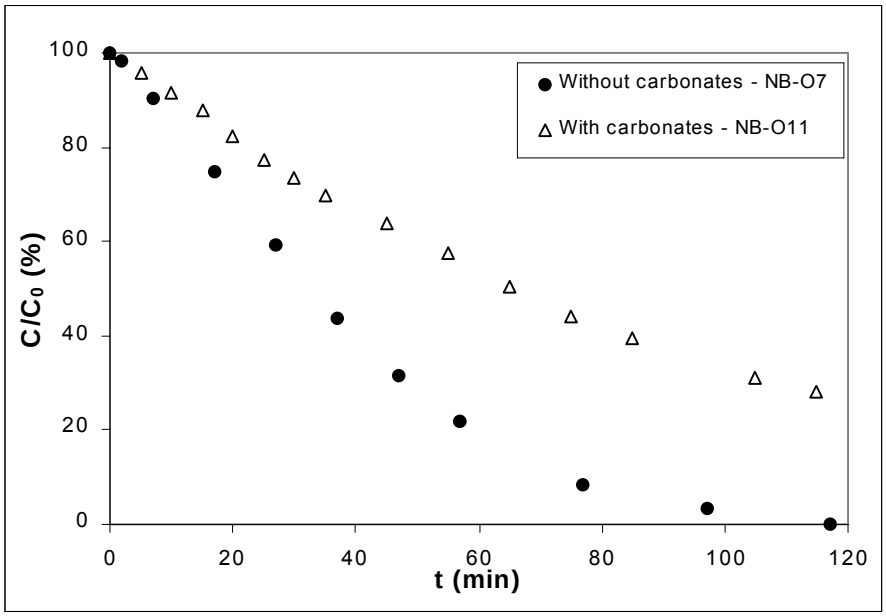

Graph 5.12. Effect of carbonates as radical scavengers on NB ozonation – Normalized concentration vs. time

Regarding the concentration of ozone in the residual gas (see Graph 5.13), it can be observed that the concentration of residual ozone is higher in presence of carbonates. The radical decomposition of ozone is inhibited by carbonates and higher amount of ozone is lost within the residual gas.

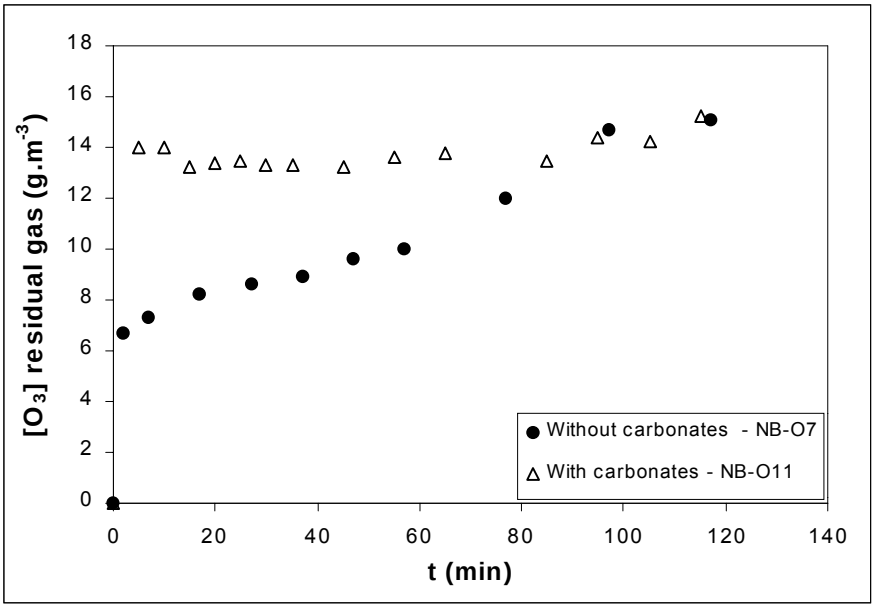

Graph 5.13. Effect of carbonates as radical scavengers on NB ozonation – Residual ozone

Nevertheless, the inhibition of the radical pathway is not complete when carbonates are present. Carbonates may act as promoters of the radical reactions responsible of the ozone decomposition when forming the superoxide radical in presence of H_2O_2 ([2.14]).

Thus, one experiment in presence of *tert*-butyl alcohol was carried out. Tert-butyl alcohol reacts very slowly with ozone (Hoigné and Bader, 1983a published a value for the kinetic constant of the direct reaction of ozone with t-BuOH of $3x10^{-2}$ $M^{-1}.s^{1}$) but reacts with hydroxyl radicals to yield inactive products that terminate the free radical mechanism (Staehelin and Hoigné, 1985). The experiment was performed at room temperature, free pH and 7.4 $g.h^{-1}$ ozone production (see section A1.2, Table NB-O12) to be compared with the experiment carried out at the same conditions without t-BuOH (NB-O2). The concentration of t-butanol used is 3 $mmol.L^{-1}$, from data presented by Hoigné and Bader (1983b). Ozone could be partially consumed by reaction with t-BuOH at high concentrations of this compound, although the kinetic constant value is very low.

As it can be seen in Graph 5.14, the presence of t-BuOH greatly inhibits the ozonation rate of NB. While NB disappears in 100 minutes in the experiment carried out without the scavenger, in presence of t-BuOH 40% of initial NB was still in solution at that time. By fitting both experiments to a pseudo-first order reaction and comparing the slopes (see Graph 5.15), it can be observed that the disappearance rate of NB is reduced in a 87% in presence of t-BuOH.

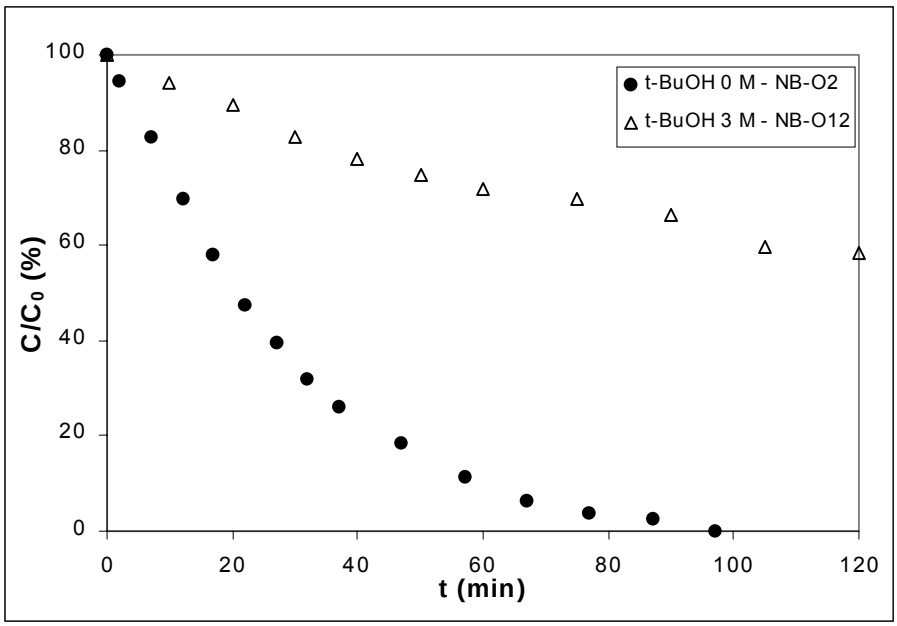

Graph 5.14. Effect of t-BuOH as radical scavenger on NB ozonation – Normalized concentration vs. time

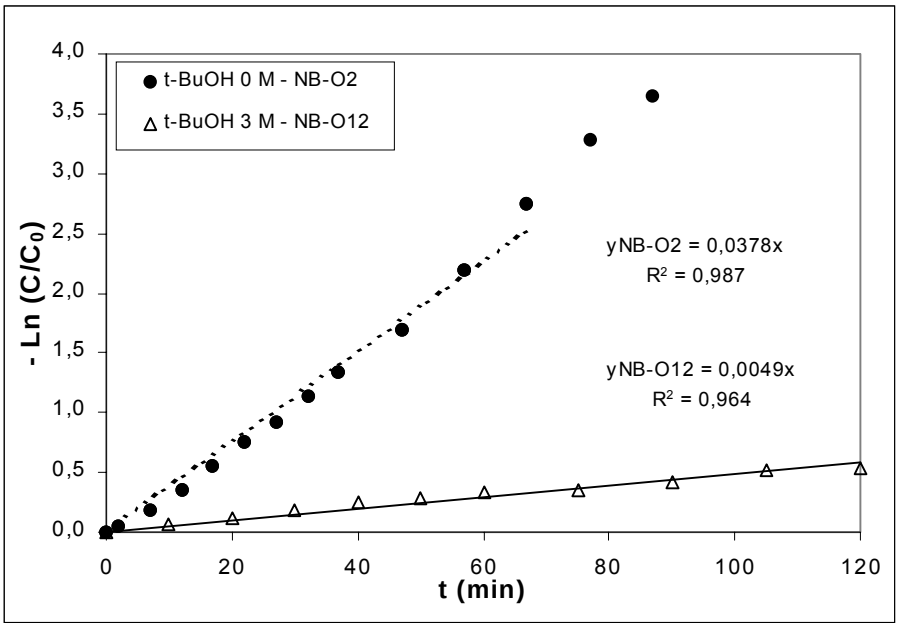

Graph 5.15. Effect of t-BuOH as radical scavenger on NB ozonation – Contribution of the OH radicals to the NB degradation

With regard to residual ozone, the addition of t-BuOH, as in the case in presence of carbonates, increases the amount of non-reacted ozone. That is, less amount of ozone is decomposed as the decomposition reaction of ozone due to hydroxyl radicals is blocked since these radicals will react preferentially with t-BuOH.

5.3.5. Biodegradability study

First of all, a BOD test was performed to a 100-ppm NB aqueous solution, determining that BOD_5 and BOD_{21} were 0. That is, the substrate was found to be non-biodegradable under the tested conditions. Besides this, an inhibition test was carried out. The inhibition of oxygen consumption by activated sludge was held by means of a dissolved oxygen detector and general guidelines are given in ISO 8192-1986. Inhibition test allows a rapid indication of the toxicity of water medium for non-acclimated biomass population. In this test, five solutions were prepared. In addition to the blank solution (without substrate) to assure that activated sludge is active, three solutions of different substrate concentration were prepared, by mixing the tested substrate with synthetic medium (peptone, urea and yeast extract) and the activated sludge (tested dilutions were 1:1000, 1:100 and 1:10). The fifth solution, with substrate and synthetic medium (without biomass), shows the physico-chemical consumption, to assure that oxygen is only

consumed by biomass and it is not consumed by any other reaction or dilution effect. The response of the sludge within three hours was followed by the decrease of the dissolved oxygen concentration in each sample. Graph 5.16 presents the results of the inhibition test carried out with NB. As it can be observed, even at 1:1000 dilution (0.1 ppm, $8.13x10^{-4}$ mmol.L^{-1}) the biological oxidation is greatly inhibited by the presence of NB. The inhibitor feature of NB was also stated in the literature under anaerobic conditions (Kameya et al., 1995). In light of these results, a 100-ppm NB solution cannot be easily degraded biologically and exhibits a high inhibition of other carbon sources.

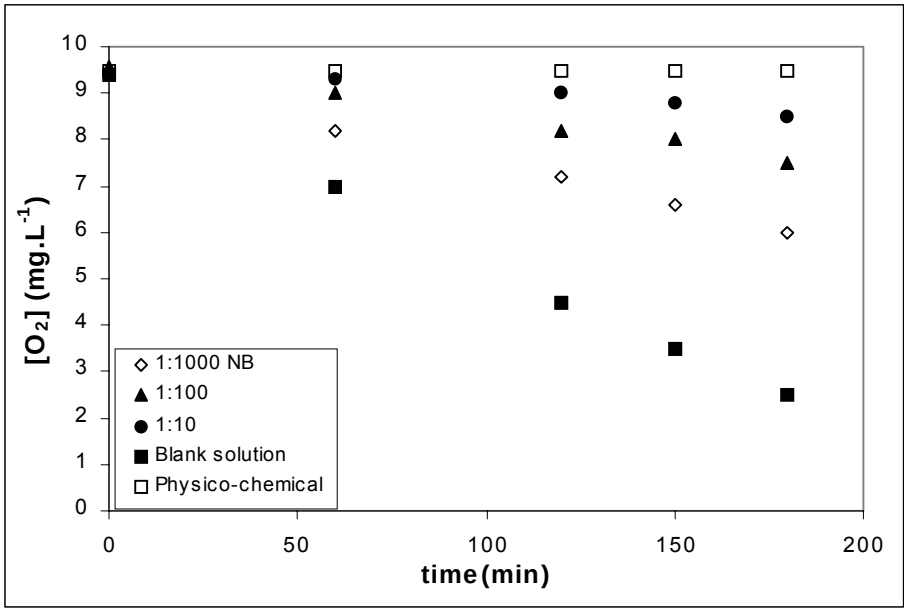

Graph 5.16. Inhibition test with a 100-ppm NB solution at dilutions 1:1000, 1:100 and 1:10.

The aim of this section was to study the effect of ozonation on the biodegradability of aqueous NB solutions. Two experiments with ca. 100 ppm NB concentration, 7.4 g.h^{-1} ozone production, free pH and room temperature have been performed. Results are presented in section A1.2, Tables NB-O13 and NB-O14. The average of these experiments is summarized in Table NB-O15 and these results are those presented in the following graphs .

The biodegradability of the solution has been tested throughout the experiment. BOD/COD and BOD/TOC ratios have been chosen as biodegradability indicators, as commented before. An increase in the BOD of a sample due to the pretreatment would indicates its greater amenability to biodegradation. Thus, an increase in the BOD/COD and BOD/TOC ratios after pretreatment is indicative of improved biodegradability due to an increase in the proportion of COD or TOC amenable to biological mineralization.

BOD has been measured at 5 and 10 days. Values obtained are plotted versus the ozone dose in Graph 5.17. As it can be noted, highest values of BOD have been obtained when the concentration of NB was reduced to less than 20% of the initial amount (after 60 minutes of treatment). The reason of this behavior will be discussed afterwards.

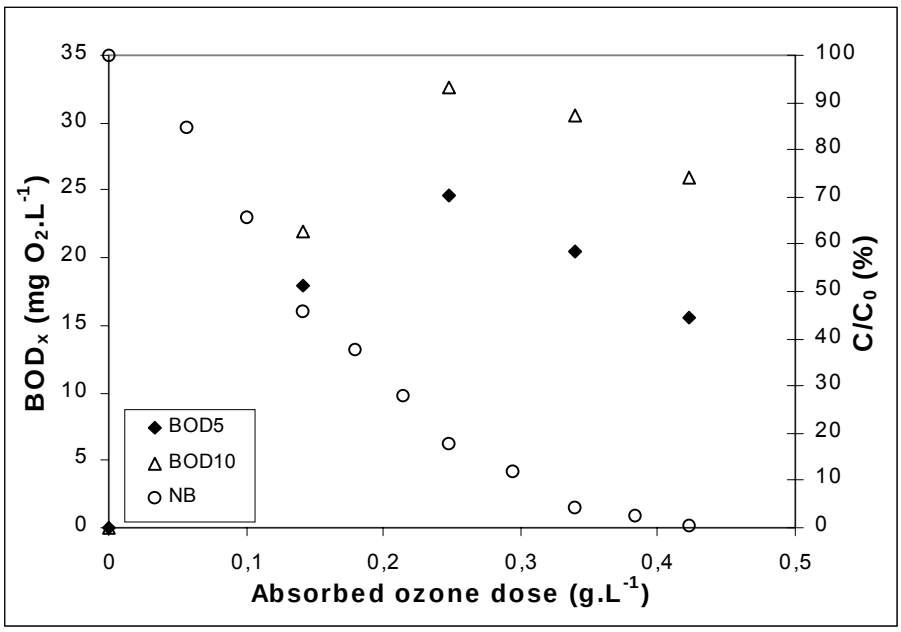

Graph 5.17. Evolution f BOD and NB normalized concentration with the absorbed ozone dose on NB ozonation

BOD_x/COD ratios and COD are shown on Graph 5.18. As it can be observed, BOD/COD ratio increases with the absorbed ozone dose but seems to be stabilized after 90 minutes of treatment (0.34 $g.L^{-1}$ ozone dose) at a value of ca. 0.3 and 0.5 for BOD_5/COD and BOD_{10}/COD, respectively. With regard to BOD_X/TOC ratios (Graph 5.19), it is increased up to ca. 0.5 for BOD_5/TOC after 60 minutes of treatment (0.25 $g.L^{-1}$ ozone dose) and ca. 0.8 for BOD_{10}/TOC at 120 minutes of treatment (0.42 $g.L^{-1}$ ozone dose). As a reference, a BOD/COD ratio of 0.4 is generally considered the cut-off point between biodegradable and difficult to biodegrade waste. Domestic waste water typically has a BOD_5/COD ratio of between 0.4 to 0.8 and BOD_5/TOC ratio between 1 to 1.6 and it is considered substantially biodegradable (Metcalf and Eddy, 1985). In light of the experimental results, optimal ozonation time was set at between 60-90 minutes.

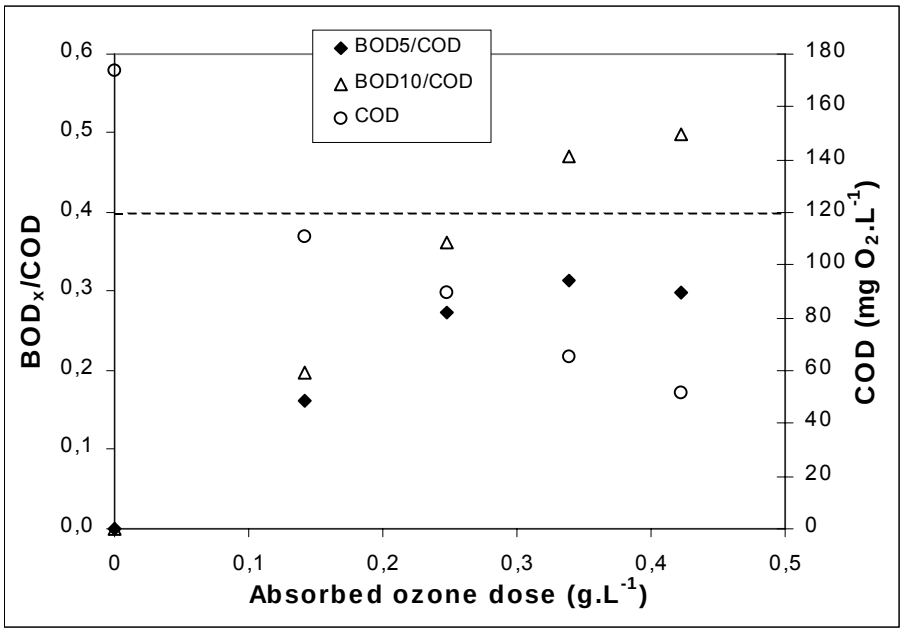

Graph 5.18. Evolution of BOD_x/COD and COD with the absorbed ozone dose on NB ozonation

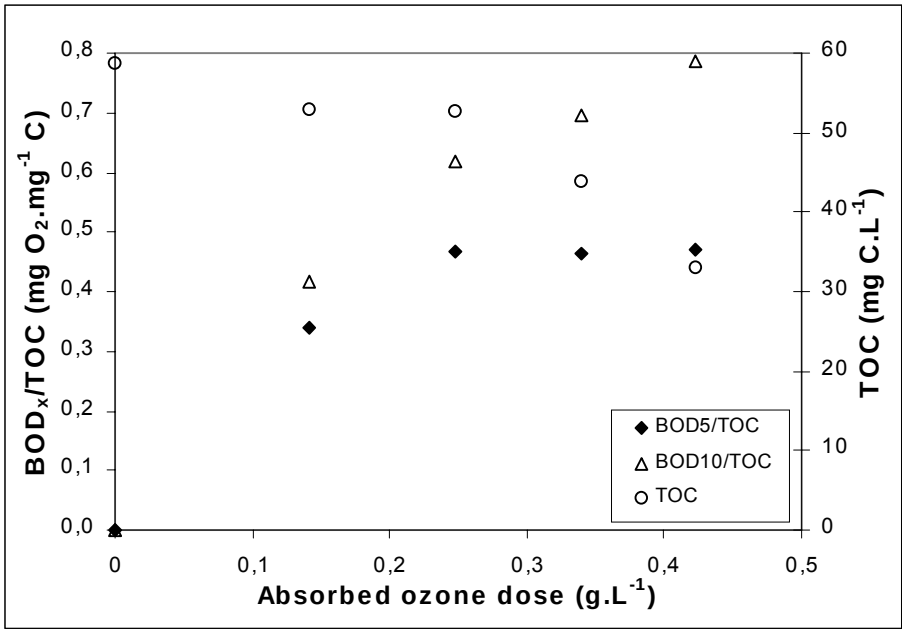

Graph 5.19. Evolution of BOD_x/TOC and TOC with the absorbed ozone dose on NB ozonation

In Figures 5.1 and 5.2 the chromatograms corresponding to the samples of the experiment NB-O15 after 30 and 60 minutes, respectively, are presented. As it can be observed, no significant differences with regard to the intermediates present are found. The three isomers of nitrophenol and 4-nitrocatecol have been detected (see section 5.10)

besides other compounds (the resolution of these chromatograms does not allow to see the peaks of the other present compounds), among which catechol is thought to be present. After 60 minutes, the concentration of the three nitrophenols have slightly decreased and they went on decreasing with time. Both NB and nitrophenols have been reported to be non-biodegradable (Urano and Kato, 1986). For nitrophenols, a BOD_5/TOC ratio of 0.05 have been reported (Takahashi et al., 1994). In that work, maximum biodegradability was achieved when nitrophenols were completely depleted from solution by means of ozonation. This fact support the idea that by-products formed at initial time (mainly nitrophenols) are not easily biodegradable, requiring further oxidation to achieve products of higher biodegradability, by which time most of the target compound has been eliminated. Besides this, the inhibition exerted by remaining NB may prevent the biodegradation of oxidation by-products. The denitrogenation has also been pointed out as a possible factor to enhance biodegradability (Takahashi et al., 1994).

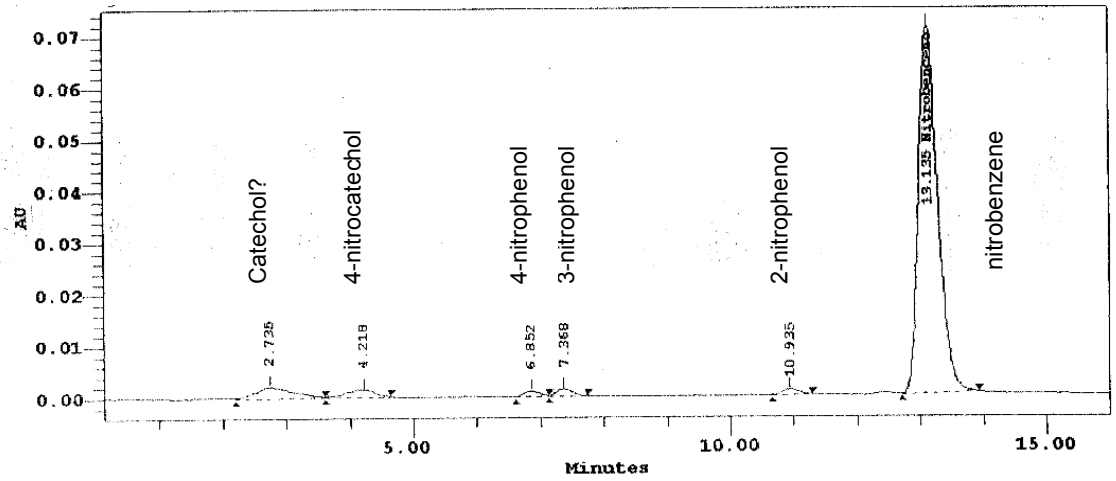

Figure 5.1. Chromatogram corresponding to sample after 30 minutes of ozonation of experiment NB-O15

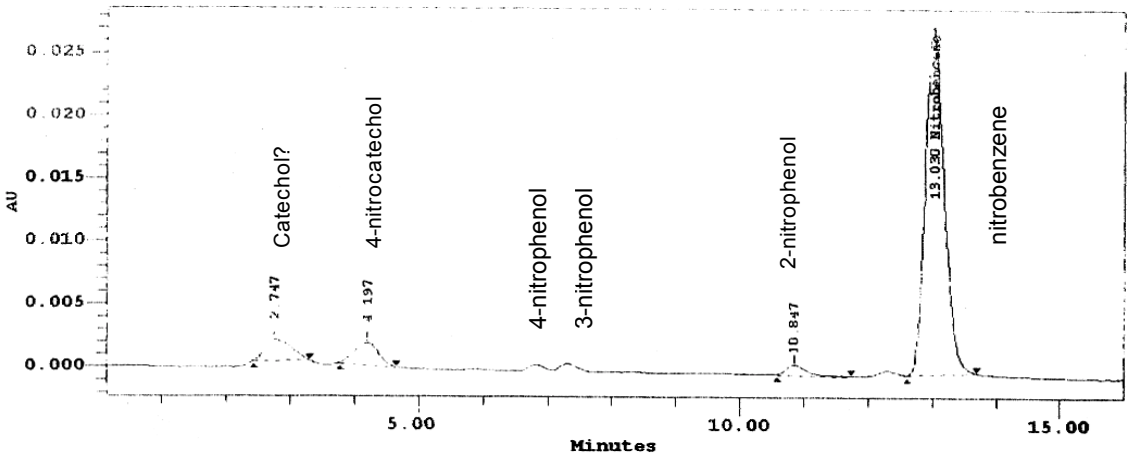

Figure 5.2. Chromatogram corresponding to sample after 60 minutes of ozonation of experiment NB-O15

Changes of the mean oxidation state of the organic carbon during the ozonation process are also presented in Graph 5.20. Oxidation state of the organic carbon can be calculated from the formula (Stumm and Morgan, 1991):

$$\text{AOS} = \text{Average Oxidation State} = \frac{4(\text{TOC} - \text{COD})}{\text{TOC}} \qquad [5.7]$$

where TOC is in mol $C.L^{-1}$ and COD in mol $O_2.L^{-1}$. Mean oxidation stages of organic carbons of several organic compounds were listed in Stumm and Morgan (1991). CH_4 is –4, benzene is –1, formaldehyde and acetic acid are 0, formic acid is +2, oxalic acid is +3 and CO_2 +4. Two stages may be found in the ozonation process. The first one (values below 0) is short, meaning that NB reacts rather rapid with ozone and forms hydroxylated aromatics, aldehydes and unsaturated carboxylic acids. In stage 2 (below 2), almost all the aromatic compounds, aldehydes and unsaturated carboxylic acids are converted to saturated carboxylic acids, such as formic acid and oxalic acid.

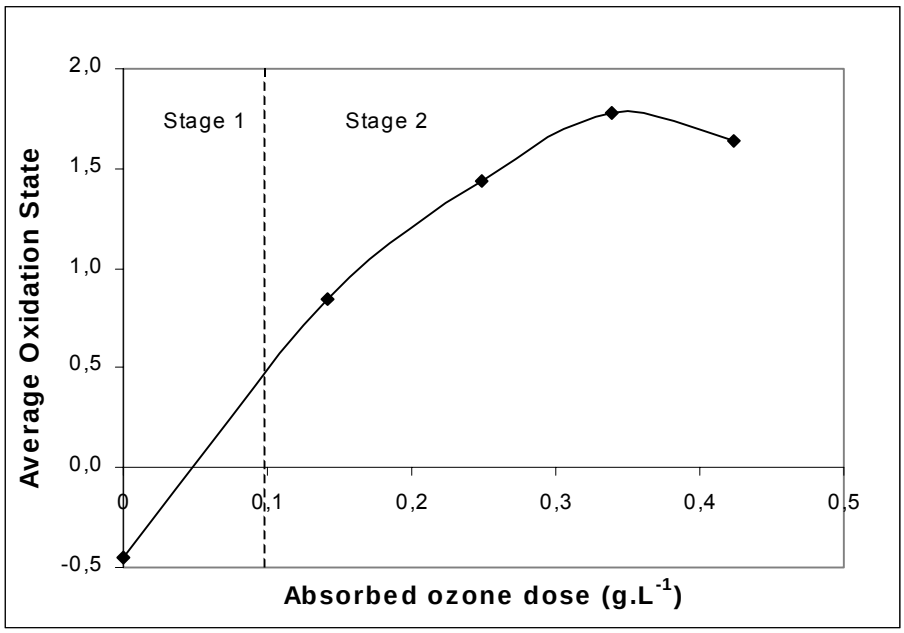

Graph 5.20. Effect of ozone dose on the average oxidation state in NB ozonation

The concentration of nitrate ion has been followed throughout the experiment. After two hours of treatment the denitration was complete while the concentration of nitrite ion in solution was completely negligible.

5.4. Ozonation combined with H_2O_2 (O_3/H_2O_2) for NB removal

5.4.1. Influence of H_2O_2 concentration

As it was mentioned in the introduction, the combination of ozone with hydrogen peroxide increases the production of hydroxyl radicals, being the global reaction

$$H_2O_2 + 2\ O_3 \rightarrow 2\ OH^{\bullet} + 3\ O_2 \qquad [1.11]$$

with the initiating step

$$HO_2^- + O_3 \rightarrow HO_2^{\bullet} + O_3^{\bullet} \qquad [1.13]$$

Hence, it would be interesting to study this combination for the degradation of NB, especially as literature points out that the main pathway of degradation of this compound is the radical one. With this aim, the following set of experiments, at room temperature and allowing pH to evolve freely were carried out.

Previously and to check the effect of hydrogen peroxide as oxidant, one experiment dosifying H_2O_2, in absence of ozone, was performed. Results are shown in section A1.3, Table NB-P. The percentage of NB removal obtained after two hours of treatment was negligible, as it can be observed in Graph 5.2. Therefore, its oxidant action will be discarded under the present working conditions. Next, two set of experiments were carried out: one dosifying the amount of hydrogen peroxide with respect to the amount of fed ozone (see section A1.3, Tables NB-OP1 to NB-OP3), and one adding it at the beginning of the experiment with respect to the amount of initial NB (see section A1.3, Tables NB-OP4 and NB-OP5). Results are compared with the experiment of single ozonation carried out in the same conditions (NB-O2a) in Graph 5.21.

As commented in the introduction chapter, diverse authors have studied the optimum H_2O_2/O_3 ratio to achieve a higher degradation rate. With different compounds it has been found a Gauss-type relation, increasing the compound removal rate as the amount of hydrogen peroxide is increased until one point, from which the reaction is inhibited, as the excess of hydrogen peroxide consumes hydroxyl radicals:

$$H_2O_2 + OH^{\bullet} \rightarrow HO_2^{\bullet} + H_2O \qquad [1.3]$$

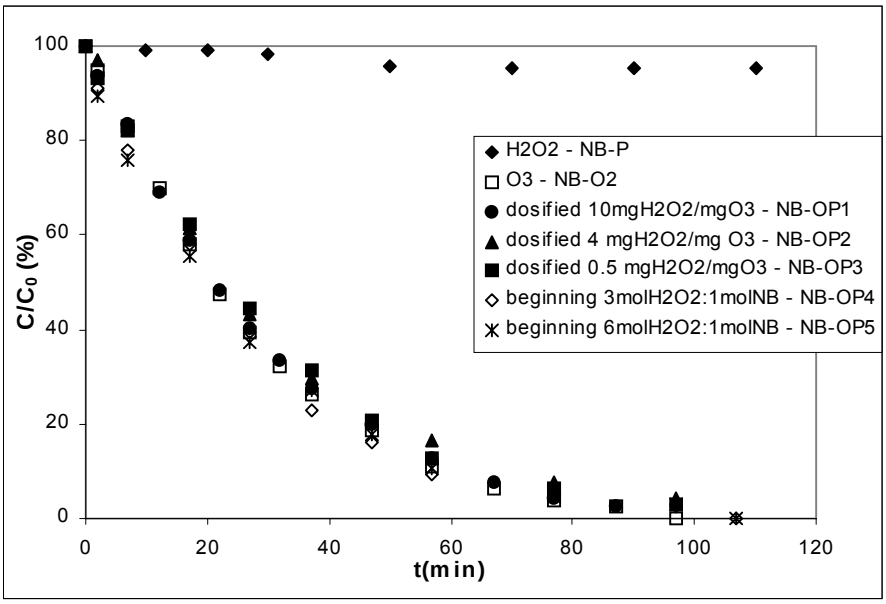

Graph 5.21. Influence of the addition of H_2O_2 to NB ozonation – Normalized concentration

For some of the studied compounds found in the literature, this optimum ratio has been found to be 0.4 mg H_2O_2/mg O_3 for trihalomethanes (Bauman and Stenstrom, 1990) and 0.5 mg H_2O_2/mg O_3 for triazines (Paillard et al., 1988). This is the reason why the ratio 0.5 mg H_2O_2/mg O_3 was checked in the experiment NB-OP3, as beforehand higher ratios were tested (NB-OP1 and NB-OP2). In the three experiments it was seen that the removal rate obtained by single ozonation was unaffected by the addition of hydrogen peroxide, even lightly inhibited. Then, hydrogen peroxide was added at the beginning of the experiment with respect to the initial amount of NB, at ratios 3:1 and 6:1 mol H_2O_2/mol NB. In this case the effect was negligible as well. At first sight these results are surprising, as it was expected that an increase in the hydroxyl radical production would be translated into an improve of the removal rate, since the process of oxidation develops through radical reactions. Nonetheless, this negligible effect of the addition of hydrogen peroxide to ozonation was already observed by Beltran et al. (1994) in the degradation of mecoprop by means of this combination.

Beltrán et al. (1998) points out that [1.13] would not be the main step to initiate the formation of hydroxyl radical but other unidentified reactions that would probably develop during single ozonation as well. Thus, byproducts of oxidation like nitrophenols, which have been identified in this oxidation system (see section 5.10) and are extremely reactive with ozone and hydroxyl radicals, could induce the formation of organic peroxide radicals. These steps would probably generate hydroxyl or other active radicals in such a way that classical initiation steps like reaction [1.13] would be less important. Therefore, no

difference between single and combined ozonation with hydrogen peroxide at low H_2O_2 concentrations would be observed.

With regard to the concentration of ozone in the residual gas (see Graph 5.22), it can be observed that the amount of residual ozone increases with the amount of H_2O_2, although values are lower that those obtained by single ozonation.

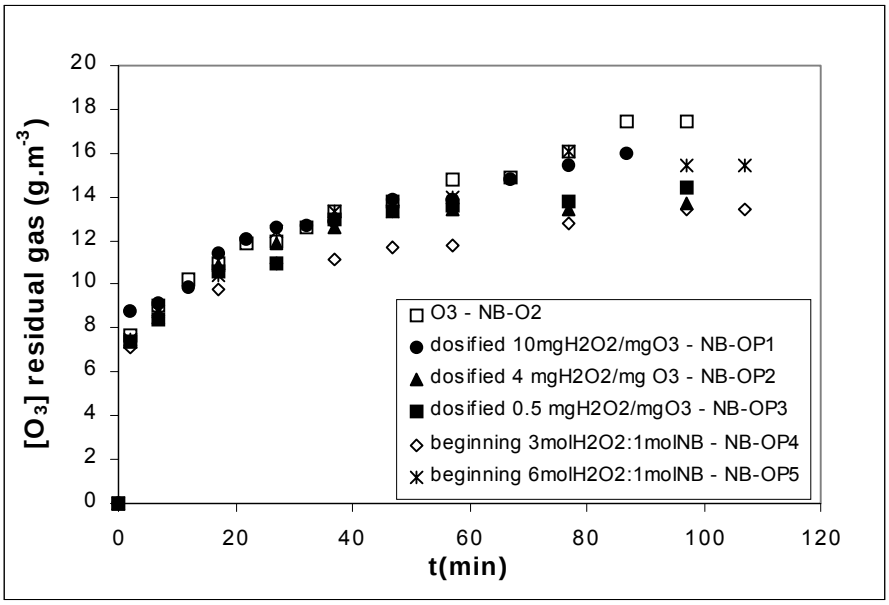

Graph 5.22. Influence of the addition of H_2O_2 to NB ozonation – Residual ozone

5.4.2. Biodegradability study

One experiment with 0.1 mol H_2O_2/mol NB (0.08 mmol.L^{-1} H_2O_2 for 100 ppm NB), 7.4 g.h^{-1} ozone production, free pH and room temperature has been carried out (see section A1.3, Table NB-OP6). A low concentration of hydrogen peroxide has been used as higher concentrations could be harmful for the biomass (Baldry (1983) reported that H_2O_2 is bactericide at concentrations above 0.15 mmol.L^{-1} , 5.1 mg.L^{-1}). Although the addition of H_2O_2 to single ozonation did not improve the removal rate of NB, it is desirable to check its effect on the biodegradability of these solutions.

BOD has been measured at 5 and 10 days and values obtained are plotted versus time in Graph 5.23. After 60 minutes of treatment over 30% of the initial amount of NB was still in the solution but BOD_5 value increased until 24 mg O_2.L^{-1}, similar to single ozonation. From this point BOD values do not decrease but seem to stabilize or even slightly increase at values of ca. 25 and 29 for BOD_5 and BOD_{10}, respectively. BOD/COD values are slightly lower than those obtained by single ozonation (see Graph 5.24).

BOD_5/COD ratio is increased from 0 to 0.20 after 60 minutes and to 0.28 after 90 minutes of treatment.

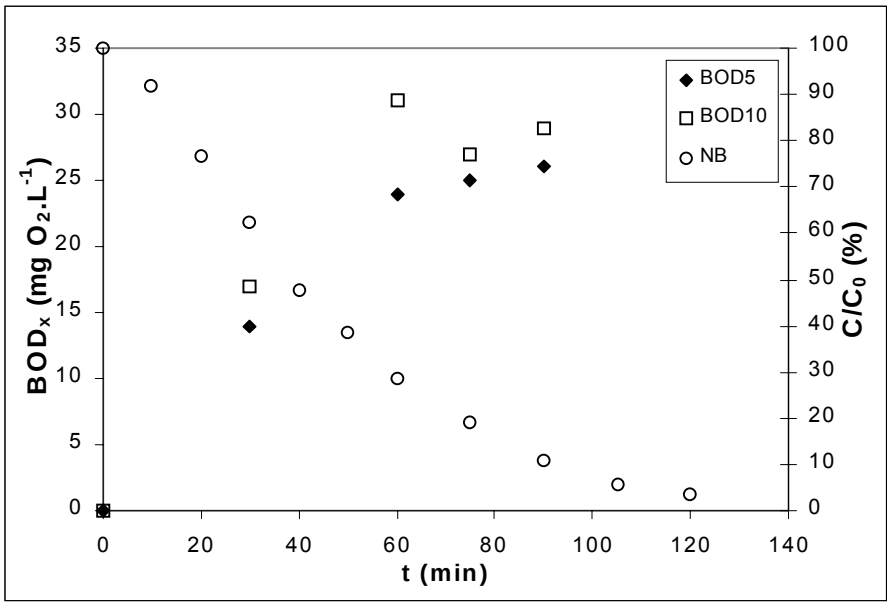

Graph 5.23. Evolution of BOD and NB normalized concentration during time with the combination O_3/H_2O_2

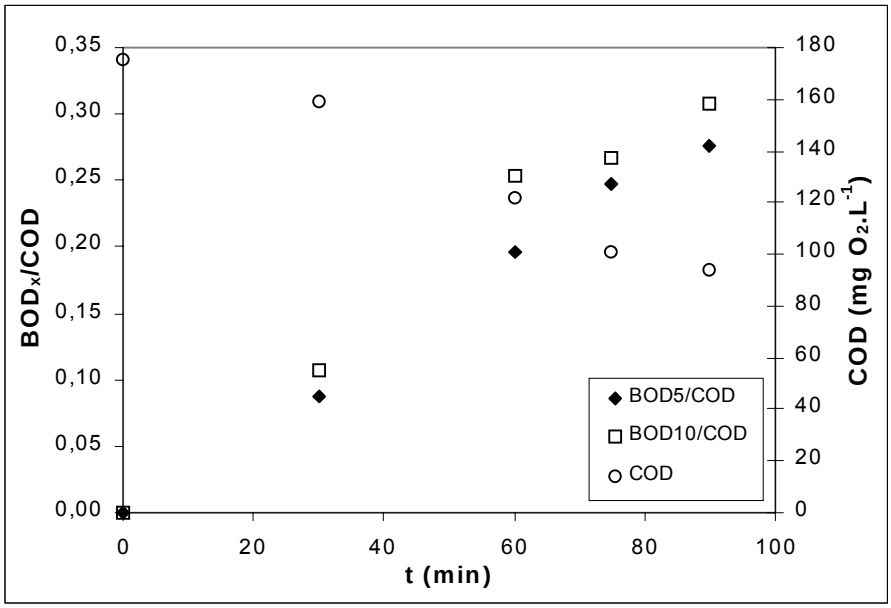

Graph 5.24. Evolution of BOD/COD ratio and COD during time with the combination O_3/H_2O_2

Regarding BOD_5/TOC ratio (see Graph 5.25), it is increased up to 0.46 after 60 minutes of treatment, similar to the value achieved by single ozonation and 0.55 after 90

minutes, slightly higher than single ozonation. BOD_{10}/TOC is increased up to 0.6 after 60 minutes and seem to stabilize afterwards.

In light of the experimental results, the addition of H_2O_2 did not improve the effect on the biodegradability of NB aqueous solutions achieved by single ozonation.

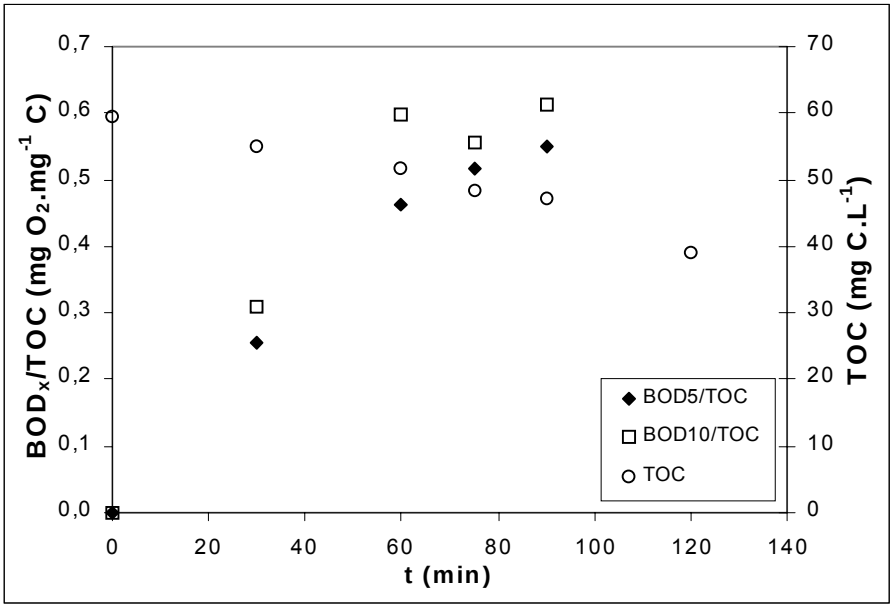

Graph 5.25. Evolution of BOD/TOC ratio and TOC during time with the combination O_3/H_2O_2

5.5. Ozonation combined with Fe(III) (O_3/Fe(III)) for NB removal

A set of experiments with the combination O_3/Fe(III) previous to the experimentation with the combination O_3/UV/Fe(III) (see section 5.8). Fe(III) salt used was $FeCl_3$ and Fe(III) was added at the beginning of the experiment with respect to the amount of initial NB, ranging from 1 to 0.01 mol Fe(III)/mol NB, at 7.4 $g.h^{-1}$ ozone production, room temperature and pH was allowed to evolve freely. Results obtained are presented in section A1.4, Tables NB-OF1 to NB-OF4. Disappearance rate is presented in Graph 5.26 and compared with the experiment of single ozonation carried out with the same conditions (NB-O2).

It can be seen that the effect of the addition of ferric ion to single ozonation is negligible or even negative. At high ratios (1:1, 0.5:1) the disappearance rate is significantly inhibited by the addition of iron. At low ratios (0.1:1 and 0.01:1), curves superpose with the results of single ozonation.

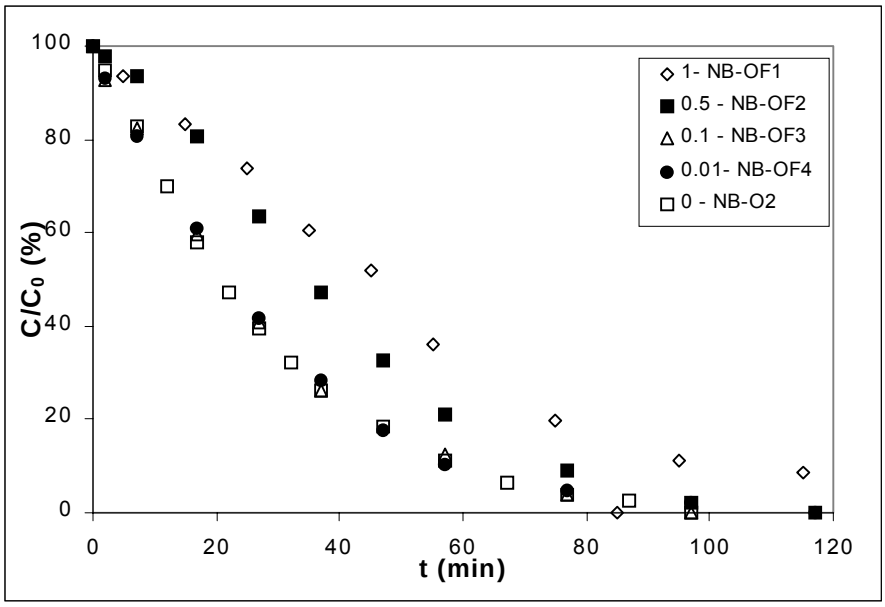

Graph 5.26. Influence of the addition of Fe(III) to the ozonation of NB – Normalized concentration

With regard to the concentration of ozone in the residual gas (see Graph 5.27), the addition of Fe(III) decreases significantly this amount, more as higher is the concentration of Fe(III). If Fe(III) is being converted to Fe(II) within the process, ozone would be being used to oxidized Fe(III) into Fe(II), decreasing the amount of ozone available for NB, fact that would also explain the behavior observed in Graph 5.27. At high Fe(III) ratios, ozone is preferably being used in the oxidation of Fe(III) in detriment of the oxidation of the target compound.

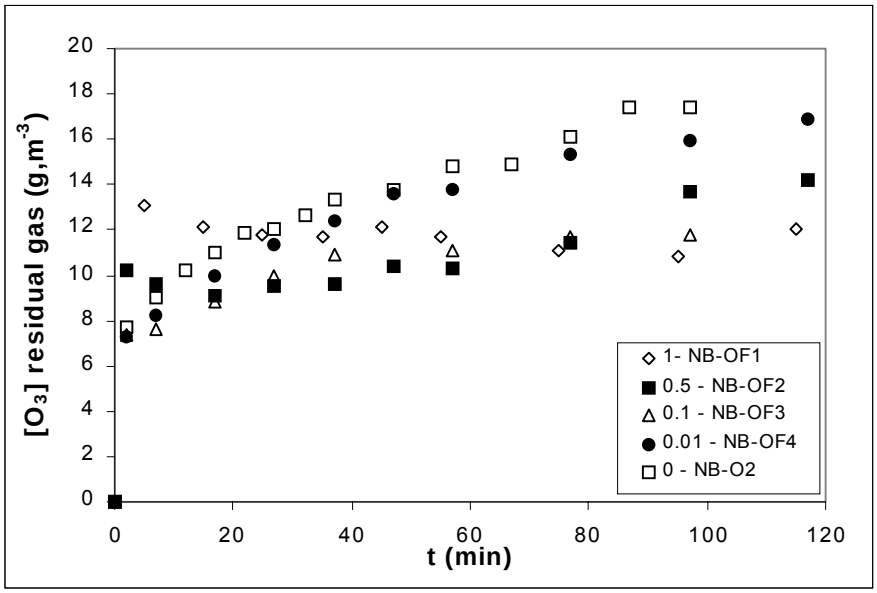

Graph 5.27. Influence of the addition of Fe(III) to the ozonation of NB – Residual ozone

5.6. Ozonation combined with UV radiation (O_3/UV) for NB removal

As with the combination O_3/H_2O_2, the process O_3/UV increases the production of hydroxyl radicals and possible ways to eliminate the pollutant. Basically, aqueous systems saturated with ozone are irradiated with UV light at a wavelength of 254 nm in a reactor convenient for such heterogeneous media. The extinction coefficient of O_3 at 254 nm is 3600 $M^{-1}.cm^{-1}$, much higher than that of H_2O_2. Besides the reactions of the ozonation process, the direct photolysis of NB and ozone and those derived from the presence of hydrogen peroxide are present. The mechanism that has been proposed for this system implies the photolytic rupture of one molecule of ozone to generate two hydroxyl radicals, but they do not act, as they recombine to produce H_2O_2 [1.7], by Peyton and Glaze (1988):

$$O_3 + H_2O \xrightarrow{h\nu < 310nm} 2\ OH^{\bullet} + O_2 \qquad [1.14]$$

$$2\ OH^{\bullet} \rightarrow H_2O_2 \qquad [1.7]$$

H_2O_2 photolizes and reacts with ozone. Both stages lead to the formation of hydroxyl radicals, being this reaction favored by the pH. Moreover, ozone reacts with the ionic form of H_2O_2 (hydroperoxide ion). Thus, it would be interesting to study the effect of the pH on this combination. Furthermore, it has been checked the use of UVA radiation (which emits in the range of wavelength of between 300 and 420 nm, with a maximum centered at 360 nm) with regard to the biodegradability of DCP solutions.

5.6.1. NB photolysis: Effect of pH

Given the aromatic nature of NB, it was studied firstly the effect of the direct photolysis on the removal of NB under the working conditions. Three experiments at pH 3, 9 and allowing pH to evolve freely were performed with UV radiation (without ozone). Results are shown in section A1.5, Tables NB-R1 to NB-R3. Previously, actinometric experiments were carried out to determine the flux of radiation emitted by the lamp and transmitted to the reactor (see section 5.1), where it was found that the flux of radiation that comes into the reactor was 23.7 $\mu Einstein.s^{-1}$ (1 Einstein = 1 mol photon).

Under these conditions, no degradation was observed after two hours of treatment at any of the studied pHs. That means that, under our working conditions, the contribution of the direct photolysis to the NB removal rate will be negligible. This fact does not mean that NB cannot be removed by means of UV radiation, but the low ratio of photons that go into the reactor and the amount of NB that goes through it may account for this. At initial

time this ratio was 0.37 mol photon/mol NB_0. In experiments carried out by the research group in another experimental device, where the ratio was 2.5 mol photon/mol NB_0, a 40% of NB removal was achieved after 60 minutes of treatment (Rodríguez et al., 2000). In that case the quantum yield (number of NB molecules that react by the number of absorbed photon) at 254 nm could be established and was found to be $(6 \pm 0.5).10^{-3}$ mol.Einstein^{-1}. This value is consistent with the one reported by Beltrán and co. (1998b), which was $(7 \pm 0.6).10^{-3}$ mol.Einstein^{-1}.

5.6.2. Combination of ozone with UV radiation: Effect of pH

One experiment with the combination O_3/UV, allowing pH to evolve freely, room temperature and 7.4 g.h^{-1} ozone production was performed (see section A1.5, Table NB-OR1 to be compared with the experiment of single ozonation (NB-O2) and direct photolysis (NB-R1) carried out at the same conditions. The NB removal rate during time for the three processes is shown in Graph 5.28.

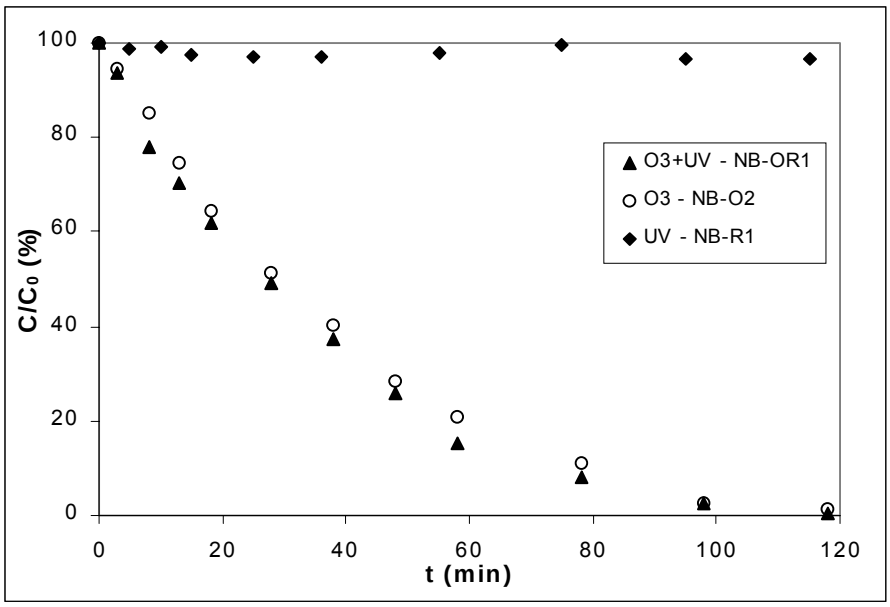

Graph 5.28. Comparison of the processes O_3, UV and O_3/UV for the removal of NB – Normalized concentration

It can be observed that the combination O_3/UV does not improve significantly the removal rate achieved by single ozonation. The ratio radiation/O_3 may justify this. At the working ozone production (7.4 g.h^{-1}) this ratio was 0.6 photon/O_3 molecule, i.e., we were working with low radiation with respect to the fed ozone. Nevertheless, when the concentration of ozone in the residual gas for the two processes is compared (see Graph 5.29), it can be seen that in the case of the O_3/UV system the concentration of residual

ozone is slightly lower. Therefore, there would be a higher decomposition of ozone into hydroxyl radicals by the ultraviolet radiation. However, this increase of the radical production is not translated into an enhancement of the NB removal rate.

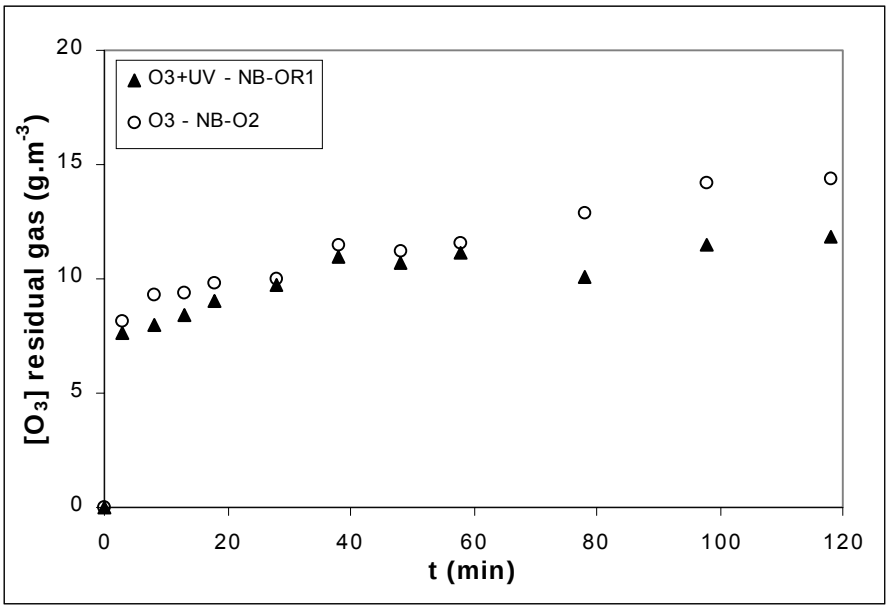

Graph 5.29. Comparison of the processes O_3 and O_3/UV for the removal of NB – Residual ozone

When increasing the ozone production, the removal rate of NB increases, as the partial pressure of ozone increases, i.e., increasing the driving force and hence the absorption rate. However, when plotting the normalized concentration of NB vs. the absorbed ozone dose instead of time (see Graph 5.30), it can be observed that both curves showed the same behavior. As with single ozonation, chemical reaction may be controlling the process. Being the dose of absorbed ozone the same for both ozone productions, the concentration of ozone in the residual gas increases, as a higher amount of non-reacted ozone is leaving the system (Graph 5.31).

To check the effect of pH in this combination, three experiments in the range 3-9 were performed to test the effect of pH in the photolytic ozonation of aqueous solutions of NB. One experiment was allowed the pH to evolve freely (NB-OR1), one was set at pH 3 acidified with H_3PO_4 (NB-OR2) and one at pH 9 buffered with borax (0.01 M $Na_2B_4O_7$, NB-OR3). The ozone production was set at 7.4 $g.h^{-1}$ and temperature was 25ºC. Graph 5.32 presents the comparison of the normalized concentration during time for the three experiments. As it was already observed in the case of single ozonation, the removal rate of NB seems to be inhibited at basic pH. The same behavior was observed when working

with higher ozone production (11.1 $g.h^{-1}$, see section A1.5 Tables NB-OR4 to NB-OR6), with smaller differences between acidic and free pH (results not shown). As it has been already commented, the production of hydroxyl radicals is favored by increasing pH. The observed behavior seems to confirm the fact mentioned in the case of single ozonation, about other initiation reactions besides the basic initiation stages that can compensate the expected differences in the removal rate of NB when increasing the pH of the medium.

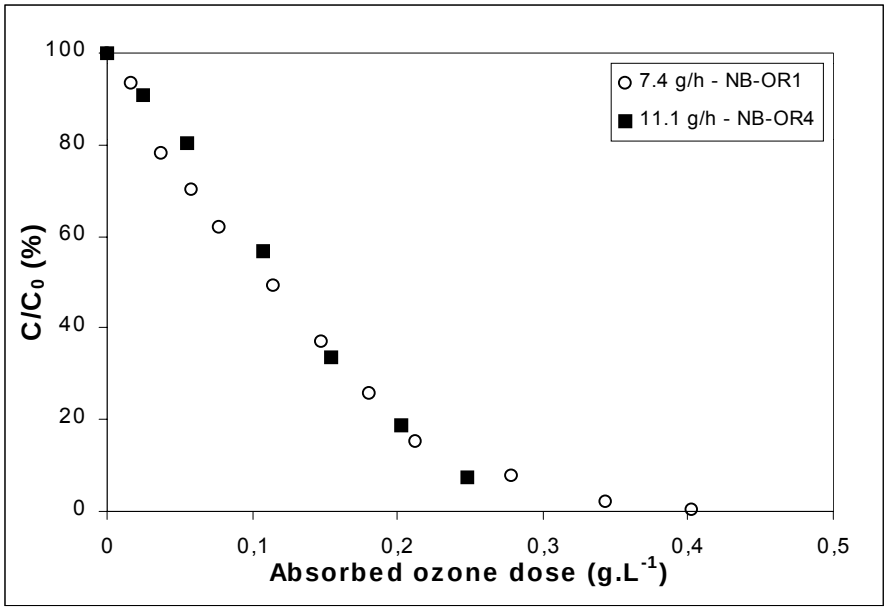

Graph 5.30. Effect of the ozone production in the removal of NB by means of the system O_3/UV – Normalized concentration

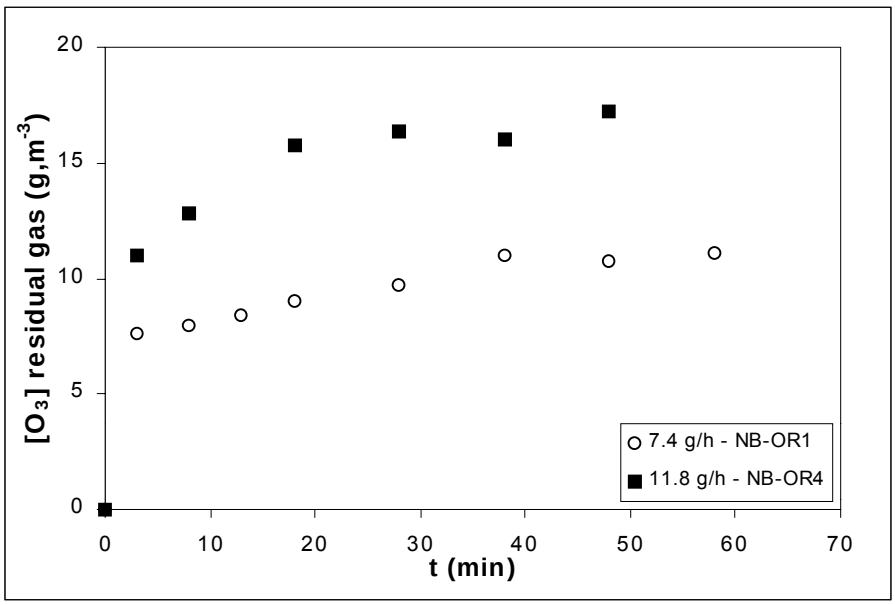

Graph 5.31. Effect of the ozone production in the removal of NB by means of the system O_3/UV – Residual ozone

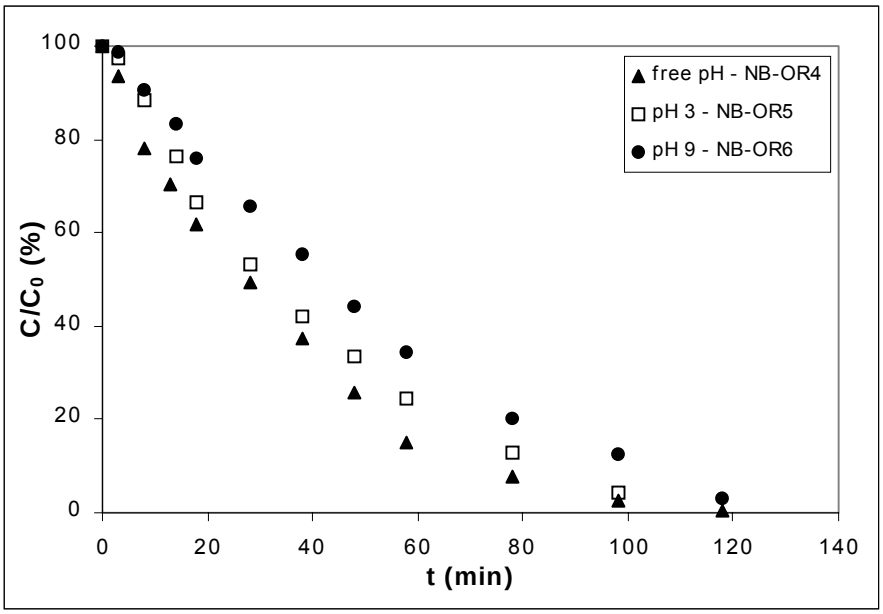

Graph 5.32. Effect of the pH in the removal of NB by means of the system O_3/UV – Normalized concentration

Nevertheless, when the concentration of ozone in the residual gas is plotted (see Graph 5.33, for an ozone production of 11.1 $g.h^{-1}$), it can be seen that the concentration of residual ozone decreases when the pH is increased, meaning that a higher amount of ozone is being decomposed into hydroxyl radicals. However, an enhancement in the removal rate is not observed. This fact may suggest that the radical pathway is not the main contribution to the removal of NB in the O_3/UV system, contrary to what stated in the literature, under the tested conditions.

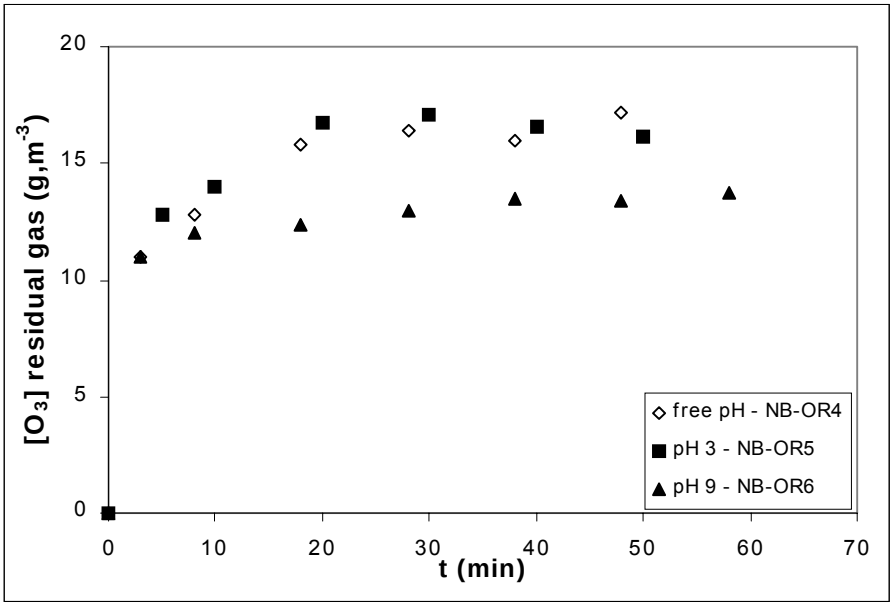

Graph 5.33. Effect of the pH in the removal of NB by means of the system O_3/UV – Residual ozone

5.6.3. The use of UVA – Biodegradability study

In this case UVA light, which emits in the range of wavelength of between 300 and 420 nm, with a maximum centered at 360 nm, was used instead of UV light to compare afterwards with the experiments with O_3/UVA/Fe. In this case, the homolysis of O_3 would be greatly reduced, as it is supposed to occur at wavelengths below 310 nm (see equation 1.14). Then, direct reaction of ozone with H_2O_2 produced is the main source of hydroxyl radicals [1.11]. But on the other hand and as it can be seen in the absorption spectrum of NB (see section 4, Figure 4.7), NB shows the capacity to absorb at higher wavelengths ranges up to ca. 400 nm. In fact, in a work carried out by our research group it was observed that wavelengths higher than 250 nm and up to 400 nm contributed in a notable manner to the degradation of NB solutions (Rodríguez et al., 2002a).

Two experiments with the combination O_3/UVA, at 7.4 $g.h^{-1}$ ozone production, room temperature and allowing pH to evolve freely were carried out and the average of both is presented (see section A1.5, Table NB-OR7). Firstly, it was desired to compare the efficiency of this combination in the removal of NB. Graph 5.34 presents the comparison of the processes O_3, O_3/UV and O_3/UVA with regard to the evolution of the normalized concentration of NB during time. As it can be seen, no difference was observed between the three processes. Nevertheless, the use of UVA instead of UV significantly improved the degree of mineralization (see Graph 5.48). The contribution of direct photolysis of NB by UVA light may account for this difference.

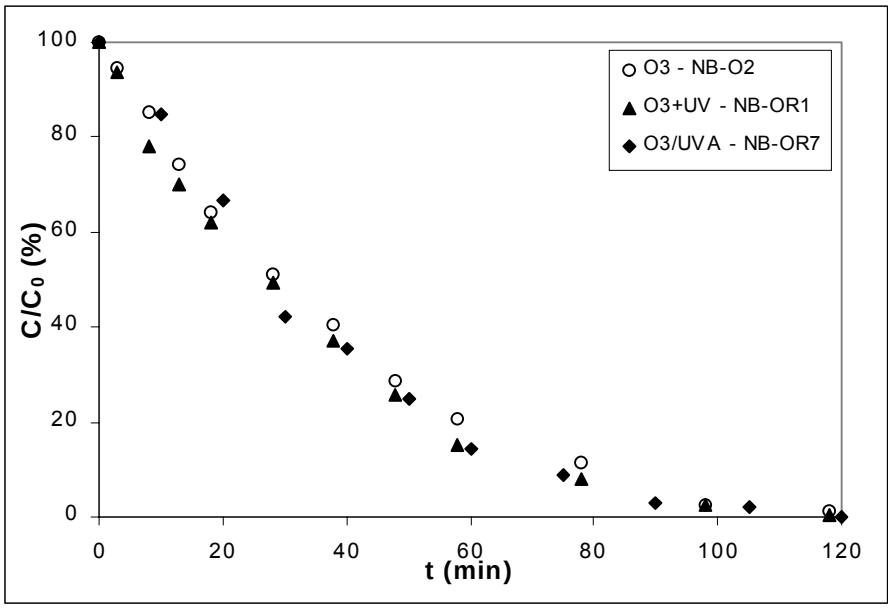

Graph 5.34. Comparison of the processes O_3, O_3/UV and O_3/UVA for the removal of NB – Normalized concentration

BOD was measured at 5 and 10 days for the process O_3/UVA and values obtained are plotted versus time in Graph 5.35. Values are considerably lower than those achieved by single ozonation. Higher values seem to be achieved between 60 and 90 minutes of treatment, when less than 15% of initial NB amount is still in solution. BOD_5 is expected to be a little bit higher and could be due to an experimental error within the BOD analysis. With regard to the intermediates present in solution, no significant differences have been observed with respect to the samples obtained by single ozonation. BOD/COD values are lower as well than those obtained by single ozonation (see Graph 5.36). BOD_5/COD ratio is increased from 0 to 0.21 after 90 minutes and BOD_{10}/COD up to 0.32 after 60 minutes of treatment. Regarding BOD_5/TOC ratio (see Graph 5.37), it is increased up to 0.43 after 90 minutes of treatment and BOD_{10}/TOC is increased up to 0.59 after 60 minutes. After 60 minutes, only 18% of TOC has been removed from the solution. These ratios are also smaller than those achieved by single ozonation. It has to be point out though that the addition of UVA to the ozonation enhanced the degree of mineralization of the NB solutions (see section 5.9, comparison of the different processes).

In light of the experimental results, the addition of UVA did not improve the effect on the biodegradability of NB aqueous solutions achieved by single ozonation.

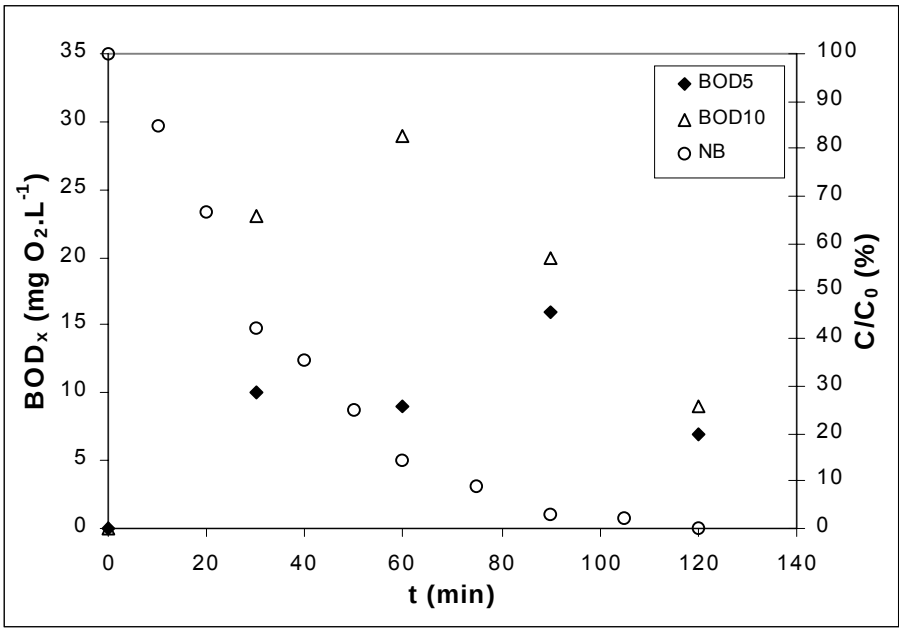

Graph 5.35. Evolution of BOD and NB normalized concentration during time with the combination O_3/UVA

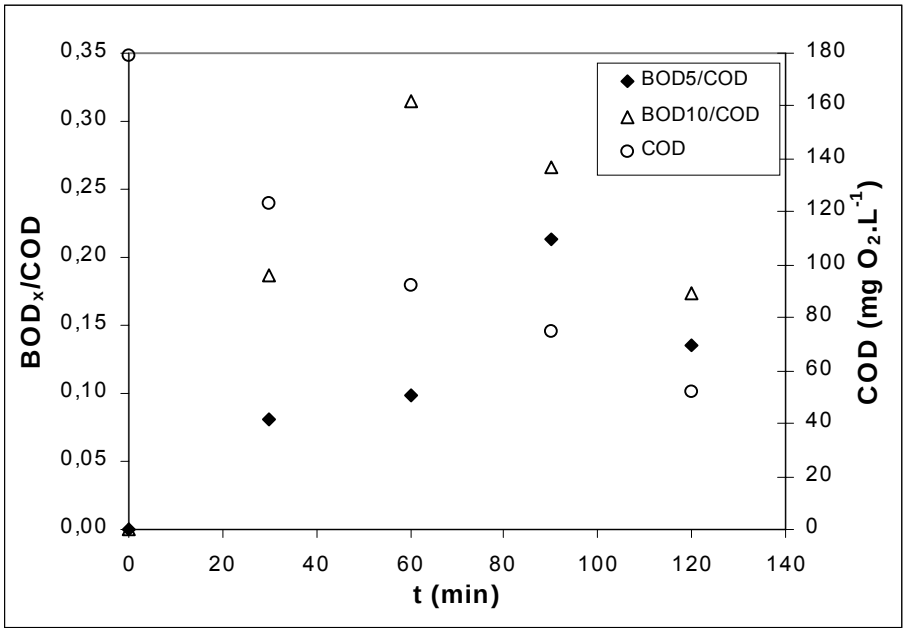

Graph 5.36. Evolution of BOD/COD ratio and COD during time with the combination O_3/UVA

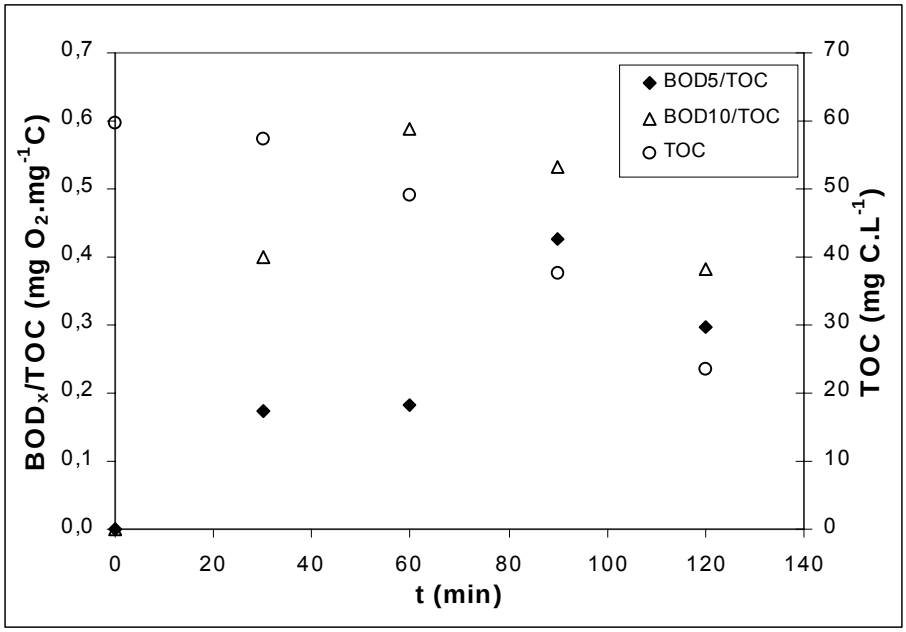

Graph 5.37. Evolution of BOD/TOC ratio and TOC during time with the combination O_3/UVA

5.7. NB removal by means of the combination O_3/UV/H_2O_2.

5.7.1. Influence of the H_2O_2 concentration

This is a very powerful method, which permits a fast and complete mineralization of pollutants. It is considered to be one of the most effective treatments for highly polluted effluents. It is the system that shows the highest number of possible pathways of degrading the target compound, as besides the possible initiating stage of the single ozonation, the contributions derived from the photolysis of ozone and hydrogen peroxide are also present.

The effect of the amount of hydrogen peroxide has been tested, by carrying out three experiments with this combination, at 7.4 $g.h^{-1}$ ozone production, room temperature and adding hydrogen peroxide at the beginning of the experiment, with respect to the initial amount of ozone. Tested ratios have been 1:1, 3:1 and 6:1 mol H_2O_2/mol NB and results are presented in section A1.6, Tables NB-ORP1 to NB-ORP3.

Graph 5.38 shows the effect of the amount of hydrogen peroxide added to the system in the removal rate of NB. It can be observed that within the range of H_2O_2 of study, at high and low amount of H_2O_2 the system seems to be slightly inhibited, while with the ratio 3:1 the removal rate of NB is equal to single ozonation. As it has already been commented, when using hydrogen peroxide it has been observed a Gauss-type relation, increasing the compound removal rate as the amount of hydrogen peroxide is increased until achieving one optimal point, from which the reaction is inhibited, as the excess of hydrogen peroxide consumes hydroxyl radicals. With the ratio 6:1 this point seems to have been exceed and the excess of hydrogen peroxide is scavenging the hydroxyl radicals. Furthermore, at the tested conditions, direct ozonation of NB seems to be the main mechanism of NB degradation. Thus, the consumption of ozone by H_2O_2 would have a negative effect in the removal rate of the substrate. In addition, the withdrawing character of the nitro group depletes the aromatic ring of electron density, holding up the attack by $OH^{\cdot}$ radicals.

With regard to the concentration of ozone in the residual gas (see Graph 5.39) no remarkable differences have been observed in the range of hydrogen peroxide concentrations tested.

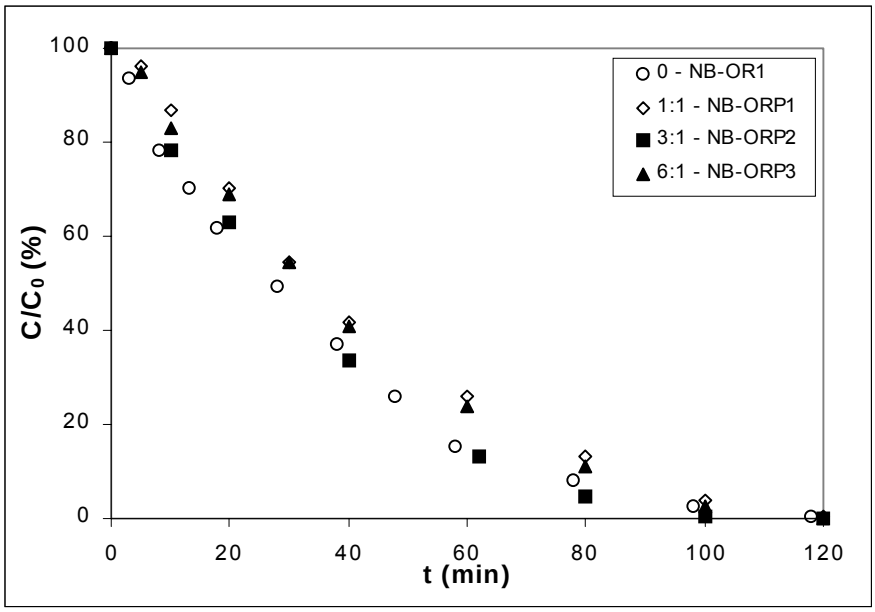

Graph 5.38. Influence of the amount of H_2O_2 in the NB removal by means of $O_3/UV/H_2O_2$ – Normalized concentration

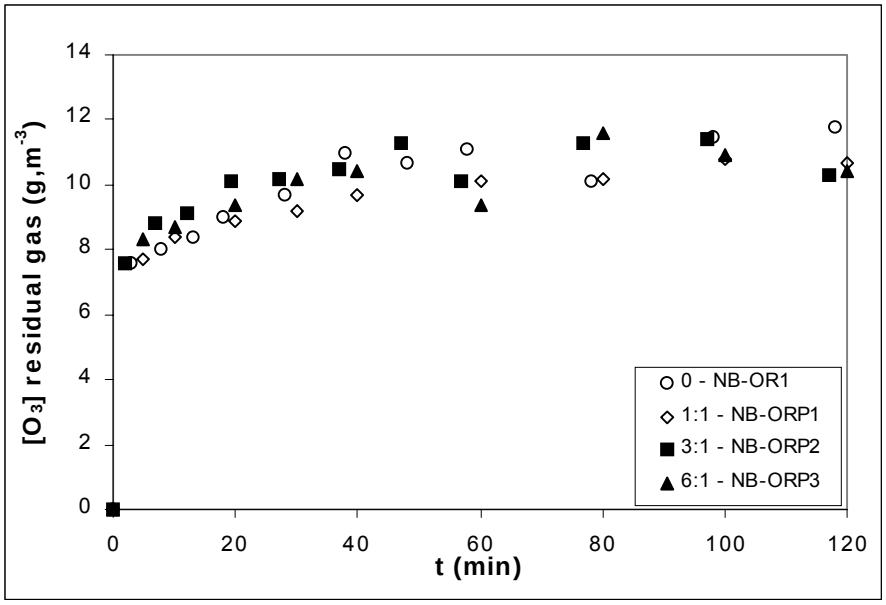

Graph 5.39. Influence of the amount of H_2O_2 in the NB removal by means of $O_3/UV/H_2O_2$ – Residual ozone

As for the decrease of the total organic carbon (TOC), the addition of H_2O_2 peroxide enhances the mineralization rate of NB achieved by the O_3/UV process. This improvement is favored by increasing the amount of hydrogen peroxide (see Graph 5.40). The improvement of TOC removal can be understood by the higher production of $OH^{\cdot}$

radicals, as the intermediates formed (e.g. nitrophenols) can react easier than nitrobenzene with hydroxyl radicals.

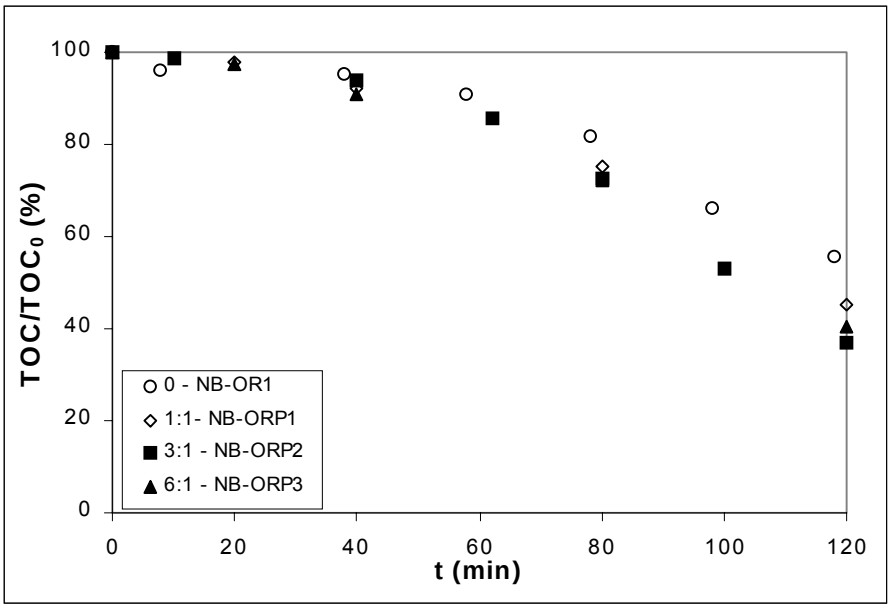

Graph 5.40. Influence of the amount of H_2O_2 in the NB removal by means of O_3/UV/H_2O_2 – Normalized TOC

5.7.2. Biodegradability study

Two experiments with 0.1 mol H_2O_2/mol NB (0.08 mmol.L^{-1} H_2O_2 for 100 ppm NB), 7.4 g.h^{-1} ozone production, free pH and room temperature were carried out and the average is presented (see section A1.6, Table NB-ORP4). The same concentration of hydrogen peroxide that in the combination O_3/H_2O_2 has been used. It is desirable to check the effect of this combination on the biodegradability of these solutions at low H_2O_2, compatible with a later biological process.

BOD has been measured at 5 and 10 days and values obtained are plotted versus time in Graph 5.41. After 60 minutes of treatment over 20% of the initial amount of NB was still in the solution and BOD_5 value increased until 19 mg O_2.L^{-1}, slightly lower than the value achieved by single ozonation. However, contrary to ozonation BOD_5 go on increasing up to 24 mg O_2.L^{-1} after 75 minutes, when ca. 12% of initial NB was in solution. BOD_{10} values are lightly higher than those achieved by single ozonation. Regarding the intermediates present, no significant differences have been observed with respect to single ozonation. The value of BOD_5/COD after 60 minutes of treatment (0.15, see Graph 5.42) is smaller than for single ozonation (0.27) but after 90 minutes results achieved by

both processes seem to be equal. BOD_5/COD ratio is increased from 0 to 0.27 after 75 minutes and to 0.32 after 90 minutes of treatment.

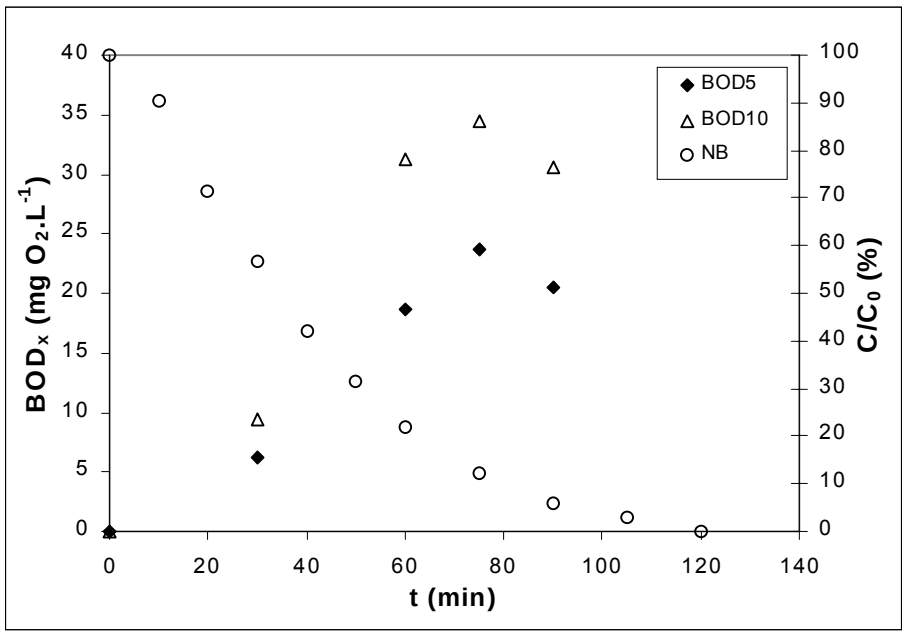

Graph 5.41. Evolution f BOD and NB normalized concentration during time with the combination O_3/UV/H_2O_2

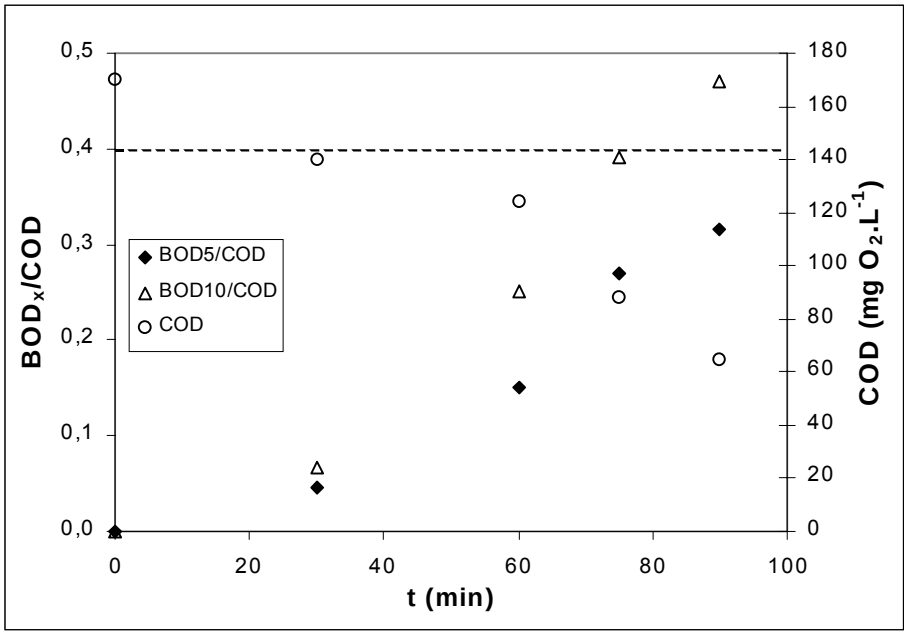

Graph 5.42. Evolution of BOD/COD ratio and COD during time with the combination O_3/UV/H_2O_2

Regarding BOD_5/TOC ratio (see Graph 5.43), it is increased up to 0.49 after 75 minutes of treatment, as attained by single ozonation. BOD_{10}/TOC are also similar to single ozonation and it is increased up to 0.6 after 60 minutes and 0.74 after 90 minutes.

In light of the experimental results, the addition of UV radiation H_2O_2 did not improve the effect on the biodegradability of NB aqueous solutions achieved by single ozonation.

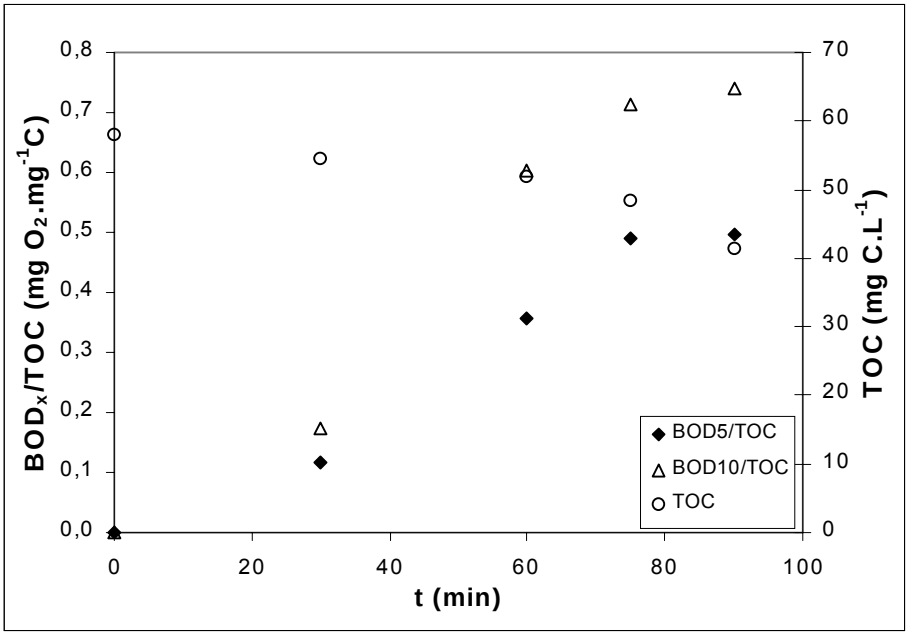

Graph 5.43. Evolution of BOD/TOC ratio and TOC during time with the combination O_3/UV/H_2O_2

5.8. NB removal by means of the combination O_3/UV/Fe(III)

In section 5.5 the effect of Fe(III) as a catalyst of single ozonation has been checked, and in previous works of the research group, the influence of Fe(III) in the NB photodegradation was studied (Rodríguez et al., 2000). In the first case the effect was found to be negligible or even inhibitory, while in the second case the combination of Fe(III) with UV radiation was found to be more effective than the application of UV radiation alone. The addition of iron ion (Fe^{3+} or Fe^{2+}) has been reported to accelerate the UV-enhanced ozonation of several pollutants (Ruppert et al., 1994; Abe and Tanaka, 1997, 1999). It was thought, then, that the combination of Fe(III) salts with the system O_3/UV could improve the results achieved by the latter.

5.8.1. Influence of Fe(III) concentration

To check the effect of this combination, three experiments with 7.4 $g.h^{-1}$ ozone production under UV irradiation were carried out by adding Fe(III) (as $FeCl_3$) at 3:1, 1:1 and 0.1:1 mol Fe(III)/mol NB_0 (2.44 to $8.1x10^{-3}$ $mmol.L^{-1}$ Fe(III)). The decrease in the pH of the solution by the addition of Fe(III) was not adjusted. Results are shown in section A1.7, Tables NB-ORF1 to NB-ORF3. The diminution of the normalized NB concentration is depicted in Graph 5.44 and compared with results obtained by the O_3/UV system at the same working conditions (NB-OR1). From the point of view of the removal rate, observed effect is negligible or inhibitory, as within the range of Fe(III) concentrations tested at high ratios (3:1 and 1:1) the removal rate is inhibited and at lower ratio (0.1:1) no difference could be observed with regard to O_3/UV.

With regard to the concentration of ozone in the residual gas (see Graph 5.45), no conclusion can be extracted as they do not present any clear tendency with the amount of Fe(III).

However, significant differences are observed with regard to TOC diminution (Graph 5.46), where the addition of ferric ion improves the mineralization rate considerably. Small amounts of ferric ion are enough to observe its catalytic effect. Higher Fe loads yielded worst results at the end of the experiments. The 1:1 ratio, however, presents an inversion of the curve that should be confirmed.

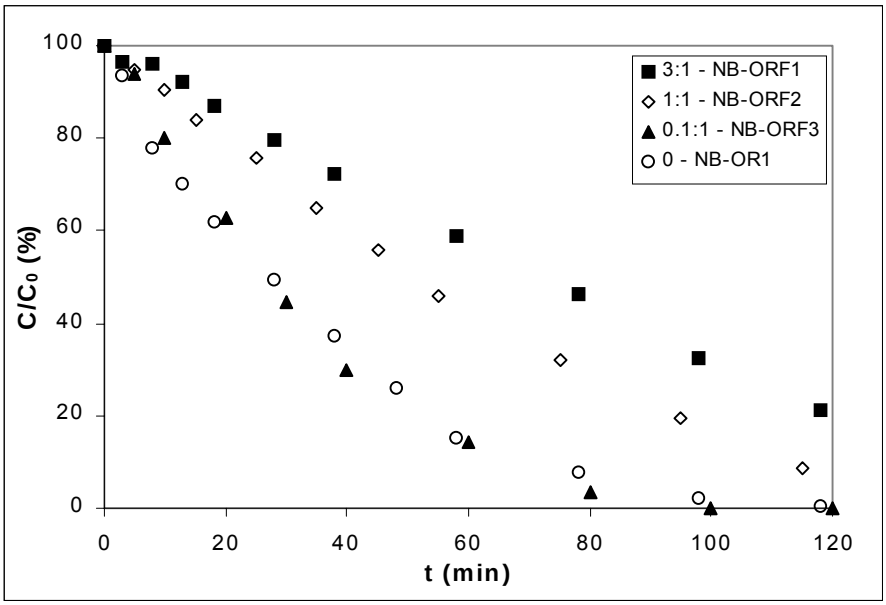

Graph 5.44. Influence of the amount of Fe(III) in the NB removal by means of O_3/UV/Fe – Normalized concentration

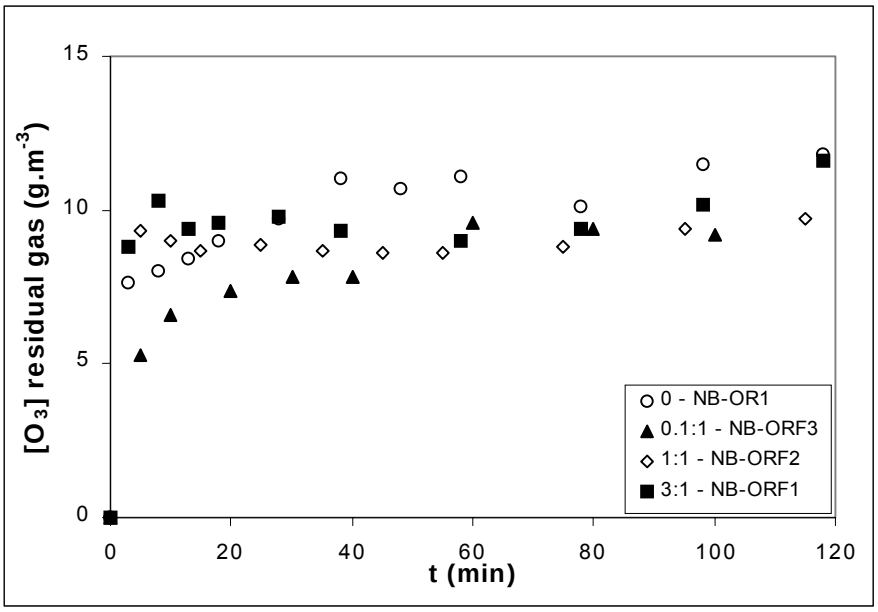

Graph 5.45. Influence of the amount of Fe(III) in the NB removal by means of O_3/UV/Fe – Residual ozone

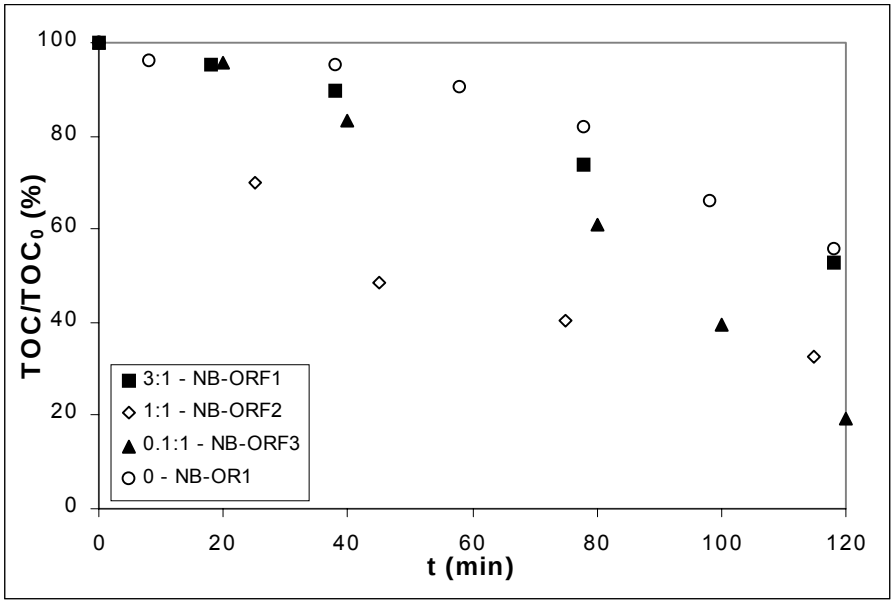

Graph 5.46. Influence of the amount of Fe(III) in the NB removal by means of O_3/UV/Fe – Normalized TOC

Three process may account for this improvement of the efficiency of the process, as mentioned in the introduction. On one hand, Fe(III) species undergo a photoredox process with UV and near-UV light, giving rise to Fe(II) and $OH^{\cdot}$ radicals according to equation [1.8] (Safarzadeh-Amiri et al., 1996; Mazellier et al., 1997):

$$Fe^{3+} \xrightarrow[H_2O]{h\nu} Fe^{2+} + OH^{\bullet} + H^{+} \qquad [1.8]$$

On the other hand, Fe(III) is considered to increase the number of hydroxyl radicals through the reduction of O_3 with the Fe^{2+} generated by the photoreduction of Fe^{3+} (Ruppert et al., 1994; Abe and Tanaka, 1999), similar to the mechanism proposed for the photo-Fenton reaction. Besides this, the initial oxidation of organic pollutants generates oxygenated intermediates, e.g. intermediates with carboxylic functional groups, which can react with Fe(III) and form complexes. These complexes are also photoactive and produce CO_2, organic radicals and ferrous ions on irradiation, contributing to the mineralization of these pollutants without the participation of hydroxyl radicals (Safarzadeh-Amiri et al., 1996; Abe and Tanaka, 1999).

$$RCO_2Fe(III) \xrightarrow{h\nu} R^{\bullet} + CO_2 + Fe(II) \qquad [1.19]$$

5.8.2. UVA vs. UV - Biodegradability study

In this case UVA light, which emits in the range of wavelength of between 300 and 420 nm, with a maximum centered at 360 nm, has been used instead of UV light. Fe(III) in aqueous solution is present mainly as $Fe(OH)^{2+}$. This complex absorbs notably in the range above 300 nm and up to 390 nm (Sefarzadeh-Amiri et al., 1996).

Two experiments with the combination O_3/UVA/Fe(III), at 7.4 $g.h^{-1}$ ozone production, room temperature and allowing pH to evolve freely were carried out (see section A1.7, Tables NB-ORF6 and NB-ORF7). Results corresponding to the latter will be presented. Firstly, it was desired to compare the efficiency of this combination in the removal of NB. Graph 5.47 presents the comparison of the processes O_3 (NB-O2), O_3/UV (NB-OR1), O_3/UVA (NB-OR7), O_3/UV/Fe (NB-ORF3) and O_3/UVA/Fe (NB-ORF7) with regard to the evolution of the normalized concentration of NB during time. As it can be seen, no significant differences were observed between the processes, although all the combinations seemed to inhibit slightly the removal rate achieved by single ozonation.

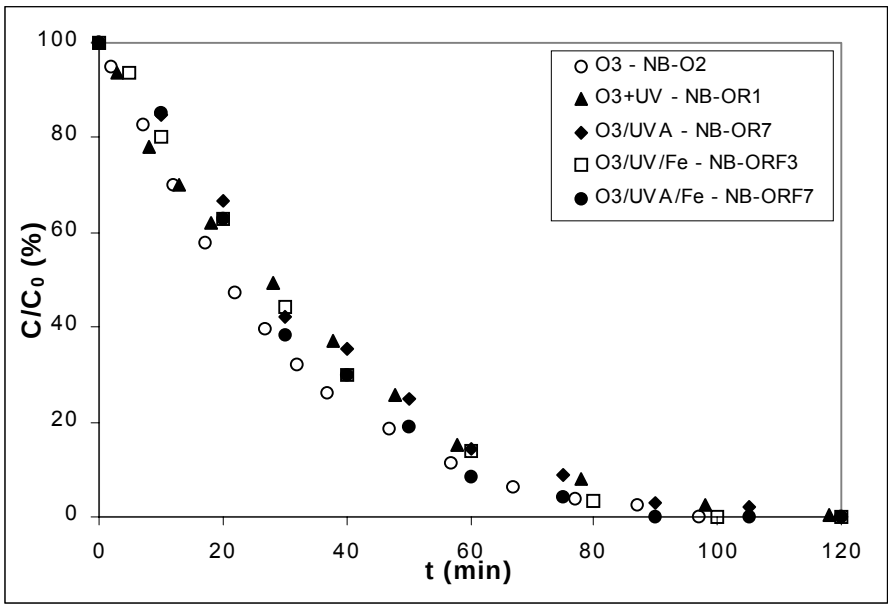

Graph 5.47. Comparison of the processes O_3, O_3/UV, O_3/UVA, O_3/UV/Fe and O_3/UVA/Fe for the removal of NB – Normalized concentration

With regard to TOC (Graph 5.48), the use of UVA instead of UV light improved the mineralization rate of the NB solutions, as it was already commented. To compare, after two hours of treatment mineralization degree achieved by O_3/UV/Fe and O_3/UVA/Fe was 80% and 91%, respectively. The combination O_3/UVA/Fe has been shown to be the most proper process for the mineralization of NB solutions.

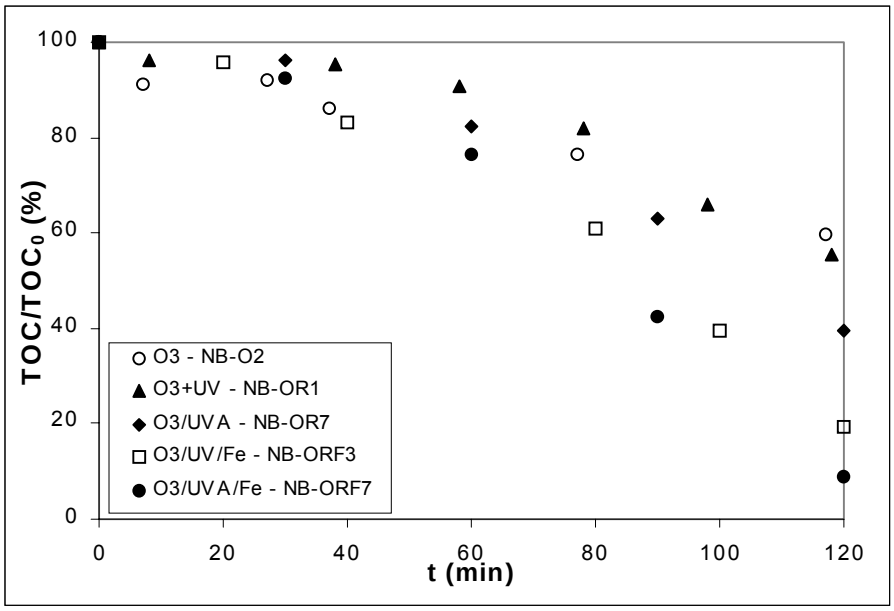

Graph 5.48. Comparison of the processes O_3, O_3/UV, O_3/UVA, O_3/UV/Fe and O_3/UVA/Fe for the removal of NB – Normalized TOC

The effect of this combination on the biodegradability of NB solutions has also been studied. BOD has been measured at 5 and 10 days for the process O_3/UVA/Fe and values obtained are plotted versus time in Graph 5.49. Values are considerably lower than those achieved by single ozonation. Higher values seem to be achieved after 60 minutes of treatment, when almost all the initial NB was depleted (less than 10% of initial NB amount was still in solution). BOD/COD values are slightly lower as well than those obtained by single ozonation (see Graph 5.50). BOD_5/COD ratio is increased from 0 to 0.20 after 60 minutes and to 0.24 after 90 minutes. BOD_{10}/COD increased up to ca. 0.35 after 60 minutes of treatment. It has to be pointed out that COD decreased strongly by means of this process: after 60 minutes COD decreased over 55%. Regarding BOD_5/TOC ratio (see Graph 5.51), it is increased to 0.30 after 60 minutes of treatment and BOD_{10}/TOC is increased up to 0.39 after 60 minutes. But in this case, after 60 minutes, 24% of TOC was removed from the solution. These ratios are also smaller than those achieved by single ozonation. It has to be point out though that the addition of UVA and Fe(III) to the ozonation enhanced the degree of mineralization of the NB solutions (see section 5.9, comparison of the different processes).

In Figures 5.3 and 5.4 the chromatograms corresponding to the samples of the experiment NB-ORF7 after 30 and 60 minutes, respectively, are shown. As it can be seen when comparing with Figures 5.1 and 5.2, new intermediates appear when UVA and Fe(III) are added. Among them, only 2-nitroresorcinol is thought to have been identified. Another difference is that the concentration of nitrophenols produced is higher with this

combination. This aspect can be especially seen in sample after 60 minutes, e.g. the concentration of 4-nitrophenol was found to be three times higher when the solution was treated by O_3/UVA/Fe. Being these compounds non-easily biodegradable, this fact could account for the lower biodegradability achieved by this combination, together with the higher mineralization degree achieved.

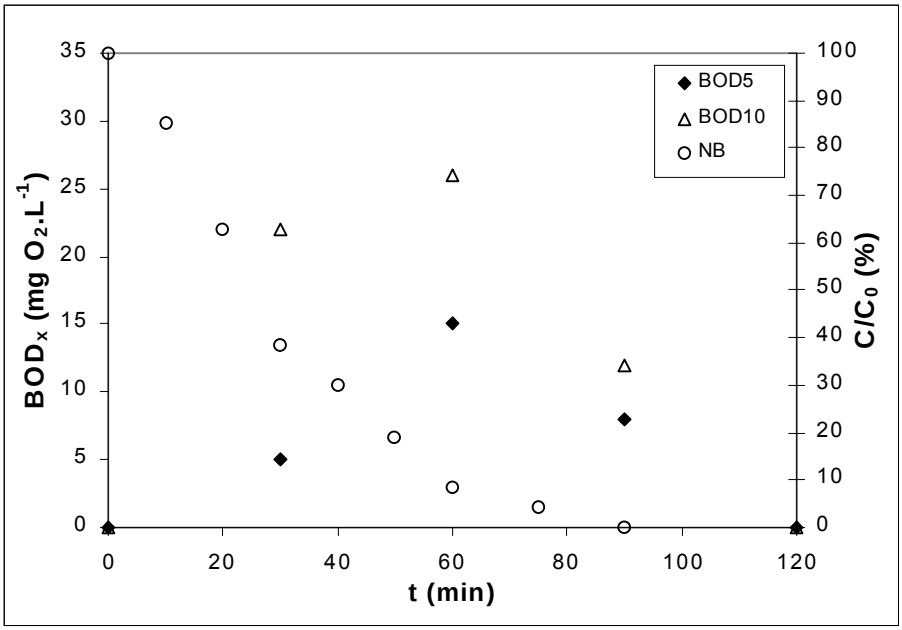

Graph 5.49. Evolution of BOD and NB normalized concentration during time with the combination O_3/UVA/Fe

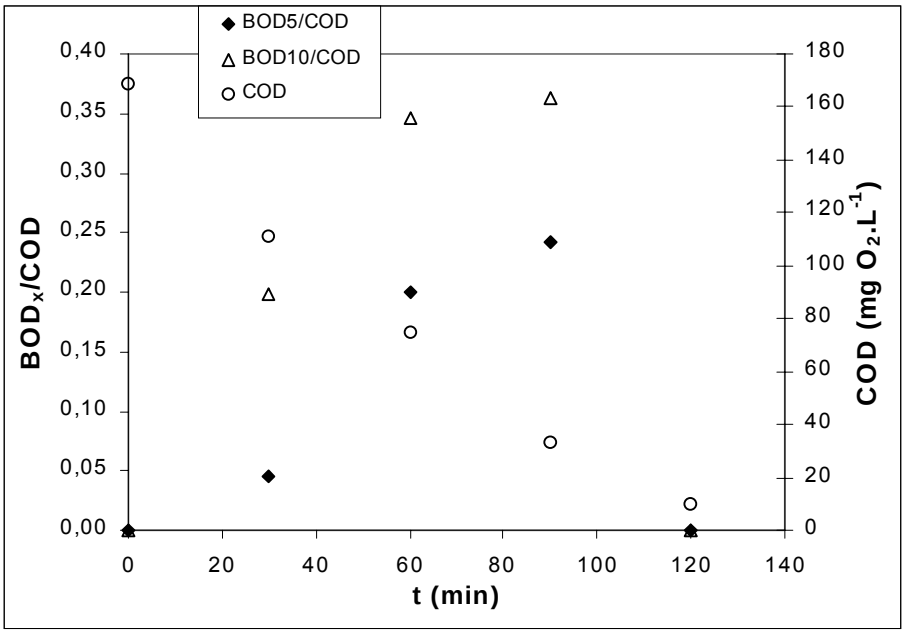

Graph 5.50. Evolution of BOD/COD ratio and COD during time with the combination O_3/UVA/Fe

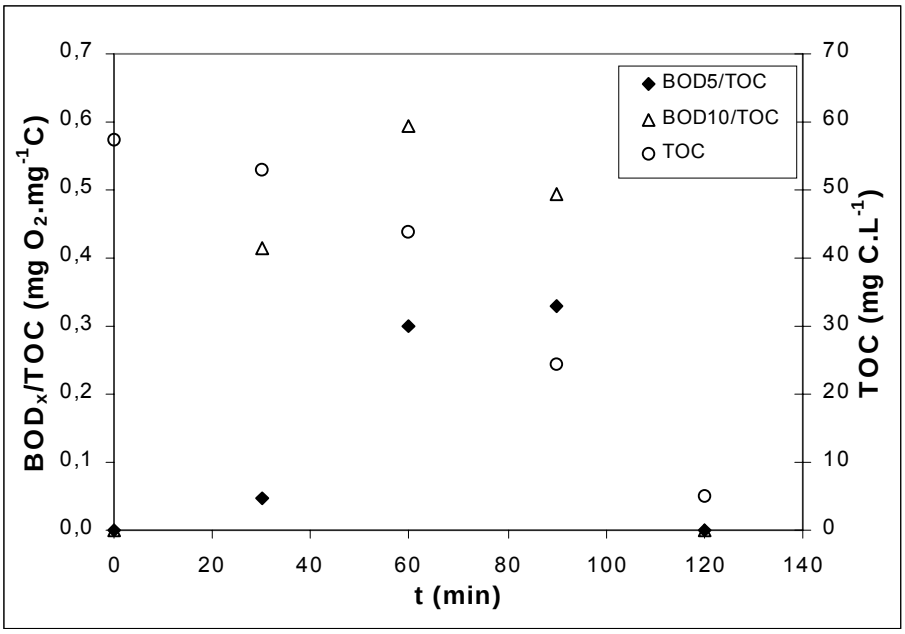

Graph 5.51. Evolution of BOD/TOC ratio and TOC during time with the combination O_3/UVA/Fe

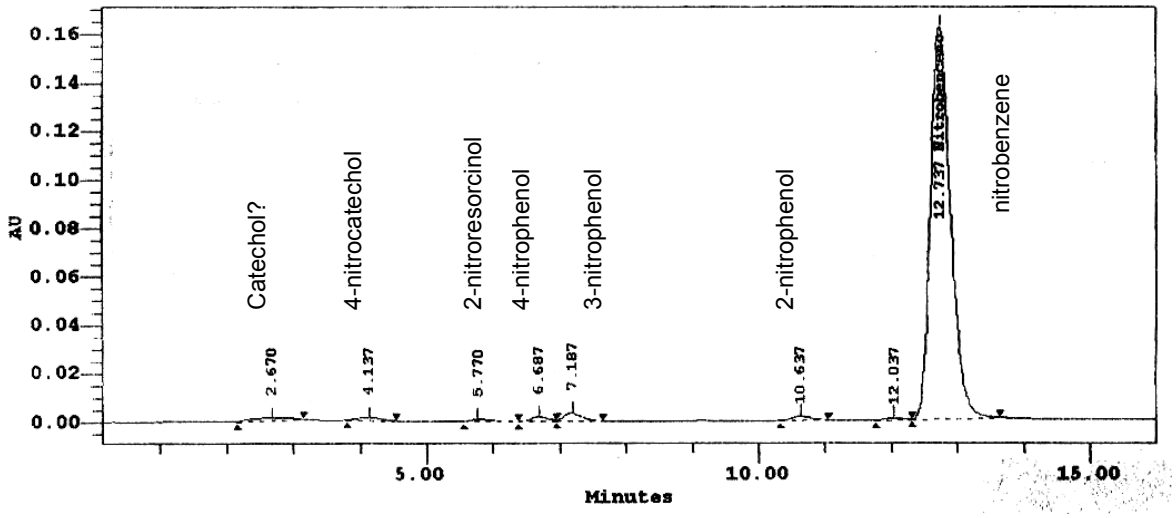

Figure 5.3. Chromatogram corresponding to sample after 30 minutes of treatment of experiment NB-ORF7 (O_3/UVA/Fe)

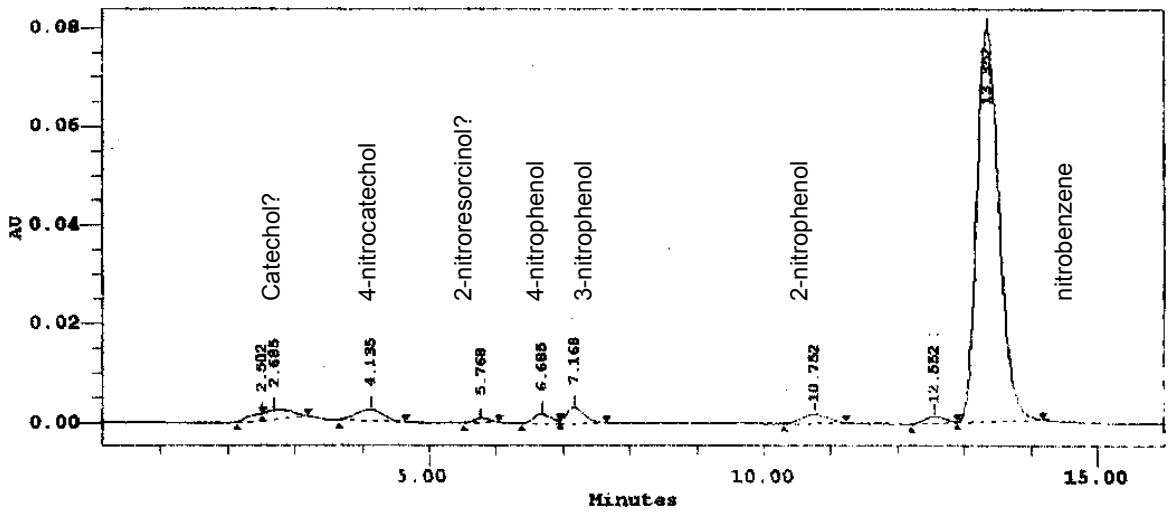

Figure 5.4. Chromatogram corresponding to sample after 60 minutes of treatment of experiment NB-ORF7 (O_3/UVA/Fe)

In light of the experimental results, the addition of UVA and Fe(III) did not improve the effect on the biodegradability of NB aqueous solutions achieved by single ozonation.

5.9. Comparison of the different studied processes for the degradation of NB

In the present section, some of the variables that have been followed in each process are to be compared among the different studied processes carried out at the same working conditions: single ozonation (NB-O2, NB-O15 for biodegradability), O_3/UV (NB-OR1, NB-OR7 for biodegradability), O_3/H_2O_2 (NB-OP4 (3:1), NB-OP6 for biodegradability (0.1:1)), O_3/UV/H_2O_2 (NB-ORP2 (3:1), NB-ORP4 for biodegradability and OI (0.1:1)) and O_3/UV/Fe(IIII) (NB-ORF3 (0.1:1), NB-ORF7 for biodegradability (0.1:1)).

5.9.1. Removal and mineralization rates

In the Graph 5.52 the normalized concentration vs. time are compared. Differences among them are rather small. It can be seen that single ozonation and O_3/H_2O_2 present the best removal rates whereas O_3/UV and O_3/UV/Fe show the slowest one.

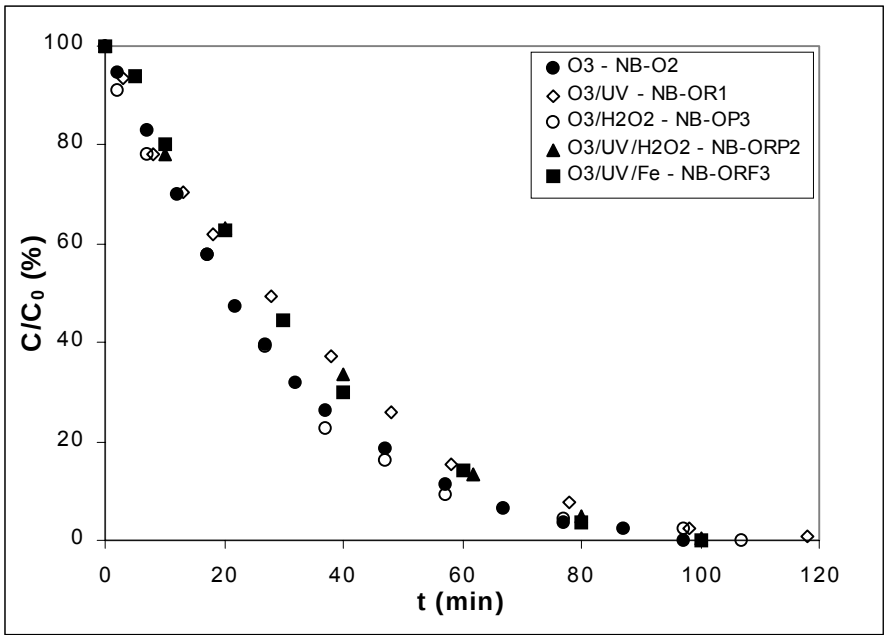

Graph 5.52. Comparison of the different processes for NB removal – Normalized concentration

Table 5.3 presents the pseudo-first order kinetic constant, the value of experimental half-life $t_{1/2}$ (that is, the time required to decrease the concentration of the reactant to half the amount present before the reaction and experimental $t_{3/4}$ (time needed to decrease to the fourth part the initial amount of NB). At the light of the results the studied processes seem to obey a pseudo-first order behavior ($t_{3/4} \approx 2 \times t_{1/2}$). Removal of nitrobenzene by an ozonation process was found to be consistent with a first order reaction equation in the literature (Baozhen and Jun, 1988).

Table 5.3. Pseudo-first order kinetic constant, $t_{1/2}$ and $t_{3/4}$ for NB removal by the different studied processes

	O_3	O_3/UV	O_3/H_2O_2 (3:1)	O_3/UV/H_2O_2 (3:1)	O_3/UV/Fe(III) (0.1:1)
k (min^{-1})	0.0363	0.027	0.0399	0.0304	0.0279
$t_{1/2}$ (min)	20.7	27.5	21.3	28.4	27.0
$t_{3/4}$ (min)	38.4	49.7	35.7	49.3	46.1

With regard to TOC (see Graph 5.53), the process exhibiting the highest mineralization rate is the combination of ozone with UV radiation and Fe(III) ion. Single ozonation and the binary combinations O_3/UV and O_3/H_2O_2 present similar results, achieving a 40-45% of TOC reduction after 120 minutes of treatment. In the case of the O_3/UV process, the TOC diminution is slower in the initial stage, attaining a higher degree

of mineralization during the second hour of treatment. With the O_3/H_2O_2 system, a stronger TOC diminution during the first 20 minutes is achieved, slowing down afterwards. With the tertiary combinations a much higher degree of mineralization is reached. Whereas with the $O_3/UV/H_2O_2$ the TOC removal is up to 63%, with the $O_3/UV/Fe(III)$ process the degree of mineralization achieved after 120 minutes is 80% (91% when UVA light was used instead of UV light). As it was commented previously, photodecarboxilation of ferric ion complexes, Fenton chemistry and photo-Fenton reaction of aqueous ferric ions with UV light may account for this improvement with regard to the other processes.

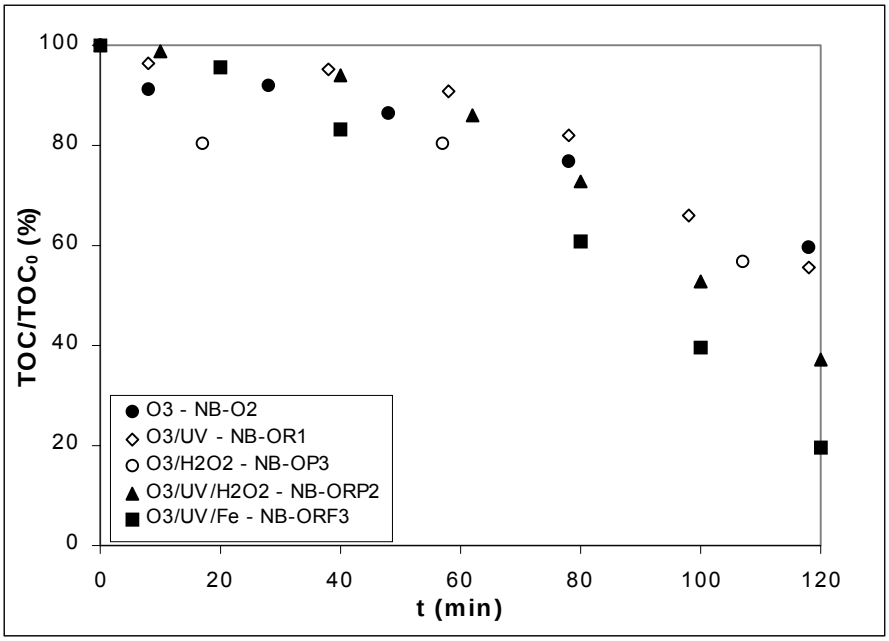

Graph 5.53. Comparison of the different processes for NB removal – Normalized TOC

Oxidation efficiency can be expressed generally in terms of an "Oxidation Index" (mol O_3/mol COD removed), abbreviated as OI, which is defined as the ratio of ozone consumed to the amount of COD removed (Kuo, 1999). Low OI values show a higher degree of utilization of ozone during the oxidation processes. Table 5.4 summarizes OI values after 30 and 60 minutes treatment by the different processes. As shown in this table, best ratios were achieved by single ozonation. None of the other studied processes improved this index. With regard to the combinations with H_2O_2, very high values have been found, what could be due to an error in the ozone residual or COD analysis.

Table 5.4. Oxidation index (mol O_3/mol COD removed) of NB by the different processes after 30 and 60 minutes of treatment

	O_3	O_3/UV	O_3/H_2O_2	O_3/UV/H_2O_2	O_3/UV/Fe(III)
After 30 minutes	1.06	1.36	*4.58*	*2.78*	1.72
After 60 minutes	1.33	1.62	*2.39*	*3.33*	1.99

Analogous to this parameter, a "mineralization index" (mol O_3/mol TOC removed) can be defined, as the ratio of ozone consumed to the amount of TOC converted to CO_2. Values are presented in Table 5.5. Single ozonation besides O_3/UV/Fe showed the best indexes. O_3/UV process exhibits an extremely high value for the first 30 minutes. As it has been commented before, initial TOC removal by means of this combination showed to be rather low.

Table 5.5. Mineralization index (mol O_3/mol TOC removed) of NB by the different processes after 30 and 60 minutes of treatment

	O_3	O_3/UV	O_3/H_2O_2	O_3/UV/H_2O_2	O_3/UV/Fe(III)
After 30 minutes	5.08	9.58	5.95	-	5.86
After 60 minutes	4.25	5.05	6.18	-	4.20

In the literature (Ku et al., 1996) a simple two-step consecutive kinetic model has been found to fit well in modeling the behavior of species during the decomposition of phenols, based on elemental mass balances of carbon and chlorine during the reaction. Thus, the mass balance of carbon is:

$$C_{total} = (NB)_{ct} + (Interme)_{ct} + (CO_2)_{ct} \qquad [5.8]$$

where

C_{total} = total initial amount of NB as carbon, mg $C.L^{-1}$

$(NB)_{ct}$ = amount of NB as carbon at time t, mg $C.L^{-1}$

$(Interme)_{ct}$ = amount of intermediates as carbon at time t, mg $C.L^{-1}$

$(CO_2)_{ct}$ = amount of inorganic carbon as carbon at time t, mg $C.L^{-1}$

The amount of CO_2 formed is calculated as the difference between the initial TOC and the TOC at a certain reaction time t. The amount of organic intermediates as carbon is calculated by the difference between the TOC and the amount of NB. Due to the complexity of the decomposition schemes of NB by advanced oxidation processes, the

simplified two-step consecutive kinetic model is used to describe the temporal behavior of reacting carbon-containing species during the reaction. Each step of the reaction is assumed to be a first-order and irreversible reaction. The model and profiles of species are derived from the following equations :

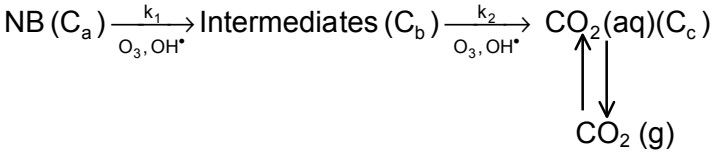

$$-r_a = -dC_a/dt = k_1 C_a \quad [5.9]$$

$$r_b = dC_b/dt = k_1 C_a - k_2 C_b \quad [5.10]$$

$$r_c = dC_c/dt = k_2 C_b \quad [5.11]$$

which yields:

$$C_a = C_{ao} e^{-k1 \cdot t} \quad [5.12]$$

$$C_b = C_{ao} k_1 (e^{-k1 \cdot t} - e^{-k2 \cdot t})/(k_2 - k_1) \quad [5.13]$$

$$C_c = C_{ao} - C_a - C_b \quad [5.14]$$

where

k_1 , k_2 = pseudo-first order rate constants for first and second decomposition steps based on carbon, respectively, min^{-1}

$C_a = (NB)_c$, amount of NB as carbon, mg $C.L^{-1}$

$C_b = (Interme)_c$, amount of intermediates as carbon, mg $C.L^{-1}$

$C_c = (CO_2)_c$, amount of inorganic carbon as carbon, mg $C.L^{-1}$

When NB is completely destroyed, equation [5.10] can be simplified and the k_2 value can be determined by:

$$\ln\left(\frac{C_b}{C_{bc}}\right) = -k_2 (t - t_{bc}) \quad [5.15]$$

t_{bc} = time required for 99% of NB to have disappeared, min

C_{bc} = concentration of (Interme) at t_{bc}, mg $C.L^{-1}$

By following this mathematical model, the values of C_a, C_b and C_c during time have been calculated for each of the processes. In the present case, t_{bc} has been set to ca. 80 min to be able to estimate k_2. Table 5.6 summarizes values of k_1 and k_2 for the different processes. Comparing the values of k_1 and k_2, the rate-determining step of mineralization of NB is presumed to be the second step. In the first step all the processes exhibit similar

mineralizing rates, while in the second step (mineralization of the intermediates formed) the mineralization rate of single ozonation is significantly enhanced by the addition of UV radiation (150%) and especially by the addition of UV combined with H_2O_2 (290%) and UV radiation and ferric ion (more than 500%).

Table 5.6. Pseudo-first order constants for the model developed by Ku et al. (1996) in the degradation of DCP (values of R^2 expressed between brackets)

Processes	k_1 (min^{-1})	k_2 (min^{-1})
O_3	0.0392 (0.98)	0.005
O_3/UV	0.0306 (0.98)	0.0074
O_3/H_2O_2 (3:1)	0.0399 (0.99)	0.0045
O_3/UV/H_2O_2 (3:1)	0.0304 (0.98)	0.0145
O_3/UV/Fe(III) (0.1:1)	0.0305 (0.98)	0.0254

One interesting parameter when comparing the mineralization degree is the calculation of efficiencies. A definition of efficiency as the ratio of TOC removed to the quantity of ozone consumed (see equation [5.16]). Assuming that one atom of oxygen in each ozone molecule is used in the process, the two other oxygen atoms being lost as molecular oxygen, the efficiency ratio is defined as (Legrini et al., 1993):

$$\text{Efficiency ratio} = \frac{\Delta\text{TOC x total volume}}{\frac{1}{8} \text{ x } [O_3] \text{ x volumen of gaseous } O_3 \text{ used}} \qquad [5.16]$$

where ΔTOC is expressed in mg $C.L^{-1}$, volumes in L and the concentration of O_3 in $mg.L^{-1}$ of gas. The factor 1/8 accounts for the molar ratio requirement of 2 moles of O_3 (96 g.) per mol of organic carbon to be oxidized (12 g.). In the Table 5.7 the efficiency ratios of the studied processes are summarized. For comparison of process efficiencies, by assuming that energy costs of light production and cost of reactives are negligible in comparison to those of ozone generation (as in our case), higher efficiencies would imply lower costs. Again, processes exhibiting highest efficiencies are O_3/UV/H_2O_2 and O_3/UV/Fe(III).

Table 5.7. Efficiency ratios for the different studied processes

Process	Efficiency ratio (%)
O_3	26
O_3/UV	29
O_3/H_2O_2 (3:1)	32
O_3/UV/H_2O_2 (3:1)	40
O_3/UV/Fe (0.1:1)	58

5.9.2. Biodegradability enhancement

As it has been mentioned in the introduction, one of the objectives would be the coupling of the AOPs with a biological process. In the literature (Takahashi et al., 1994) it has been reported that the ozonation of several nitrophenols enhanced their biodegradability, presenting a maximum, from which biodegradability started decreasing. The biodegradability indicators used throughout the present work have been BOD_5/COD and BOD_5/TOC ratios. Graphs 5.54 and 5.55 present the variation of those ratios during time for all the studied processes. Highest BOD_5/COD ratios have been attained after 90 minutes of treatment. This ratio has been increased from 0 to 0.32 by means of single ozonation and the O_3/UV/H_2O_2 process. Highest BOD_5/TOC ratios have also been reached after 90 minutes, achieving a value of up to 0.55 by means of O_3/H_2O_2 and ca. 0.5 by single ozonation and O_3/UV/H_2O_2. As a reference, a BOD_5/COD ratio of 0.4 is generally considered the cut-off point between biodegradable and difficult to biodegrade waste. Domestic waste water typically has a BOD_5/COD ratio of between 0.4 to 0.8 and BOD_5/TOC ratio between 1 to 1.6 and it is considered substantially biodegradable (Metcalf and Eddy, 1985). In light of the experimental results, single ozonation would be the chosen process to enhance the biodegradability of the NB solutions and the treatment time would be set to 60-90 minutes.

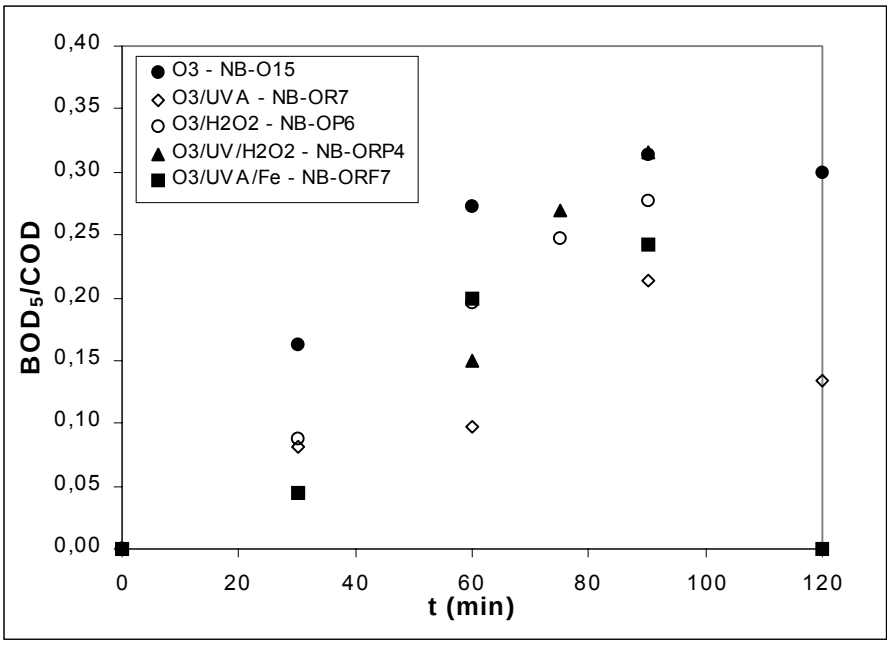

Graph 5.54. Comparison of the different processes for NB removal – BOD_5/COD ratio

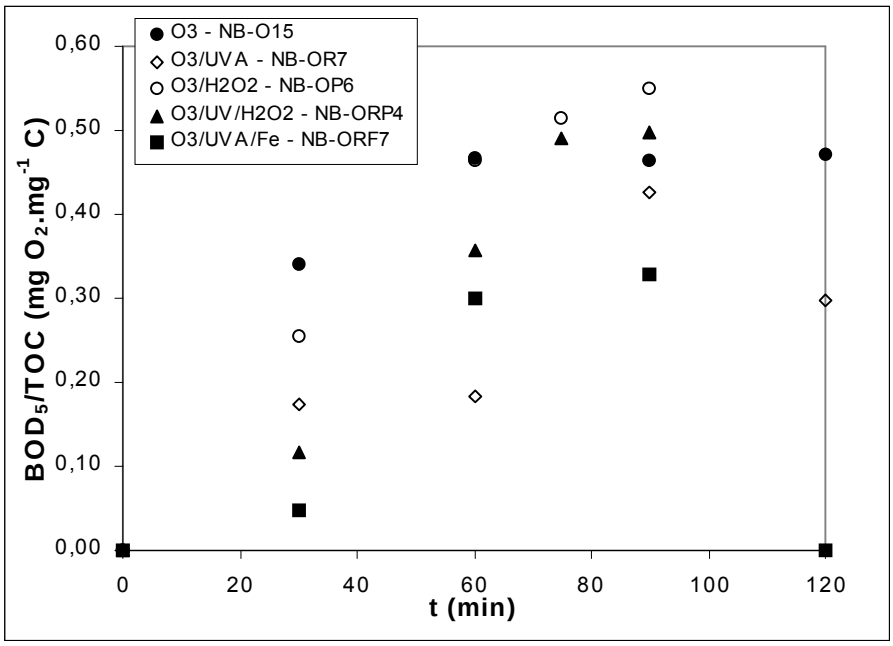

Graph 5.55. Comparison of the different processes for NB removal – BOD_5/TOC ratio

5.9.3. Cost estimation

The evaluation of the treatment costs is one of the most important aspects. The overall costs are represented by the sum of the capital costs, the operating costs and maintenance. For a full-scale system these costs strongly depend on the nature and the

concentration of the pollutants, the flowrate of the effluent and the configuration of the reactor (Andreozzi et al., 1999). An estimation of costs have been made in this section, regarding the operating costs for the processes plotted in Graphs 5.52 and 5.53. Costs of reagents (*Chemical Market Reporter* (2000)) and electricity are shown in Table 5.8. Cost associated to the production of ozone (which includes the price of O_2 and electrical cost) and electricity has been obtained from industrial references (*Note*: nowadays, 1 $ ~ 1 €).

Table 5.8. Cost of the reagents used in the studied processes

Reagent	Basis	Cost (€)
O_3	kg	2.93
Electricity	KW.h	0.03
H_2O_2, 35%	lb	0.245
$FeCl_3$ technical grade	kg	0.255

Costs have been calculated for 60 and 120 minutes of treatment and as the ratio to the amount of NB removed and to the amount of TOC mineralized. Results are presented in Table 5.9. All the studied processes exhibit similar costs respect to the amount of NB removed. This cost increases with time because at initial time is when the disappearance rate is highest. With respect to the amount of TOC removed, O_3/UV/Fe(III) appears to be the most attractive option for NB degradation. It has to be pointed out that this cost would decrease considerably if solar light were used (Giménez et al., 1999).

Table 5.9. Comparison of costs among the studied processes

Processes	€/kg NB rem (60 min)	€/kg NB rem (120 min)	€/kg C rem (60 min)	€/kg C rem (120 min)
O_3	13.65	21.89	108.8	90.77
O_3/UV	12.98	22.15	199.9	83.83
O_3/H_2O_2 (3:1)	18.90	21.62	99.59	85.89
O_3/UV/H_2O_2 (3:1)	14.93	24.54	*159.2*	67.85
O_3/UV/Fe(III) (0.1:1)	12.45	21.35	63.34	44.02

5.10. Identification of intermediates

Some of the samples were analyzed by HPLC/MS to identify the products of the oxidation of NB. The standards used for the identification were: 2-nitrophenol, 3-nitrophenol, 4-nitrophenol, 4-nitrocatechol, 2-nitroresorcinol, catechol, resorcinol, hydroquinone, benzoic acid and p-benzoquinone. Analyzed samples belonged to the processes O_3, O_3/UVA and O_3/UVA/Fe. The main conclusions are presented below:

a) Nitrophenols

The presence of two isomers, 3- and 4-nitrophenol was detected in all the processes. 2-nitrophenol was also observed in the ozonated samples and in the other processes it is also thought to be produced.

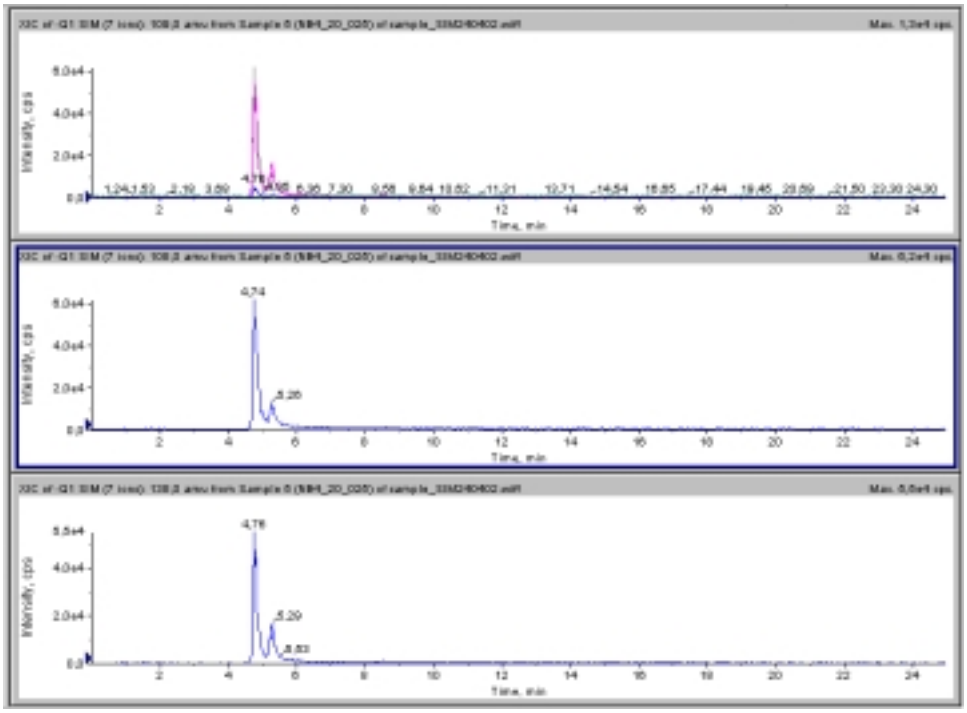

b) Nitrocatechol, nitroresorcinol

Nitrocatechol was identified as an ozonation byproduct and it is thought to be identified in the other processes as well. Nitroresorcinol and nitrohidroquinone are thought to have been identified in some of the samples as well.

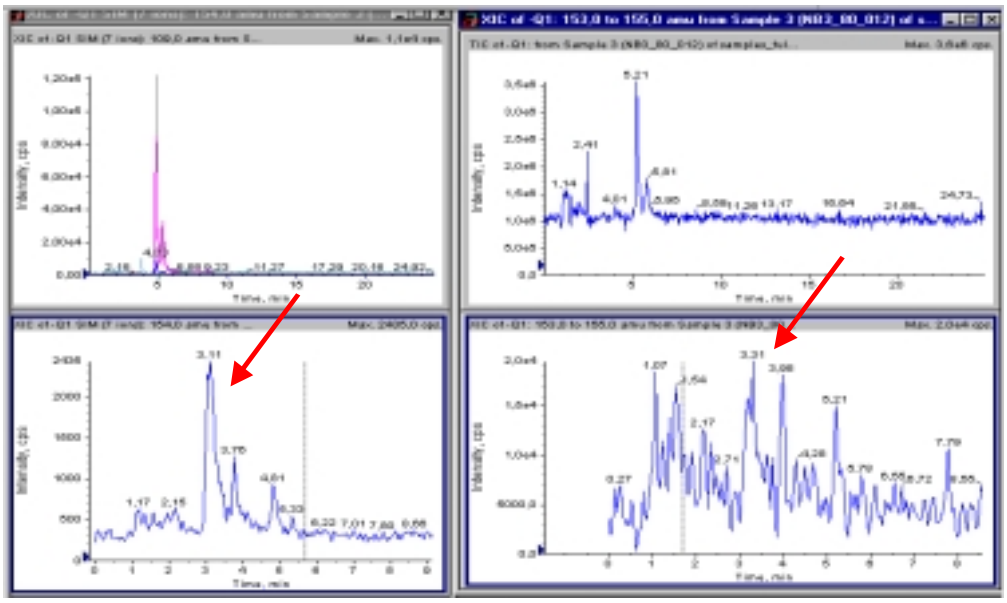

c) Catechol, resorcinol, hydroquinone

Catechol is thought to be identified is ozonated samples. Hydroquinone and resorcinol have not been detected

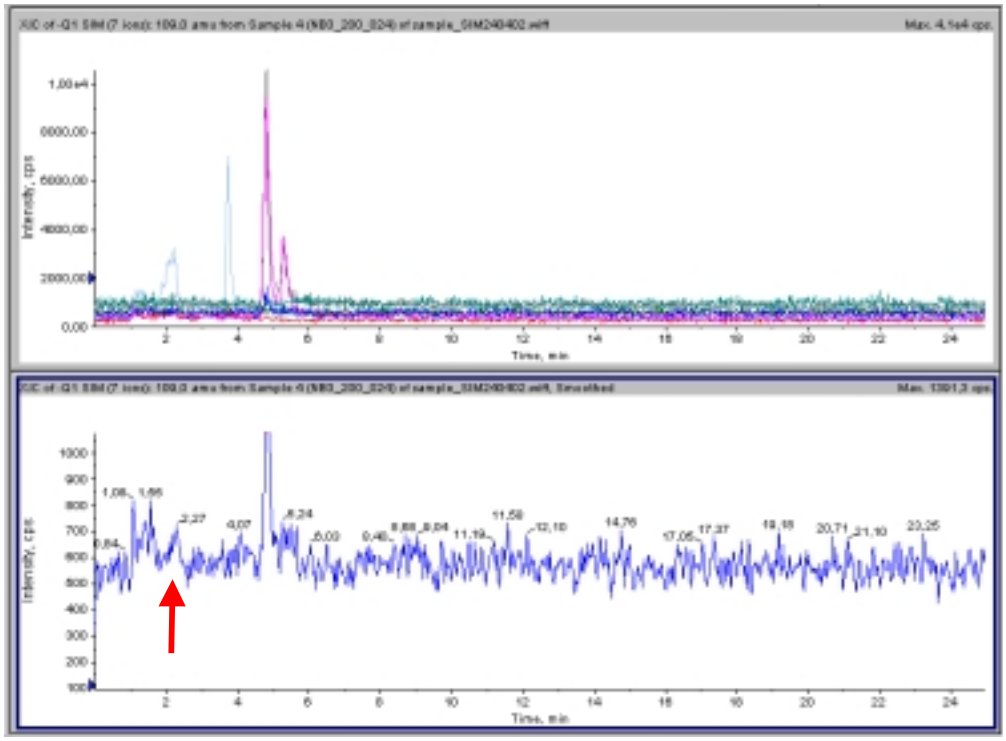

d) P-benzoquinone, benzoic acid

They were not observed in any of the samples. The reason could be a low concentration in samples, a high detection limit using this technique or both.

As it has been commented, the three nitrophenols have been identified (see Figure 5.5) as the main intermediates of nitrobenzene (especially 4-nitrophenol), as it has been reported by other authors (Lipczynska-Kochany, 1991; Beltrán et al., 1998a,b). This phenol was formed from electrophilic substitution reactions, both from the direct attack of ozone or hydroyl radicals. In the literature the mechanism for the ozonation of nitrophenol has been proposed (Beltrán et al., 1999a) and it is shown in Figure 5.6. Once nitrophenol is formed, the following intermediates through ozone direct reactions can be deduced from the phenol ozonation mechanism (Mokrini, 1998). Thus, it would expected that compounds such as nitrodihydroxybenzenes (nitroresorcinol, nitrocatechol, nitrohidroquinone) are formed. Nitrocatechol has been also identified among the intermediates, confirming this hypothesis. Through the aromatic ring breaking, unsaturated carboxylic acids (e.g., nitromuconic acid) would be formed, and from them, lower molecular weight compounds. Nitroresorcinols and nitromuconic acid can also be formed from reactions with hydroxyl radicals, where hydroperoxide anion is also formed. Catechol is thought to have been also identified, suggesting that direct dissociation of the nitro group from the aromatic ring before cleavage is produced. In the literature it has also been reported that the nitro group is split from the aromatic ring to produce the nitrate ion (Gilbert and Zinecher, 1980; Baozhen and Jun, 1988; Takahashi et al., 1994), and this fact has been verified experimentally by following the concentration of nitrate ion. With regard to the low molecular weight compounds, Caprio et al. (1984) identified formic acid, oxalic acid, glyoxal and glyoxylic acid among them. Beltrán et al. (1998a,b) have also identified by means of GC/MS the presence of benzaldehide as ozonation intermediate and 2,6-dinitrobenzaldehide and 3-nitro-1,2-benzenedicarboxylic acid among the intermediates formed by O_3/UV.

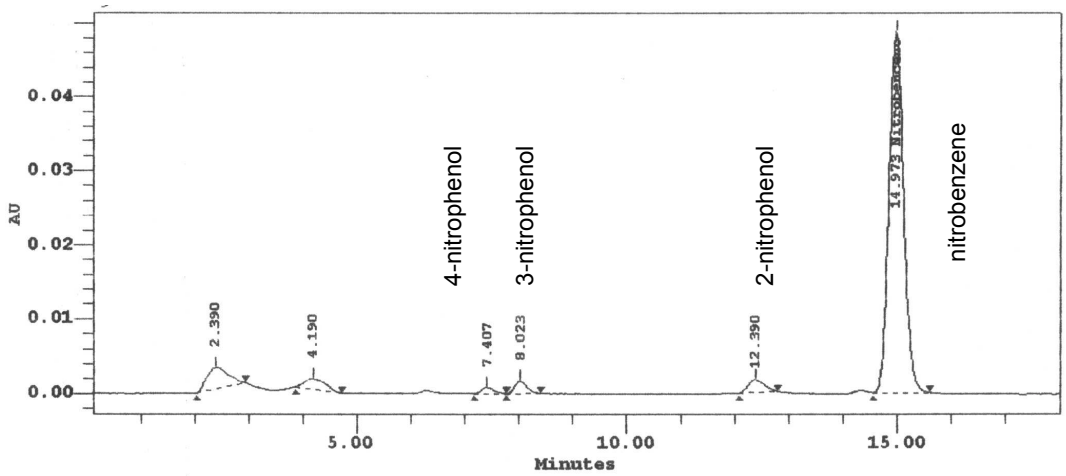

Figure 5.5. HPLC chromatogram corresponding to sample 120 min of the experiment NB-O8

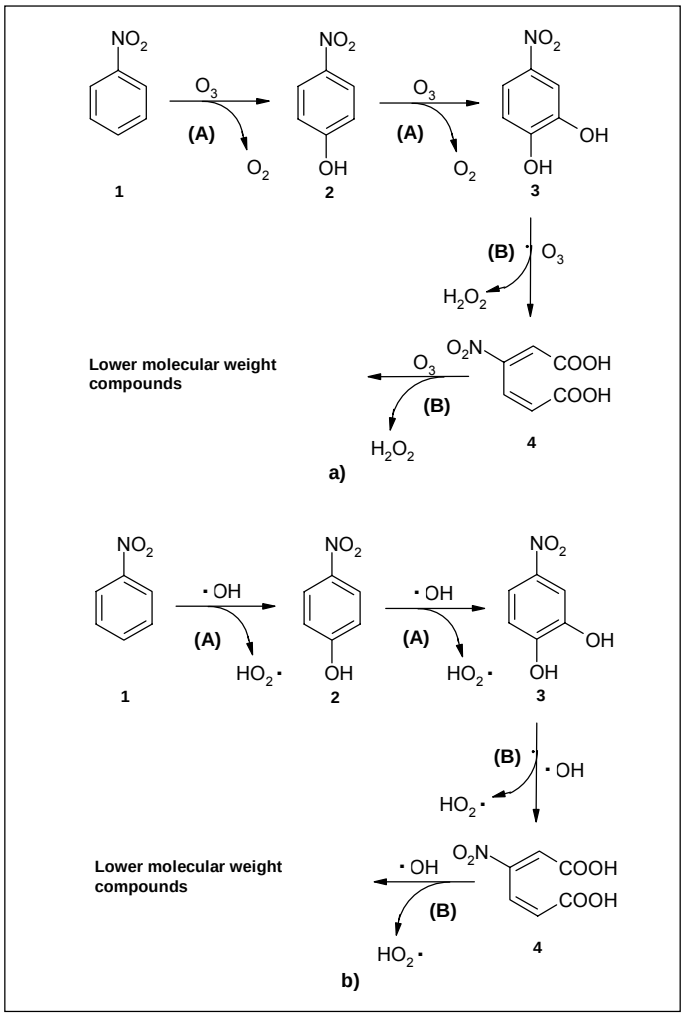

Figure 5.6. Proposed mechanism for the ozonation of nitrobenzene (Beltrán et al., 1999a) through a) ozone direct reactions and b) hydroxyl radical reactions: (A) electrophilic substitution, (B) dipolar cycloaddition, (1) NB, (2) 4-nitrophenol, (3) nitroresorcinol and (4) nitromuconic acid

2,4-DICHLOROPHENOL (DCP)

5.11. Previous experiments with DCP – Stripping with oxygen

The effect of an "ozone-free" oxygen flow on aqueous solutions of DCP at 25ºC was checked. Results are shown in Appendix 1.8, Table DCP-S. A 9% loss of compound was found after two hours of treatment. An equivalent TOC diminution was observed. After 30 minutes of bubbling oxygen (approximate time necessary to make DCP disappear in next AOPs experiments) a 3% DCP was removed. This amount will be considered negligible and it will be assumed that the degree of DCP removal by means of any AOP will be produced by the action of these combinations without contribution of the stripping.

5.12. Single ozonation of DCP

In the first series of experiments, the effect of single ozonation on the degradation and biodegradability of DCP was studied. The influence of ozone production, pH, initial DCP concentration and scavengers on the degradation of DCP was checked, as well as the effect of single ozonation on the biodegradability of these solutions. Moreover, the stoichiometric coefficient of the reaction between ozone and DCP was determined. Results are shown on Appendix 1.9, Tables DCP-O1 to DCP-O15. In the following graphs, most of results have been plotted versus the *absorbed* ozone dose. Mass transfer of ozone from the gaseous to the aqueous phase can be a limiting factor, causing a part of applied ozone to be lost in the off-gas. The *absorbed* ozone dose is thus more informative because it indicates the amount of dissolved ozone available for oxidation. The absorbed ozone dose was calculated by subtracting the concentration of ozone in the off-gas from the inlet concentration.

5.12.1. Influence of the ozone production.

Aqueous solutions of ca. 100 ppm DCP (in the range 90-100 ppm (0.55-0.61 $mmol.L^{-1}$)) were treated by single ozonation, changing the production of ozone from 7.4 $g.h^{-1}$ (21 $g.m^{-3}$, concentration of ozone in the inlet gas) to 4.1 $g.h^{-1}$ (11.5 $g.m^{-3}$). The lower production rates are unstable and with higher production rates, DCP disappears very fast. The pH was allowed to evolve freely (ca. 5 to 3) and temperature of the experiments was 21-22ºC. Results are shown on section A1.9, Tables DCP-O1 to DCP-O3.

Graphs 5.56 and 5.57 present the evolution of the normalized DCP concentration and the amount of DCP removed vs. time. It can be observed that the amount of DCP removed vs. time increases with the ozone production and the DCP removal rate increases linearly with the production (r^2 = 0.94, see Table 5.10). The removal rate of DCP was found to be ca. 2.5 times higher than of NB (see Tables 5.1 and 5.10). The nitro group, an electron-withdrawing group, deactivates the aromatic ring for the direct reaction of ozone with NB while the presence of a OH donor group make phenolic compounds strongly reactive towards ozone.

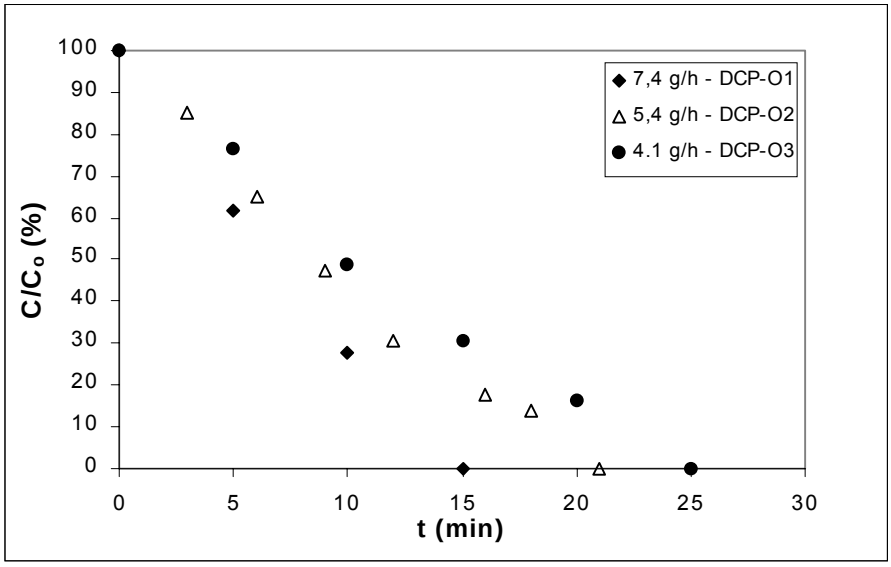

Graph 5.56. Influence of the ozone production on DCP ozonation – Normalized concentration

Table 5.10. Effect of the production of ozone on the initial removal rate of DCP.

Ozone production ($g.h^{-1}$)	DCP removal rate ($mg.min^{-1}$)
4.1	80.1
5.4	109
7.4	127

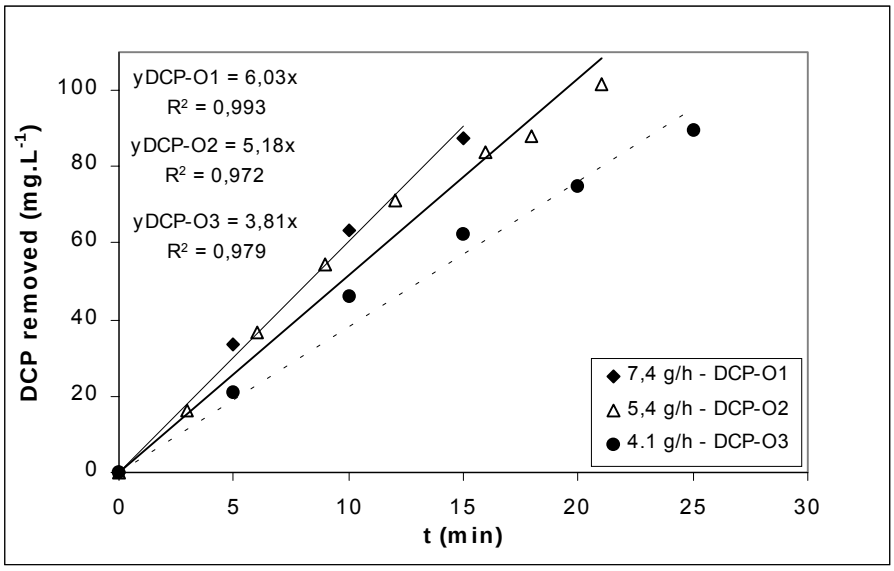

Graph 5.57. Influence of the ozone production on DCP ozonation – Amount of DCP removed vs. time

When the production of ozone is increased, the driving force enhances as well as the absorption rate. However, if the amount of DCP removed is plotted versus the absorbed ozone dose, it does not seem to depend on the ozone production (see Graph 5.58). This may suggest that for the conditions tested mass transfer is lightly controlling the process (probably at initial time), however the reaction kinetics appear to be mostly chemical reaction controlled, as it was already observed in the case of nitrobenzene.

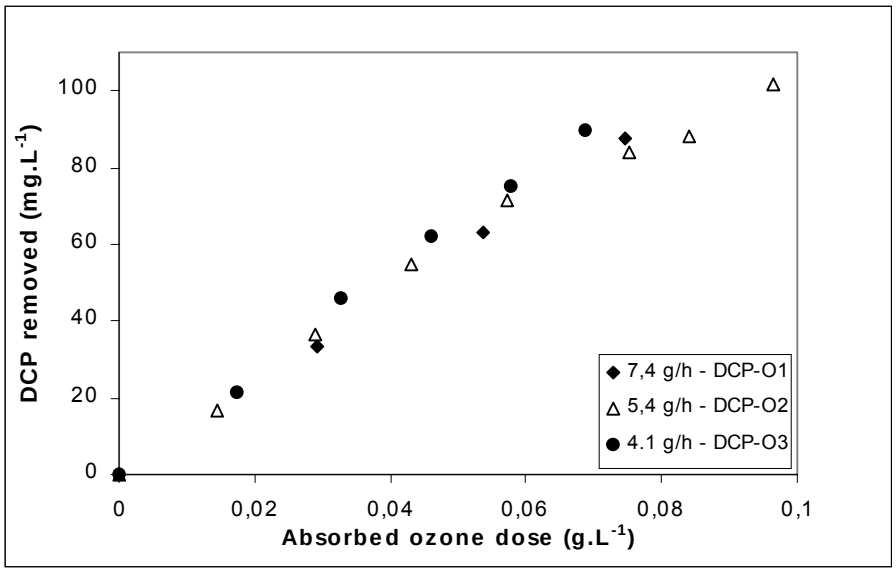

Graph 5.58. Influence of the ozone production on DCP ozonation – Amount of DCP removed vs. absorbed ozone dose.

With regard to residual ozone (see Graph 5.59), no significant differences were found between 4.1 and 5.1 $g.h^{-1}$, however residual ozone increased dramatically for 7.4 $g.h^{-1}$. Residual ozone increases with production because less ozone is taken advantage of in the oxidation process. Plateaus were not observed in this case.

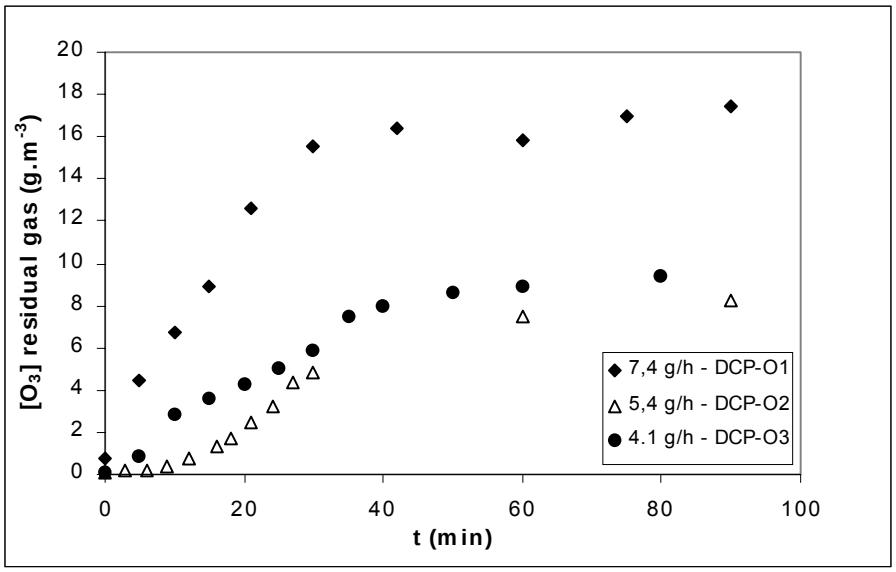

Graph 5.59. Influence of the ozone production on DCP ozonation – Residual ozone.

Dissolved ozone was measured for the experiments DCP-O3 and DCP-O15 (see Graph 5.60). No significant differences have been found between these two experiments regarding dissolved ozone concentration, however the presence of dissolved ozone immediately after the beginning of ozonation would confirm that for the testing conditions, reaction may be mainly controlling the process and takes place in the liquid phase.

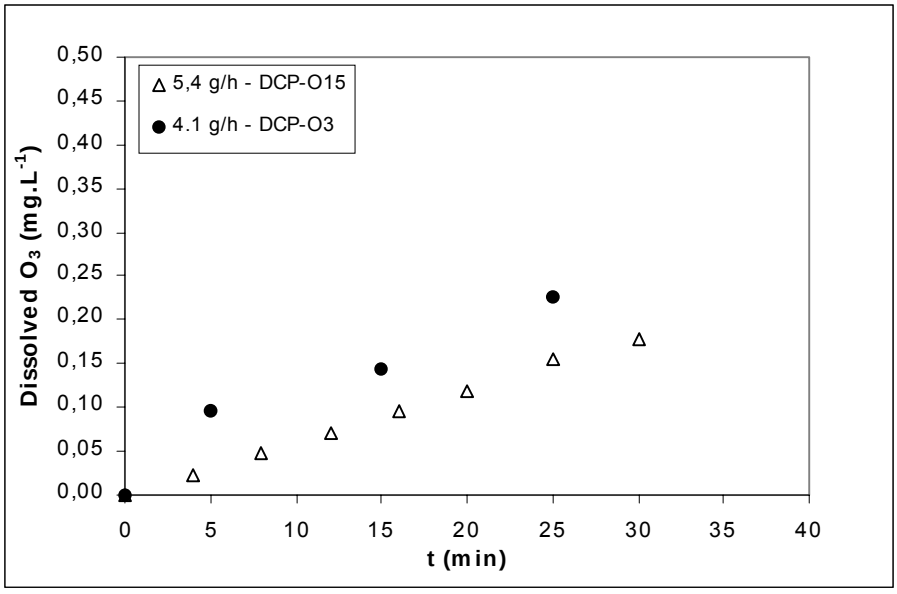

Graph 5.60. Influence of the ozone production on DCP ozonation – Dissolved ozone.

From the data presented in Graph 5.58 of the amount of DCP removed and of ozone consumed (calculated as the absorbed ozone dose multiplied by the volume of treated solution, 21 L), the stoichiometric coefficient for the reaction of ozone and DCP can be *estimated*. Data and initial slopes (this coefficient has to be estimated at initial times, as afterwards intermediates are produced and will affect this value) are shown in Graph 5.61. The *stoichiometric coefficient* has been found to be 2.6-2.9 mol O_3 consumed per mol DCP removed in the range of production tested. Regarding the stoichiometric coefficient, it has been determined to be 2 in the literature. Hoigné and Bader (1983a) found a value of 2.5 for aromatic compounds. Trapido et al. (1997) found a value of 1.89 at pH=2.5. Benitez et al. (2000) determined a stoichiometric coefficient of ca. 2 for the ozonation of DCP at a pH range of between 2-3. More recently, Qiu et al. (2002) has found a value of 2.04 for the ozonation of 2,4-CP at free pH. It has to be taken into account that our value of the stoichiometric coefficient is only an estimation, as a pilot plant is not suitable for this kind of calculation and this work has not been carried out in high excess of DCP to assure the total consumption of ozone practically at an instantaneous rate by DCP and not by the intermediates products formed.

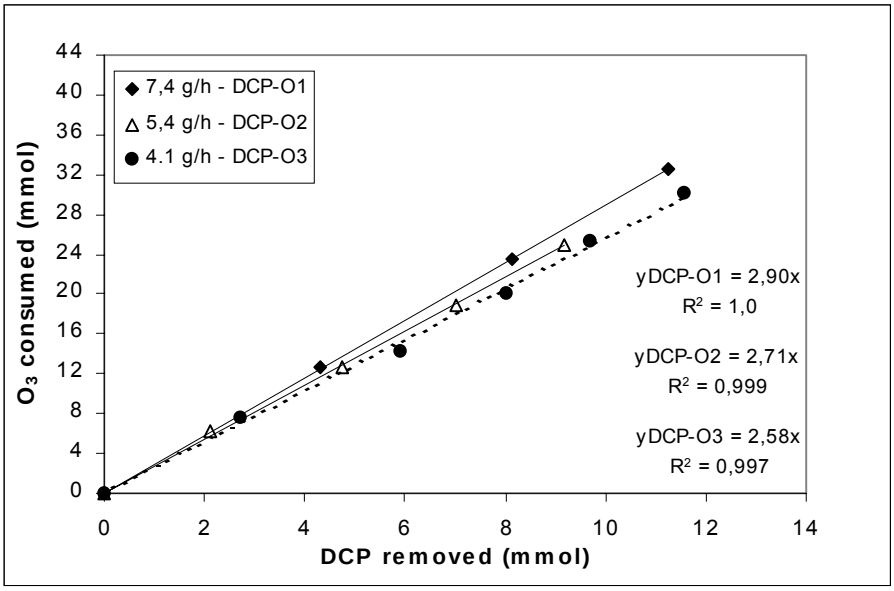

Graph 5.61. Stoichiometric coefficient for the reaction of DCP with ozone.

With regard to the decrease of TOC, TOC removal rate seems to increase with the ozone production (see Graph 5.62). A similar stoichiometric coefficient can be calculated for the organic carbon (see Graph 5.63). In this case, a value of 3-4 mol O_3 consumed per mol C mineralized has been found.

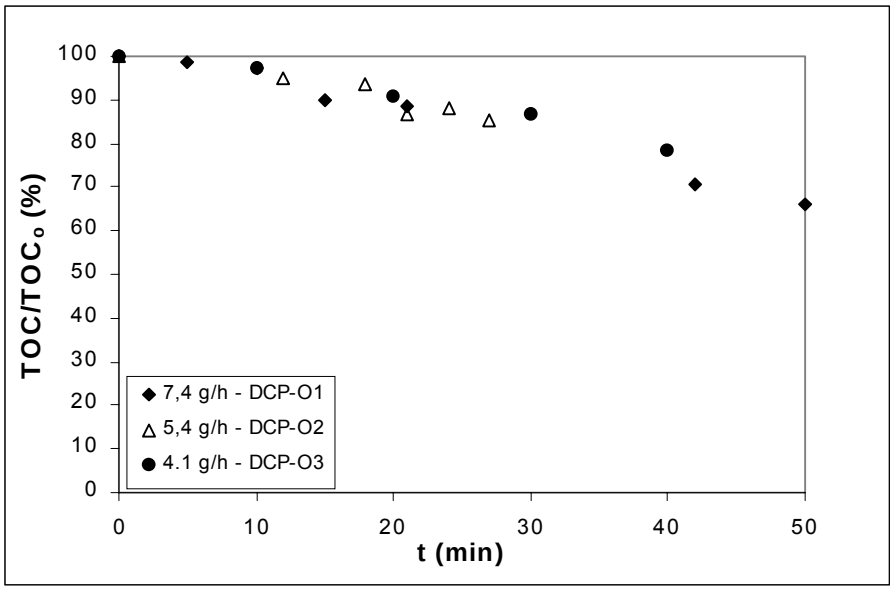

Graph 5.62. Influence of the ozone production on DCP ozonation – Normalized TOC

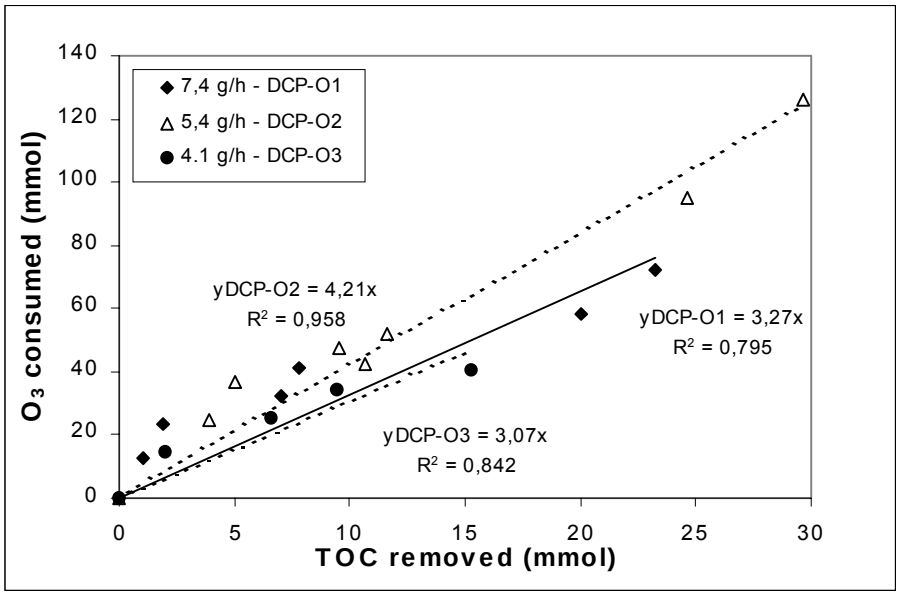

Graph 5.63. Stoichiometric coefficient for the removal of TOC on DCP ozonation

5.12.2. Ozonation at basic pH.

As mentioned in the NB section, pH is one of the most important variables in the ozonation processes, due to the catalytic action of the hydroxyl ion in the ozone decomposition (Staehelin and Hoigné, 1985):

$$O_3 + OH^- \rightarrow O_2^{\bullet} + HO_2^{\bullet} \qquad (k = 70\ M^{-1}.s^{-1}) \qquad [2.4]$$

In the present case, only pH 9 (0.01 M $Na_2B_4O_7$ (borax)) has been checked. Other pHs have not been tested because of the high amount of salts needed in the pilot plant. The production of ozone was set at 5.4 $g.h^{-1}$ and results are shown in section A1.9, Table DCP-O4.

Graph 5.64 shows the comparison of this experiment with the one carried out at free pH and with the same ozone production (DCP-O2) for the normalized DCP concentration. As it can be observed, the disappearance rate of DCP increases at basic pH. When increasing pH ozone starts to decompose and OH radicals are produced, which are stronger oxidants than ozone itself. Another process that occurs at higher pH is the dissociation of DCP to dichlorophenoxide ions, which can rapidly react with ozone by direct pathway. Hoigné and Bader (1983b) indicated that for many dissociating organic compounds, the rate of ozonation increases rapidly with the degree of dissociation. Because of the extremely fast reaction of the dichlorophenoxide ion, the overall reaction rate is accelerated rapidly with the solution pH. Benítez and co. (2000) estimated a value of 1569 $M^{-1}s^{-1}$ for the rate constant of ozone towards non-dissociated species and $6.1x10^8$ $M^{-1}s^{-1}$ for the dissociated species. Similar values have been lately publish by Qiu and co. (2002), who have determined a value of 3000 $M^{-1}s^{-1}$ for the rate constant of 2,4-DCP molecules against $7.7x10^8$ $M^{-1}s^{-1}$ for phenolate ions.

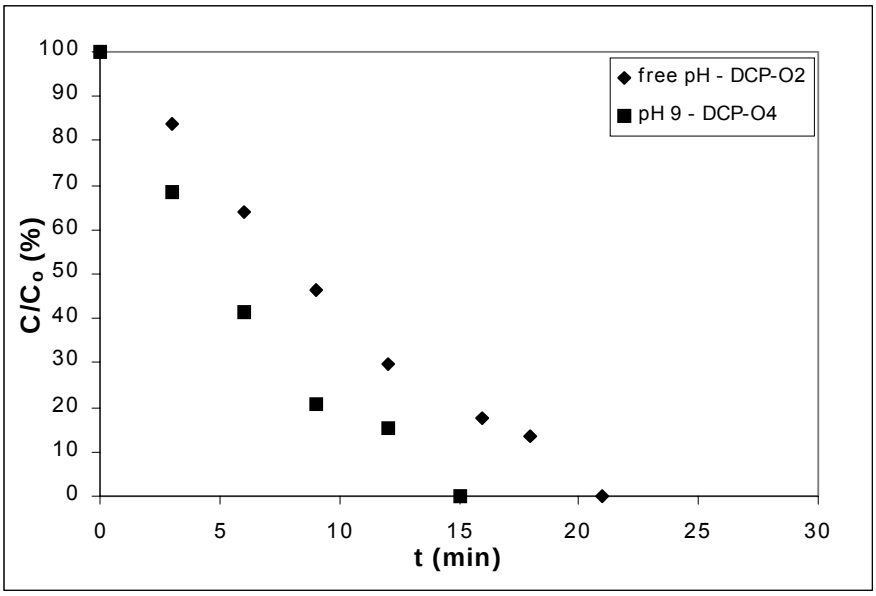

Graph 5.64. Comparison of the normalized DCP concentration evolution at basic and free pH by ozonation.

Regarding the concentration of residual ozone in the gas phase, at pH 9 practically no residual ozone was detected while DCP was still present in the solution, starting

increasing from that point (see Graph 5.65). Similar results can be expected for the concentration of dissolved ozone. As for TOC (Graph 5.66), an increase in the TOC removal rate was observed under basic conditions and at short reaction times.

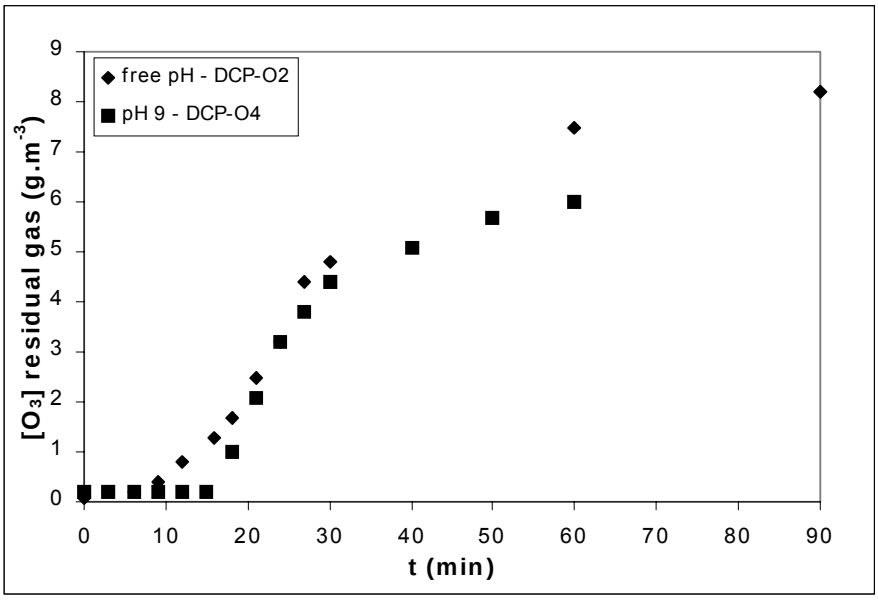

Graph 5.65. Influence of pH on the ozonation of DCP - Residual ozone.

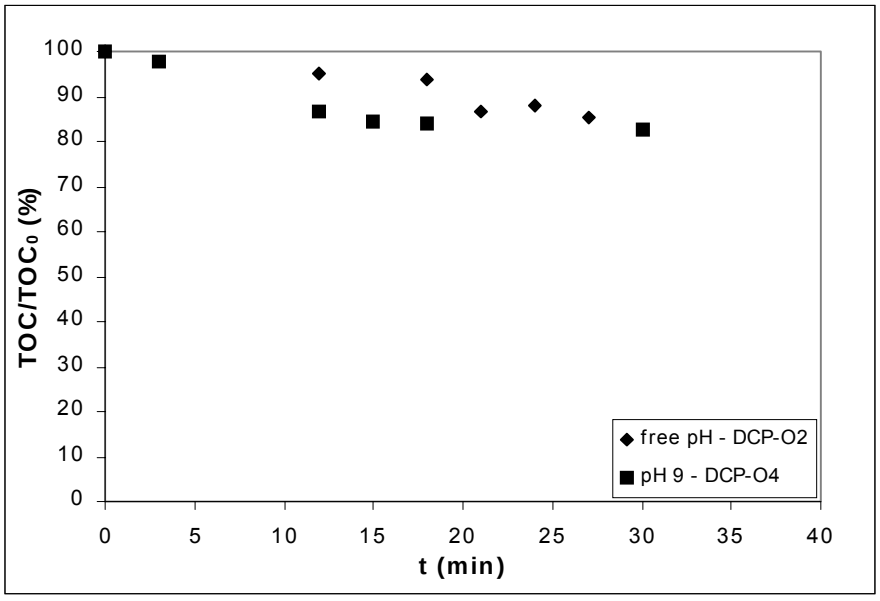

Graph 5.66. Comparison of the normalized TOC removal at basic and free pH by ozonation.

5.12.3. Influence of the initial concentration.

To check the effect of the initial concentration, two experiments with ca. 200 ppm as initial DCP concentration, room temperature and allowing the pH to evolve freely were carried out at ozone productions 5.4 and 7.4 $g.h^{-1}$ (see section A1.9, Table DCP-O5 and DCP-O6) and compared with experiments DCP-O2 and DCP-O1, respectively. The evolution of the normalized concentration versus time is shown in Graph 5.67. As already mentioned in the section 5.12.1, the DCP disappearance rate does not seem to depend on the ozone production, but decreases when the initial concentration is increased. It can be seen that at a certain reaction time (or equivalent absorbed ozone dose), an increase in the initial concentration diminishes the conversion, although the disappearance rate increases (see Graph 5.69).

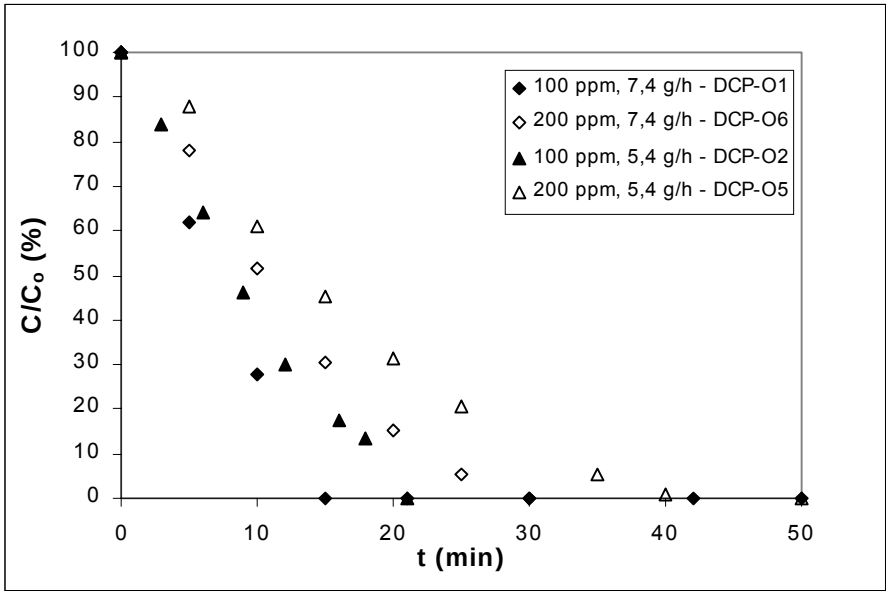

Graph 5.67. Influence of the initial concentration on DCP ozonation at two different ozone productions – Normalized concentration

The initial behavior of this process follows a pseudo-first order kinetics. By fitting the logarithm of the normalized concentration to a straight line (see Graph 5.68) it is obtained for the four experiments the pseudo-first order kinetic constants that are summarized in Table 5.11. Kinetic constants were found to be ca. 2 times higher for 100 ppm than 200 ppm. Compared to NB, they are ca. 3 times higher. Results are in good agreement with those previously reported in the literature (Trapido et al., 1997).

Table 5.11. Pseudo-first order kinetic constants as a function of the initial DCP concentration and the ozone production.

Initial DCP conc. ($mg.L^{-1}$)	Ozone production ($g.h^{-1}$)	k (min^{-1})
102	5.4	0.102
210	5.4	0.0541
87	7.4	0.122
193	7.4	0.0733

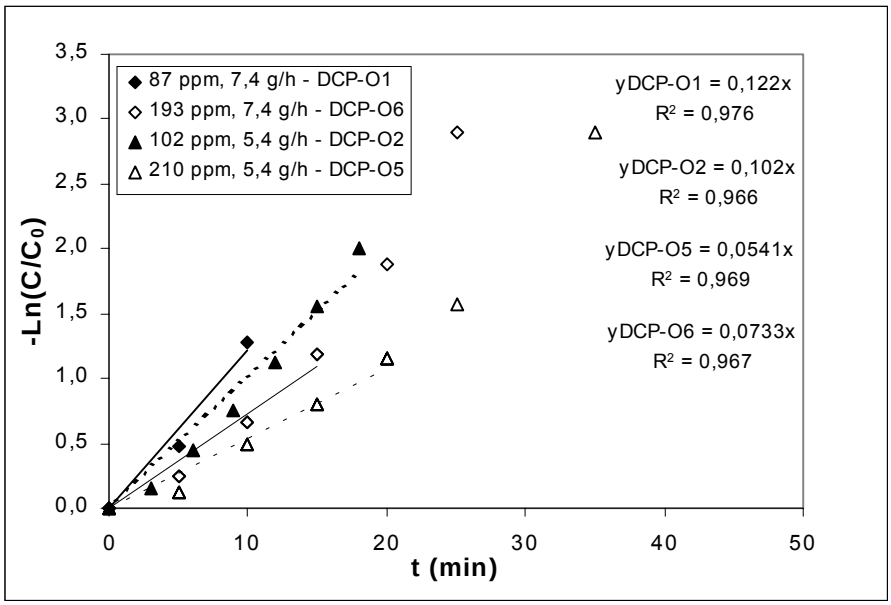

Graph 5.68. Influence of the initial concentration on DCP ozonation at two different ozone productions – Estimation of the pseudo-first order kinetic constants

With regard to the variation of the DCP removal rate as a function of time, it is possible to see that it depends on the initial concentration and slightly on the production of ozone, as it is shown in Graph 5.69: it increases with the concentration and with the ozone production. Table 5.12 summarizes the DCP removal rates and the stoichiometric coefficient calculated for each experiment.

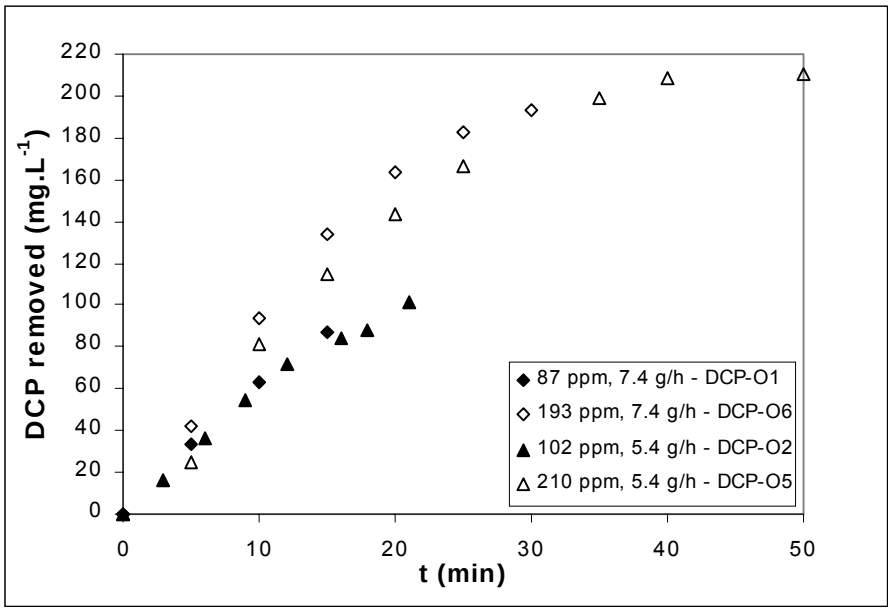

Graph 5.69. Influence of the initial concentration on DCP ozonation at two different ozone productions – DCP removal rate.

Table 5.12. Effect of DCP initial concentration on the initial removal rate of DCP by ozonation and calculation of stoichiometric coefficients.

Initial DCP conc. ($mg.L^{-1}$)	Ozone production ($g.h^{-1}$)	DCP removal rate ($mg.min^{-1}$)	Stoichiometric coefficient (mol O_3 cons/mol DCP rem)
102	5.4	109	2.71
210	5.4	148	2.23
87	7.4	127	2.90
193	7.4	180	2.55

With regard to residual ozone (Graph 5.70) during time, it can be observed that it decreases when increasing the initial concentration, as the amount of non-reacted ozone that leaves the system is smaller.

Graph 5.71 shows the evolution of the normalized TOC with the absorbed ozone dose. It seems to be almost independent of the production of ozone. The TOC removal rate decreases when increasing the initial DCP concentration. The amount of TOC removed during time allows us to calculate the mineralizing rate, which is summarized in the Table 5.13 with the stoichiometric coefficient (mol of ozone consumed per mol of carbon mineralized). Previous studies (Esplugas et al., 1994; Kuo, 1999) indicated that the rate of mineralization of chlorophenols followed apparent first-order kinetics as expressed by equation [5.17]

$$-\frac{dTOC}{dt} = k_{TOC} TOC \qquad [5.17]$$

Accordingly, the degradation rate of DCP was expressed by the apparent first-order rate constant on the basis of TOC removal, and listed in Table 5.13 as well (see Graph 5.72). These kinetic constants are found to be in the same order of magnitude than those reported by Kuo (1999).

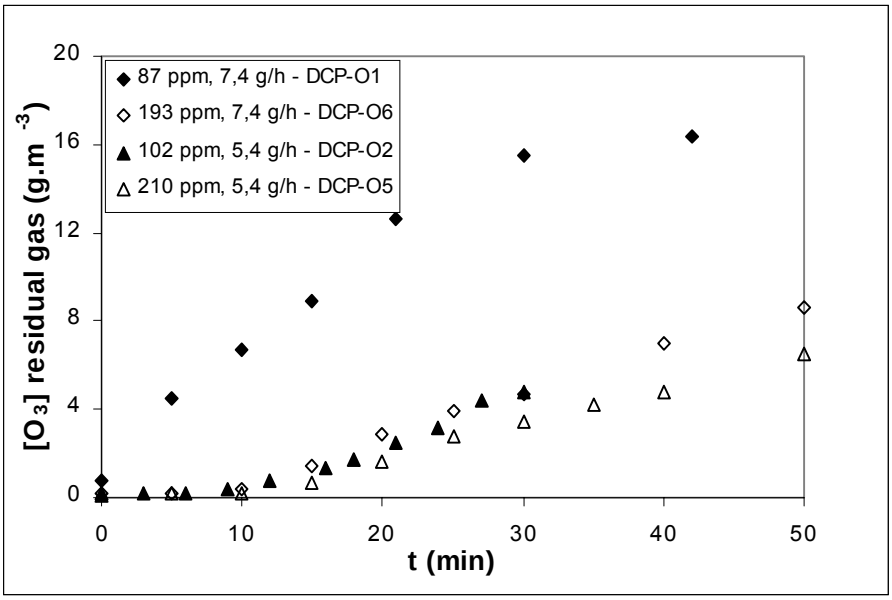

Graph 5.70. Influence of the initial concentration on DCP ozonation at two different ozone productions – Residual ozone.

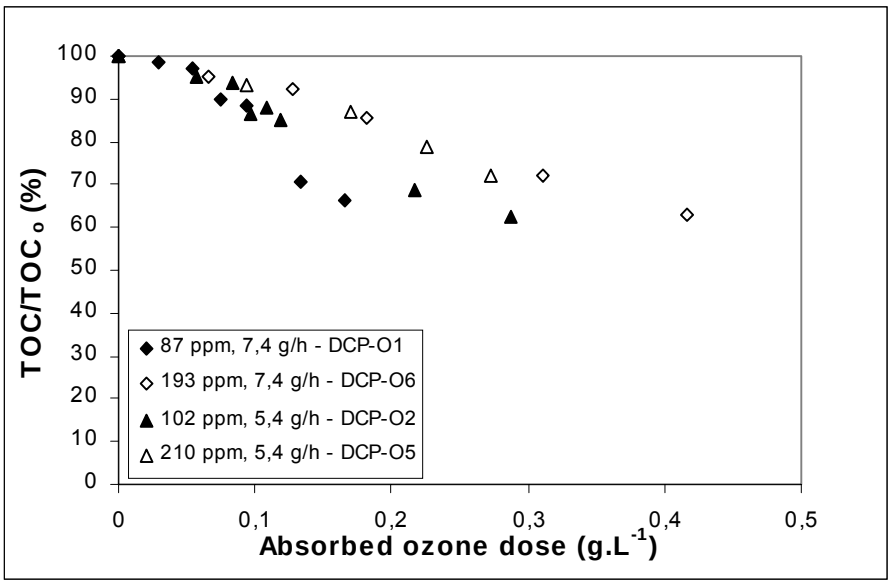

Graph 5.71. Influence of initial concentration on DCP ozonation at two different ozone productions – Normalized TOC

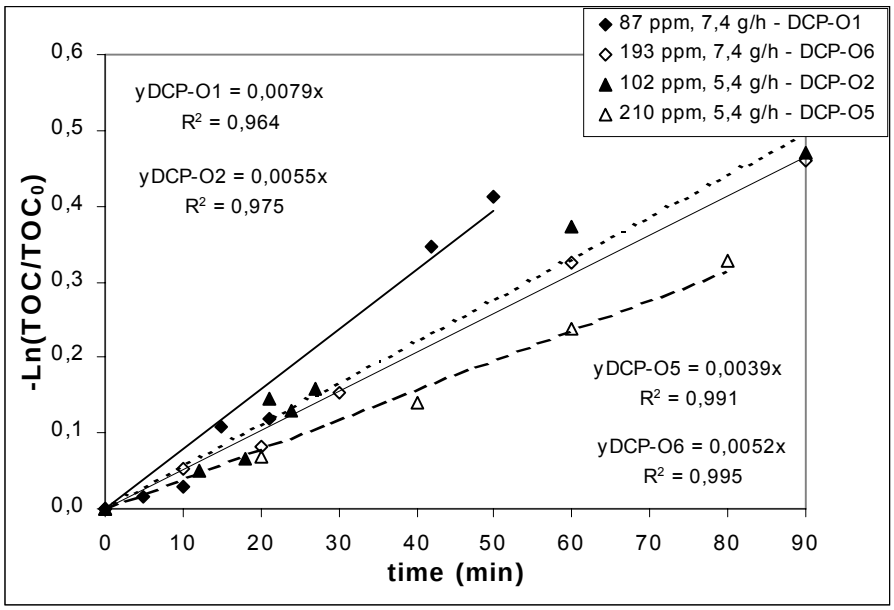

Graph 5.72. Influence of the initial concentration on DCP ozonation at two different ozone productions – Estimation of TOC apparent first-order kinetic constant

Table 5.13. Effect of DCP initial concentration on the mineralization rate of DCP by ozonation and estimation of stoichiometric coefficients.

Initial DCP conc. ($mg.L^{-1}$)	Ozone prod. ($g.h^{-1}$)	Mineralization rate ($mg\ C.min^{-1}$)	k_{TOC} (min^{-1})	Stoichiometric coefficient (mol O_3 cons/mol C rem)
102	5.4	4.36	0.0055	4.21
210	5.4	6.74	0.0039	3.11
87	7.4	5.44	0.0079	3.27
193	7.4	7.88	0.0052	3.38

5.12.4. Influence of hydroxyl radical scavengers: t-BuOH.

As previously commented, in the ozonation processes, the attack of ozone can be undertaken directly (direct attack) or through its decomposition into hydroxyl radicals (radical pathway). In this sense, one experiment in presence of tert-butanol, which does not react with ozone (Hoigné and Bader, 1983a published a value for the kinetic constant of the direct reaction of ozone with t-BuOH of $3x10^{-2}\ M^{-1}.s^{1}$) at room temperature, free pH and 5.4 $g.h^{-1}$ ozone production (see section A1.9, Table DCP-O7) was carried out to compare with the experiment carried out at the same conditions without t-BuOH (DCP-O2). The concentration of t-butanol used is 3 $mmol.L^{-1}$, from data presented by Hoigné and Bader (1983b). Ozone could be partially consumed by reaction with t-BuOH at high concentrations of this compound, although the kinetic constant value is very low. As it can be observed in Graph 5.73, the presence of t-BuOH does not inhibit the disappearance

rate of DCP. This fact may suggest that the main mechanism of ozone attack at this pH is the direct one. As for the residual ozone, the addition of t-BuOH increases the amount of non-reacted ozone (see Graph 5.74). That is, less amount of ozone is decomposed into OH radicals. If OH radicals are produced but no difference is observed in the DCP removal rate, this fact would confirm that the direct ozone attack is the main pathway. Hautaniemi et al. (1998) also found that ozonation at low pH proceed through the reactions with molecular ozone.

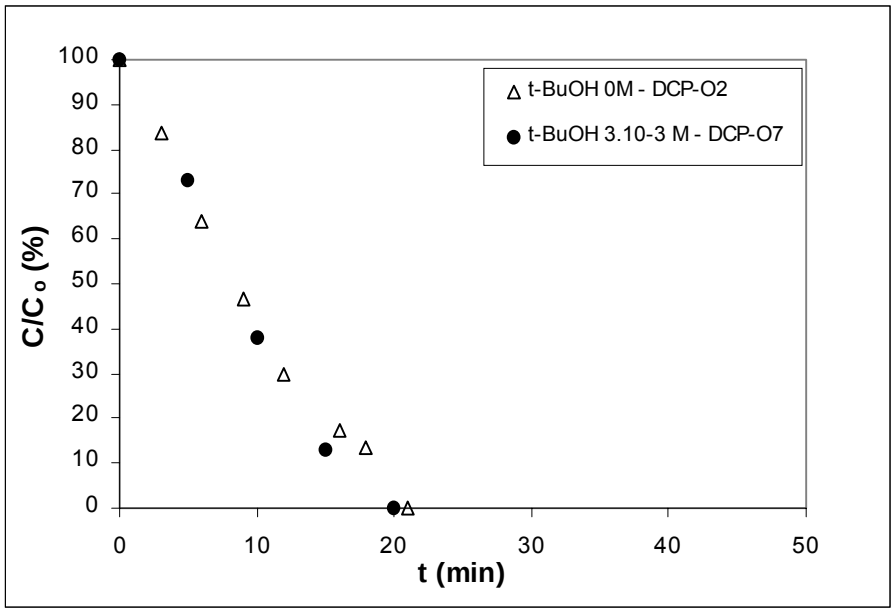

Graph 5.73. Influence of t-BuOH as radical scavenger on DCP ozonation – Normalized concentration

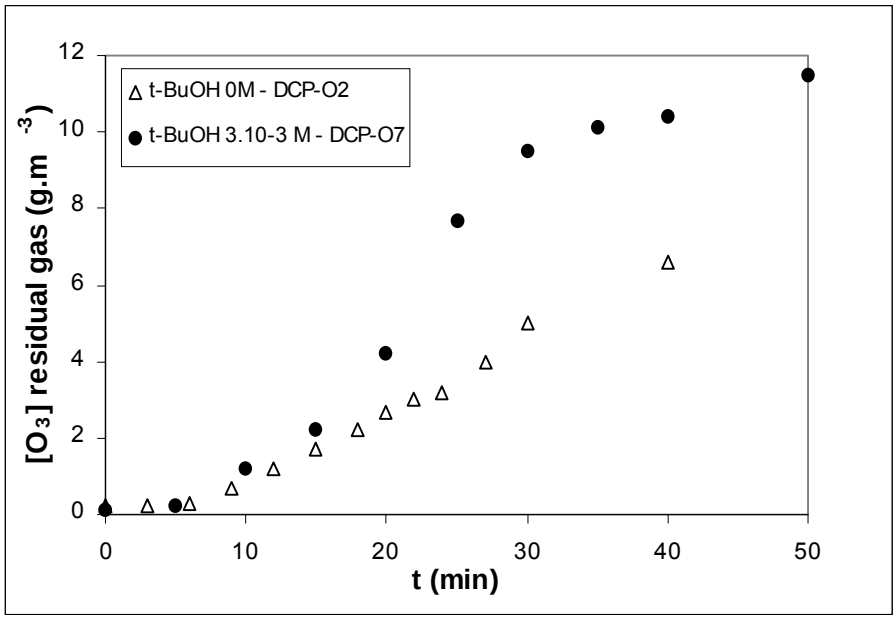

Graph 5.74. Influence of t-BuOH as radical scavenger on DCP ozonation – Residual ozone.

5.12.5. Influence of the ozonation pre-treatment on the biodegradation of DCP.

First of all, a BOD test was performed to a 100-ppm DCP aqueous solution, determining that BOD_5 and BOD_{21} were 0. That is, the substrate was non-biodegradable under the tested conditions. Besides this, the same inhibition test that was carried out with NB has been performed with DCP. Graph 5.75 presents the results of the inhibition test carried out with DCP. As it can be observed, even at 1:1000 dilution (0.1 ppm, 6.13×10^{-4} mmol.L^{-1}) the biological oxidation is clearly inhibited by the presence of DCP and total inhibition occurred at 1:10 dilution. In light of these results, a 100-ppm DCP solution cannot be easily degraded biologically and exhibits a strong inhibition of the biodegradation of other carbon sources.

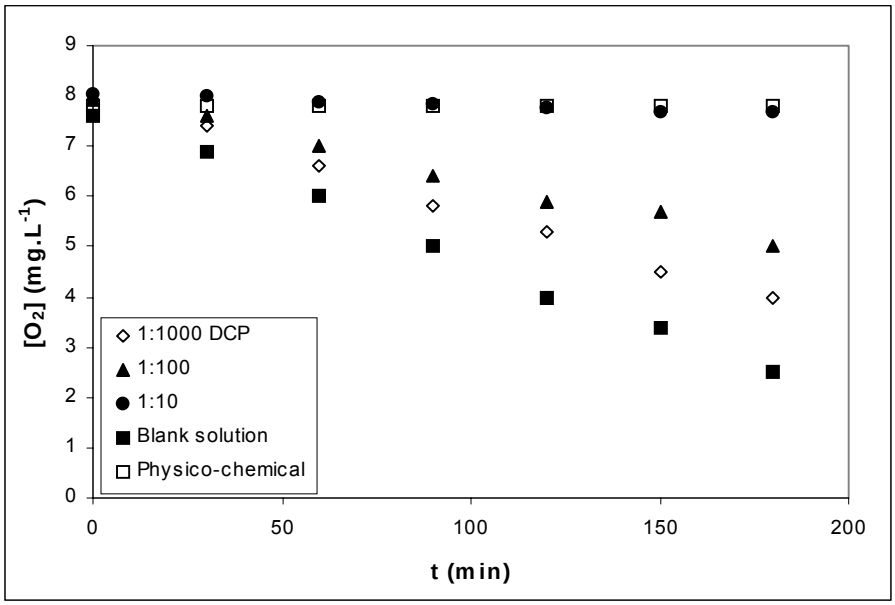

Graph 5.75. Inhibition test of a 100-ppm DCP solution at dilutions 1:1000, 1:100 and 1:10.

This section is divided into two parts. In the first one, the effect of ozonation on the biodegradability of aqueous solutions of DCP has been studied. BOD/COD and BOD/TOC ratios have been chosen as biodegradability indicators and the average oxidation state has been used to indicate changes on the degree of oxidation throughout the process. Results are presented in section A1.9, Tables DCP-O8 to DCP-O13. Experiments have been repeated several times, as BOD and COD are analytical methods of intrinsic error. The average of these experiments is summarized in Table DCP-O14 and these results are those presented in the following graphs. In the second part, biodegradation of the pre-ozonated solution has been carried out in two semi-continuous stirred tank reactors (with non-acclimated sludge and with previously acclimated to phenol sludge) at different

hydraulic retention times. Kinetic studies based on the Monod model have also been developed.

a) Results of ozonation experiments and BOD tests

The ozone production in the pilot plant was set at 5.4 $g.h^{-1}$, as this production allowed us to follow the concentration of the target compound. Results have been plotted versus the absorbed ozone dose. As it can be observed in Graph 5.76, DCP is completely removed after an ozone dose of 0.12 $g.L^{-1}$ (corresponding to ca. 30 minutes of ozonation treatment). At this moment, only 14% of TOC has been depleted. The biodegradability of the solution has been tested throughout the experiment. BOD/COD and BOD/TOC ratios have been chosen as biodegradability indicators, as commented before.

BOD has been measured at 5, 10 and 21 days. Values obtained are plotted versus the ozone dose in Graph 5.76. As it can be noticed, BOD increases considerably when the concentration of DCP is less than 10% of the initial amount, obtaining the highest value at the point that all DCP has been depleted from the solution. This behavior could be attributed to two reasons:

- Inhibition exerted by remaining 2,4-DCP prevents the biodegradation of oxidation by-products and/or
- by-products formed at initial time are not easily biodegradable, requiring further oxidation to achieve products of higher biodegradability, by which time most of the target compound has been eliminated.

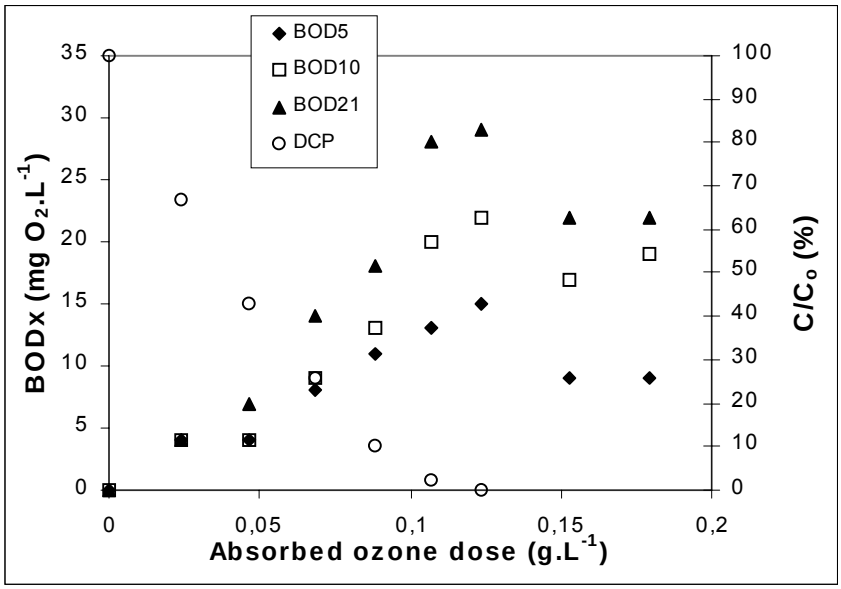

Graph 5.76. Evolution of BOD and DCP normalized concentration with the absorbed ozone dose on DCP ozonation

BOD_x/COD and BOD_x/TOC ratios are shown on Graphs 5.77 and 5.78, respectively. As it can be observed, both ratios increase substantially in the range between 0.09 and 0.12 $g.L^{-1}$ absorbed ozone dose, being 0.25 and 0.4 for BOD_5/COD and BOD_5/TOC after an ozone dose of 0.12 $g.L^{-1}$, respectively (0.48 and 0.77 for the same ratios at 21 days). As a reference, a BOD/COD ratio of 0.4 is generally considered the cut-off point between biodegradable and difficult to biodegrade waste.

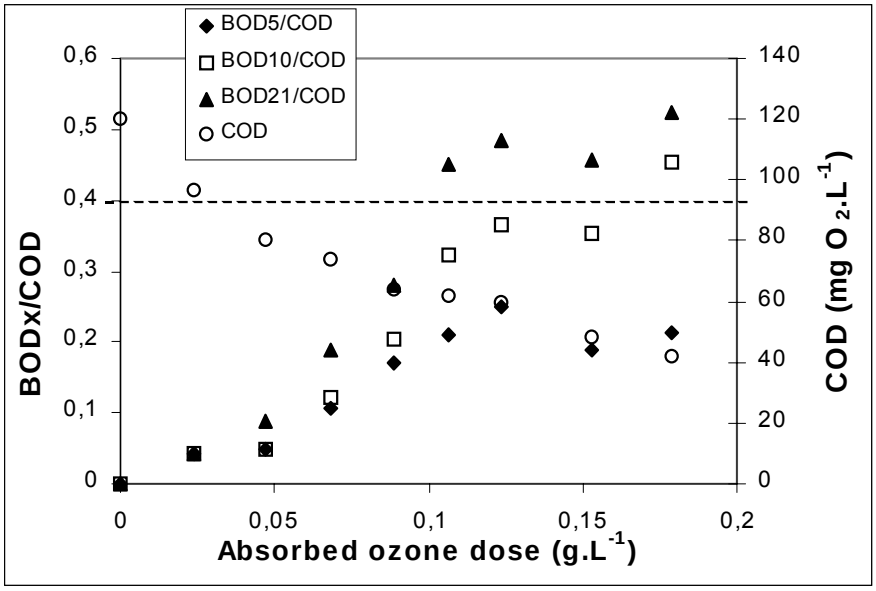

Graph 5.77. Changes in BOD_X/COD ratio and COD with the absorbed ozone dose on DCP ozonation

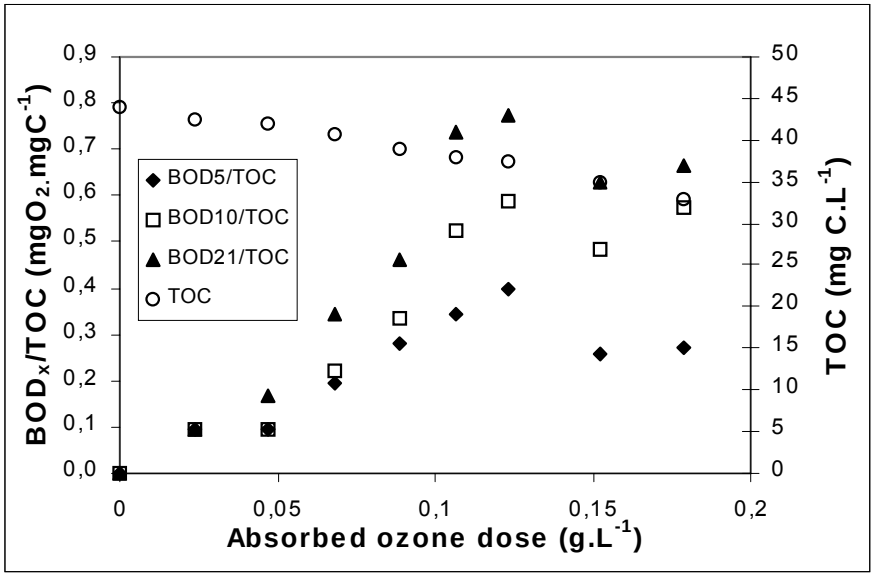

Graph 5.78. Changes in BOD_x/TOC ratios and TOC with the absorbed ozone dose on DCP ozonation

In light of the experimental results, optimal ozonation time was set at between 25-30 minutes, when DCP completely disappears. As it can be seen in section 5.18 (Figures 5.7 and 5.8), chlorobenzoquinone has been identified among the intermediates. This compound was found to disappear after 25 minutes of treatment. At this time, less than 5% of the initial DCP was present. Among the remaining compounds after 25 minutes, resorcinol is thought to have been identified. The depletion of DCP and chlorobenzoquinone may account for the increase of biodegradability, as both compounds may be inhibitory for the other carbon sources.

COD/TOC yields interesting information on how chemical substances in the effluent become more oxidized, meaning lower ratios higher degree of oxidation (for alkanes this parameter ranges theoretically between 4 and 5.3 and very oxidized substances such as oxalic acid yield a degree of 0.6, provided of course there are no other oxidizable elements such as sulphur or nitrogen) (Marco et al., 1997). This ratio was found to decay considerably (44% after an ozone dose of 0.12 $g.L^{-1}$, see Graph 5.79), meaning that organic substances present in the solution have a higher degree of oxidation.

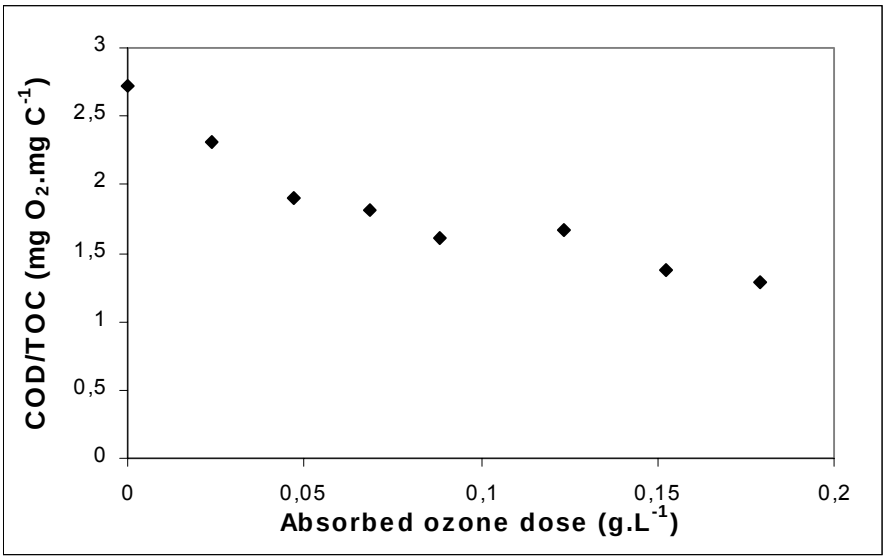

Graph 5.79. COD/TOC evolution with the absorbed ozone dose on DCP ozonation

Changes of the average oxidation state of the organic carbon during the ozonation process are also presented in Graph 5.80. Oxidation state of the organic carbon can be calculated from the equation [5.9]. Three stages may be found in the ozonation process. The first one (values below 0) is very short, meaning that DCP reacts rapidly with ozone and forms hidroxylated aromatics, aldehydes and unsaturated carboxylic acids. In stage 2 (below 2), almost all the aromatic compounds, aldehydes and unsaturated carboxylic

acids are converted to saturated carboxylic acids, such as formic acid and oxalic acid. At the point that all the DCP has been removed from the solution, the oxidation state is found to be 1.5. In the third stage, saturated carboxylic acids, like formic and oxalic, comprise the appreciable amount of TOC that still remains in solution, as this compounds are quite resistant to ozone.

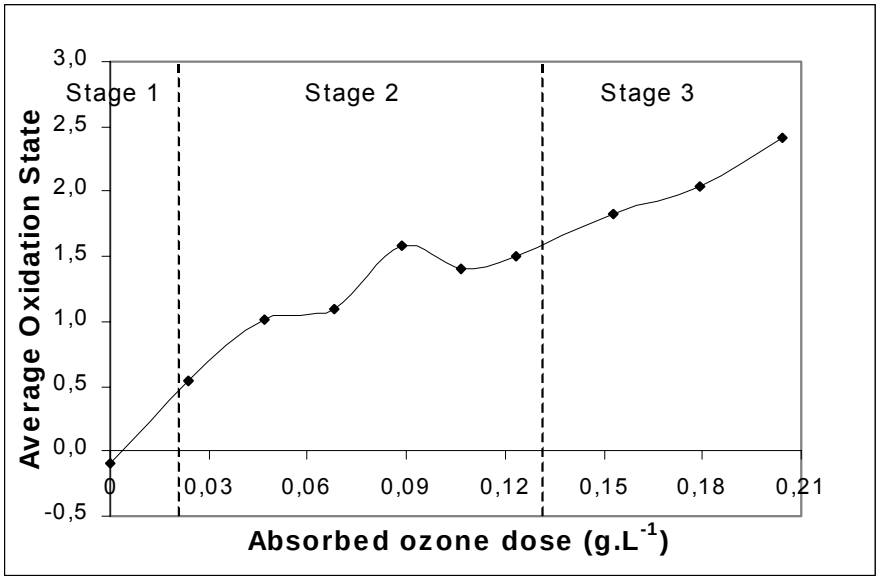

Graph 5.80. Effect of ozone dose on the oxidation state of DCP by ozonation

Inorganic chloride was formed continuously during the ozonation, thereby proving that dechlorination takes place in the oxidation processes. The concentration of chloride ion increased linearly during the first 30 minutes of treatment (see Table DCP-O10) and continued after the complete disappearance of initial DCP. For 94% of DCP conversion, the achieved degree of dechlorination has been found to be 54% and at a 100% of DCP conversion (30 minutes of treatment), 70% (Graph 5.81, Table DCP-O9), indicating the presence of chlorinated intermediates. These results are in concurrence with Trapido et al. (1997), who reported a 62% dechlorination for a 97% of DCP conversion.

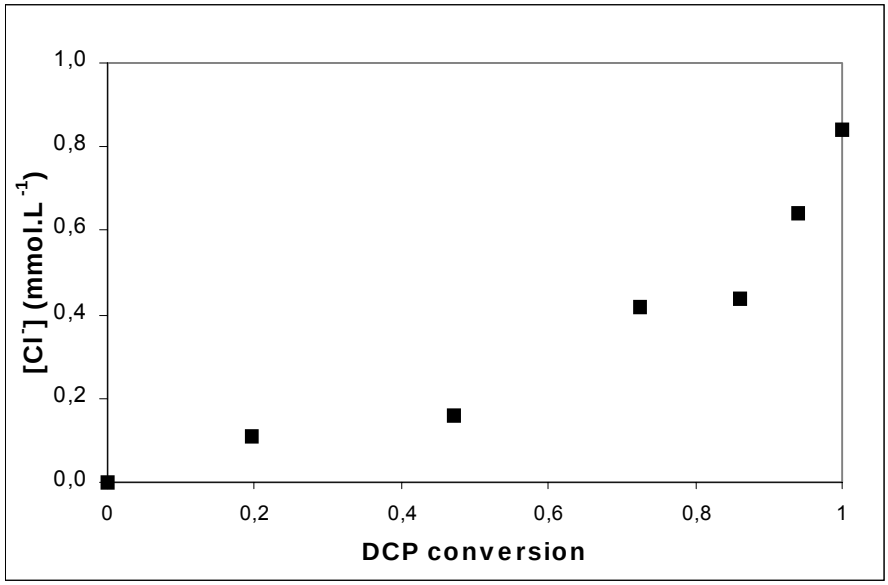

Graph 5.81. Variation of chloride ion with the conversion of DCP on DCP ozonation

b) Aerobic biological degradation of pre-ozonated solution.

From results presented above, it was decided to fix an ozonation treatment time of 30 min, corresponding to an absorbed ozone dose of 0.12 $g.L^{-1}$, when DCP was completely removed. This solution was feed to two biological reactors, one with activated sludge coming from the waste water treatment plant in Gavà (Barcelona) and one with biomass previously acclimated to phenol, which has similar chemical structure to probable formed intermediates and it is known to be slightly biodegradable (BOD_5/COD ratio for 100-ppm aqueous phenol solution was found to be 0.12 by Ben Abderrazik et al., 2002).

1. Acclimated to phenol reactor

1.5 $g.L^{-1}$ of activated sludge was acclimated for 10 days to a 100-ppm phenol solution as sole carbon source. Then, the pre-treated solution, mixed with the 100-ppm phenol solution, was fed to the reactor in different percentages and at different HRTs (hydraulic retention times). This percentage was increased progressively until achieving 100% of the pre-ozonated solution as sole carbon source. Table 5.14 shows a summary of the acquired data for each of the tested conditions, once the reactor was assumed to be in steady state. Results presented show the average of data compiled through the cycle (between brackets, number of samples) and the error calculated for a 95% confidence level by means of standard deviation and T student. Graph 5.82 shows the evolution of initial TOC (TOC_i, after feeding the reactor), final TOC (TOC_f) and TOC removed (TOC_r) for 100% of pre-treated solution and HRT of 12 hours. Similar graphs have been obtained for the other conditions tested (results not shown). It can be observed in Table 5.14 that since the first conditions studied there was a TOC removal of 38% up to

a 88% for the mixture 70/30. The percentage of TOC removal increased with the organic load rate (OLR). When feeding 100% of the pre-treated solution the percentage of final TOC increased slightly. Further investigation has to be carried out to test the optimal reactor configuration.

Table 5.14. Summary of experimental results with acclimated to phenol reactor

Feed (% phenol/ /% pret. sol)	HRT (days)	OLR (mg $C.L^{-1}.day^{-1}$)	TOC_i (mg$C.L^{-1}$)(1) (# samples)	TOC_f (mg$C.L^{-1}$)(1) (# samples)	% TOC removal
80/20	10	9.4	21.51 ± 1.75 (3)	13.32 ± 1.47 (3)	38.08
80/20	5	16.0	18.07 ± 0.7 (3)	4.15 ± 0.17 (3)	77.03
80/20	2	36.5	36.73 ± 2.16 (4)	4.57 ± 0.73 (4)	87.56
70/30	2	34.5	34.73 ± 0.98 (4)	4.10 ± 0.16 (4)	88.19
50/50	2	27.1	26.59 ± 1.35 (4)	5.65 ± 0.61 (4)	78.75
30/70	2	20.7	22.71 ± 0.5 (3)	6.04 ± 0.03 (3)	73.40
0/100	2	16.4	22.13 ± 1.2 (11)	12.28 ± 0.76 (19)	44.51
0/100	1	30.5	30.8 ± 0.78 (6)	12.77 ± 0.63 (6)	58.54
0/100	0.5	65.6	32.66 ± 1.13 (8)	17.05 ± 0.94 (8)	47.80

(1) Error has been calculated for a 95% confidence level

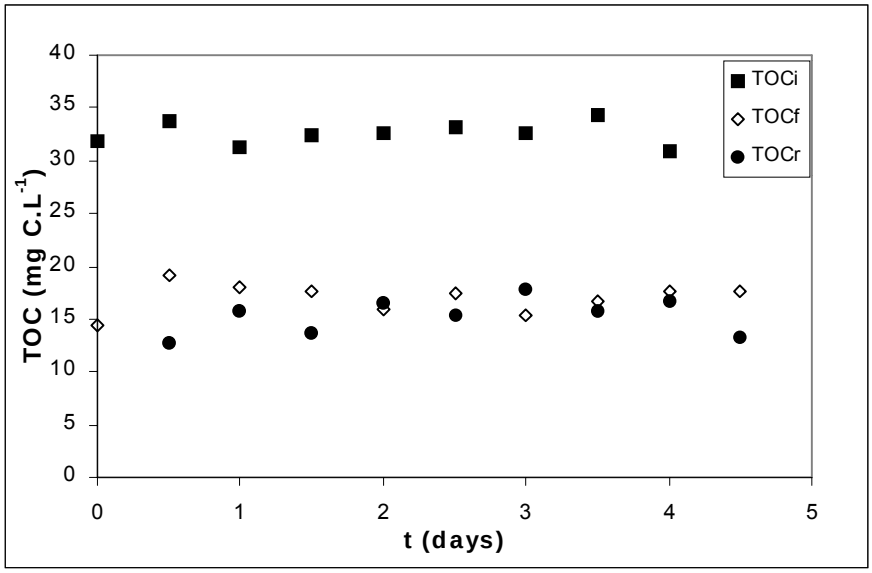

Graph 5.82. Initial, final and removed TOC for the acclimated reactor operating at 100% of pre-treated solution and HRT = 12 hours.

2. Activated sludge reactor

Activated sludge of this reactor was not previously acclimated to phenol. 1.5 $g.L^{-1}$ of sewage sludge as inoculum and a mixture of municipal waste water and our pre-treated solution was used as feeding mixture at different percentages and at different HRTs. This percentage was also increased until achieving 100% of the pre-ozonated solution. As with the acclimated reactor, Table 5.15 shows a summary of the compiled data for each of the tested conditions, once the reactor was assumed to be in steady-state. It can be seen that since the first studied conditions there was a TOC removal of 32%. For a HRT of 2 days it was found a ca. 80% of TOC removal for the different percentages of mixture tested (see Graph 5.83). That would offer the possibility of co-digesting the pre-ozonated effluent together with a municipal waste water at different percentages of mixture. Regarding feeding 100% of the pre-treated solution, the percentage of TOC removal decreased, but for HRT of one day it was found to be ca. 70%. That means that the reactor can work at short HRTs, being those similar to municipal waste water plants. At HRT of 12 h, final TOC increased lightly, meaning that a fraction of this solution could not be biodegraded within 12 hours. As in the previous case, further investigation has to be carried out regarding the reactor configuration and non-biodegradable intermediates. Nevertheless, better results have been obtained with the non-acclimated reactor, meaning that sludge coming from a municipal waste water plant could be suitable for the treatment of the pre-ozonated solutions. Graph 5.84 shows the evolution of initial TOC (TOC_i, after feeding the reactor), final TOC (TOC_f) and TOC removed (TOC_r) for 100% of pre-treated solution and HRT of 12 hours. Similar graphs have been obtained for the other conditions tested (results not shown).

Table 5.15. Summary of experimental results with the non-acclimated reactor

Feed (% w.w. / % pret. sol)	HRT (days)	OLR (mg $C.L^{-1}.day^{-1}$)	TOC_i ($mgC.L^{-1}$)(1) (# samples)	TOC_f ($mgC.L^{-1}$)(1) (# samples)	% TOC removal
80/20	10	19.5	21.62 ± 2.09 (5)	14.69 ± 1.42 (8)	32.05
80/20	5	33.4	40.61 ± 6.79 (4)	13.55 ± 1.68 (4)	66.63
80/20	2	55.6	54.72 ± 4.68 (6)	9.73 ± 0.81 (6)	82.22
70/30	2	55.2	56.18 ± 3.80 (8)	11.38 ± 0.75 (12)	79.74
50/50	2	46.2	51.32 ± 3.73 (6)	10.84 ± 1.23 (7)	78.88
30/70	2	21.9	47.42 ± 0.86 (3)	9.44 ± 0.38 (5)	80.09
0/100	2	15.2	18.88 ± 0.56 (4)	8.64 ± 1.08 (5)	54.24
0/100	1	28.2	25.66 ± 1.38 (7)	8.29 ± 1.10 (7)	67.69
0/100	0.5	55.6	28.36 ± 1.59 (7)	14.32 ± 1.39 (5)	49.51

(1) Error has been calculated for a 95% confidence level

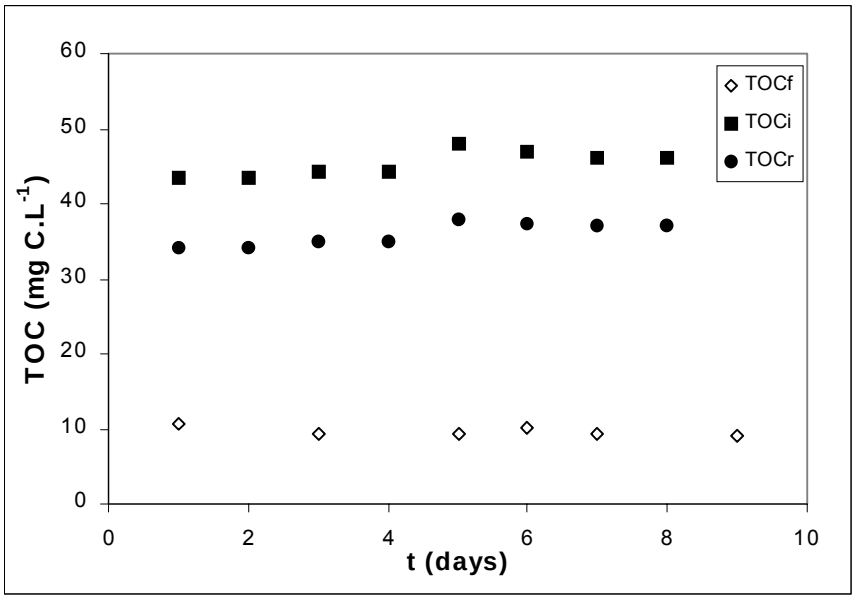

Graph 5.83. Initial, final and removed TOC for the non-acclimated reactor operating with the mixture 30% w.w / 70% pret.sol and HRT = 2 days.

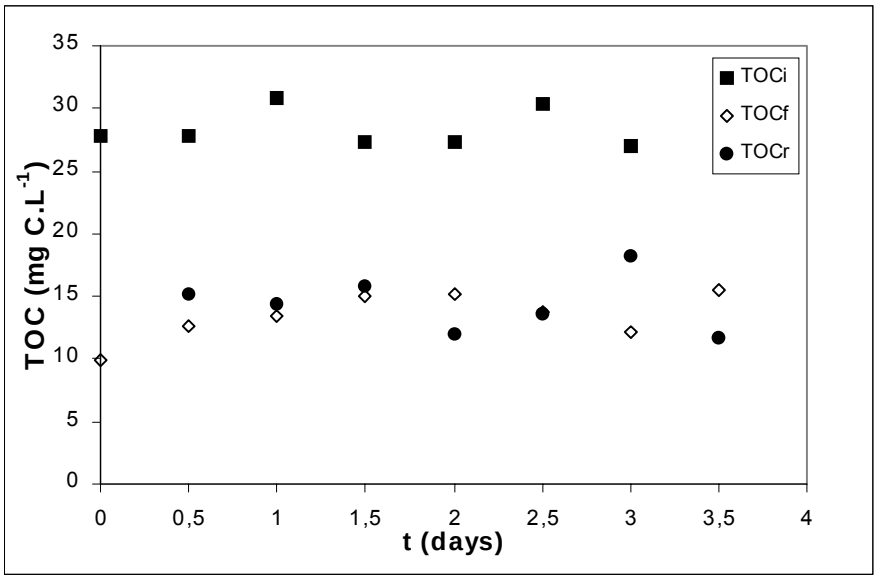

Graph 5.84. Initial, final and removed TOC for the non-acclimated reactor operating at 100% of pre-treated solution and HRT = 12 hours.

Graph 5.85 shows the percentage of TOC removal for mixtures 50/50 and 30/70 w.w./pre-treated solution with 2 days of HRT, and 100% pre-treated solution at HRT of 2 days, 1 day and 12 hours. As it can be seen, the mixtures ww/pre-ozonated solution show a high percentage of TOC removal, offering a good possibility of co-digesting the pre-ozonated DCP effluent together with a municipal waste water. Biological reactor can

perform with 100% pre-treated solution, achieving a TOC removal up to 80% for HRT 1 day.

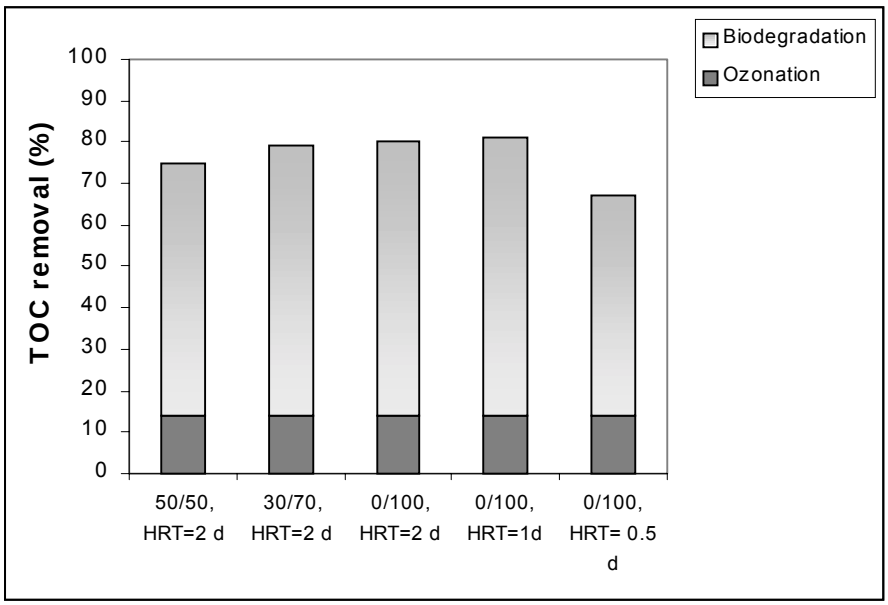

Graph 5.85. TOC removal by means of the combined ozonation-biological degradation of different mixtures w.w./pre-treated DCP solution and different HRT

3. Kinetic study

Monod (1949) has been the most widely kinetic model used to describe the processes of aerobic degradation of compounds dissolved in wastewaters, in absence of inhibition, which can be expressed as:

$$-\frac{1}{X}\frac{dS}{dt} = \frac{k\,S}{k_S + S} \qquad [5.18]$$

where X is the concentration of biomass (g of TVSS.L^{-1}), S is the concentration of substrate which can be biodegraded by the biomass (DOC in the present case), k is the substrate utilization constant and k_s is the saturation constant.

Chudoba (1990) showed that a zero order kinetic described the single-component substrate removal very satisfactorily. But it was unsuitable for a multicomponent substrate removal, which was found to be described by a first-order kinetic. Assuming that the intermediates formed in the pre-ozonization process follow Monod model and that the evolution of DOC with time follows a first-order kinetic (as the obtained solution is a muticomponent system, meaning that $k_{s(DOC)}$ >> DOC), the kinetic equation will be:

$$-\frac{1}{X}\frac{dDOC}{dt} = k_{DOC}\frac{DOC}{k_{s(DOC)} + DOC} = \frac{k_{DOC}}{k_{S(DOC)}}DOC = k'_{DOC}\,DOC \qquad [5.19]$$

where k'_{DOC} is a function of the biomass activity given by a physiological state of microorganisms.

Graphs 5.86 to 5.89 shows results for the kinetic study. Other kinetic models derived from linearizations of Monod model have been tested, but results showed no good agreement with the proposed models. By using equation [5.19], two different kinetics have been found in the non-acclimated reactor when HRT was 2 days, indicating that one part of the effluent could be more easily biodegraded. Studies carried out with 100% pre-treated solution in both reactors show a good r^2 value, as it can be observed in Graphs 5.88 and 5.89, however the associated errors have shown to be rather high. In those cases, only one zone was observed. Table 5.16 summarizes the values obtained for k'_{DOC} for the tested conditions with both reactors. As it can be observed, kinetic constants of the same order of magnitude were found for acclimated and non-acclimated sludge working at the same HRT. Values for the non-acclimated reactor were slightly higher than the acclimated (e.g., 0.69 and 0.80 L.g $TSS^{-1}.h^{-1}$ for the acclimated and non-acclimated, respectively, and HTR of 12 h). The explanation for this behavior might be that the chemical structure of the ozonation by-products is different from phenol, being better accepted by the activated sludge which has not been exposed to phenol before.

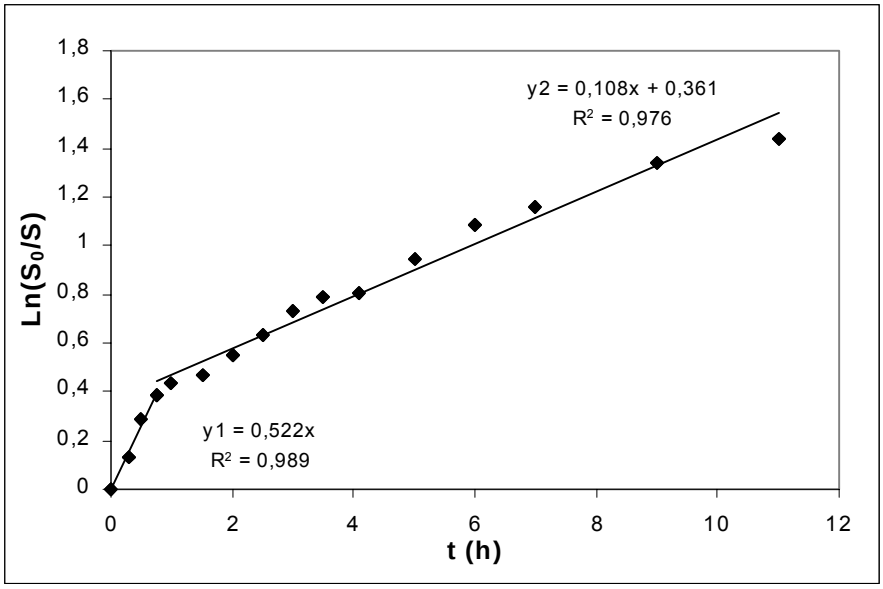

Graph 5.86. Kinetic study of the biodegradation of the 50/50 solution carried out in the non-acclimated reactor. Conditions: T = 22ºC, pH ≈ 7.2, TVSS = 0.37 $g.L^{-1}$, HRT = 2 days

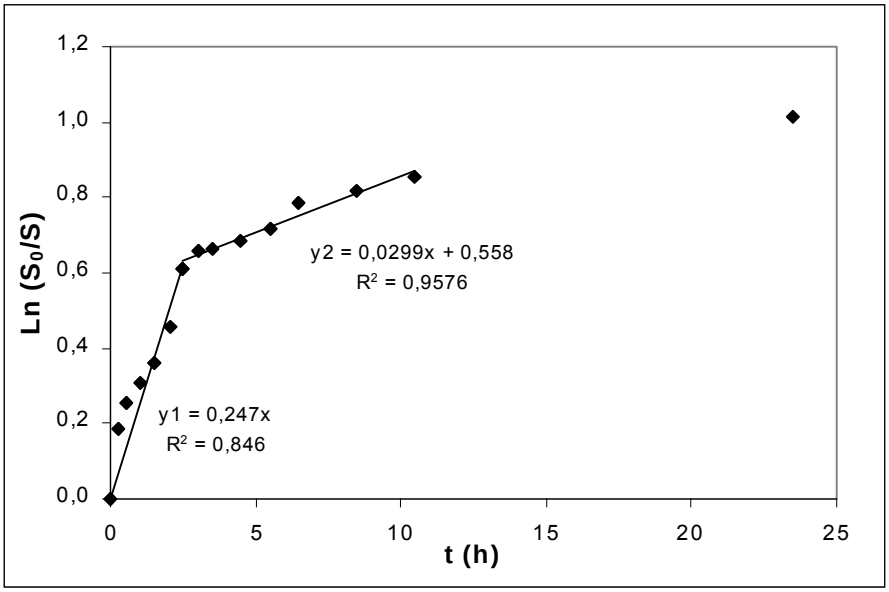

Graph 5.87. Kinetic study of the biodegradation of 100% pre-treated solution carried out in the non-acclimated reactor. Conditions: T = 22ºC, pH ≈ 7.2, TVSS = 0.21 g.L^{-1}, HRT = 2 days

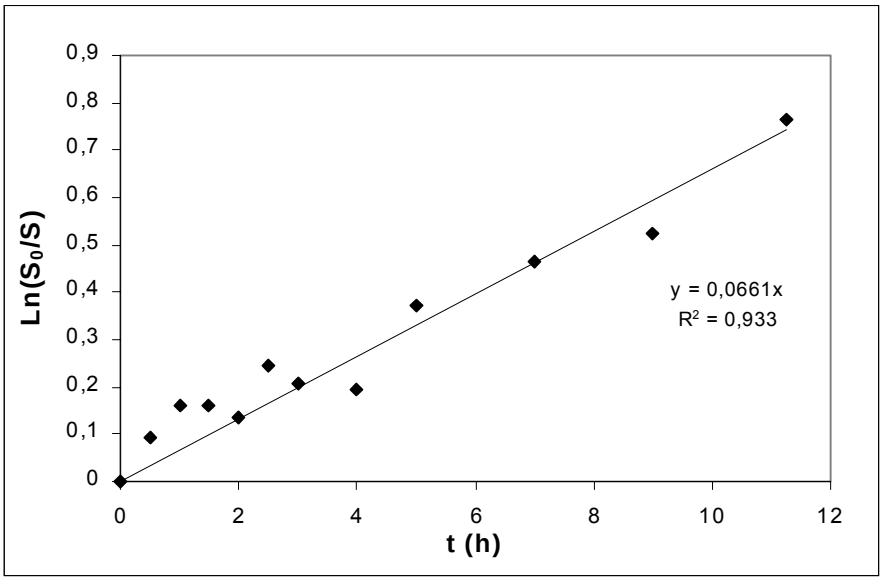

Graph 5.88. Kinetic study of the biodegradation of 100% pre-treated solution carried out in the non-acclimated reactor. Conditions: T = 21ºC, pH ≈ 7.2, TVSS = 0.1 g.L^{-1}, HRT = 1 day

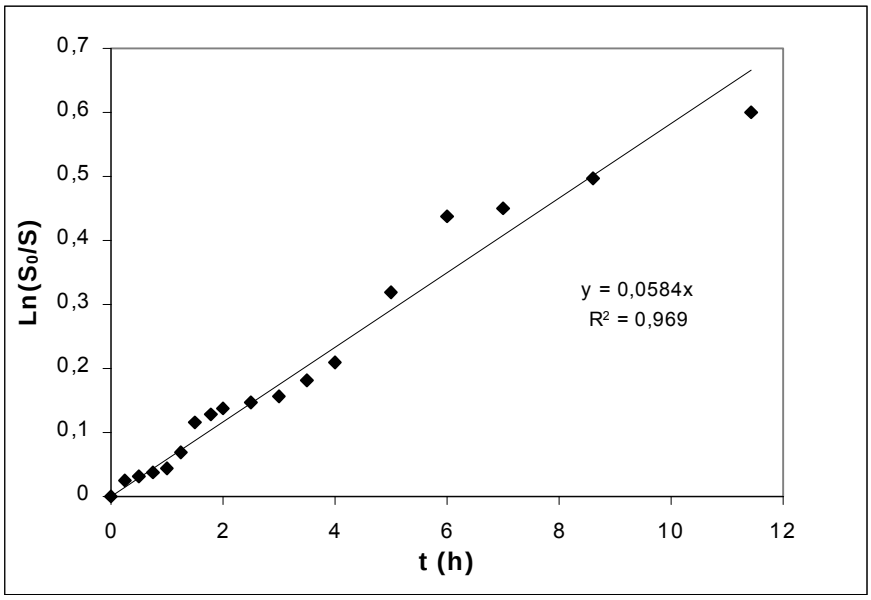

Graph 5.89. Kinetic study of the biodegradation of 100% pre-treated solution carried out in the acclimated reactor. Conditions: T = 22ºC, pH ≈ 7.2, TVSS = 0.11 g.L^{-1}, HRT = 1 day

Table 5.16. Kinetic constants of the biodegradation of pre-ozonated solution

REACTOR	HRT (Days)	k'_{DOC} (L.g TVSS^{-1}.h^{-1}) (r^2) (1st part)	k'_{DOC} (L.g TVSS^{-1}.h^{-1}) (r^2) (2nd part)
Acclimated (0/100)	1	0.531 (0.96)	-
Acclimated (0/100)	0.5	0.693 (0.97)	-
Non-acclimated (50/50)	2	0.522 (0.99)	0.108 (0.98)
Non-acclimated (0/100)	2	0.247 (0.85)	0.0299 (0.96)
Non-acclimated (0/100)	1	0.661 (0.93)	-
Non-acclimated (0/100)	0.5	0.796 (0.90)	-

5.13. Ozonation combined with H_2O_2 (O_3 / H_2O_2) for DCP removal

The characteristic of this process is that in slow kinetics conditions, the main step for the production of hydroxyl radicals is the reaction between ozone and the ionic form of hydrogen peroxide ([1.13]) enhancing, at least theoretically, the oxidation rate. Since in section 5.12.4 has been seen that the radical mechanism does not have influence in the degradation of DCP at free pH, therefore it is not expected that the addition of H_2O_2 significantly enhances the process, but it is desirable to check its influence in the biodegradability of DCP solutions.

$$O_3 + HO_2^- \rightarrow O_3^{\cdot} + HO_2^{\cdot} \qquad [1.13]$$

5.13.1. Influence of H_2O_2 concentration

In the set of experiments DCP-OP1 to DCP-OP3, the effect of the addition of hydrogen peroxide at different mol H_2O_2/mol DCP ratios has been studied. The comparison of the normalized concentration during time with the experiment of single ozonation carried out at the same conditions (DCP-O14) is shown in Graph 5.90. As it was expected, only a slight increase of the disappearance rate has been observed.

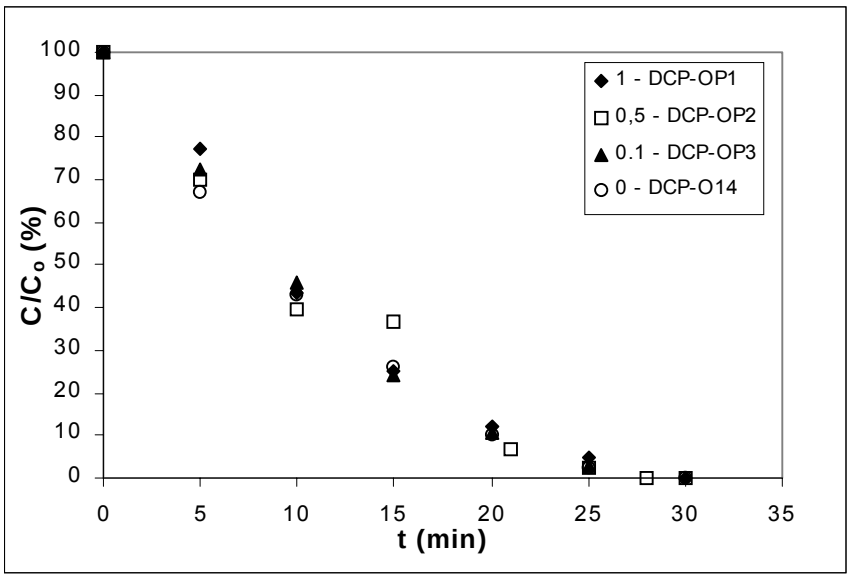

Graph 5.90. Influence of the addition of H_2O_2 to DCP ozonation – Normalized concentration.

With regard to TOC, the addition of H_2O_2 significantly increases the mineralization rate, more as higher is its concentration and at longer times (see Graph 5.91). That means that although not affecting the disappearance rate of DCP, the addition of H_2O_2 improves the degradation of the intermediates formed. This point is confirmed with the

data of dissolved ozone. As it can be observed in Graph 5.92, the concentration of residual dissolved ozone is greatly reduced when H_2O_2 is added to the system, meaning that more ozone is being decomposed.

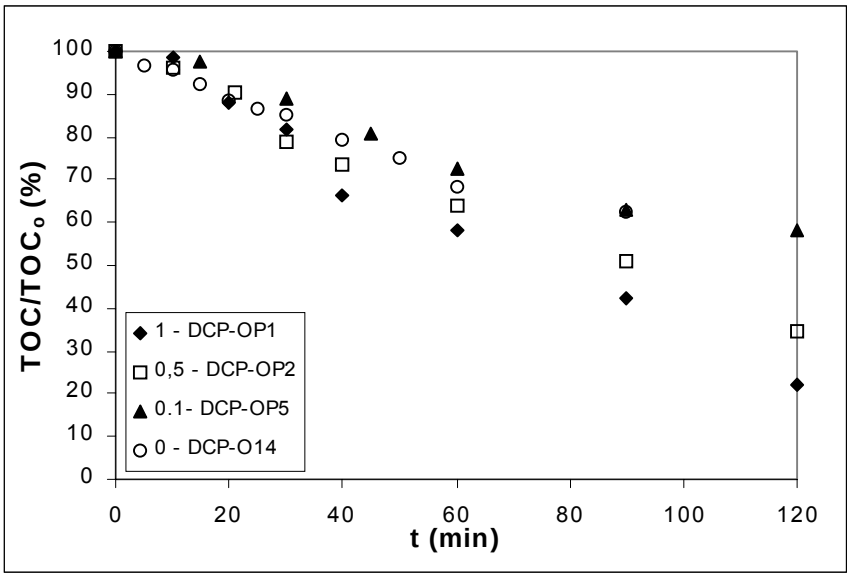

Graph 5.91. Influence of the addition of H_2O_2 to DCP ozonation – Normalized TOC

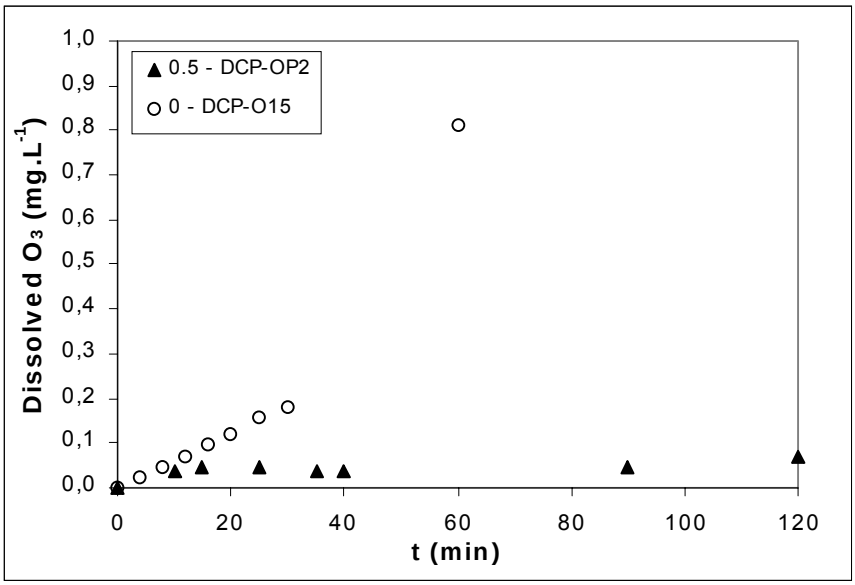

Graph 5.92. Influence of the addition of H_2O_2 to DCP ozonation – Dissolved ozone.

Graph 5.93 illustrates data of residual hydrogen peroxide for the experiments with 0.5 and 0.1 mol H_2O_2/mol DCP. The concentration of H_2O_2 has been measured by means of a Quantofix (Macherey-Nagel) peroxide test in the range 0-100 mg H_2O_2 .L^{-1}. In view of these results, it has been decided to perform the biodegradability study with the 0.1 ratio

(Baldry (1983) reported that H_2O_2 is bactericide at concentrations above 0.15 mmol.L^{-1} , 5.1 mg.L^{-1}).

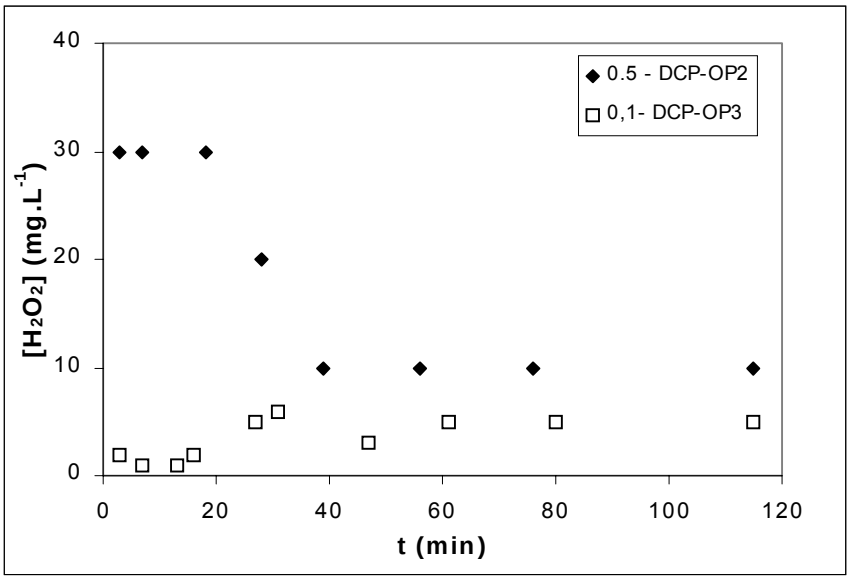

Graph 5.93. Concentration of residual H_2O_2 for the experiments with 0.5 and 0.1 mol H_2O_2/ mol DCP in the O_3/H_2O_2 process

5.13.2. Biodegradability study

Two experiments with 0.1 mol H_2O_2/mol DCP were performed (see section A1.10, Tables DCP-OP3 and DCP-OP4) and the average values of these two experiments are summarized in Table DCP-OP5. As in the previous section, the AOS will be used to follow changes on the degree of oxidation throughout the process and BOD/COD and BOD/TOC ratios are used as biodegradability indicators.

AOS changes are presented and compared with the experiment of single ozonation carried out at the same conditions (DCP-O14) in Graph 5.94. No significant differences have been found with regard to single ozonation, although it seems that the degree of oxidation starts increasing earlier and gives the impression to stabilize at longer times, meaning that no further oxidation could be achieved although increasing the ozonation time.

BOD values achieved by this combination are similar to those achieved by single ozonation (see Graph 5.95). Unlike this one, the BOD values do not reach a maximum when DCP disappears from solution, until after 45 minutes of treatment (16 mg O_2.L^{-1}). BOD/COD ratios are analogous to those found for single ozonation (see Graph 5.96)

however a difference is observed in the value at 45 minutes. BOD_5/COD ratio is increased from 0 to 0.3 after 45 minutes of treatment.

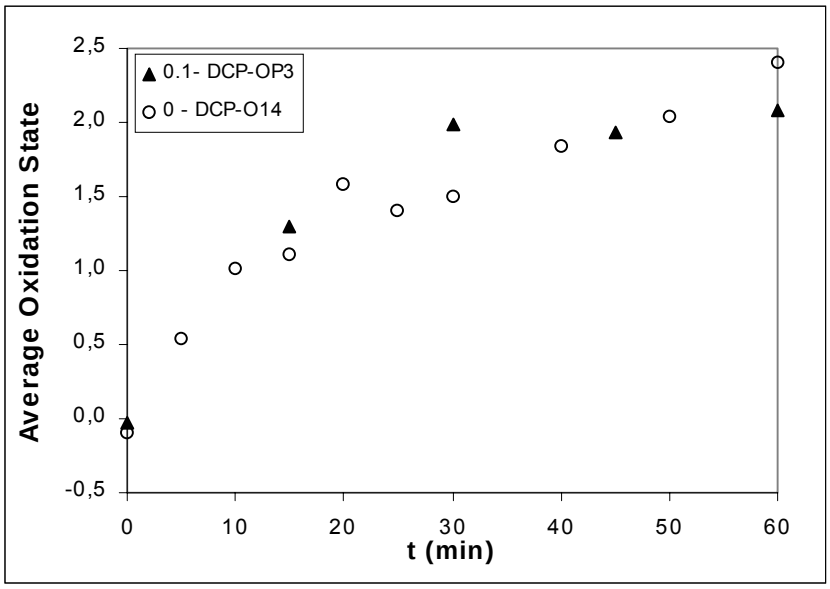

Graph 5.94. Effect of the addition of H_2O_2 to DCP ozonation – Average oxidation state.

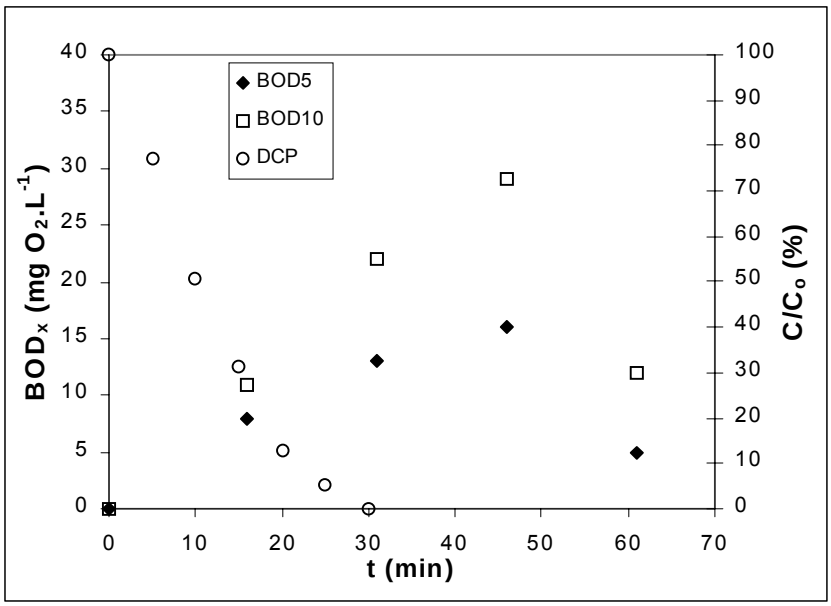

Graph 5.95. Evolution of BOD and DCP normalized concentration during time at 0.1 mol H_2O_2/mol DCP in the O_3/H_2O_2 process

BOD/TOC values are shown in Graph 5.97. Analogous to BOD/COD ratio, values are similar to those obtained by single ozonation during the first 30 minutes. BOD_5/TOC ratio increases from 0 to 0.55 after 45 minutes of treatment.

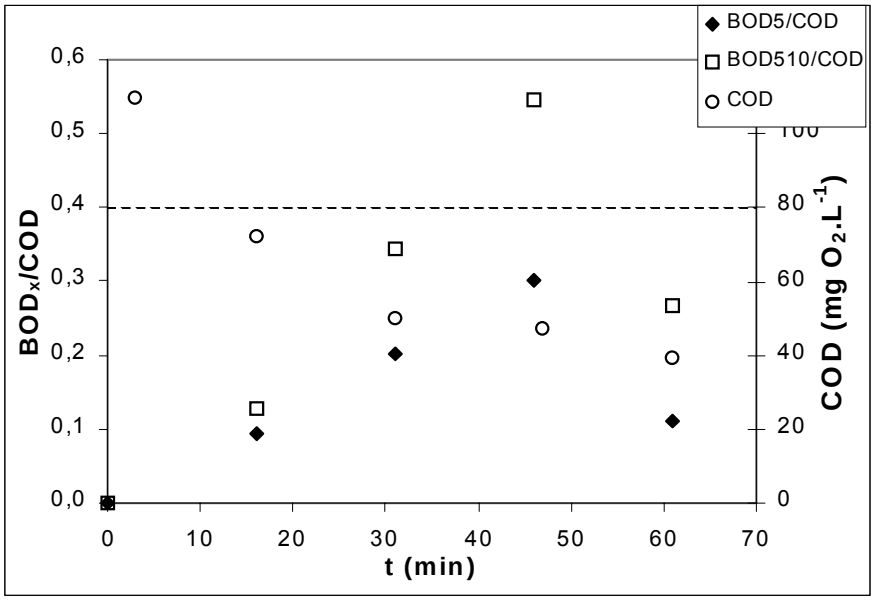

Graph 5.96. Evolution of BOD/COD ratio and COD during time at 0.1 mol H_2O_2/mol DCP in the O_3/H_2O_2 process

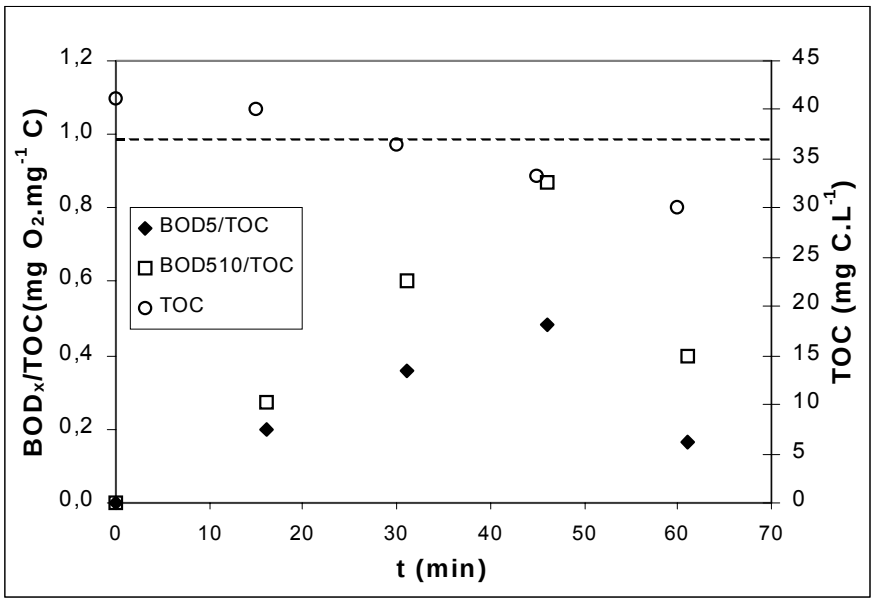

Graph 5.97. Evolution of BOD/TOC ratio and TOC during time at 0.1 mol H_2O_2/mol DCP in the O_3/H_2O_2 process

5.14. Ozonation combined with UV (O_3/UV) for DCP removal

Just as in the process O_3/H_2O_2, the combination O_3/UV increases the production of hydroxyl radicals and possible ways to eliminate the pollutant. Besides the reactions of the ozonation process, the photolysis of ozone, DCP and those derived of the presence of hydrogen peroxide are present (see section 1.3.6.2.3). As for the combination O_3/H_2O_2, its influence in the biodegradability of DCP solutions warrants further study. The effect of an increase of the initial DCP concentration has also been studied.

5.14.1. Influence of initial DCP concentration.

Two experiments with ca. 100 and 200 ppm were performed with the combination O_3/UV, 5.4 $g.h^{-1}$ ozone production, room temperature and allowing the pH to progress freely (see Tables DCP-OR1 and DCP-OR2, respectively). The evolution of the normalized concentration vs. the treatment time is presented in Graph 5.98. The initial behavior of the process follows a pseudo-first order kinetics. By fitting the logarithm of the normalized concentration to a straight line (Graph 5.99) the pseudo-first order kinetic constants have been obtained, with values (shown in the graph) lower than those by single ozonation. Trapido et al. (1997) also reported that UV-radiation decelerated the ozonation of DCP at pH=2.5. Hautaniemi et al. (1998) found that the degradation rate of chlorophenols was not enhanced either by the combination of ozone with UV radiation compared with ozonation alone at pH=2.5.

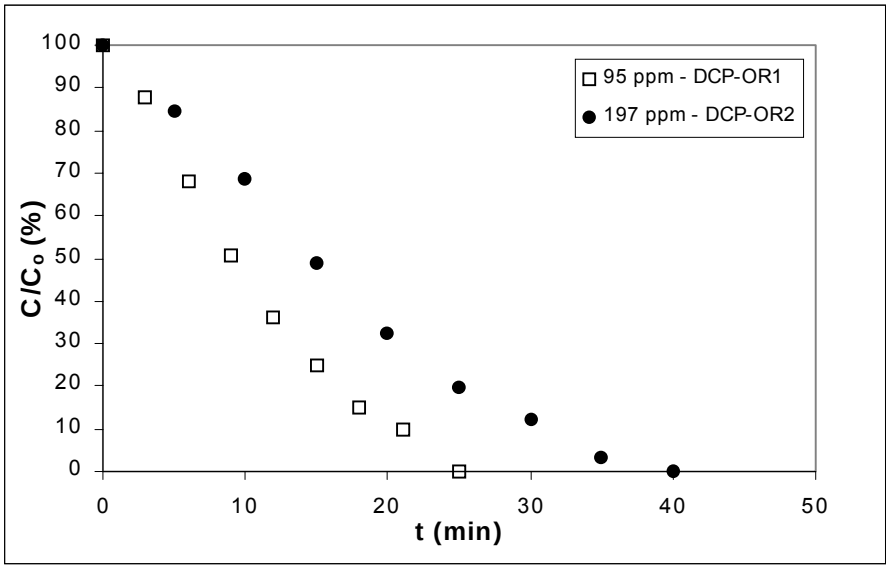

Graph 5.98. Influence of the initial concentration in the removal of DCP by O_3/UV – Normalized concentration

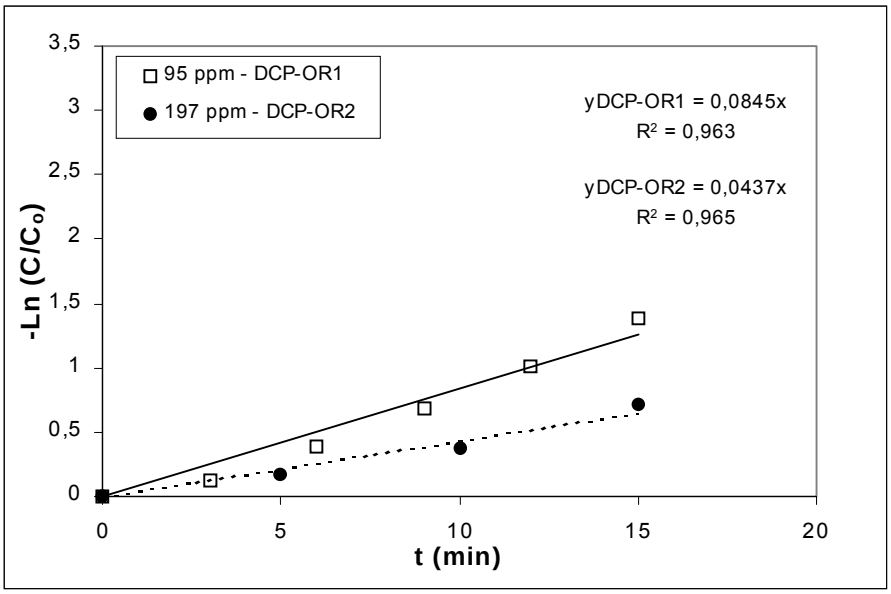

Graph 5.99. Estimation of the pseudo-first order kinetic constants for DCP removal by O_3/UV

Concerning the DCP removal rate, it is found to increase with the initial concentration, and values are also similar to those obtained by single ozonation (109 and 139 $mg.min^{-1}$ for DCP-OR1 and DCP-OR2, respectively). By representing the ozone consumed versus the amount of DCP removed, a stoichiometric coefficient of 3 has been obtained for 100 ppm initial concentration in comparison with 2.7 obtained by single ozonation.

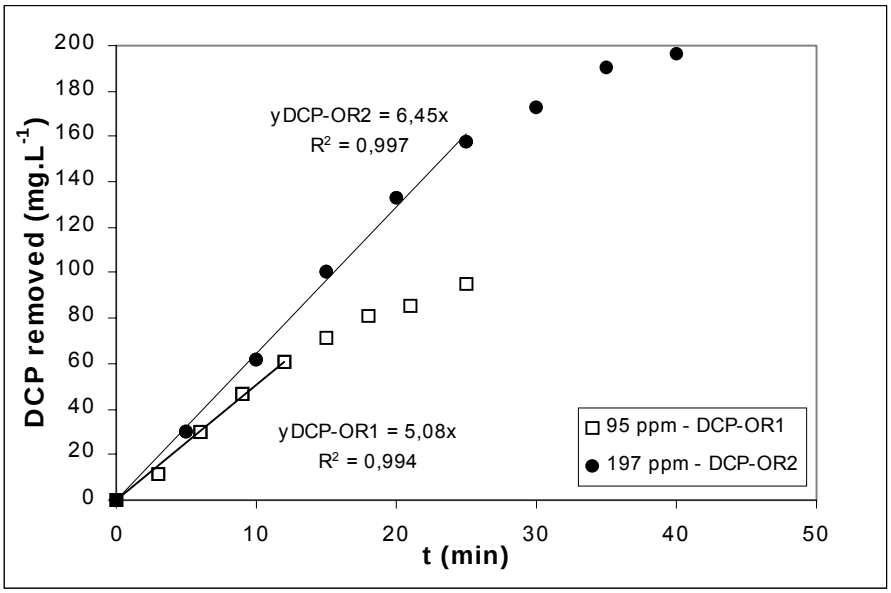

Graph 5.100. DCP removal rate by the combination O_3/UV

As regards to the concentration of residual ozone in the off-gas (Graph 5.101), it was found to increase when the initial concentration decreases, as less ozone reacts in the system.

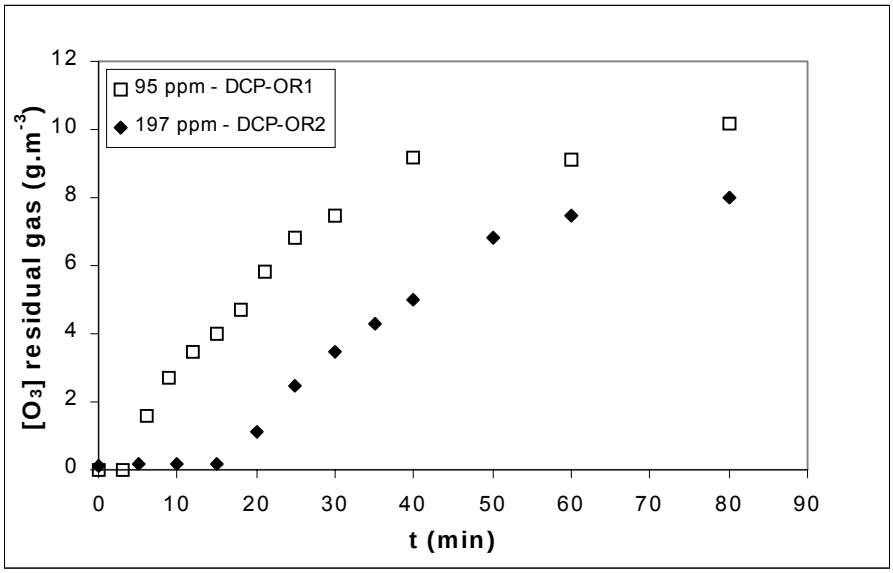

Graph 5.101. Influence of the initial concentration in the removal of DCP by O_3/UV – Residual ozone

However, the concentration of residual dissolved ozone for the experiment DCP-OR3 has been compared with the experiment with single ozonation (DCP-O15) and found to be slightly lower (Graph 5.102), as more ozone is being decomposed by the action of the light.

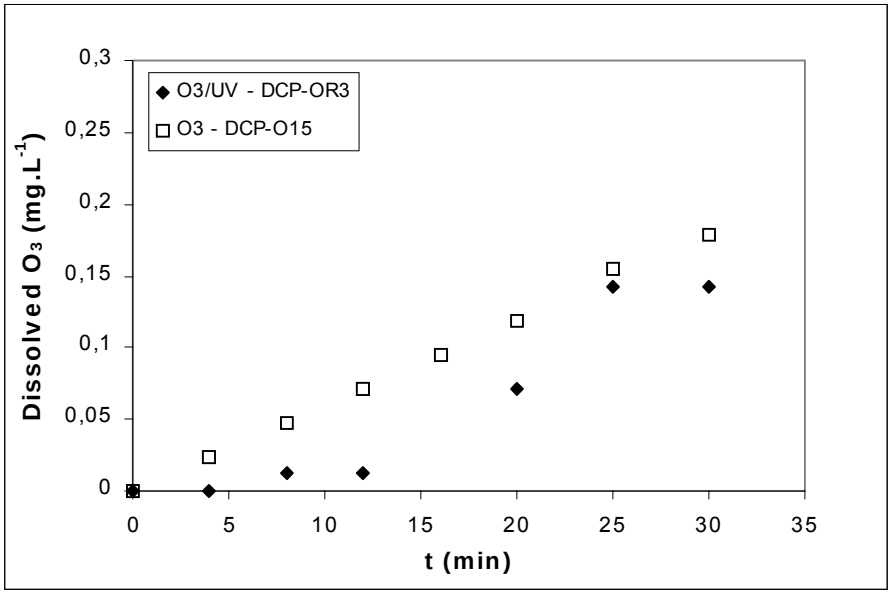

Graph 5.102. Comparison of the residual dissolved ozone for the processes O_3 and O_3/UV

Graph 5.103 shows the descent of the normalized TOC during time. TOC removal rate decreases as the initial concentration increases. The addition of UV to the ozonation of DCP solutions increased ca. 50% the degree of mineralization, in agreement with results reported by Kuo (1999). Mineralizing rate has been estimated (Graph 5.104) as well and found to be ca. 1.5 times higher than the ones achieved by single ozonation (7.2 and 8.2 mg C.min^{-1} for DCP-OR1 and DCP-OR2, respectively).

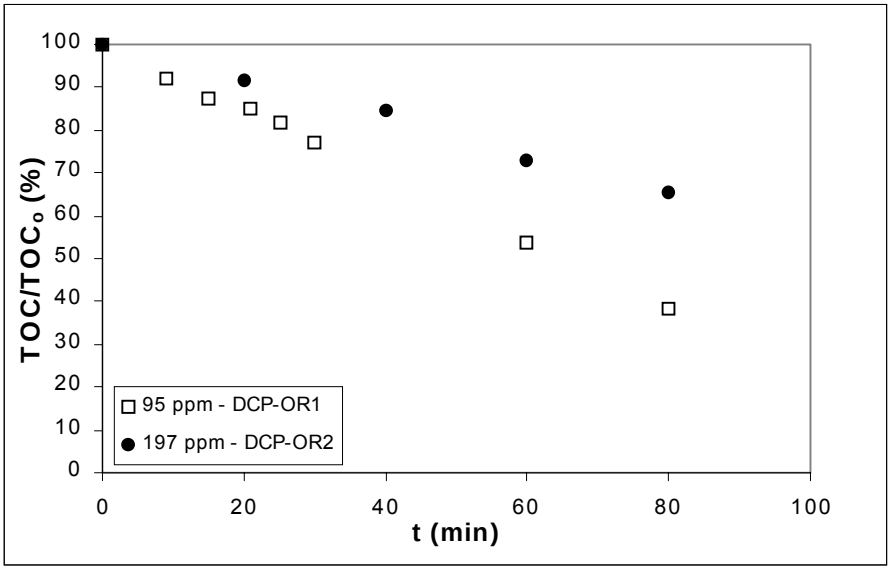

Graph 5.103 . Influence of the initial concentration in the removal of DCP by O_3/UV – Normalized TOC

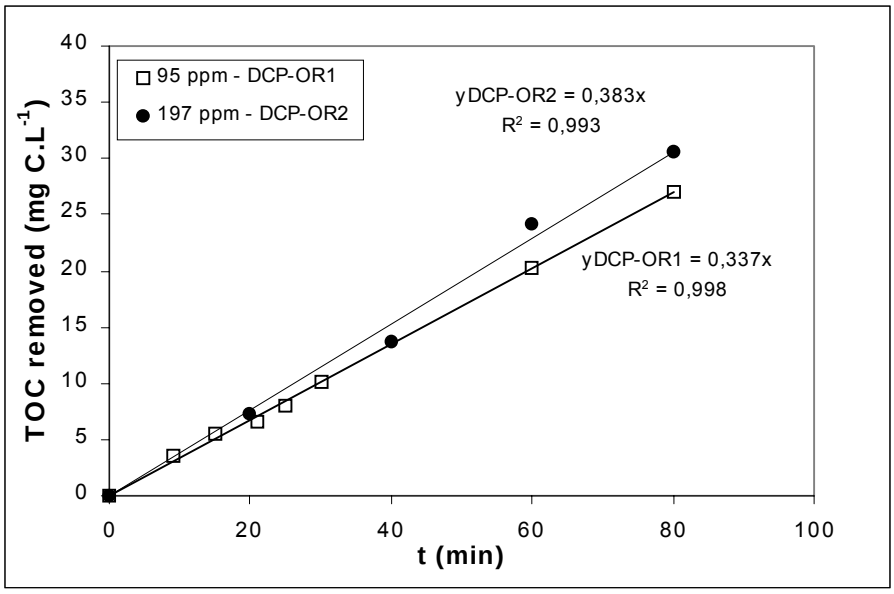

Graph 5.104. Influence of the initial concentration in the DCP mineralization rate by O_3/UV

5.14.2. Biodegradability study

One experiment with the combination O_3/UV with initial DCP concentration ca. 100 ppm and 5.4 $g.h^{-1}$ ozone production was performed (see section A1.11, Table DCP-OR4) in order to follow the different variables related to the biodegradability of the solution, i.e. BOD and COD. As in the preceding sections, the AOS will be used to follow changes on the degree of oxidation throughout the process and BOD/COD and BOD/TOC ratios are used as biodegradability indicators.

AOS changes are presented and compared with the experiment of single ozonation carried out at the same conditions (DCP-O14) in Graph 5.105. The degree of oxidation achieved by the combination O_3/UV is smaller than by single ozonation.

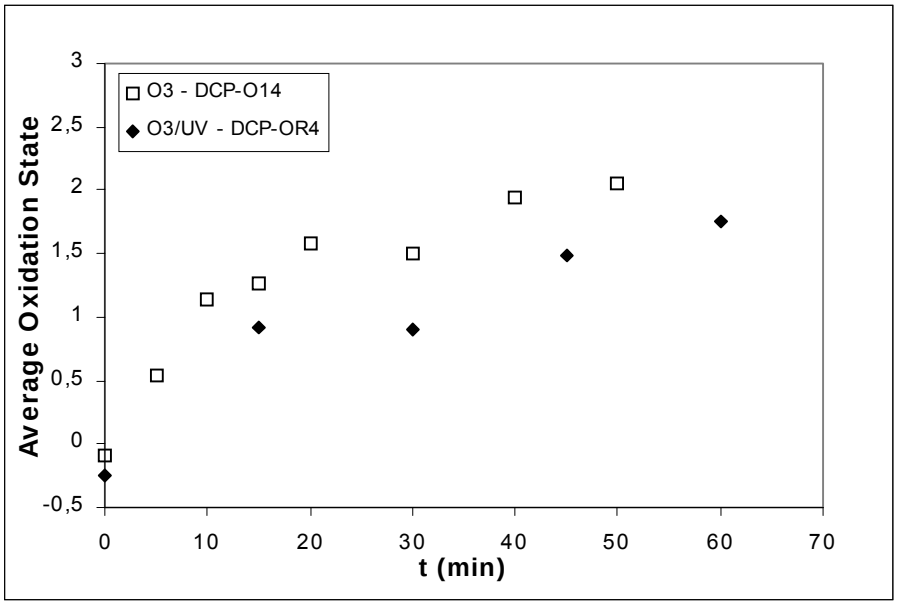

Graph 5.105. AOS achieved by the processes O_3 and O_3/UV in DCP removal

BOD values achieved by this combination are lower than the ones achieved by single ozonation (see Graph 5.106). Contrasting this one, BOD values do not reach a maximum, but go on increasing in the range of time tested. BOD/COD ratios are lower as well to those found for single ozonation (see Graph 5.107). BOD_5/COD ratio is increased only from 0 to 0.14 after 45 minutes of treatment. Parallelly, BOD_5/TOC is increased merely from 0 to 0.23 after 45 minutes of treatment (see Graph 5.108). With regard to the intermediates, there are two remarkable differences: (1) chlorobenzoquinone was not produced as intermediate and (2) new intermediates appeared, which could not be

identified (see section 5.18, Figure 5.9). When DCP was depleted from solution, those intermediates were still present.

In view of the experimental results, the addition of UV did not improve the effect on the biodegradability of DCP aqueous solutions achieved by single ozonation.

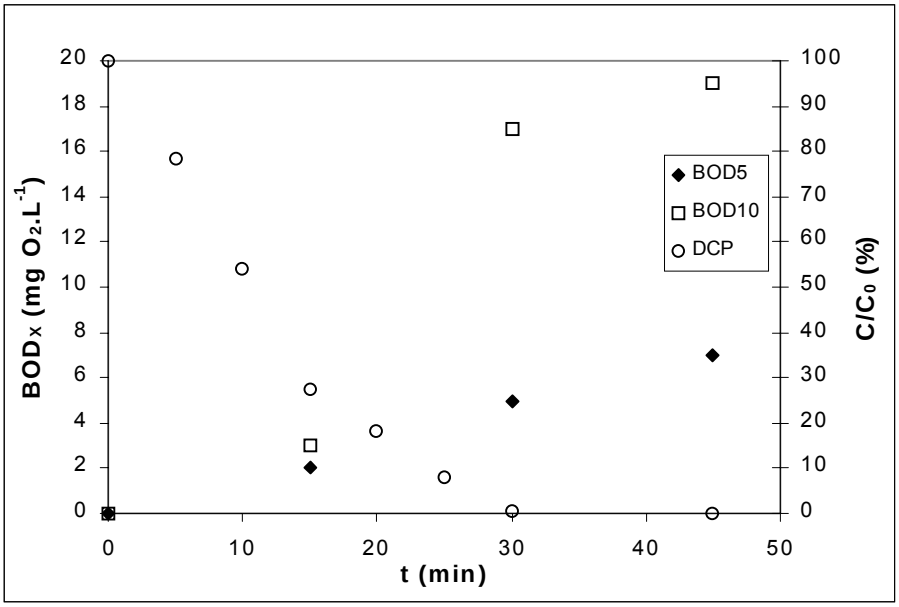

Graph 5.106. Evolution of BOD and DCP normalized concentration for the combination O_3/UV

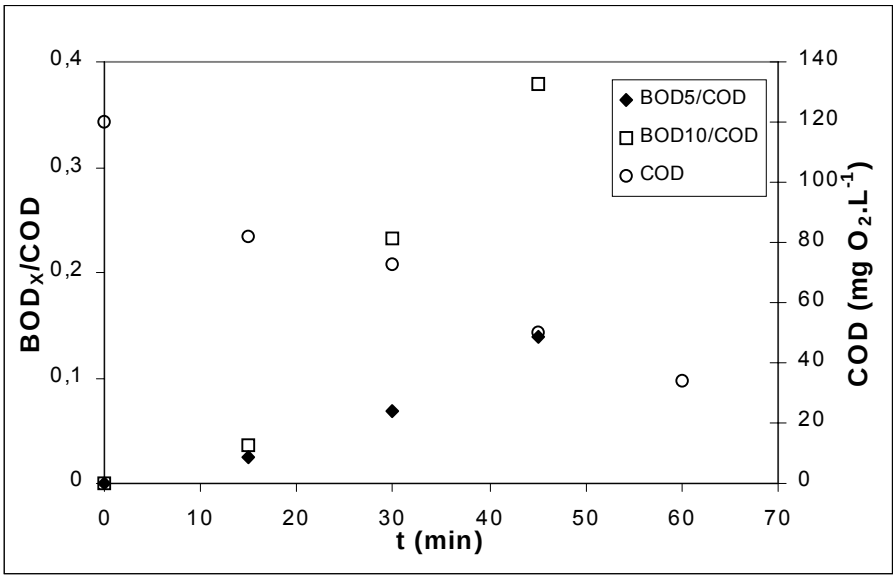

Graph 5.107. Evolution of the BOD_x/COD ratio and COD for the combination O_3/UV

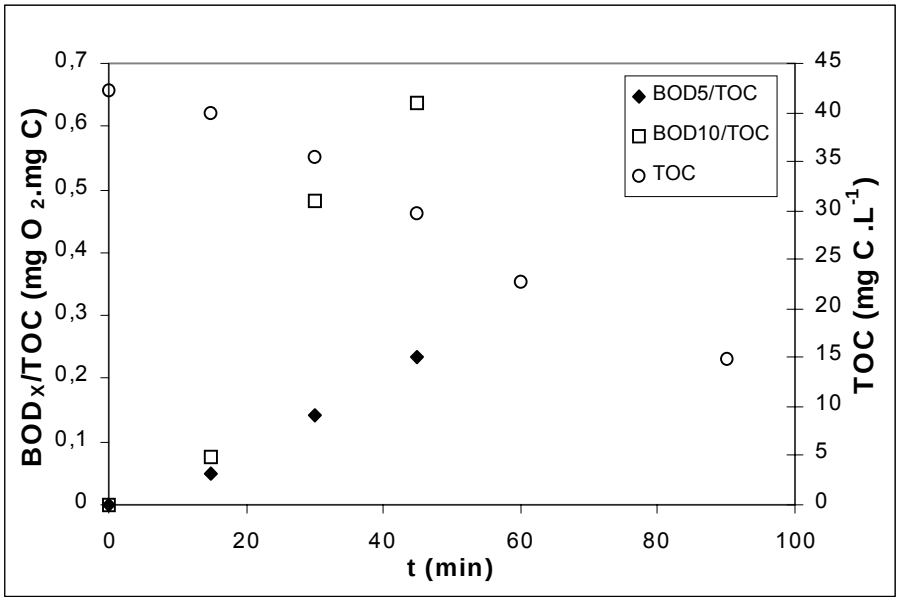

Graph 5.108. Evolution of the BOD_x/TOC ratio and TOC for the combination O_3/UV

5.15. DCP removal by means of the combination O_3/UV/H_2O_2

In this combination, the influence of the addition of UV radiation and hydrogen peroxide to ozonation has been checked only regarding to biodegradability of the DCP aqueous solutions. Two experiments with the combination O_3/UV/H_2O_2 with initial DCP concentration ca. 100 ppm, 5.4 $g.h^{-1}$ ozone production and 0.1 mol H_2O_2/mol DCP were performed (see section A1.12, Tables DCP-ORP1 and DCP-ORP2) in order to follow the different variables linked to the biodegradability, i.e. BOD and COD and mineralization (TOC) of the solution. The average of both experiments has been calculated and it is shown in Table DCP-ORP3. As in the prior sections, the AOS will be used to follow changes on the degree of oxidation throughout the process and BOD/COD and BOD/TOC ratios as biodegradability indicators. Plotted results are those corresponding to the average calculated (DCP-ORP3).

AOS changes are presented and put side by side with the experiment of single ozonation carried out at the same conditions (DCP-O14) in Graph 5.109. The degree of oxidation attained by the combination O_3/UV/H_2O_2 is rather similar than the one achieved by single ozonation.

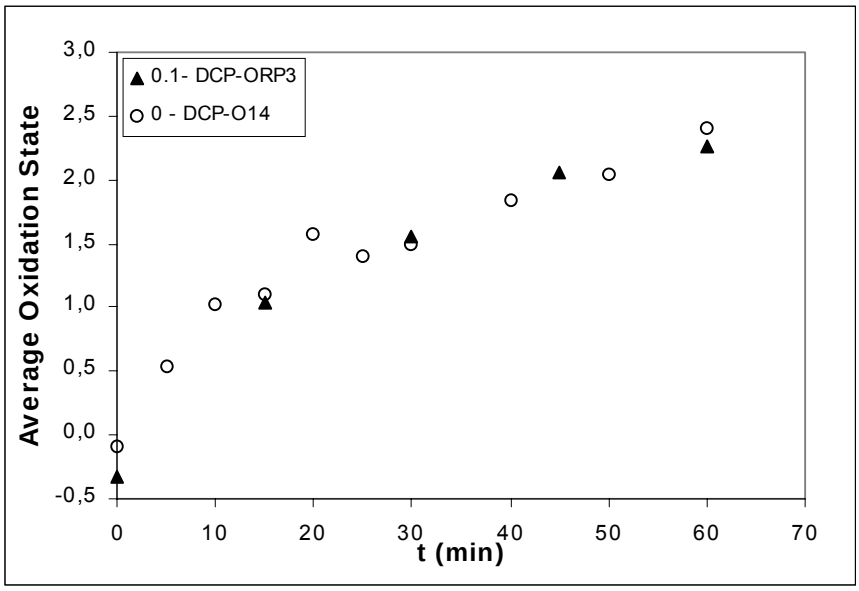

Graph 5.109. Influence of the addition of H_2O_2 and UV radiation to DCP ozonation – Average Oxidation State

BOD values achieved by this combination are slightly smaller than those attained by single ozonation and O_3/H_2O_2 (see Graph 5.110). Similarly to what observed with the combination O_3/H_2O_2, BOD values does not reach a maximum when all the DCP disappears, but seem to decrease after 45 minutes of treatment. Disappearance rate of DCP has been estimated to be 85 $mg.min^{-1}$. BOD/COD ratios are analogous as well to those found for the combination O_3/H_2O_2 (see Graph 5.111). BOD_5/COD ratio is increased from 0 to 0.28 after 45 minutes of treatment.

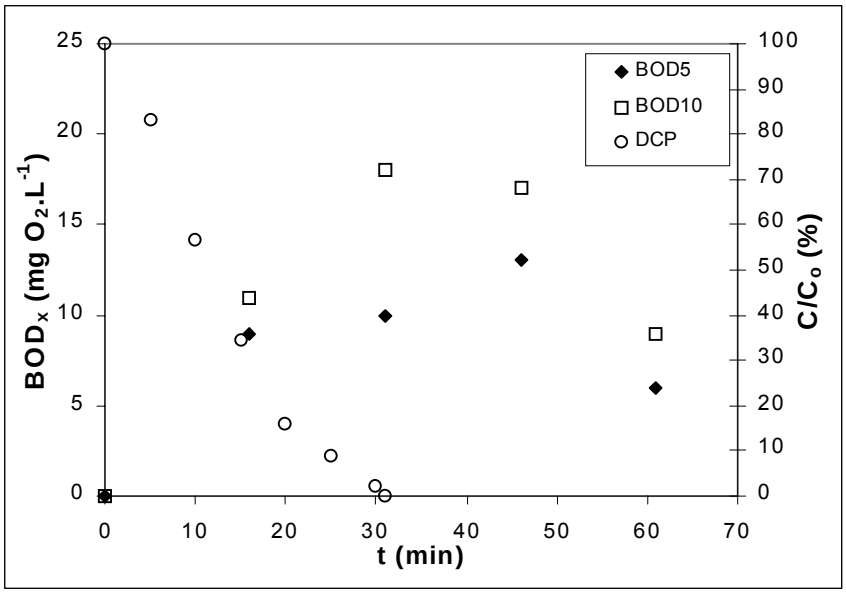

Graph 5.110. Evolution of BOD and DCP normalized concentration during time with the combination $O_3/UV/H_2O_2$

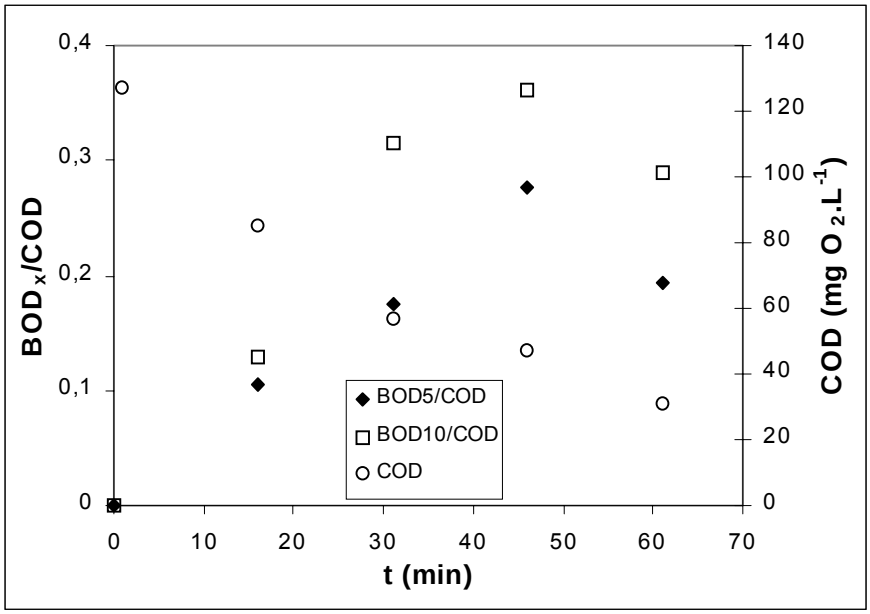

Graph 5.111. Evolution of BOD_x/COD ratio and COD during time with the combination $O_3/UV/H_2O_2$

Although the degree of mineralization achieved by this combination is higher than by the combination O_3/H_2O_2, values of BOD/TOC ratios are quite similar as BOD values were found to be a slightly lower. BOD_5/TOC is increased from 0 to 0.44 after 45 minutes of treatment (see Graph 5.112). Mineralization rate has been estimated to be 6.6 mg C.min^{-1}.

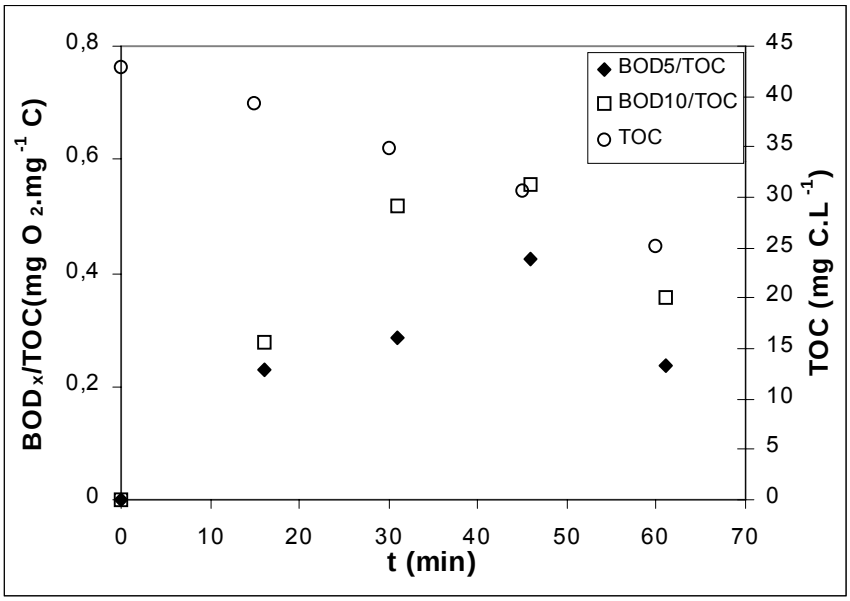

Graph 5.112. Evolution of BOD/TOC ratio and TOC during time with the combination $O_3/UV/H_2O_2$

With regard to the intermediates, they have found to be rather similar to those for the O_3/UV process. Chlorobenzoquinone was not produced as intermediate either, while new intermediates appeared, which could not be identified. When DCP was depleted from solution, those intermediates were still present as well (see section 5.18, Figure 5.10).

The combination O_3/UV/H_2O_2 has not been found either to improve the effect of single ozonation in the biodegradability of the DCP solutions.

5.16. DCP removal by means of the combinacion O_3/UV/Fe(III)

The addition of iron ion (Fe^{3+} or Fe^{2+}) has been reported to accelerate the UV-enhanced ozonation of several pollutants (Abe and Tanaka, 1997, 1999). Thus, the effect of the addition of Fe(III) salts and UV light to single ozonation on the degradation and biodegradability of DCP has been studied. The influence of the Fe(III) concentration (expressed as mol Fe(III)/mol DCP), type of Fe(III) salt, the use of Fe(II) instead of Fe(III) and the use of UVA instead of UV light on the degradation of DCP was checked, as well as the effect of this catalytic ozonation on the biodegradability of these solutions. Results are shown on section A1.13, Tables DCP-ORF1 to DCP-ORF9.

5.16.1. Influence of Fe(III) concentration.

Three experiments were carried out with DCP initial concentration ca. 90 ppm, 5.4 $g.h^{-1}$ ozone production, UV light, free pH, room temperature and adding $FeCl_3$ ranging from 1.63 to 0.1 mol Fe(III)/mol DCP (1 to $6.1x10^{-2}$ $mmol.L^{-1}$ of Fe(III)). They are presented in Tables DCP-ORF1 to DCP-ORF3 and compared with the experiment performed in absence of Fe(III) (DCP-OR1). The addition of Fe(III) to the O_3/UV process showed to decrease the DCP removal rate (see Graph 5.113), more as the concentration is increased, as was observed with NB. However, with regard to TOC, the addition of Fe(III) increases slightly the mineralization rate (see Graph 5.114), although the difference is not as high as observed with NB. Mineralization rate increases with the concentration, although no differences are observed between 1.63 and 0.5 ratios.

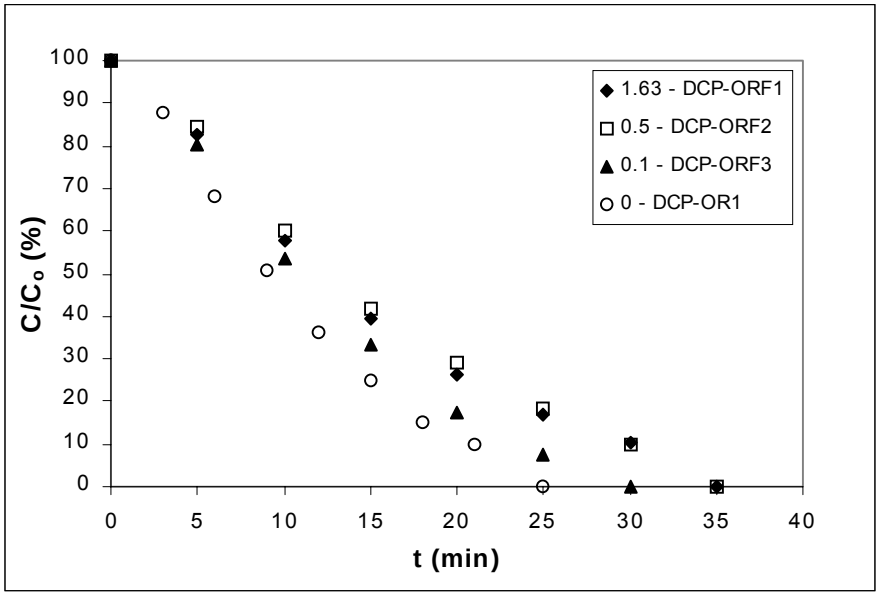

Graph 5.113. Influence of the Fe(III) concentration in the DCP removal by means of O_3/UV/Fe – Normalized concentration

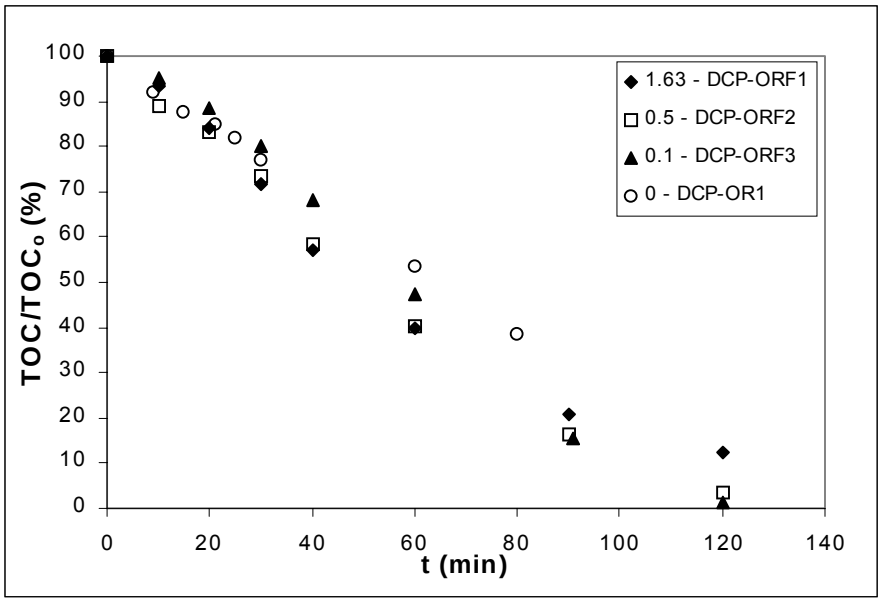

Graph 5.114. Influence of Fe(III) concentration in the combination O_3/UV/Fe(III) - Normalized TOC

As it has been mentioned in the introduction and section 5.8, photodecarboxilation of ferric ion complexes ([1.19]), Fenton chemistry and photo-Fenton reaction of aqueous ferric ions with UV light ([1.16]) may account for this higher efficiency.

With regards to the concentration of ozone in the residual gas, the addition of Fe(III) has been found to decrease the amount of non-reacted ozone with respect to

single ozonation (DCP-O14) and O_3/UV (DCP-OR1). It has also been observed the plateaus already detected in the case of NB.

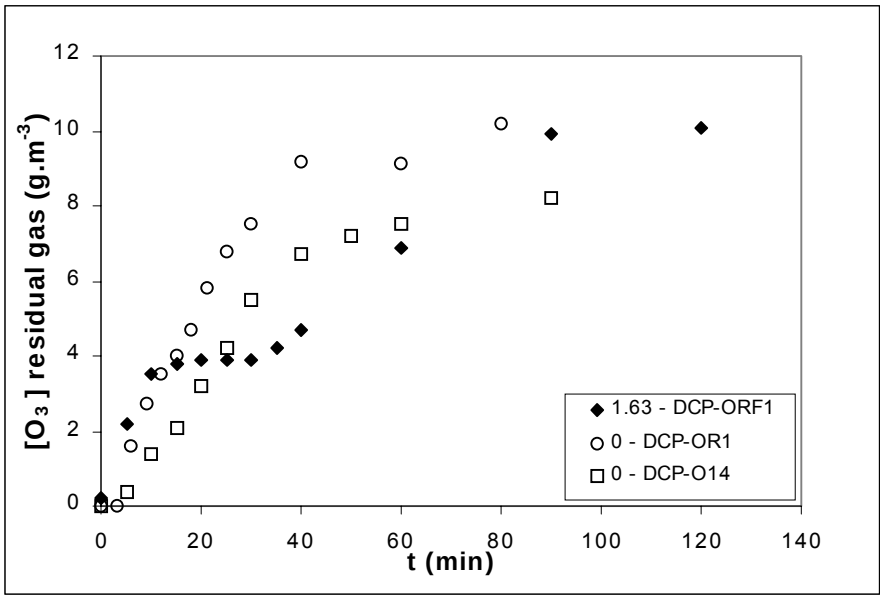

Graph 5.115. Influence of Fe(III) concentration in the DCP removal by means of O_3/UV/Fe(III) – Residual ozone

5.16.2. Influence of Fe(III) salt.

The influence of the type of Fe(III) salts on the catalytic ozonation of DCP solutions has also been tested. Chloride ions have been reported to be hydroxyl radical scavengers (Maletzky and Bauer, 1998), so the degradation of DCP solutions by means of sulphate and chloride Fe(III) salts has been compared. Experiments DCP-ORF1 and DCP-ORF4 have been carried out with ca. 90 ppm initial DCP concentration, 5.4 $g.h^{-1}$ ozone production, UV light, free pH (by adding the Fe(III) salt initial pH drops to ca. 3), room temperature and 1.63 mol Fe(III)/mol DCP (1 $mmol.L^{-1}$) as $FeCl_3$ and $Fe_2(SO_4)_3$, respectively.

No significant differences between chloride and sulphate salts have been observed with regard to concentration (see Graph 5.116), TOC (see Graph 5.117) or concentration of ozone in the residual gas (Graph 5.118). Thus, no scavenger effect derived from the use of chloride ion has been observed in the DCP removal by means of O_3/UV/Fe under the testing conditions. Glaze and Kang (1989) had already mentioned that chloride is not a significant scavenger of hydroxyl radicals except at a very low pH values.

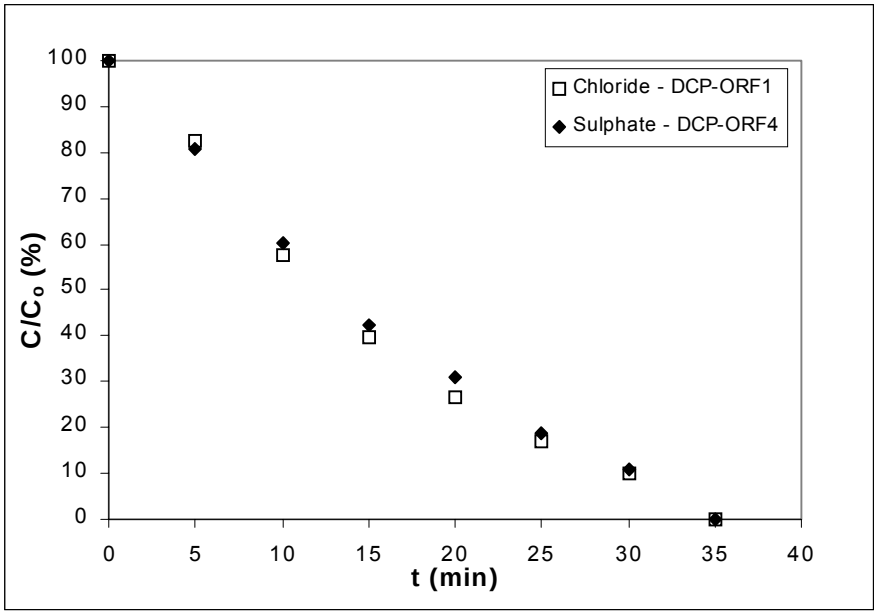

Graph 5.116. Influence of Fe(III) salt in the DCP removal by means of O_3/UV/Fe – Normalized concentration

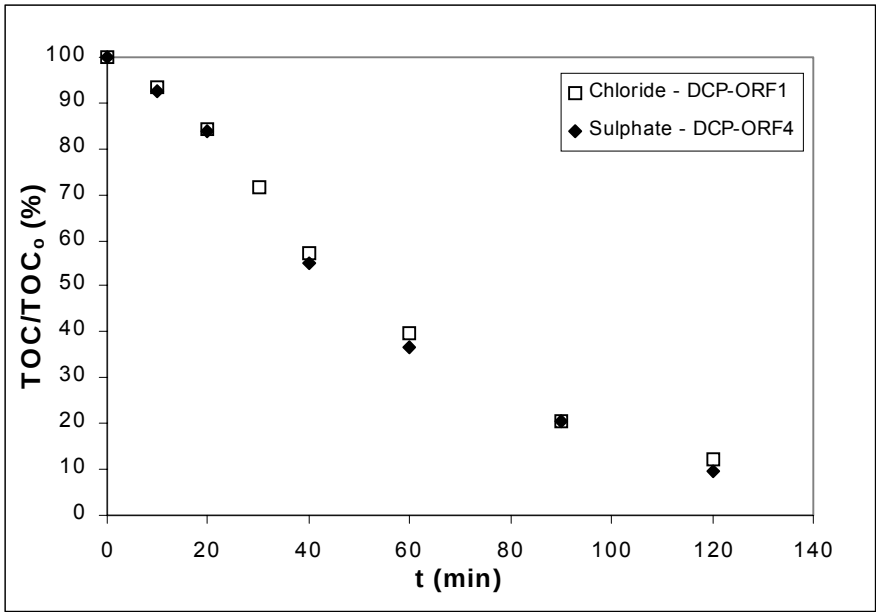

Graph 5.117. Influence of Fe(III) salt in the DCP removal by means of O_3/UV/Fe – Normalized TOC

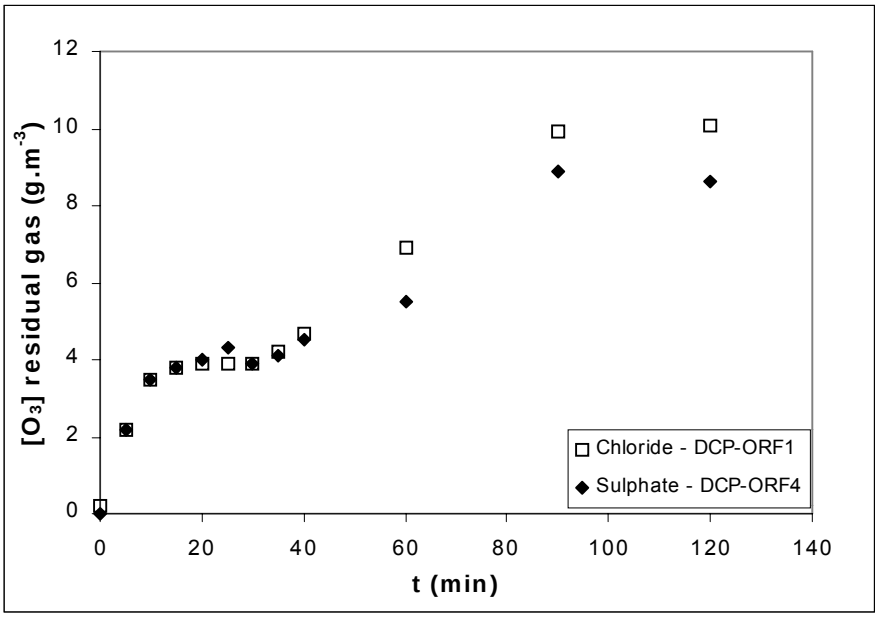

Graph 5.118. Influence of Fe(III) salt in the DCP removal by means of O_3/UV/Fe – Residual ozone

5.16.3. Fe(III) vs. Fe(II)

Besides the influence of the ferric salt used, the effect of the iron ion (Fe(III) or Fe(II)) has also been studied. Two experiments performed at the same conditions (5.4 $g.h^{-1}$ ozone production, UV light, free pH, room temperature and 1.63 mol Fe/mol DCP (1 $mmol.L^{-1}$) $Fe_2(SO_4)_3$ and $FeSO_4$ are to be compared. Results are presented in Tables DCP-ORF4 and DCP-ORF5 and compared in Graphs 5.119 and 5.120.

With regards to the normalized concentration (Graph 5.119), the use of Fe(II) diminishes the DCP removal rate. When Fe(II) is used, an initial induction period can be observed, increasing the time necessary for the complete disappearance of DCP from the solution (35 minutes with Fe(III) and ca. 60 minutes with Fe(II)), although the disappearance rate after this initial period are similar. The oxidation of Fe(II) into Fe(III) may account for this delay time, as 0.43 mg O_3 are consumed per mg of Fe(II) (Langlais et al., 1991). As for TOC (Graph 5.120), the initial mineralization rate with Fe(II) seems to be lightly restrained, deriving in a smaller TOC reduction at short and medium times in comparison with the chloride salt. Nevertheless, final TOC removed achieved by the two species was found to be the same. At the light of these results, Fe(III) seems to be a better catalyst for this process under the tested conditions.

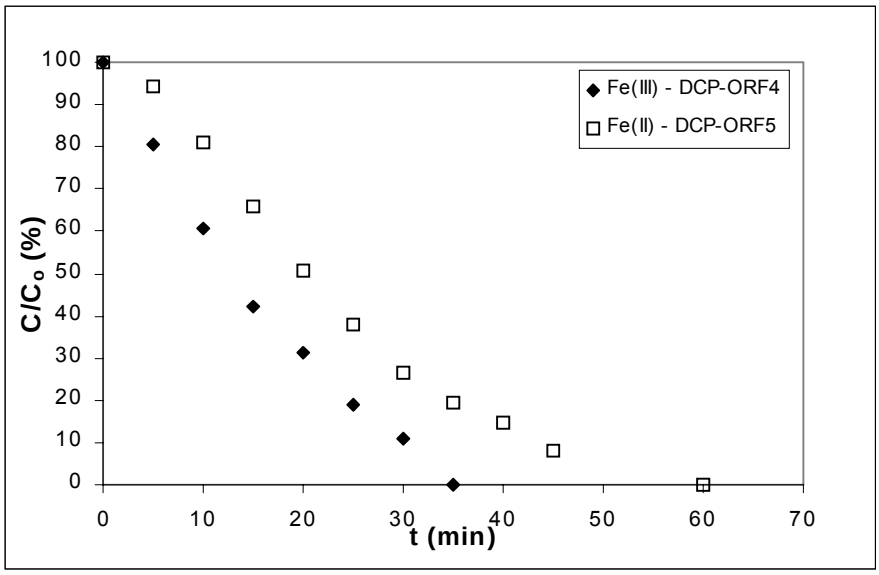

Graph 5.119. Fe(III) vs. Fe(II) in the DCP removal by means of O_3/UV/Fe – Normalized concentration

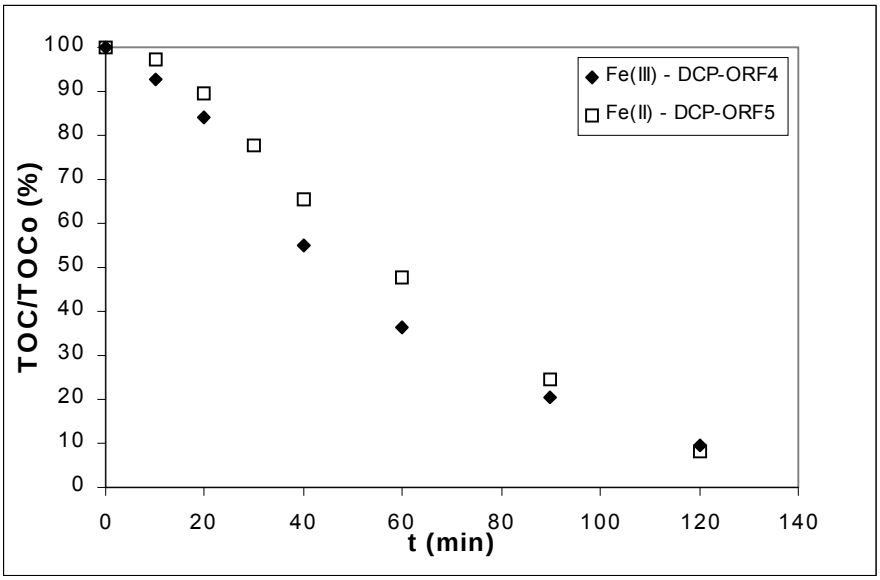

Graph 5.120. Fe(III) vs. Fe(II) in the DCP removal by means of O_3/UV/Fe – Normalized TOC

5.16.4. Biodegradability study

Two experiments with the combination O_3/UV/Fe(III) with ca. 90 ppm initial DCP concentration, 5.4 $g.h^{-1}$ concentration, free pH, room temperature and 0.1 mol Fe(III)/mol DCP as $FeCl_3$ were performed in order to check the effect of this combination in the biodegradability of the DCP solutions. The ratio 0.1 was chosen as low Fe(III) amounts have shown to be effective in this combination. Results are accessible in Tables DCP-

ORF6 and DCP-ORF7, and a summary of these two in Table DCP-ORF8. Data present in the following graphs correspond to DCP-ORF8.

Graph 5.121 depicts changes of the average oxidation state (AOS) during the time of experimentation. The degree of oxidation throughout the process shows to be lower than by single ozonation. TOC values are greatly lower when the solution is treated by means of O_3/UV/Fe. The higher degree of mineralization rather than oxidation achieved by this process may account for this behavior.

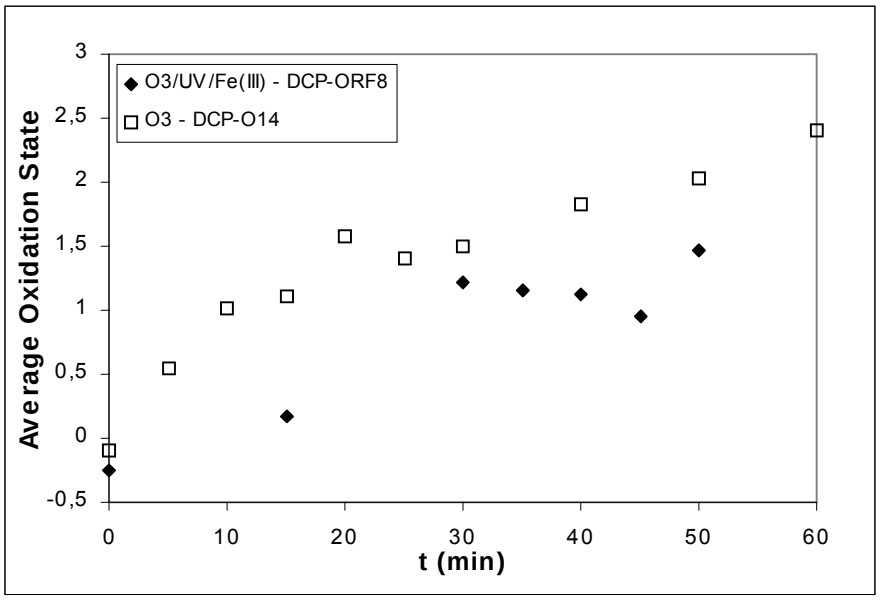

Graph 5.121. AOS achieved by the processes O_3 and O_3/UV/Fe(III) in DCP removal

With regards to BOD, measured values were rather similar than those achieved by single ozonation. Analogous to the latter, maximum BOD values are found when almost all DCP has been removed from the solution up to a value of 16 mg $O_2.L^{-1}$ (see Graph 5.122).

BOD/COD values were slightly higher than those of single ozonation. BOD_5/COD ratio was increased from 0 to 0.28 after 30 minutes of treatment while BOD_{21}/COD achieved a value of 0.60 after 30 minutes and up to 0.7 after 40 minutes of treatment. BOD/TOC values were even higher, as the degree of mineralization achieved was significantly higher than by single ozonation. BOD_5/TOC increased from 0 to 0.52 after 30 minutes of treatment while BOD_{21}/TOC up to 1.3 after 40 minutes (see Graphs 5.123 and 5.124).

Intermediates were rather similar to those produced by single ozonation. Chlorobenzoquinone was detected as well, although the concentration seemed to be

smaller in this process. This compound was removed earlier from the solution: after 15 minutes chlorobenzoquinone was not present. Therefore, biodegradability between 15 and 30 minutes may be higher than by single ozonation.

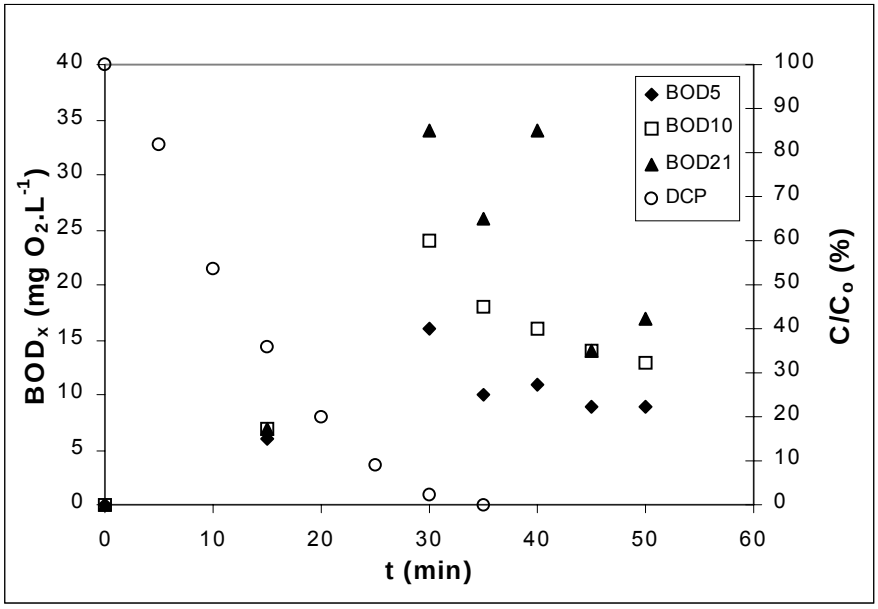

Graph 5.122. Evolution of BOD and DCP normalized concentration for the combination O_3/UV/Fe(III)

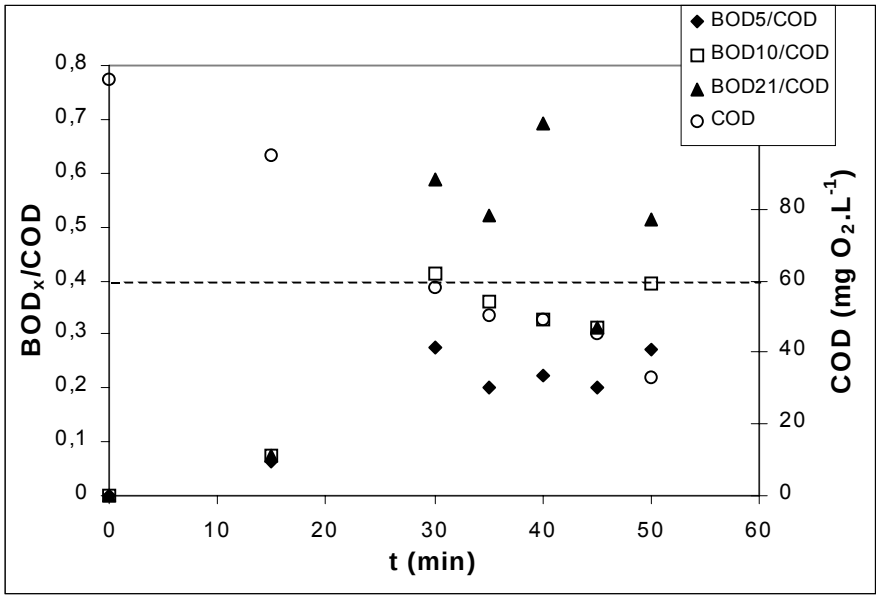

Graph 5.123. Evolution of BOD_x/COD ratio and COD for the combination O_3/UV/Fe(III)

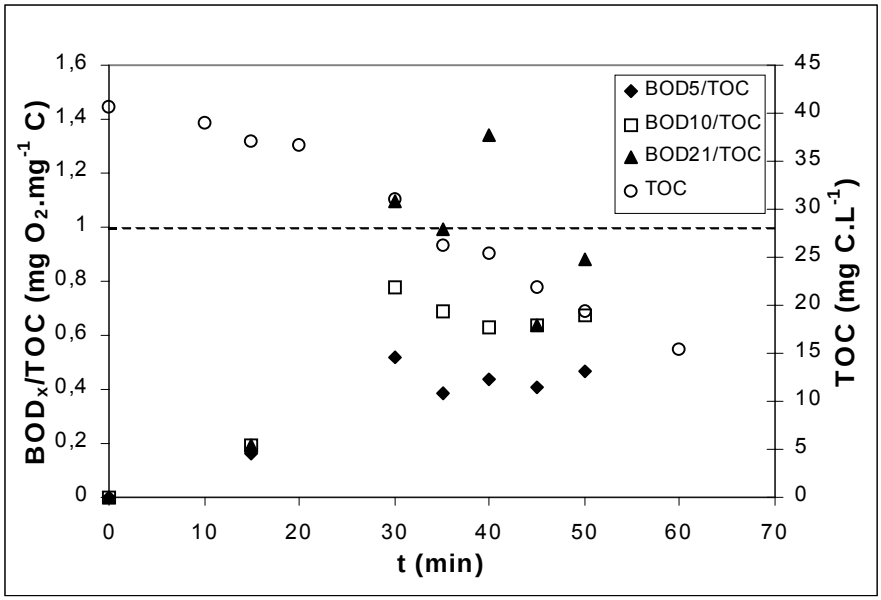

Graph 5.124. Evolution of BOD_x/TOC ratio and TOC for the combination O_3/UV/Fe(III)

5.16.5. UVA vs. UV

UVA light, which emits in the range of wavelength of between 300 and 420 nm, with a maximum centered at 360 nm, is representative of the atmospheric solar emission and suitable for iron solutions, as Fe(III) species have been found to absorb greatly in the range of between 290 and 390 nm (Safarzadeh-Amiri et al., 1996). For this reason, one experiment with ca. 90 ppm initial DCP concentration, 5.4 $g.h^{-1}$ ozone production, 0.1 mol Fe(III)/mol DCP as $FeCl_3$, free pH, room temperature and UVA light instead of UV (253.7 nm) was performed (see Table DCP-ORF9). The same experiment was also carried out without Fe(III) (O_3/UVA, see Table DCP-OR5). Both experiments are to be compared with the experiments carried out at the same conditions by single ozonation (DCP-O14), O_3/UV (DCP-OR1) and Fe(III) catalytic ozonation with UV light (DCP-ORF8).

Graph 5.125 depicts the normalized concentration during time for the experiments cited above. As it can be observed, processes involving the use of Fe(III) slightly inhibit the disappearance rate of DCP. However, this inhibition is lower when using UVA instead of UV light.

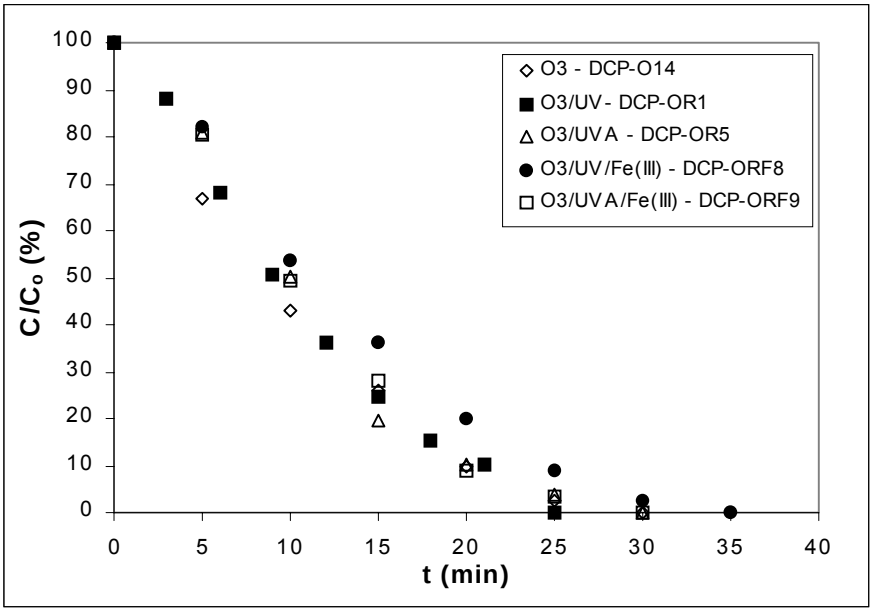

Graph 5.125. Comparison of the processes involving O_3, UV(A) and Fe(III) in DCP removal – Normalized concentration

With regard to TOC (see Graph 5.126), the addition of both UV(A) or UV(A)/Fe(III) strongly increases the mineralization rate with respect to single ozonation, especially when using Fe(III), but results obtained have been similar to those achieved by UV light. To compare, after one hour of treatment, mineralization degree achieved by single ozonation, O_3/UV(A) and O_3/UV(A)/Fe(III) has been 32%, 46-47% and 60-62%, respectively. Best results have been attained with the combination O_3/UVA/Fe(III), although no significant differences between the use of UVA instead of UV light have been found.

As for the average oxidation state (Graph 5.127), higher degrees of oxidation have been reached by single ozonation. When using UVA or UV(A)/Fe(III), the AOS seem to stabilize after 30 minutes of treatment. The combinations O_3/UV/Fe and O_3/UVA/Fe have been shown to be the best processes for the mineralization of DCP solutions.

BOD_5/COD ratios have been compared as well in Graph 5.128. As it can be observed, O_3/UVA/Fe(III) seems to exhibit the better efficiency to improve the biodegradability of the DCP aqueous solutions, as BOD_5/COD ratio is increased up to 0.31 and 0.37 after 30 and 40 minutes of treatment, respectively. Nevertheless, it has to be pointed out that experiments with UV and UVA/Fe(III) have been performed only once and differences observed in the BOD/COD ratio could be due to an experimental error, especially in the case of O_3/UV, which is surprisingly lower.

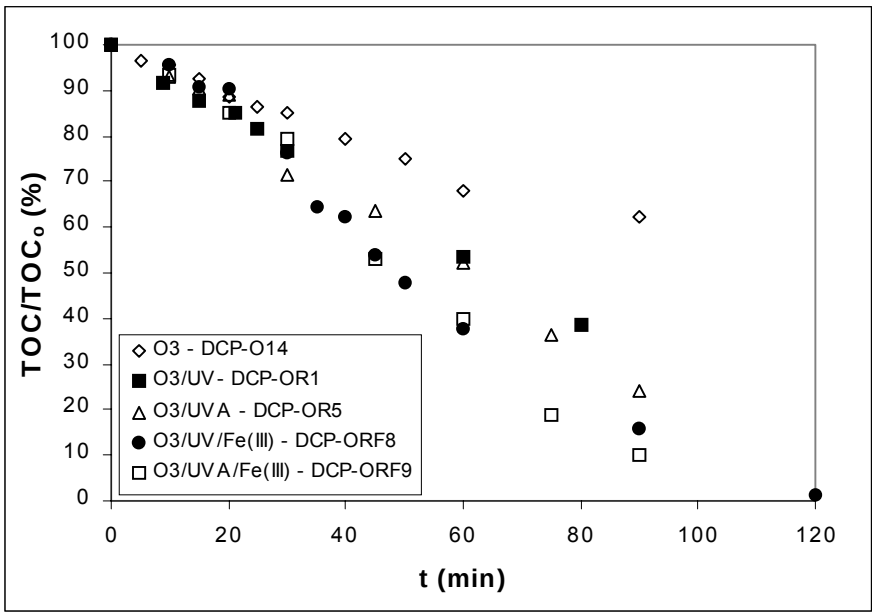

Graph 5.126. Comparison of the processes involving O_3, UV(A) and Fe(III) in DCP removal – Normalized TOC

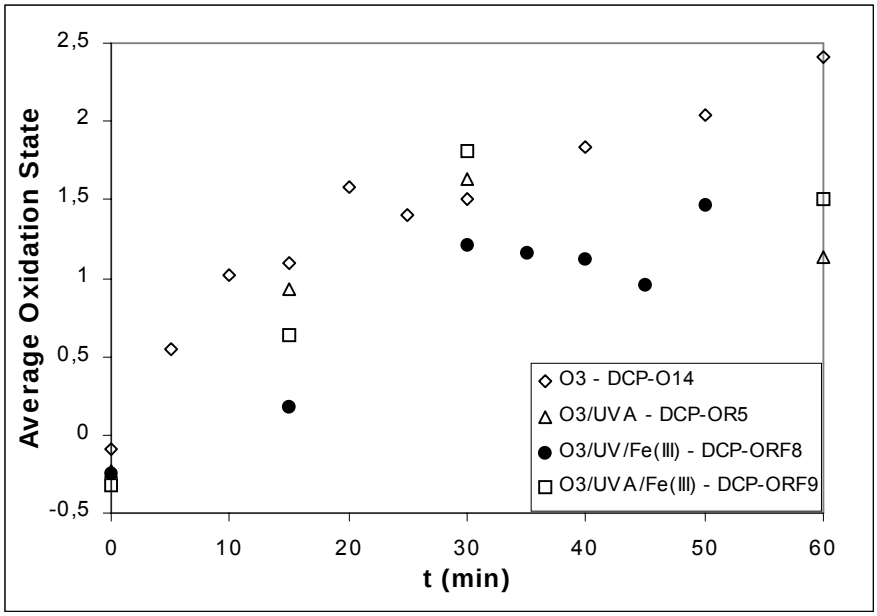

Graph 5.127. Comparison of the processes involving O_3, UV(A) and Fe(III) in DCP removal – AOS

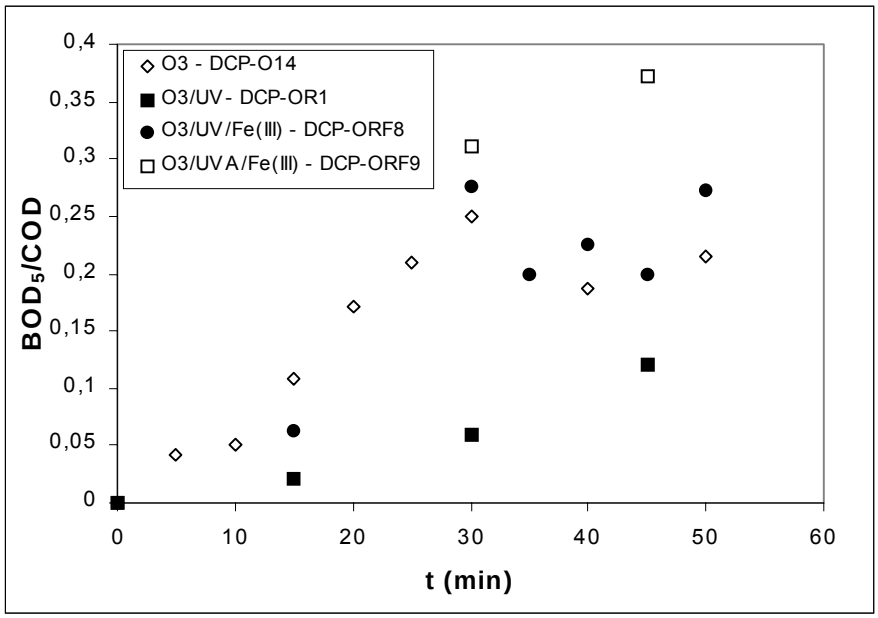

Graph 5.128. Comparison of the processes involving O_3, UV(A) and Fe(III) – BOD_5/COD ratio for DCP removal

5.17. Comparison of the different studied processes for the degradation of DCP.

In the present section, some of the different variables that have been commented in the discussion of each process are to be compared among the different studied processes: single ozonation (O_3, DCP-O14), ozonation combined with UV radiation (O_3/UV, DCP-OR4), ozonation combined with hydrogen peroxide (O_3/H_2O_2, DCP-OP5), ozonation combined with UV radiation and hydrogen peroxide ($O_3/UV/H_2O_2$, DCP-ORP3) and ozonation combined with UV radiation and Fe(III) ion (O_3/UV/Fe(III), DCP-ORF8).

5.17.1. Removal and mineralization rates

In the Graph 5.129 the normalized concentration vs. time are compared. It can be observed that single ozonation presents the best results whereas ozonation combined with UV radiation and Fe(III) shows the slowest ones. Regarding the absorbed ozone dose (Graph 5.130) differences are even smaller, showing all the tested processes the same behavior.

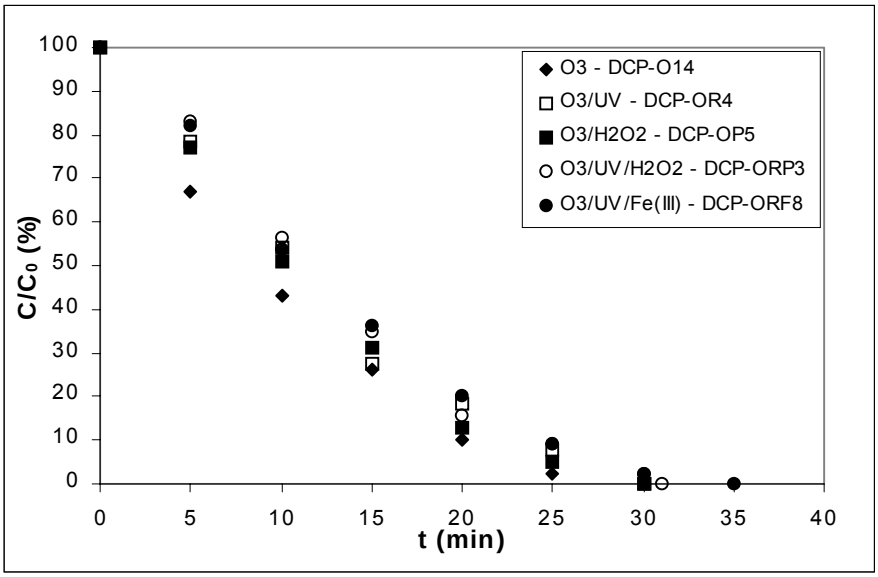

Graph 5.129. Comparison of the different processes for DCP removal – Normalized concentration vs. time

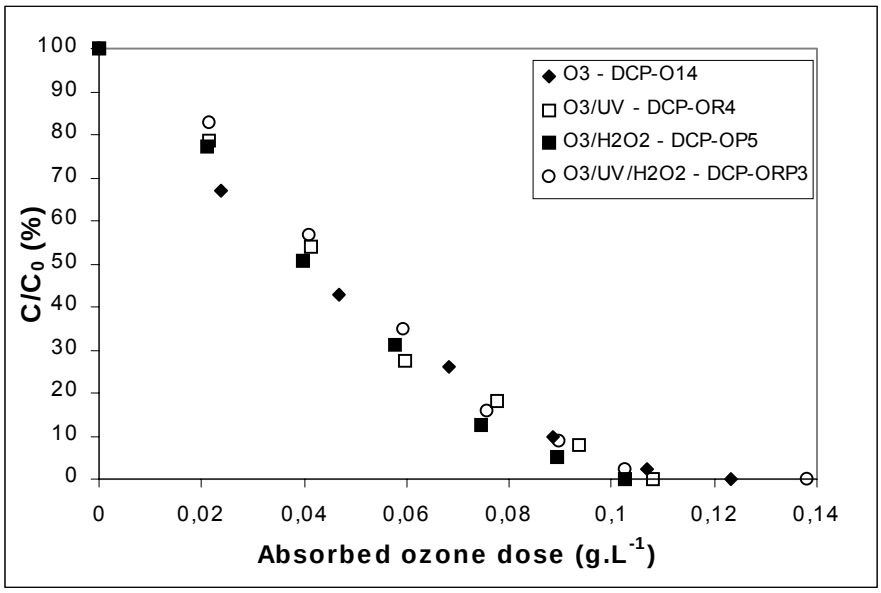

Graph 5.130. Comparison of the different processes for DCP removal – Normalized concentration vs. absorbed ozone dose

Table 5.17 presents the pseudo-first order kinetic constant, the value of experimental half-life $t_{1/2}$ (that is, the time required to decrease the concentration of the reactant to half the amount present before the reaction) and experimental $t_{3/4}$ (time needed to decrease the concentration to the fourth-part of the initial amount). Nevertheless, at the light of the results none of the processes seem to obey a first order behavior ($t_{3/4} \neq 2 \times t_{1/2}$). As it has been reported in the literature (Qiu et al., 2002; Benítez et al., 2000) the overall reaction of DCP is second order with first order each in the

concentration of ozone and DCP. Compared to NB, kinetic constants have been found to be 2.5-3 times higher in DCP removal.

Table 5.17. Pseudo-first order kinetic constant, $t_{1/2}$ and $t_{3/4}$ for DCP removal by the different studied processes

	O_3	O_3/UV	O_3/H_2O_2	O_3/UV/H_2O_2 (0.1:1)	O_3/UV/Fe(III) (0.1:1)
k (min^{-1})	0.0876	0.0813	0.0729	0.0643	0.0728
$t_{1/2}$ (min)	8.5	10.6	10.2	11.5	11.0
$t_{3/4}$ (min)	15.3	16.7	16.3	17.6	18.5

With regard to TOC, the process exhibiting the highest mineralization rate is the combination of ozone with UV radiation and Fe(III) ion (see Graph 5.131). Single ozonation and the O_3/H_2O_2 process present similar results, achieving a 37% of TOC reduction after 90 minutes of treatment. The addition of UV radiation to both processes increases the mineralization rate, attaining a ca. 65% of mineralization after 90 minutes by means of both processes. With the O_3/UV/Fe(III) process, the degree of mineralization achieved after 90 minutes is 84% and ca. 100% after two hours of treatment. As it was commented in the introduction, photodecarboxilation of ferric ion complexes, Fenton chemistry and photo-Fenton reaction of aqueous ferric ions with UV light may account for this improvement with regard to the other processes.

As it has been commented before, the literature points out that the mineralization rate of chlorophenols follows apparent first-order kinetics (Esplugas et al., 1994; Kuo, 1999). Accordingly, the degradation rate of DCP is expressed by the apparent first-order rate constant on the basis of TOC removal and listed in Table 5.18. The three processes that have been found to follow a first-order behavior are O_3, O_3/UV and O_3/H_2O_2. The mineralization rate of the other two processes has been found to be more linear, with a slope of 0.696 min^{-1} for O_3/UV/H_2O_2 and 0.903 min^{-1} for O_3/UV/Fe(III) in the expression:

$$\frac{TOC}{TOC_0} = 100 - (slope)\cdot t$$

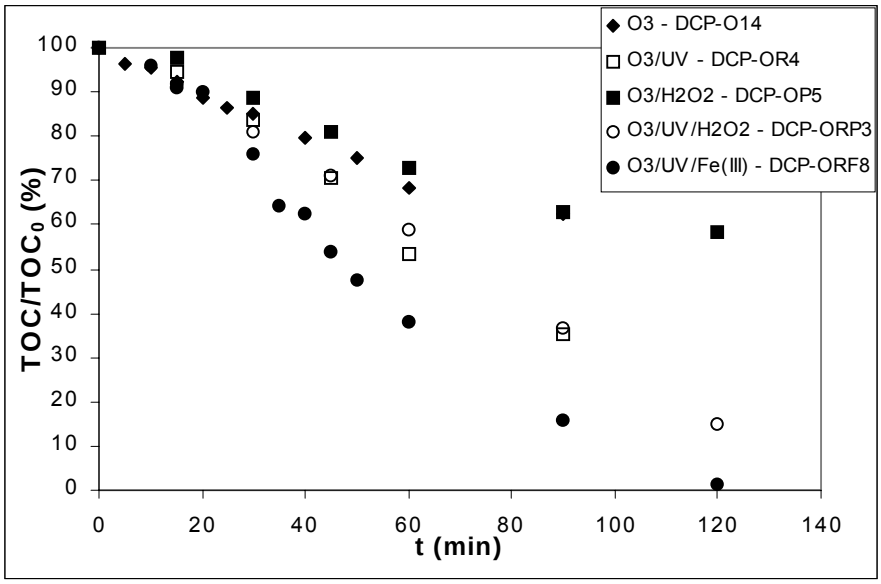

Graph 5.131. Comparison of the different processes for DCP removal – Normalized TOC vs. time

Table 5.18. Pseudo-first order kinetic constant and mineralization rate of DCP by the different studied processes

	O_3	O_3/UV	O_3/H_2O_2	O_3/UV/H_2O_2 (0.1:1)	O_3/UV/Fe(III) (0.1:1)
k (h^{-1})	0.336	0.618	0.282	-	-
TOC removed (mg C.min^{-1})	5.01	6.60	3.77	6.58	8.58

Graph 5.132 shows the percentage of dechlorination for three of the tested processes: single ozonation (DCP-O9), O_3/H_2O_2 (DCP-OP1) and O_3/UV/Fe(III) (DCP-ORF7). As it can be observed, higher and faster dechlorination degrees are obtained by the combination O_3/H_2O_2 rather than with single ozonation. This could be explained by that the predominant pathway in the initial degradation of DCP by O_3/H_2O_2 is considered to be direct dechlorination via a nucleophilic displacement of chloride (by $OH^{\cdot}$) while ozonation is presumably initiated by electrophilic addition of ozone molecules. Nevertheless, with both single ozonation and O_3/H_2O_2 a ca. 100% dechlorination is achieved after 60 minutes of treatment. Results for the combination O_3/UV/Fe(III) seem surprising, as only 50% dechlorination is attained.

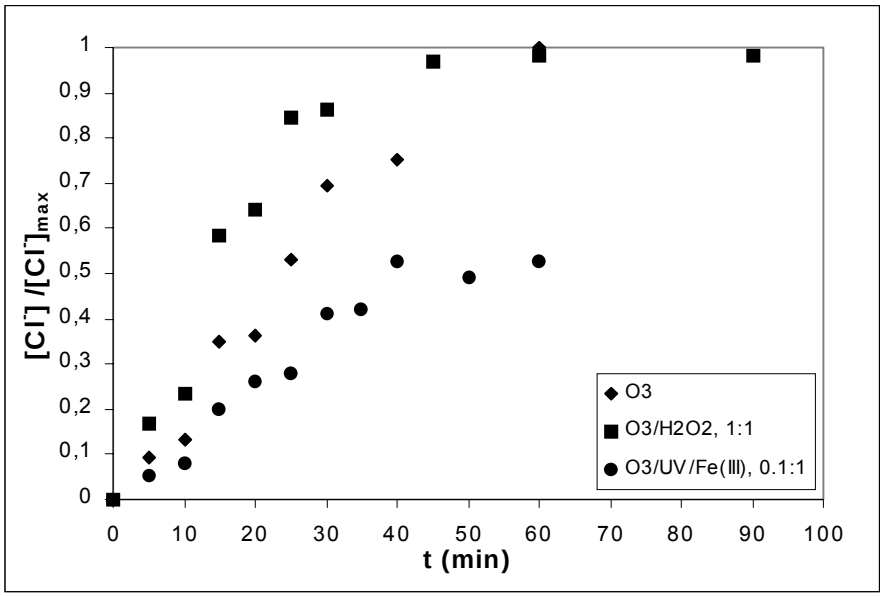

Graph 5.132. Comparison of the different processes for DCP removal – Percentage of dechlorination

Oxidation efficiency can be expressed generally in terms of an "Oxidation Index", abbreviated as OI, as it has been already commented in section 5.9. Low OI values show a higher degree of utilization of ozone during the oxidation processes. Table 5.19 summarizes OI values after 30 and 60 minutes treatment by the different processes, except O_3/UV/Fe(III), for which absorbed ozone dose cannot be calculated. As shown in this table, OI attained by single ozonation is only decreased by the combination O_3/UV/H_2O_2 in a 25-30%. This could be due to the higher radical production, resulting in faster DCP decomposition rates. Thus less ozone is required for decomposing the same amount of DCP.

Table 5.19. Oxidation index (mol O_3/mol COD) of DCP by the different processes after 30 and 60 minutes of treatment

	O_3	O_3/UV	O_3/H_2O_2	O_3/UV/H_2O_2	O_3/UV/Fe(III)
After 30 minutes	1.37	1.53	1.90	0.98	-
After 60 minutes	1.60	1.31	1.63	1.20	-

Analogous to this parameter, a "mineralization index" can be defined, as the ratio of ozone consumed to the amount of TOC converted to CO_2. Values are presented in Table 5.20. As it can be observed, with regard to TOC this index is greatly improved by the addition of UV (44% decrease with respect to single ozonation).

Table 5.20. Mineralization index (mol O_3/mol TOC) of DCP by the different processes after 30 and 60 minutes of treatment

	O_3	O_3/UV	O_3/H_2O_2	O_3/UV/H_2O_2	O_3/UV/Fe(III)
After 30 minutes	4.74	2.67	5.56	3.15	-
After 60 minutes	3.65	2.08	3.56	2.44	-

As it has been mentioned in section 5.9, a simple two-step consecutive kinetic model has been found in the literature (Ku et al., 1996) to fit well in modeling the behavior of species during the decomposition of phenols, based on elemental mass balances of carbon and chlorine during the reaction. Thus, the mass balance of carbon is:

$$C_{total} = (DCP)_{ct} + (Interme)_{ct} + (CO_2)_{ct} \quad [5.20]$$

where

C_{total} = total initial amount of DCP as carbon, mg $C.L^{-1}$

$(DCP)_{ct}$ = amount of DCP as carbon at time t, mg $C.L^{-1}$

$(Interme)_{ct}$ = amount of intermediates as carbon at time t, mg $C.L^{-1}$

$(CO_2)_{ct}$ = amount of inorganic carbon as carbon at time t, mg $C.L^{-1}$

The amount of CO_2 formed is calculated as the difference between the initial TOC and the TOC at a certain reaction time t. The amount of organic intermediates as carbon is calculated by the difference between the TOC and the amount of DCP. Due to the complexity of the decomposition schemes of phenols by advanced oxidation processes, the simplified two-step consecutive kinetic model is used to describe the temporal behavior of reacting carbon-containing species during the reaction (Ku et al., 1996). Each step of the reaction is assumed to be a first-order and irreversible reaction. The model and profiles of species are derived from the following equations :

$$DCP\,(C_a) \xrightarrow[O_3, OH^{\bullet}]{k_1} Intermediates\,(C_b) \xrightarrow[O_3, OH^{\bullet}]{k_2} CO_2(aq)(C_c) \rightleftarrows CO_2\,(g)$$

$$-r_a = -dC_a/dt = k_1C_a \quad [5.9]$$

$$r_b = dC_b/dt = k_1C_a - k_2C_b \quad [5.10]$$

$$r_c = dC_c/dt = k_2C_b \quad [5.11]$$

which yields:

$$C_a = C_{ao}e^{-k1\cdot t} \quad [5.12]$$

$$C_b = C_{ao}k_1(e^{-k1\cdot t} - e^{-k2\cdot t})/(k_2-k_1) \quad [5.13]$$

$$C_c = C_{ao} - C_a - C_b \quad [5.14]$$

where

k_1 , k_2 = pseudo-first order rate constants for first and second decomposition steps based on carbon, respectively, min^{-1}

$C_a = (DCP)_c$, amount of DCP as carbon, mg $C.L^{-1}$

$C_b = (Interme)_c$, amount of intermediates as carbon, mg $C.L^{-1}$

$C_c = (CO_2)_c$, amount of inorganic carbon as carbon, mg $C.L^{-1}$

When DCP is completely destroyed, equation [5.10] can be simplified and the k_2 value can be determined by:

$$\ln(\frac{C_b}{C_{bc}}) = -k_2\,(t - t_{bc}) \quad [5.15]$$

t_{bc} = time required for 99% of DCP to have disappeared, min

C_{bc} = concentration of (Interme) at t_{bc}, mg $C.L^{-1}$

By following this mathematical model, the values of C_a, C_b and C_c during time have been calculated for each of the processes. In the present case, t_{bc} has been set to 30 min. Table 5.21 summarizes values of k_1 and k_2 for the different processes. Comparing the values of k_1 and k_2, the rate-determining step of mineralization of DCP is presumed to be the second step. In the first step all the processes exhibit similar mineralizing rates, while in the second step (mineralization of the formed intermediates) the mineralization rate of single ozonation is significantly enhanced by the addition of UV radiation (150%), UV combined with H_2O_2 (110%) and especially by the addition of UV radiation and ferric ion (330%).

Table 5.21. Pseudo-first order constants for the model developed by Ku et al. (1996) in the degradation of DCP (values of R^2 expressed between brackets)

Processes	k_1 (min^{-1})	k_2 (min^{-1})
O_3	0.0876 (0.99)	0.0057 (0.93)
O_3/UV	0.0904 (0.95)	0.0142 (0.99)
O_3/H_2O_2 (0.1:1)	0.0892 (0.93)	0.0051 (0.96)
O_3/UV/H_2O_2 (0.1:1)	0.0869 (0.94)	0.0120 (0.96)
O_3/UV/Fe(III) (0.1:1)	0.0835 (0.94)	0.0245 (0.99)

5.17.2. Biodegradability enhancement

Biodegradability indicators used throughout the present work have been BOD_5/COD and BOD_5/TOC ratios. The variation of those ratios during time for all the studied processes are shown in Graphs 5.133 and 5.134. The highest BOD_5/COD ratios have been achieved after 30 minutes of treatment, when DCP was completely depleted from solution. Best ratios have been achieved by O_3/UV/Fe (0.28) and single ozonation (0.25). Maximum ratios are similar to those found for NB, however treatment time has been reduced from 90 to 30 minutes. Highest BOD_5/TOC ratios have also been reached after 30 minutes by O_3/UV/Fe (0.52) and single ozonation (0.4), similar to NB as well. In light of the experimental results and due to the small differences between O_3 and O_3/UV/Fe, single ozonation would be used to enhance the biodegradability of the DCP solutions and the treatment time would be set to ca. 30 minutes.

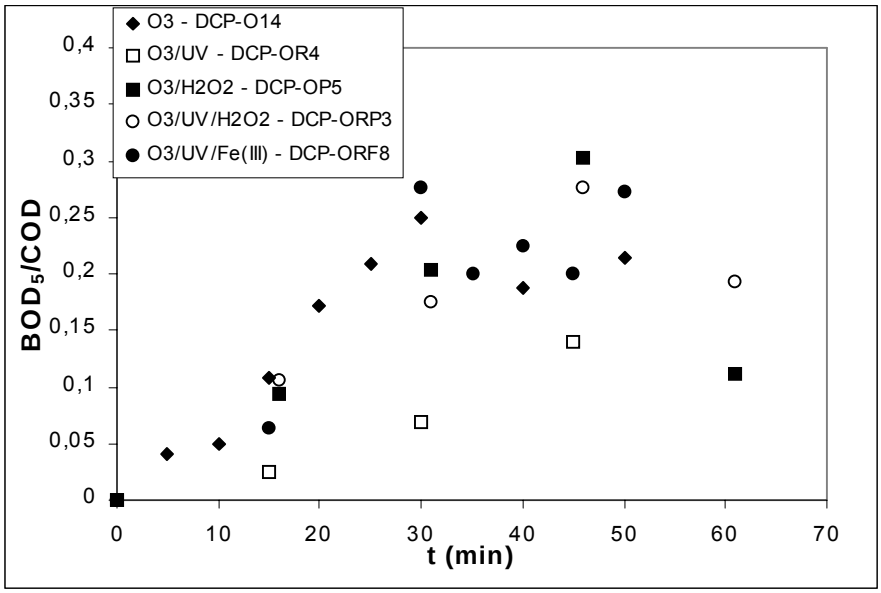

Graph 5.133. Comparison of the different processes for DCP removal – BOD_5/COD ratio

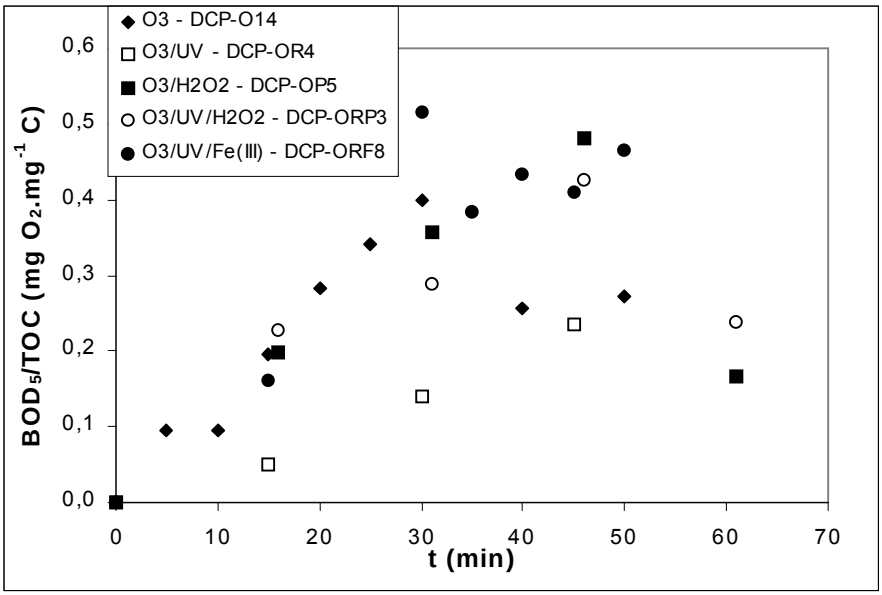

Graph 5.134. Comparison of the different processes for DCP removal – BOD_5/TOC ratio

5.17.3. Cost estimation

As it has been already performed with NB, an estimation of costs has been made in this section, regarding the operating costs for the processes that have been compared in this section. Costs of reagents and electricity were shown in Table 5.8. Costs have been calculated for 30 and 60 minutes of treatment and as the ratio to the amount of NB removed and to the amount of TOC mineralized. Results are shown in Table 5.22. With regard to kg of DCP removed, single ozonation shows the lowest costs while regarding kg of TOC mineralized O_3/UV/Fe is the most attractive option for DCP degradation. It has to be pointed out that this cost would decrease if solar light was used. Compared to NB, cost have been found to be ca. 2 times smaller.

Table 5.22. Comparison of costs among the studied processes

Processes	€/kg DCP rem (30 min)	€/kg DCP rem (60 min)	€/kg C rem (30 min)	€/kg C rem (60 min)
O_3	3.77	7.53	57.96	53.82
O_3/UV	3.99	7.98	56.63	40.21
O_3/H_2O_2 (0.1:1)	4.00	7.97	75.23	65.06
O_3/UV/H_2O_2 (0.1:1)	4.20	8.37	49.14	44.85
O_3/UV/Fe(III) (0.1:1)	4.26	8.50	41.18	31.37

5.18. Identification of intermediates

The change of colorless initial solution to pinkish or yellowish indicates the formation of reaction intermediates with aromatic structures. As it was commented in section 5.12.4, the dechlorination at 100% of DCP conversion was not complete, indicating the presence of chlorinated intermediates. Chlorobenzoquinone was identified by means of HPLC as reaction by-product but contrary to a previous research (Abe and Tanaka, 1997), chlorohidroquinone has not found among the formed intermediates. Qiu and co. (2002) and Duguet and co. (1987) pointed out the existence of chlorinated polymers. Hydroquinone, muconic acid and glycolic acid have been detected by Yu and Hu (1994) in the ozonation of DCP solutions at pH 3. Monochlorophenols, monochlorobenzenediols, dichlorobenzenediols, and several other organic chlorides were identified by GC/MS in the ozonation of DCP by Qiu and co. (2002). Nevertheless, toxicity of different dichlorophenols (among them, 2,4-DCP) solutions after ozonation has been studied by Trapido and co. (1997) by using *Daphnia magna* 24 hours test, finding that after an ozonation time that caused 90-95% reduction of DCP level, the ozonated samples possessed only minor or even no advers effects to the organism *Daphnia magna*.

Samples were analyzed by means of HPLC to identify the products of the oxidation of DCP. The standards used for the identification were: chlorohidroquinone, 4,6-dichlororesorcinol, chlorobenzoquinone, hidroquinone, resorcinol, p-benzoquinone, formic acid and oxalic acid. Among them, only chlorobenzoquinone has been clearly identified.

Ozonation : In Figures 5.7 and 5.8 the chromatograms corresponding to samples after 10 and 25 minutes of the experiment DCP-O13, respectively, are shown. As it can be seen, the peak at ca. 6.7 minutes, which was identified as chlorobenzoquinone, disappeared after 25 minutes of treatment. At this time, less than 5% of the initial DCP was present. Among the remaining compounds at this time, resorcinol is thought to have been identified. The depletion of DCP and chlorobenzoquinone may account for the increase of biodegradability observed at this time.

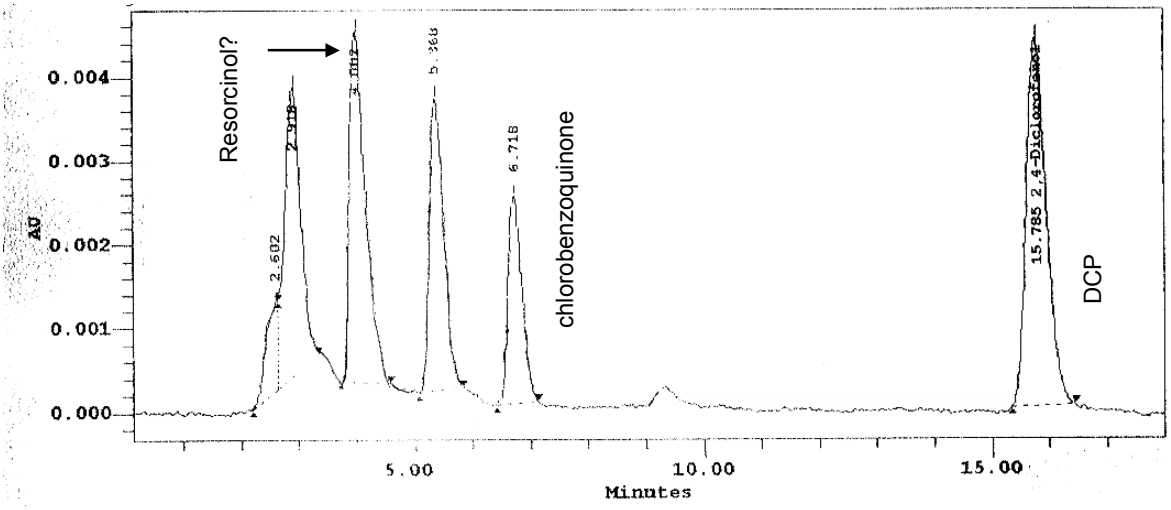

Figure 5.7. Chromatogram corresponding to sample after 10 minutes of ozonation of experiment DCP-O13

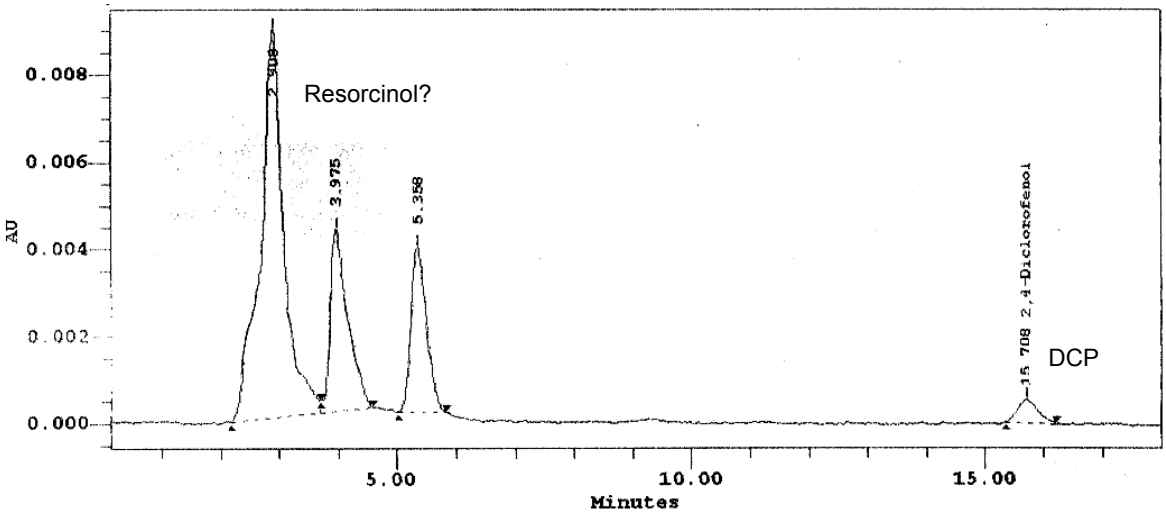

Figure 5.8. Chromatogram corresponding to sample after 25 minutes of ozonation of experiment DCP-O13

O_3/UV: With regard to the intermediates, there are two remarkable differences: chlorobenzoquinone was not produced as intermediate, while new intermediates appeared, which could not be identified (see Figure 5.9). When DCP was depleted from solution, those intermediates were still present.

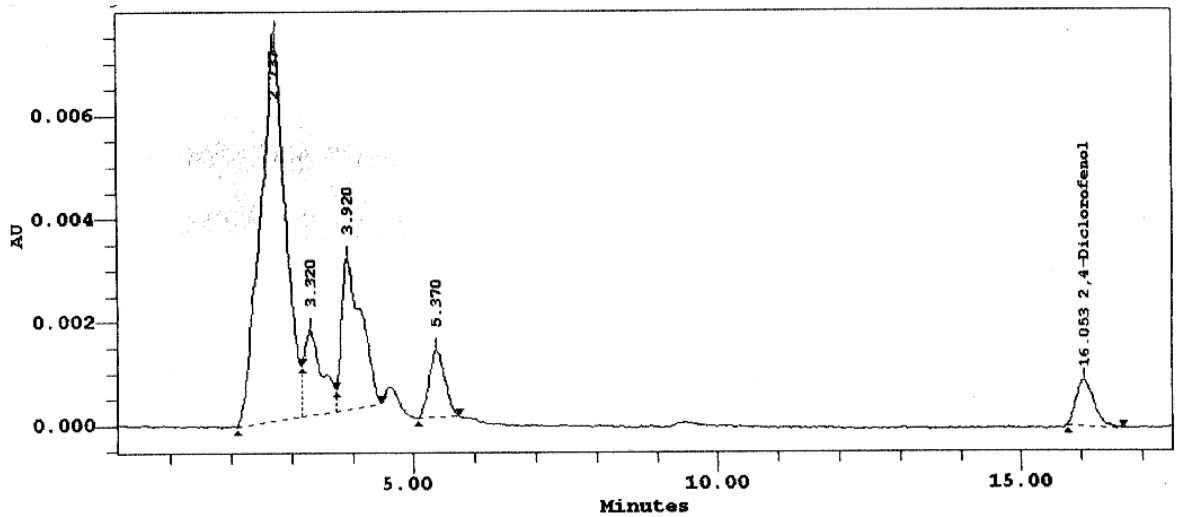

Figure 5.9. Chromatogram corresponding to sample after 21 minutes of treatment of experiment DCP-OR1

O_3/UV/H_2O_2: Intermediates are rather similar to those found for the photolytic ozonation. Chlorobenzoquinone was not produced as intermediate either, while new intermediates appeared, which could not be identified. When DCP was depleted from solution, those intermediates were still present as well. (see Figure 5.10).

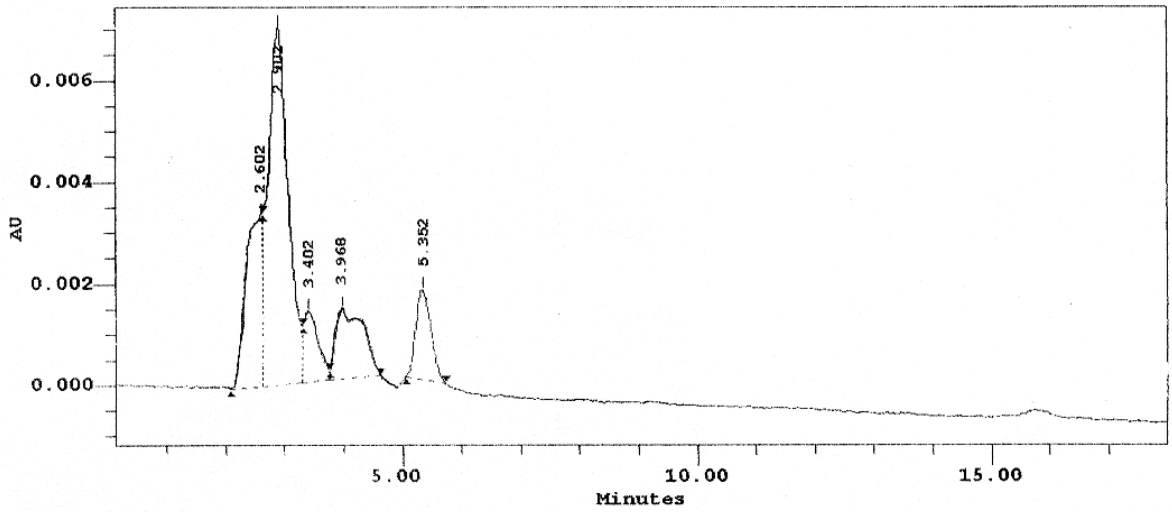

Figure 5.10. Chromatogram corresponding to sample after 30 minutes of treatment of experiment DCP-ORP3

O_3/UV/Fe: Intermediates were rather similar to those produced by single ozonation (see Figure 5.11). Chlorobenzoquinone was detected as well, although the concentration was seemed to be smaller. This compound was removed earlier from the solution: after 15

minutes chlorobenzoquinone was not present. Thus, biodegradability between 15 and 30 minutes may be higher than by single ozonation.

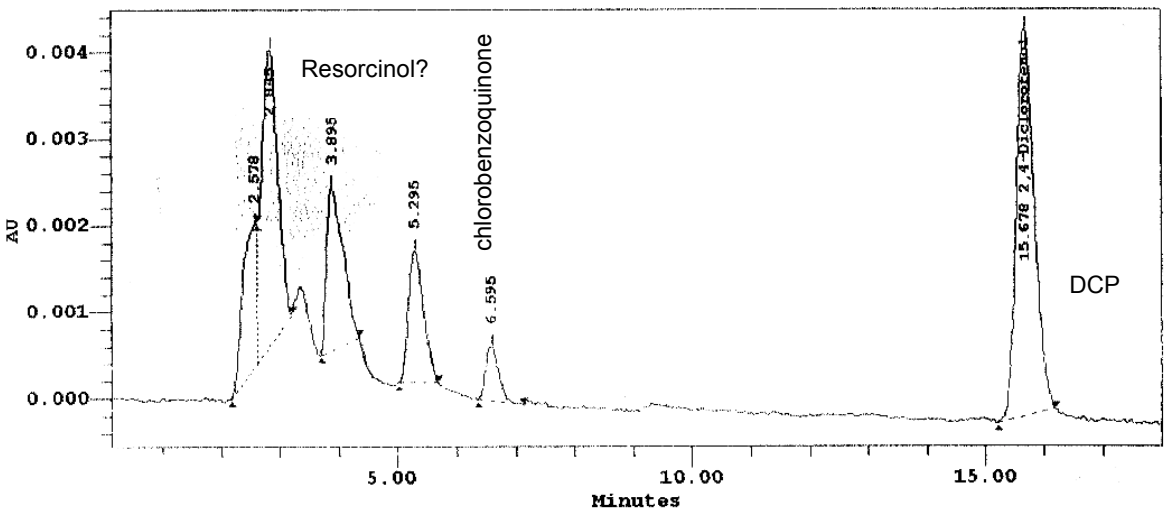

Figure 5.11. Chromatogram corresponding to sample after 10 minutes of treatment of experiment DCP-ORF8

6. Sequential Ozonation and biological oxidation of waste waters: a model including biomass inhibition by residual oxidant

Activated sludge processing has traditionally been the usual approach for the treatment of municipal sewage and wastewater from many industrial activities. However, it is not feasible to treat toxic or recalcitrant substances, since these reduce the biodegradation performance and eventually could inhibit the process (Beltran et al., 2000a).

Ozone or ozone-based technologies have been shown to effectively oxidize recalcitrant compounds in wastewater to more readily biodegradable oxidation products that can be treated using a conventional aerobic biological treatment (Sontheimer et al., 1978; Marco et al., 1997; Ledakowicz and Gonera, 1999). In this sense, the interest in the development of sequential chemical and biological processes for the treatment of wastewater has considerably grown (Scott and Ollis, 1995, 1997). Thus, the need for credible, useful engineering models for such an integrated flow system increases. Previously, kinetic forms arising in simple reaction networks for treatment of recalcitrant wastewaters initially containing non-biodegradable materials have been explored (Esplugas and Ollis, 1996; Scott and Ollis, 1996), and those models shown to produce results reflective of the modest quantitative literature available to date.

A central kinetic feature, previously unexplored, in engineering models of two-step chemical followed by biological oxidation, is the potential impact of residual oxidant (e.g. ozone or hydrogen peroxide) on the bioreactor performance. Ozone is known to be a strong germicidal agent (Sulzer et al., 1959; Morris, 1975; Lezcano et al., 1999; Rennecker et al., 1999), so ozone residuals could reduce the number of viable cells present in the biological reactor. The concentration of ozone that kills bacteria has been reported to be from 0.04 to 0.1 ppm (volume) by Stockinger (1959). Hamelin et al. (1978) observed the killing capacity of ozone at concentrations higher than 10 ppm v. The mechanism of inactivation of bacteria by ozone is still not well known. Studies on *Escherichia coli* suggested that lesions to deoxyribonucleic acid (DNA) might be responsible for killing of bacteria by ozone (Hamelin and Chung, 1974; Hamelin et al., 1977, 1978). Other works pointed out that ozone destroys the function of the bacterial cell membrane via oxidation of membrane components such as proteins and lipids (Scott and Lesher, 1963; Komanapalli and Lau, 1996). The kinetics of disinfection with ozone has attracted considerable attention during the last years (Perrich et al., 1975; Zhou and Smith, 1994; Hunt and Mariñas, 1997, 1999; Rennecker et al., 1999) for the rational design of ozone disinfection contactors.

The present study reports a new engineering model incorporating this "residual oxidant effect" on the bioreactor in the integrated chemical/biological sequence. This model is created by combining classical chemostat kinetics with a recent model for the kinetics of ozone disinfection of wastewater treatment effluents applied to an activated sludge system. This new model predicts the bioreactor performance under various loadings of biodegradable intermediates, recalcitrant starting materials, and residual oxidant (ozone in the present case). These results would help to identify the regimes wherein a preconditioning of the bioreactor feed by an interposed air stripping operation would be necessary to reduce the residual ozone oxidant (Beltran et al, 2000 a,b) would be necessary. Similar models could be applied for other oxidants used in a chemical pretreatment, e.g. hydrogen peroxide residuals derived from processes such as UV/H_2O_2, O_3/H_2O_2, $O_3/UV/H_2O_2$ or Fenton processes, which may be expected to have some negative impact on the bioreactor performance.

6.1. Model Development.

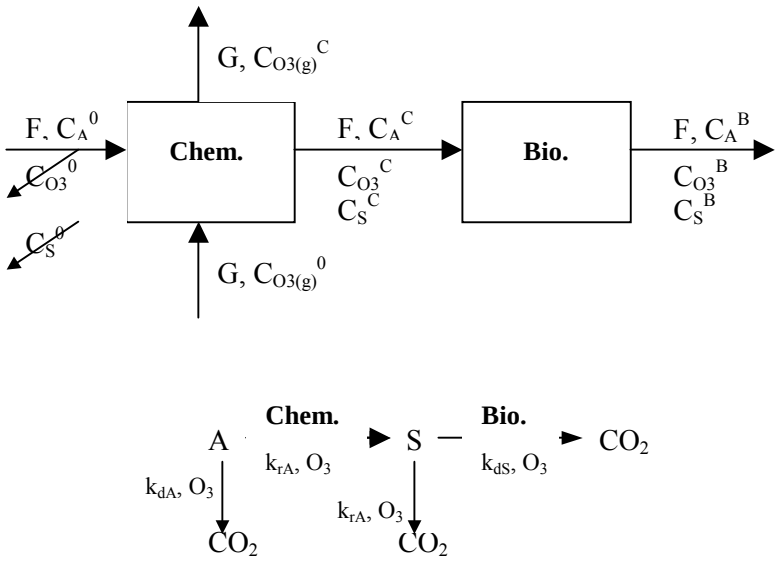

Figure 6.1. Scheme of the system and reactions taking place

As before (Esplugas and Ollis, 1996; Scott and Ollis, 1996; Esplugas et al., 2001), a simple kinetic model based on consecutive reactions is used: a non-biodegradable substance (A) is converted through ozonation in the chemical reactor into a single biodegradable intermediate (S), which may be consumed in a later biological step (Figure

6.1). Both chemical and biological reactor are considered continuous stirred tank reactors (CSTR) for convenience here.

For the simulation, model solutions have been found by using a quasi-Newton algorithm (Excel, Microsoft Office), with a precision of 10^{-9} and convergence of 10^{-8}.

6.1.1. Mathematical model for the chemical reactor

The chemical oxidation kinetics for ozone reactions are taken as second order, and predict oxidation reactor effluent levels for the three substances: A, S and ozone, the variations of which with the reactor residence time (θ_C) are given by equations [6.1-6.3]:

$$C_A^C = \frac{C_A^0}{1+\theta_C(k_{rA}+k_{dA})C_{O_3}^C} \qquad [6.1]$$

$$C_S^C = \frac{\theta_C k_{rA} C_{O_3}^C}{1+\theta_C k_{rS} C_{O_3}^C} C_A^C = \frac{\theta_C k_{rA} C_{O_3}^C}{1+\theta_C k_{rS} C_{O_3}^C} \cdot \frac{C_A^0}{1+\theta_C(k_{rA}+k_{dA})C_{O_3}^C} \qquad [6.2]$$

$$C_{O_3}^C = \frac{\theta_C D_{O_3}}{1+\theta_C\left[(k_{rA}+k_{dA})C_A^C + k_{rS}C_S^C\right]} \qquad [6.3]$$

where ozone dose rate D_{O3} is defined as:

$$D_{O_3} = \frac{G}{V_C}(C_{O_3(g)}^0 - C_{O_3(g)}^C)$$

From [6.1], [6.2] and [6.3] we obtain a cubic equation for $C_{O3}{}^C$ [6.4]:

$$\frac{D_{O_3}}{k_{rS}} + \left(D_{O_3}\theta_C(1+B) - \frac{1}{\vartheta_C k_{rS}} - C_A^0 B\right)C_{O_3}^C - \left[(1+B) + \theta_C C_A^0(2k_{rA}+k_{dA)}) - \theta_c^2 k_{rS} D_{O_3} B\right](C_{O_3}^C)^2 - (\theta_C k_{rS} B)(C_{O_3}^C)^3 = 0$$

[6.4]

where $B = \frac{k_{rA}+k_{dA}}{k_{rS}}$.

For the simulation, the following values or ranges of values for each variable have been considered: $C_A{}^0$ = 5 mol.m^{-3}; D_{O3} = 3-10 mol.m^{-3}.h^{-1} and k_{rA}, k_{rS}, k_{dA} = 10^2 - 10^7 m^3.mol^{-1}.h^{-1} (Yao and Haag, 1991, see Table 6.1)

Table 6.1. Rate constants for direct reaction of ozone with some potential organic drinking water contaminants.

Compound Name	k_{O3} ($m^3.mol^{-1}.h^{-1}$)
Lindane	≤ 144
Trichloroethylene	$5.4.10^5$
Hexachlorocyclopentadiene	$3.2.10^5$
Endrin	≤ 72
m-Dichlorobenzene	2052
PCB's	180-3240
Carbofuran	$2.2.10^6$
Azobenzene	$7.9.10^5$
Aldicarb	$1.6.10^8 – 1.6.10^9$
2,4-D	4000
2,4,5-TP	$3.2.10^4$
Atrazine	$(2.2\text{-}8.6).10^4$

6.1.2. Mathematical model for the biological reactor

A new engineering kinetic model incorporating the "residual oxidant effect" on the bioreactor in the integrated chemical/biological oxidation sequence is developed here by combining classical chemostat kinetics (Bailey and Ollis, 1986; Esplugas and Ollis, 1996; Scott and Ollis, 1996) with a new model for the kinetics of ozone (Hunt and Mariñas, 1997, 1999). To make the model simpler, we assume that no reaction of A takes place in the bioreactor (it is not biodegradable, nor does it react appreciably with ozone).

a) Classical chemostat kinetics

The use of a continuous stirred tank reactor to extend the duration of culture of microbes was developed in the 1950s by Novick and Szilard, and Monod. The realization that a CSTR could be used to maintain microbial growth at steady state value, which could be varied from any growth rate up to the maximum μ_{max} was an important advance (Bailey and Ollis, 1986; Blanch and Clark, 1996; Grady et al., 1999). The growth rate model used is the one developed by Monod (Monod, 1950) based on the observations of the growth of *E. coli* at various glucose concentrations, where it is assumed that only one substrate (the growth-limiting substrate, S) is important in determining the rate of cell proliferation.

$$\mu = \frac{\mu_{max} S}{K_S + S} \quad [6.5]$$

where μ_{max} is the maximum specific growth rate of the cells and K_S is the value of the limiting nutrient concentration, which results in a growth rate of half the maximum value. Values of μ_{max} vary with the type of organism and the value of K_S depends on the nature of the substrate. This simple model has been shown also to model activated sludge kinetics (more complete forms including endogenous and exogenous metabolism are also known).

The mass balances for the viable biomass (N) and substrate (S) in a CSTR are presented below [6.6-6.7]:

$$\frac{dN}{dt} = \frac{F}{V_B}(N_0 - N) + \mu N = 0 \quad [6.6]$$

$$\frac{dS}{dt} = \frac{F}{V_B}(S_0 - S) - \frac{1}{Y_{N/S}}\mu N = 0 \quad [6.7]$$

At steady state and when the feed stream is sterile (N_0=0) two solutions are possible:

$N_{SS} = 0$ or $\mu_{SS} = F/V_B = D$

For the second solution and using the Monod equation, the following expressions can be applied to determine the concentration of S and viable biomass in the outlet of the biological reactor:

$$S_{SS} = \frac{D K_S}{\mu_{max} - D} \quad [6.8]$$

$$N_{SS} = Y_{N/S}\left(S_0 - \frac{D K_S}{\mu_{max} - D}\right) \quad [6.9]$$

b) Hunt and Mariñas model (Hunt and Mariñas, 1999)

These authors investigated and modeled the apparent chemical and inactivation reactions taking place during the disinfection of *Escherichia coli* with ozone in the presence of humic acid (representing organic matter). The authors introduced a new variable, X, for the concentration of “fast” ozone demand constituents in *E. coli* cells (number of reactive groups, e.g., double bonds C=C in cell membrane). A relationship

between the batch cell inactivation kinetics and the kinetics for the reaction between molecular ozone and the fast-reacting portion of *E. coli* cells was established. At initial time, this relationship is stoichiometric,

$$X_0 = \alpha_0 N_0 \qquad [6.10]$$

but is found to evolve non-linearly over time:

$$\left(\frac{N}{N_0}\right) = \left(\frac{X}{X_0}\right)^{k_i/k_x} \qquad [6.11]$$

where k_i is the second order inactivation rate constant of the reaction of living cells with ozone:

$$\frac{dN}{dt} = -k_i C_{O_3}^B N \qquad [6.12]$$

and k_X is the second order rate constant for the reaction of ozone with the fast ozone demand groups:

$$\frac{dC_{O_3}^B}{dt} = -k_X C_{O_3}^B X \qquad [6.13]$$

The value of k_i was found to be 138 $L.mg^{-1}.s^{-1}$ at 20°C and the quotient k_i/k_x equal to 80 for *E. coli* by Hunt and Mariñas (1999). Lezcano et al. (1999) also found for the inactivation of six bacterial strains by ozone to be represented by a second order kinetic expression depending on both dissolved ozone and microorganism concentration.

It was also found that only a 5.6% loss of the fast-reacting constituents in *E. coli* corresponded to 99% inactivation of this microorganism. That means that this variable (X) can be considered almost constant and the balance of ozone can be simplified by setting the production rate of X proportional to the growth rate of viable cells at all the times. The value of α_0 was found to be $1.62.10^8$ O_3 molecules/CFU, similar to the value found by Scott and Lesher (1963), who reported that at a concentration of ozone that kills 50% of a culture, the number of molecules of ozone consumed per bacterium killed was approximately 2.10^7.

c) Mathematical model for the biological reactor

A model, which is derived from the combination of the chemostat equations and the model of the bacterial inactivation kinetics of ozone developed by Hunt and Mariñas, is presented below. Mass balances for ozone, S, fast ozone-demand constituents (X) and viable cells (N) are presented in equations [6.14-6.17], respectively:

$$D\,(C_{O_3}^{C} - C_{O_3}^{B}) = k_X C_{O_3}^{B} X + k_{rS} C_{O_3}^{B} C_S^{B} \qquad [6.14]$$

$$D\,(C_S^{C} - C_S^{C}) = \frac{\mu_{max} C_S^{B}}{K_S + C_S^{B}} \frac{N}{Y_{N/S}} + k_{rS} C_{O_3}^{B} C_S^{B} \qquad [6.15]$$

$$D\,X = \left(\frac{\mu_{max} C_S^{B}}{K_S + C_S^{B}} \right) N\,\alpha - k_x C_{O_3}^{B} X \qquad [6.16]$$

(It has to be considered the contribution to X from all (viable + dead) cells, because even dead cells still have reactive groups towards ozone, per Hunt and Mariñas data (1999)).

$$D = \frac{\mu_{max} C_S^{B}}{K_S + C_S^{B}} - k_i C_{O_3}^{B} \qquad [6.17]$$

From [6.17],

$$D + k_i C_{O_3}^{B} = \frac{\mu_{max} C_S^{B}}{K_S + C_S^{B}} \qquad [6.18]$$

and the concentration of S in the outlet as a function of the concentration of ozone is:

$$C_S^{B} = \frac{K_S (D + k_i C_{O_3}^{B})}{\mu_{max} - (D + k_i C_{O_3}^{B})} \qquad [6.19]$$

From [6.15], [6.18] and [6.19] the concentration N of viable cells as a function of ozone concentration can be obtained:

$$N = \frac{D\,C_S^{C}\,Y_{N/S}}{D + k_i C_{O_3}^{B}} - \frac{Y_{N/S}\,(D + k_{rS} C_{O_3}^{B})\,K_S}{\mu_{max} - (D + k_i C_{O_3}^{B})} \qquad [6.20]$$

From [6.16] and [6.18] the concentration of fast ozone demand groups, again as f(C_{O3}^{B}) is:

$$X = \frac{(D + k_i C_{O_3}^B)}{(D + k_X C_{O_3}^B)} N \alpha \qquad [6.21]$$

and from [6.14], [6.18] and [6.21] an expression for the concentration of ozone C_{O3}^B in the bioreactor outlet stream:

$$\frac{D}{(D + k_i C_{O_3}^B)} \left(\frac{C_{O_3}^C}{C_{O_3}^B} - 1 \right) = \frac{k_X N \alpha}{(D + k_X C_{O_3}^B)} + \frac{k_{rS} K_S}{\mu_{max} - (D + k_i C_{O_3}^B)} \qquad [6.22]$$

Simplified model

To simplify the system, we first consider that the reaction of S with ozone is unimportant (S disappears mainly through reaction with biomass). The resultant, simplified equations obtained for the concentration of cells, fast ozone demand constituents and ozone are [6.23-6.25]:

$$N = \frac{D\, Y_{N/S}}{D + k_i C_{O_3}^B} \left(C_S^C - \frac{K_S}{\left(\frac{\mu_{max}}{D + k_i C_{O_3}^B} \right) - 1} \right) \qquad [6.23]$$

$$X = \frac{D}{k_x} \left(\frac{C_{O_3}^C}{C_{O_3}^B} - 1 \right) \qquad [6.24]$$

$$\frac{(D + k_X C_{O_3}^B)}{k_X} \left(\frac{C_{O_3}^C}{C_{O3}^B} - 1 \right) = Y_{N/S}\, \alpha \left(C_S^C - \frac{K_S}{\frac{\mu_{max}}{D + k_i C_{O_3}^B} - 1} \right) \qquad [6.25]$$

These equations can be further simplified by considering the limiting cases where $k_i C_{O3}^B >> D$ or $k_i C_{O3}^B << D$.

For the simulations, the following literature ranges of values have been considered for the variables (in brackets, chosen values): μ_{max} = 0.5-1.22 h^{-1} (0.8) (Blanch and Clark, 1996); K_S= 0.01-0.05 $mol.m^{-3}$ (0.02) (Nielsen and Villadsen, 1994; Blanch and Clark, 1996); $Y_{N/S}$ = $1.6.10^{-10}$ – $2.2.10^{-10}$ mol cells.mol^{-1} S ($1.9.10^{-10}$) (Nielsen and Villadsen, 1994); N = 10^{-13} – 10^{-9} mol cells.m^{-3} (Bailey and Ollis, 1986); k_i = 10^3 - $2.4.10^7$ $m^3.mol^{-1}.h^{-1}$

($2.4.10^4$ and $2.4.10^7$) (Hunt and Mariñas, 1997, 1999; Lezcano et al., 1999); $k_X = k_i/80$ (Hunt and Mariñas, 1999); $k_{rS} = 10^4 – 10^7$ $m^3.mol^{-1}.h^{-1}$ (10^4)

6.2. Calculated Results and Discussion

6.2.1.Results for the chemical reactor

For the variable range shown, among the three roots of the cubic equation [6.4] are two negative and one positive solutions; only the latter has physical meaning. Results for an arbitrary chosen residence time of 0.8 h are presented in Table 6.2 for various ozone dose rates (D_{O3}). Graphs 6.1 to 6.3 illustrate the evolution with the residence time of C_{O3}^C, C_A^C and C_S^C when the kinetic constants are taken to be 10^4 $m^3.mol^{-1}.h^{-1}$. At a constant dose rate, no differences are observed when the ozone kinetic constants are increased to 10^7 $m^3.mol^{-1}.h^{-1}$ with regard to C_S^C and C_A^C, while C_{O3}^C decreases in a complementary fashion (Figures not shown).

Table 6.2. Evolution of the main variables in the chemical reactor with the dose of ozone.

Ozone dose ($mol.m^{-3}.h^{-1}$)	$k_{rA}=k_{rS}=k_{dA}=k$ ($mol.m^{-3}$)	C_{O3}^C ($mol.m^{-3}$)	C_A^C ($mol.m^{-3}$)	C_S^C ($mol.m^{-3}$)
3	10^2	$4.57.10^{-3}$	2.887	0.773
3	10^4	$4.59.10^{-5}$	2.884	0.774
3	10^7	$4.59.10^{-8}$	2.884	0.774
5	10^2	$1.13.10^{-2}$	1.777	0.845
5	10^4	$1.14.10^{-4}$	1.770	0.845
5	10^7	$1.12.10^{-7}$	1.789	0.846
10	10^2	0.62	0.0497	0.0487
10	10^4	0.502	$6.2.10^{-4}$	$6.2.10^{-7}$
10	10^7	0.5	~ 0	~ 0

As it can be observed, the concentration of ozone grows with the residence time, as the reactants disappear and the ozone dose rate remains constant. As it was expected, the disappearance rate of A increases with the dose of ozone. It can also be seen that the intermediate S presents a maximum. This maximum appears earlier when the dose of ozone is increased. S goes to zero as a consequence of a second order kinetics and a constant ozone dosing rate.

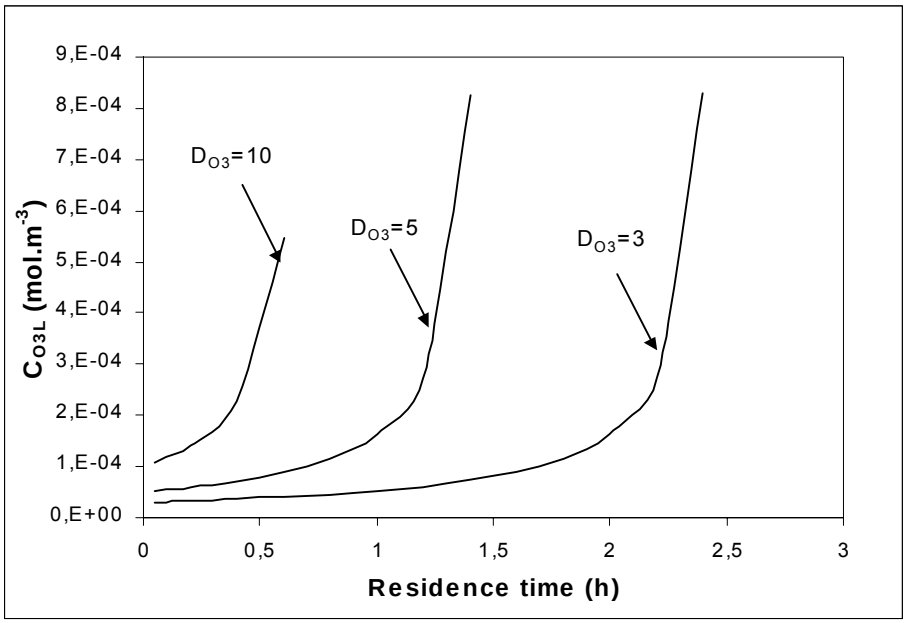

Graph 6.1. Ozone concentration (C_{O3}^{C}) vs. residence time for ozone doses rates of 3, 5 and 10 mol.m^{-3}.h^{-1} (k = 10^4 m^3.mol^{-1}.h^{-1})

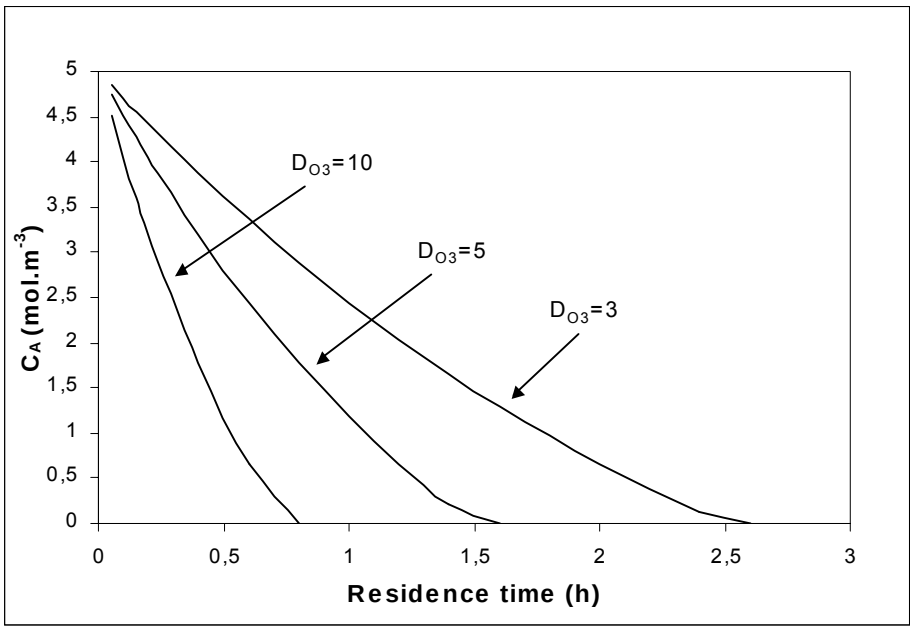

Graph 6.2. Concentration of A (C_A^C) vs residence time for ozone doses rates of 3, 5 and 10 mol.m^{-3}.h^{-1} (k=10^4 m^{-}.mol^{-1}.h^{-1})

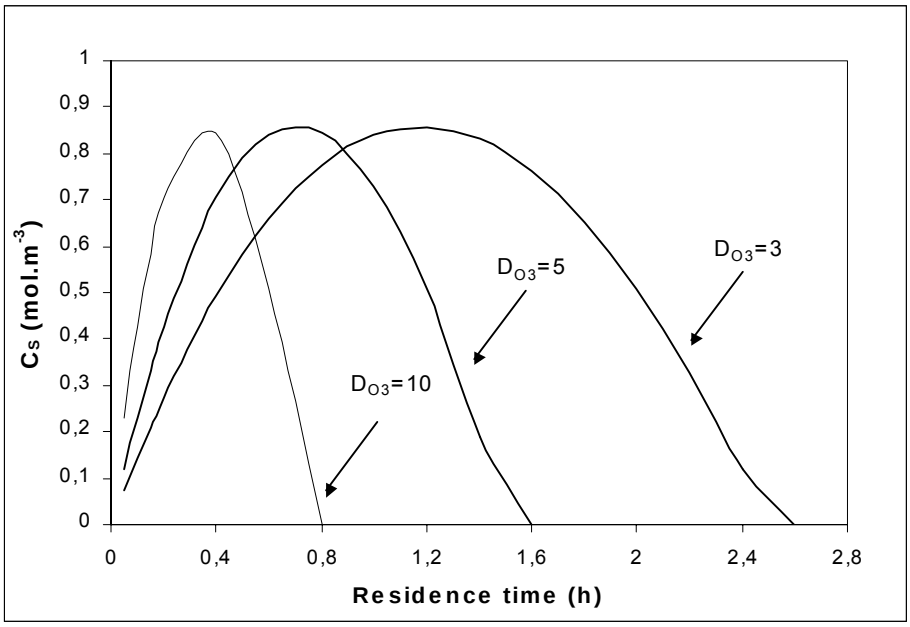

Graph 6.3. Concentration of S (C_S^C) vs. residence time for ozone dose rates of 3, 5 and 10 mol.m^{-3}.h^{-1} (k = 10^4 m^3.mol^{-1}.h^{-1})

6.2.2. Results for the biological reactor

Two cases are considered for the modeling of the biological reactor. In the first one, we assume that no reaction of S with the ozone present in the system takes place (equations [6.19] and [6.23-6.25]). The second case adds this reaction in the system (equations [6.19-6.22]). For the simulation of both cases we take the solution of the chemical reactor to receive an ozone dose of 5 mol.m^{-3}.h^{-1} and the kinetic constants to have a value is 10^4 m^3.mol^{-1}.h^{-1} with regard to C_S^C, but changing the concentration of ozone in the inlet of the biological reactor (or outlet of the chemical reactor) to test its impact in the performance of the biological reactor.

Three solutions are found for equation [6.25], of which two are positive and within 15% of each other. In Table 9.3 the results for the smaller one are presented. Graphs 6.4 to 6.7 show the evolution of C_s^B, C_{O3}^B, N and X with the residence time for an inlet concentration of ozone (C_{O3}^C) between 5.10^{-3} and 0 mol.m^{-3} when a value of k_i equal to $2.4.10^4$ m^3.mol^{-1}.h^{-1} is used.

Table 6.3. Results not considering the reaction of S with the ozone present in the system.

$[O_3]$ inlet (mol/m^3)	k_i ($m^3.mol^{-1}.h^{-1}$)	Res. Time[(1)] (h)	N [(2)] ($mol.m^{-3}$)	$[1-(N/N_{max})]x100$ (% cells killed)	X[(3)] ($mol.m^{-3}$)	$1-(X/X_{max})x100$ (% fod destroyed)	$[O_3]$ outlet (mol/m^3)
10^{-3}	$2.4.10^{4}$	7	$3.8.10^{-11}$	78.1	0.0245	4.3	$5.6.10^{-6}$
10^{-3}	$2.4.10^{7}$	7-8	$3.8.10^{-11}$	78.1	0.0245	4.3	$5.6.10^{-9}$
5.10^{-4}	$2.4.10^{4}$	4-6	$6.2.10^{-11}$	61.3	0.0251	1.95	$2.8.10^{-6}$
5.10^{-4}	$2.4.10^{7}$	4-6	$6.2.10^{-11}$	61.3	0.0251	1.95	$2.8.10^{-9}$
10^{-4}	$2.4.10^{4}$	1.9	$1.2.10^{-10}$	23.8	0.0255	0.39	5.10^{-7}
10^{-4}	$2.4.10^{7}$	2	$1.2.10^{-10}$	23.8	0.0255	0.39	5.10^{-10}
5.10^{-5}	$2.4.10^{4}$	1.7	$1.4.10^{-10}$	13.1	0.0256	0	$2.5.10^{-7}$
10^{-5}	$2.4.10^{4}$	1.4	$1.6.10^{-10}$	3.1	0.0256	0	$5.4.10^{-8}$
0	------	1.3	$1.6.10^{-10}$	0	0.0256	0	0

(1) Earliest non-washout residence time.

(2) N corresponding to the plateau value for high residence times.

(3) X corresponding to the plateau value for high residence times.

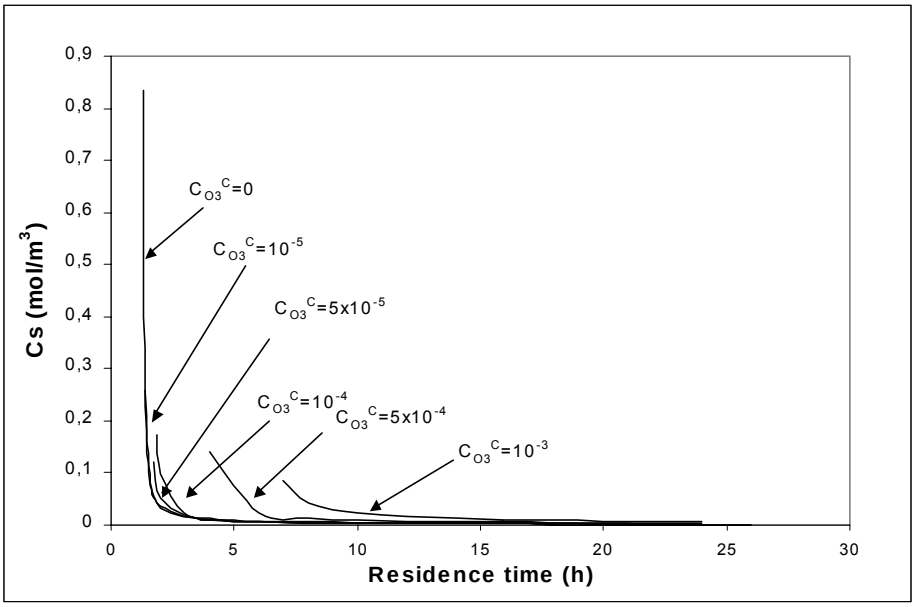

Graph 6.4. Concentration of S (C_S^C) vs. residence time ($k_i = 2.4x10^4\ m^3.mol^{-1}.h^{-1}$)

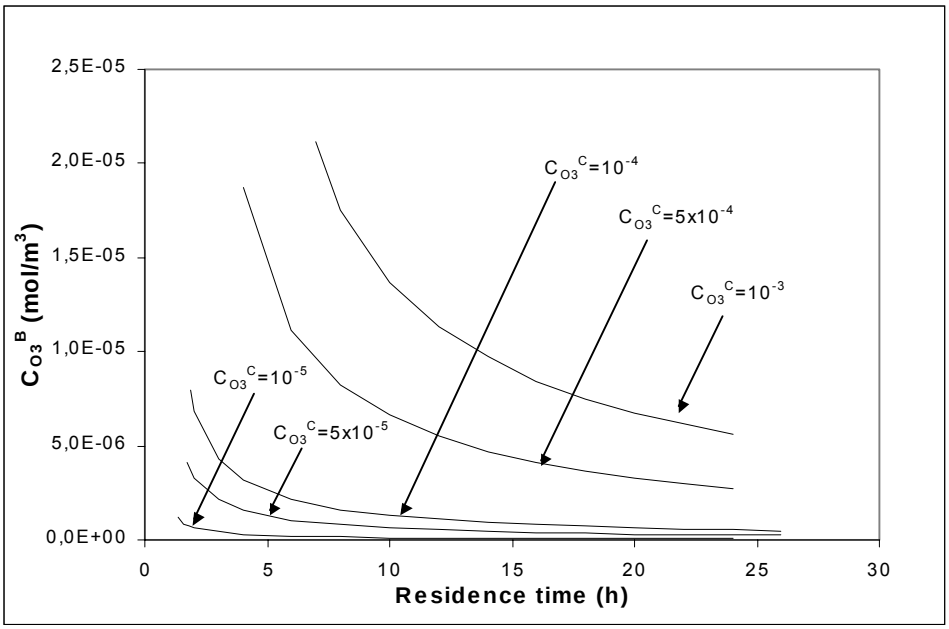

Graph 6.5. Concentration of ozone (C_{O3}^{B}) vs. residence time (k_i = 2.4x10^4 m^3.mol^{-1}.h^{-1})

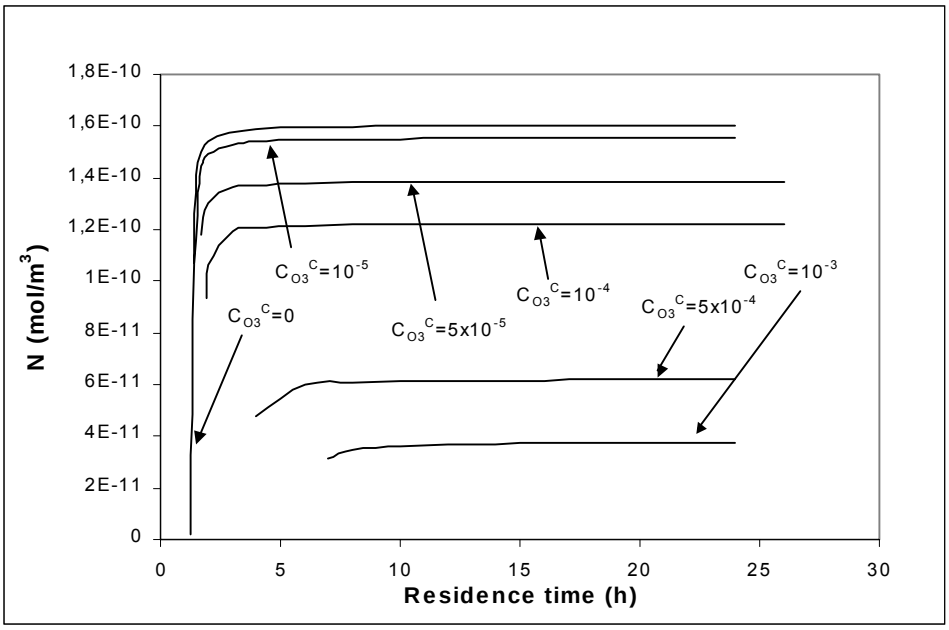

Graph 6.6. Concentration of viable cells (N) vs. residence time (k_i = 2.4x10^4 m^3.mol^{-1}.h^{-1})

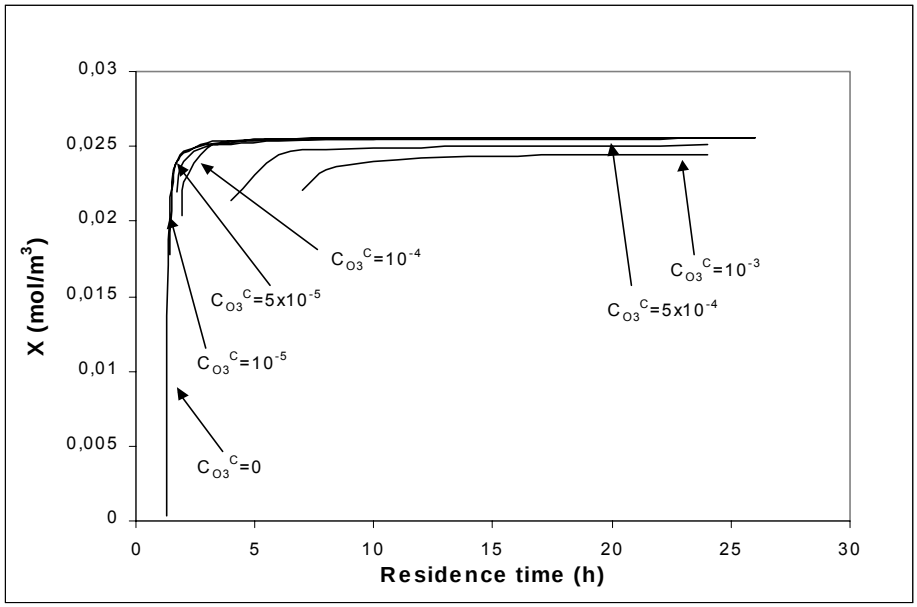

Graph 6.7. Concentration of fast ozone demand groups (X) vs. residence time (k_i = 2.4x10^4 m^3.mol^{-1}.h^{-1})

In these graphs it can be noticed that as the concentration of ozone in the inlet of the biological reactor increases, there is a larger range of dilution rates for which there is no solution (wash-out), and the system has a useful solution (C_s^b >0) only at higher residence times. It can also be seen that as the concentration of ozone increases, differences between N and N_{max} (when there is no ozone in the system) become more important: when the inlet concentration of ozone is 10^{-3} mol/m^3, the amount of live biomass has been decreased in about 78%, whereas at 5.10^{-4} and 5.10^{-5} mol/m^3 it has been reduced in 61% and 13%, respectively. Differences in X are smaller, verifying the assumption of considering X almost constant (and therefore X production rate is proportional to N growth rate). Even more simplified expressions could be applied if the inlet concentration of ozone is higher than 10^{-3} mol/m^3 (0.48 ppm) or smaller than 5.10^{-5} mol/m^3 (0.0024 ppm), where the assumptions that $k_i.C_{O3}^b$ >> D and $k_i.C_{O3}^b$ << D, respectively, are valid.

For the second case (adding the reaction of S with ozone), only one positive root of equation [6.22] exists. Results are presented in Table 6.4. Graphs 6.8 to 6.11 show the evolution of C_s^B, C_{O3}^B, N and X with the residence time for an inlet concentration of ozone (C_{O3}^C) between 5.10^{-3} and 0 mol.m^{-3} when a value of k_i = 2.4.10^4 m^3.mol^{-1}.h^{-1} is used.

Table 6.4. Results considering the reaction of S with the ozone present in the system

$[O_3]$ inlet (mol/m^3)	k_i ($m^3.mol^{-1}.h^{-1}$)	Res. Time[(1)] (h)	N [(2)] ($mol.m^{-3}$)	$1-(N/N_{max})x100$ (% cells killed)	X[(3)] ($mol.m^{-3}$)	$1-(X/X_{max})x100$ (% fod destroyed)	$[O_3]$ outlet (mol/m^3)
10^{-2}	$2.4.10^4$	1.3	$3.5.10^{-11}$	78.1	0.0242	5.5	$6.1.10^{-6}$
10^{-3}	$2.4.10^4$	1.3	$8.7.10^{-11}$	45.6	0.0253	1.2	$1.4.10^{-6}$
10^{-4}	$2.4.10^4$	1.3	$1.4.10^{-10}$	12.5	0.0256	0	2.10^{-7}
10^{-5}	$2.4.10^4$	1.3	$1.6.10^{-10}$	0	0.0256	0	$2.1.10^{-8}$
0	------	1.3	$1.6.10^{-10}$	0	0.0256	0	0

(1) Earliest non-washout residence time.

(2) N corresponding to the plateau value for high residence times.

(3) X corresponding to the plateau value for high residence times

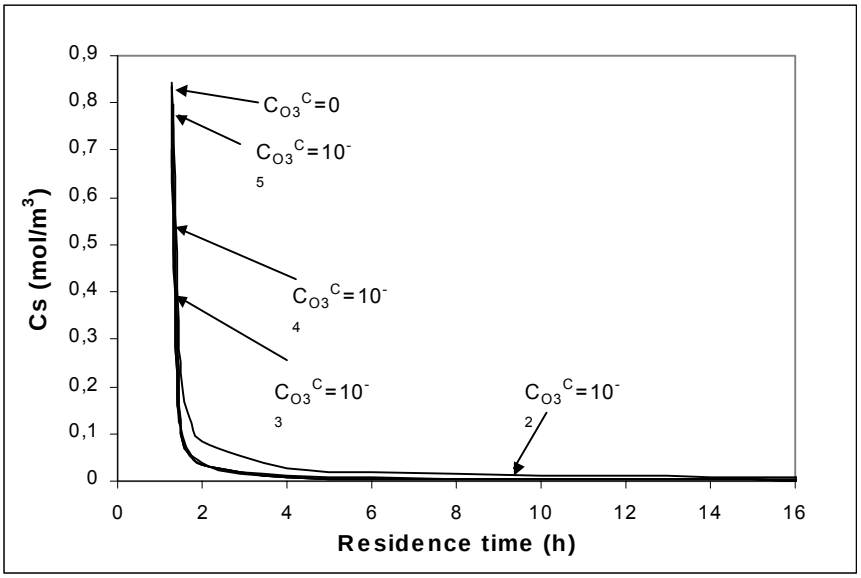

Graph 6.8. Concentration of S (C_S^C) vs. residence time ($k_i = 2.4x10^4\ m^3.mol^{-1}.h^{-1}$)

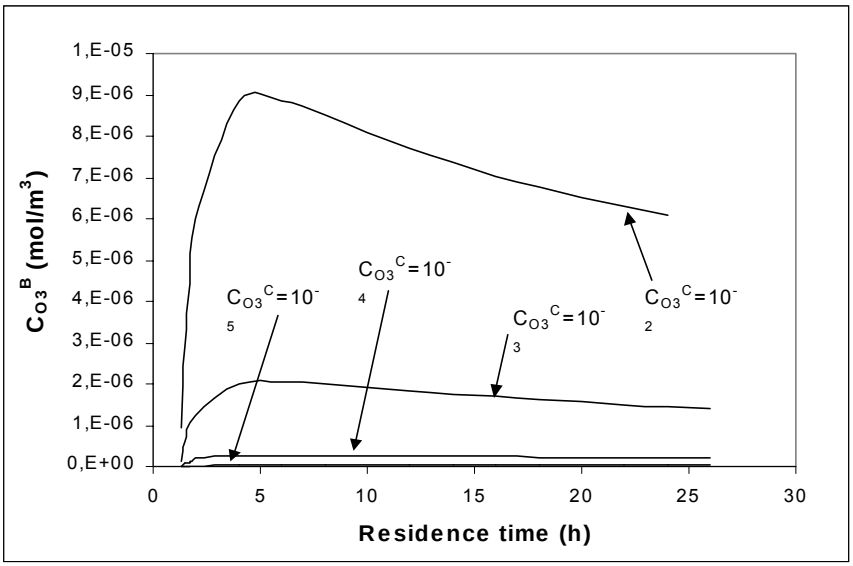

Graph 6.9. Concentration of ozone (C_{O3}^B) vs. residence time ($k_i = 2.4x10^4\ m^3.mol^{-1}.h^{-1}$)

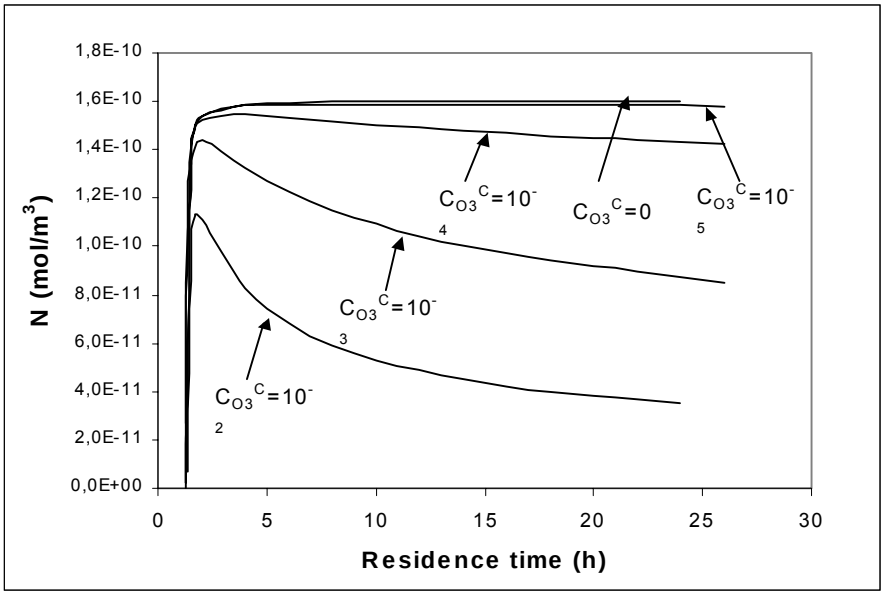

Graph 6.10. Concentration of viable cells (N) vs. residence time (k_i = 2.4x10^4 m^3.mol^{-1}.h^{-1})

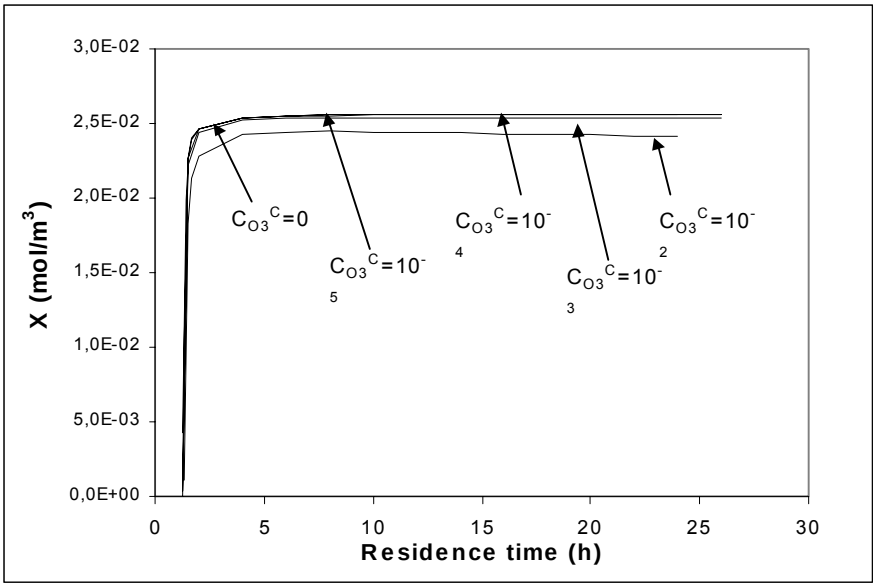

Graph 6.11. Concentration of fast ozone demand groups (X) vs. residence time (k_i = 2.4x10^4 m^3.mol^{-1}.h^{-1})

From these graphs it can be seen that although increasing the inlet concentration of ozone in the inlet of the biological reactor, no significant differences are found between the earliest times for which non-washout solutions appear. The shape of the curve representing the concentration of ozone as a function of the residence time in the biological reactor changes with respect to the first case, presenting a maximum corresponding to the time when almost all S has been oxidized. Then, the concentration of ozone begins to decrease as ozone reacts with the biomass present (N begins also to decrease). Important result is variation of N (thus bioreactor performance) with time.

Related to the previous conclusion, no effect is observed while S is present and start decreasing when almost all S has been consumed. As the inlet concentration of ozone increases, differences between N and N_{max} become more important: when the inlet concentration of ozone is 10^{-2} mol/m^3 the amount of biomass has been diminish in 75%, whereas at 10^{-4} mol/m^3 it has only been reduced in 12%. Significant differences between X and X_{max} or C_s^b and $C_s^b{}_{max}$ are not observed.

Results of the combined chemical and biological reactor process for the first and second case are presented in Tables 6.5 and 6.6, respectively. Those derived from an ozone dose in the chemical reactor of 10 mol.m^{-3}.h^{-1} are not presented, as the concentration of ozone in the inlet of the biological reactor is too high and a wash-out situation is observed in the second reactor.

From the results of this investigation,

- A simulation model has been developed for prediction of A (pollutant), S (biodegradable intermediate), N (viable cells), X (fast ozone demand groups) and ozone (dissolved) vs. residence time in a bioreactor in presence of ozone residuals.
- The effect of ozone residual is increasingly important as ozone increases.
- Depending on the value of the kinetic constant for the reaction of the substances with ozone, the general case can be simplified by assuming that the reaction of S with the ozone present in the bioreactor is unimportant.
- This model would allow predicting when or if an intervening ozone stripper is needed between the ozonation reactor and the bioreactor.
- Similar models could be applied for other oxidants used in chemical pretreatment, e.g. hydrogen peroxide.

Table 6.5. Summary of the results of the chemical reactor + biological reactor (not considering the reaction of S with ozone)

Ozone dose ($mol.m^{-3}.h^{-1}$)	$k_{rA}=k_{rS}=k_{dA}=k$ ($mol.m^{-3}$)	$C_{O3}^{C\,(1)}$ ($mol.m^{-3}$)	$C_A^{C\,(1)}$ ($mol.m^{-3}$)	$C_S^{C\,(1)}$ ($mol.m^{-3}$)	K_i ($m^3.mol^{-1}.h^{-1}$)	$N^{(2)}$ ($mol.m^{-3}$)	$N^{(2)}$ ($cells.L^{-1}$)	% killed cells $^{(2)}$	$X^{(2)}$ ($mol.m^{-3}$)	$C_{O3}^{B\,(2)}$ ($mol.m^{-3}$)	$C_S^{B\,(2)}$ ($mol.m^{-3}$)
3	10^4	$4.6.10^{-5}$	2.88	0.77	$2.4.10^4$	$1.3.10^{-10}$	$7.8.10^{10}$	14%	0.0234	$2.7.10^{-7}$	0.0128
					$2.4.10^7$	$1.3.10^{-10}$	$7.8.10^{10}$	14%	0.0234	$2.7.10^{-10}$	0.0128
3	10^7	$4.6.10^{-8}$	2.88	0.77	$2.4.10^4$	$1.47.10^{-10}$	$8.9.10^{12}$	0%	0.0235	$2.7.10^{-10}$	0.001
					$2.4.10^7$	$1.47.10^{-10}$	$8.9.10^{12}$	0%	0.0235	0	0.001
5	10^4	10^{-4}	1.77	0.85	$2.4.10^4$	$6.2.10^{-11}$	$3.7.10^{10}$	24%	0.0255	5.10^{-7}	$1.47.10^{-3}$
					$2.4.10^7$	$6.2.10^{-11}$	$3.7.10^{10}$	24%	0.0255	5.10^{-10}	$1.47.10^{-3}$
5	10^7	10^{-7}	1.79	0.85	$2.4.10^4$	$1.6.10^{-10}$	$6.0.10^{10}$	0%	0.0256	(5.10^{-9})	0.001
					$2.4.10^7$	$1.6.10^{-10}$	$6.0.10^{10}$	0%	0.0256	(0)	0.001

(1) For a residence time in the chemical reactor of 0.8 h.

(2) For a residence time in the biological reactor of 24 h.

Table 6.6. Summary of the results of the chemical reactor + biological reactor (considering the reaction of S with ozone)

Ozone dose ($mol.m^{-3}.h^{-1}$)	$k_{rA}=k_{rS}=k_{dA}$ $=k$ ($mol.m^{-3}$)	$C_{O3}^{C\,(1)}$ ($mol.m^{-3}$)	$C_A^{C\,(1)}$ ($mol.m^{-3}$)	$C_S^{C\,(1)}$ ($mol.m^{-3}$)	K_i ($m^3.mol^{-1}.h^{-1}$)	$N^{(2)}$ ($mol.m^{-3}$)	$N^{(2)}$ ($cells.L^{-1}$)	% killed cells $^{(2)}$	$X^{(2)}$ ($mol.m^{-3}$)	$C_{O3}^{B\,(2)}$ ($mol.m^{-3}$)	C_S^{B} ($mol.m^{-3}$)
3	10^4	$4.6.10^{-5}$	2.88	0.77	$2.4.10^4$	$1.39.10^{-10}$	$8.3.10^{10}$	5%	0.0235	$1.02.10^{-7}$	$1.17.10^{-3}$
3	10^7	$4.6.10^{-8}$	2.88	0.77	$2.4.10^4$	$1.47.10^{-10}$	$8.9.10^{10}$	0%	0.0235	0	$1.10.10^{-3}$
5	10^4	10^{-4}	1.77	0.85	$2.4.10^4$	$1.4.10^{-10}$	$8.4.10^{10}$	13%	0.0256	2.10^{-7}	$1.24.10^{-3}$
5	10^7	10^{-7}	1.79	0.85	$2.4.10^4$	$1.6.10^{-10}$	$9.6.10^{10}$	0%	0.0256	0	0.001

(1) For a residence time in the chemical reactor of 0.8 h.

(2) For a residence time in the biological reactor of 24h

7. Conclusions and recommendations

7.1. Conclusions.

The results obtained in the study have allowed to formulate the following conclusions:

1) Advanced Oxidation Processes based on ozone have shown to be efficient in the degradation and biodegradability enhancement of NB and DCP aqueous solutions.

2) NB removal rates ranged from 37 $mg.min^{-1}$ (at 4.1 $g.h^{-1}$ ozone production) to 78 $mg.min^{-1}$ (at 14.6 $g.h^{-1}$ ozone production), whereas DCP removal rate ranged from 80 to 127 $mg.min^{-1}$ at 4.1 and 7.4 $g.h^{-1}$ ozone production, respectively. Thus, DCP removal rate was found to be ca. 2 times higher than NB.

3) Stoichiometric coefficients of the reaction of ozone with NB and DCP have been estimated to be ca.4.0 and 2.7 mol O_3 consumed per mol of compound removed, respectively.

4) Regarding the effect of pH in single ozonation, this variable seemed not to have an important effect on the removal of NB within the studied range (3 to 9). Only at pH 9 the ozonation of NB was slightly inhibited. However, in the case of DCP solutions, an enhancement of the removal and mineralization rate was observed when pH was increased.

5) The evolution of the concentration of both substances has been adjusted to a first-order kinetics with respect to the pollutant concentration. Pseudo-first order kinetic constants of single ozonation have been found to be ca. 3 times higher for DCP than NB. The withdrawing character of the nitro group, which depletes the aromatic ring from electron density, may account for this behavior. When the initial concentration was doubled, these constants were reduced to half its value. Values of pseudo-first order kinetic constants are in the order of magnitude of those found in the literature.

6) Both carbonates and t-BuOH showed a great inhibition effect on the ozonation of NB solutions, pointing out the importance of the radical pathway in the removal of this compound at the testing conditions. On the other hand, no effect was observed in the removal rate of DCP solution when t-BuOH was added to the system: at low pHs, ozonation of DCP proceeds through reactions with molecular ozone.

7) Single ozonation showed to be effective to enhance the biodegradability of NB and DCP solutions. In the case of NB solutions, BOD_5/COD and BOD_5/TOC ratios were increased from 0 to 0.27 and 0.5 respectively, after an ozone dose of 0.25 $g.L^{-1}$ (corresponding to 60 minutes of treatment). With DCP solutions, those ratios were improved from 0 to 0.25 and 0.4 respectively, after an ozone dose of 0.12 $g.L^{-1}$ (30 minutes of treatment). Highest BOD values have been observed when these compounds were removed from solution. This behavior could be attributed to the inhibition character of both substances and/or that byproducts formed at initial time are not easily biodegradable, requiring further oxidation.

8) Optimum treatment times for a combined ozonation pre-treatment and biological oxidation process have been found to be ca. 30 and 60 minutes for DCP and NB, respectively, under the tested conditions. In the case of DCP solutions, this pre-ozonated effluent was fed to aerobic reactors, showing that sludge coming from a municipal waste water plant could be suitable for the treatment of the pre-treated solutions. A percentage of TOC removal of up to 80% has been achieved by means of the coupled ozonation-biological oxidation of DCP solutions.

9) The addition of hydrogen peroxide to single ozonation of NB and DCP solutions showed no effect in the removal rate nor in the biodegradability of these solutions. With regard to the degree of mineralization, it was found to increase with the hydrogen peroxide concentration.

10) The combination of ozone with UV radiation did not improve the removal rate nor biodegradability achieved by single ozonation. Regarding the mineralization of these solutions, the addition of UV light slightly increased the percentage of TOC removed in case of DCP solutions, whereas no enhancement was observed in case of NB.

11) The addition of both UV radiation and hydrogen peroxide increased significantly the degree of mineralization achieved by single ozonation, from ca. 40 to 65% after 120 and 90 minutes of treatment in case of NB and DCP, respectively. No increase was observed in the removal rate and biodegradability.

12) The combination O_3/UV/Fe(III) showed the best degrees of mineralization with both compounds. Compared to single ozonation, the percentage of TOC removed was increased from ca. 40 to 80% after 120 and 90 minutes of treatment in case of NB and DCP, respectively. Photodecarboxilation of ferric ion complexes, Fenton chemistry and reactions of aqueous ferric ions with UV light may account for this

improvement. When UVA was used instead of UV light, degree of mineralization was enlarged up to 90%. This combination seemed to slightly increased the biodegradability of DCP solutions.

13) To enhance the biodegradability of NB and DCP solutions single ozonation showed to be the most proper process, whereas to mineralize these solutions the use of the combination O_3/UVA/Fe(III) is proposed.

14) The three isomers of nitrophenol and nitrocatechol have been identified among the intermediates generated in the treatment of NB solutions. Chlorobenzoquinone has been detected when DCP solutions where treated by means of single ozonation and O_3/UV/Fe.

15) Operating costs for the treatment of NB and DCP by means of these AOPs have been found to be ca. 13 €/kg NB removed (after 60 minutes) and 4 €/kg DCP (after 30 minutes) removed for all the tested processes. With regard to TOC, O_3/UV/Fe is the most attractive option, with ca. 63€ and 41€/kg TOC removed for NB and DCP, respectively.

16) A simulation model has been developed for prediction of A (pollutant), S (biodegradable intermediate), N (viable cells), X (fast ozone demand groups) and ozone (dissolved) vs. residence time in a bioreactor in presence of ozone residuals. This model would allow predicting when or if an intervening ozone stripper is needed between the ozonation reactor and the bioreactor.

7.2. Recommendations

- The combination O_3/UV/Fe has shown to be very effective in the mineralization of NB and DCP solutions. Further investigation should be carried out within this field, concerning for example to:
    - The use of solar light instead of UVA lamps
    - The use of other catalysts instead of iron to work in a broader range of pH

- To follow the concentration of dissolved ozone throughout the experiment to perform kinetic calculations.

- To identify the unknown intermediates to establish a possible mechanism of reaction and relate to changes in the biodegradability of solutions.

- To carry out further investigation in the coupling of AOPs and biological processes, especially regarding:
    - The use of other operating conditions (pH, ozone production, hydrogen peroxide or iron concentration…) to improve biodegradability of solutions
    - To upgrade the reactor configuration for the biological process.
    - To set up an experimental installation for the coupled ozonation-biological oxidation working in continuous to check the developed mathematical model.

- To apply similar models to the one developed for biological reactors working in presence of residual ozone to other oxidants used in chemical pre-treatment, e.g. hydrogen peroxide.

- To model the mass transfer of ozone by means of a venturi injector

8. Glossary

Symbols		Unit
a	Volumetric interfacial area	$m^2.m^{-3}$
C	Concentration (in general)	$mg.L^{-1}$
C_A^0	Concentration of A in the inlet of the chemical reactor	$mol.m^{-3}$
C_A^B	Concentration of A in the outlet of the biological reactor	$mol.m^{-3}$
C_A^C	Concentration of A in the outlet of the chemical reactor	$mol.m^{-3}$
C_G	Bulk concentration of ozone in the gas phase	$mg.L^{-1}$
C_L	Bulk concentration of ozone in the liquid phase	$mg.L^{-1}$
C_L^*	Liquid concentration of ozone in equilibrium with the bulk gas concentration	$mg.L^{-1}$
$C_{O3(g)}^0$	Ozone concentrat. in the gas stream in the inlet of the chemical reactor	$mol.m^{-3}$
$C_{O3(g)}^C$	Ozone concentration in the gas stream in the outlet of the chemical reactor	$mol.m^{-3}$
C_{O3}^0	Ozone concentrat. in the liquid stream in the inlet of the chemical reactor	$mol.m^{-3}$
C_{O3}^B	Ozone concentration in liquid stream in the outlet of the biological reactor	$mol.m^{-3}$
C_{O3}^C	Ozone concentration in liquid stream in the outlet of the chemical reactor	$mol.m^{-3}$
C_S^0	Concentration of S in the inlet of the chemical reactor	$mol.m^{-3}$
C_S^B	Concentration of S in the outlet of the biological reactor	$mol.m^{-3}$
C_S^C	Concentration of S in the outlet of the chemical reactor	$mol.m^{-3}$
D	$=1/\theta_B$ = dilution rate	h^{-1}
D_{O3}	Diffusion coefficient	$m^2.s^{-1}$
D_{O3}	Ozone dose	$mol\ O_3.m^{-3}.h^{-1}$
F	Volumetric flow rate of the liquid stream	$m^3.h^{-1}$
G	Volumetric flow rate of the gas stream	$m^3.h^{-1}$
k_G	Gas film mass transfer coefficient	$m.s^{-1}$

k_i	Inactivation rate constant of the reaction of cells with ozone	$m^3.mol^{-1}.h^{-1}$
k_L	Liquid film mass transfer coefficient	$m.s^{-1}$
K_La	Over-all mass transfer coefficient	s^{-1}
k_{rA}, k_{dA}	Second order kinetic constants for the reaction of ozone with A	$m^3.mol^{-1}.h^{-1}$
k_{rS}, k_{dS}	Second order kinetic constants for the reaction of ozone with S	$m^3.mol^{-1}.h^{-1}$
K_S	Half-velocity constant	$mol.m^{-3}$
k_X	second order rate constant of the reaction of ozone with the fast ozone demand groups	$m^3.mol^{-1}.h^{-1}$
m	Specific mass transfer rate or mass flow rate	$mg.L^{-1}.s^{-1}$
N	Concentration of cells	$mol.m^{-3}$
n_M	Mols of species M	mol
q	Modulus of the density flux vector	$Einstein.m^{-2}.s^{-1}$
r	Correlation coefficient	
S	Concentration of substrate in Monod model	$mol.m^{-3}$
t	Time	min
T	Temperature	ºC
V_B	Volume of the biological reactor	m^3
V_C	Volume of the chemical reactor	m^3
W_{abs}	Absorbed radiation flow	$Einstein.s^{-1}$
X	Concentration of fast ozone demand groups	$mol.m^{-3}$
$Y_{N/S}$	Yield coefficient	mol cells produced. mol^{-1} S consumed

Greek alphabetic		**Unit**
Φ	Quantum yield	mol. mol $photon^{-1}$ = $mol.Einstein^{-1}$
λ	Wavelength	nm
μ	Absorption	cm^{-1}
	Specific growth rate	h^{-1}
μ_{max}	Maximum specific growth rate	h^{-1}
θ_B	Residence time in the biological reactor	h
θ_C	Residence time in the chemical reactor	h

Abbreviations		Unit
AOP	Advanced Oxidation Processes	
BOD	Biological Oxygen Demand	mg $O_2.L^{-1}$
COD	Chemical Oxygen Demand	mg $O_2.L^{-1}$
DCP	2,4-dichlorophenol	
DOC	Dissolved Organic Carbon	mg $C.L^{-1}$
HPLC	High Performance Liquid Chromatography	
HTR	Hydraulic Retention Time	day, hour
M	Molar	$mol.L^{-1}$
NB	Nitrobenzene	
OFX	Experiments with the combination O_3/Fe(III)	
OPX	Experiments with the combination O_3/H_2O_2	
ORFX	Experiments with the combination O_3/UV/Fe(III)	
ORPX	Experiments with the combination $O_3/UV/H_2O_2$	
ORX	Experiments with the combination O_3/UV	
OX	Experiments of single ozonation	
TOC	Total Organic Carbon	mg $C.L^{-1}$
TSS	Total Suspended Solids	$g.L^{-1}$
TVSS	Total Volatile Suspended Solids	$g.L^{-1}$
UV	Ultraviolet	
WW	Waste water	

9. Publications derived from this work

9.1. Publications

- CONTRERAS, S.; RODRÍGUEZ, M.; AL-MOMANI, F.; SANS, C. and ESPLUGAS, S. (2002) "Contribution of the ozonation pre-treatment to the biodegradation of aqueous solutions of 2,4-dichlorophenol", *Water Research* (submitted)

- CONTRERAS, S.; OLLIS, D.F. and ESPLUGAS, S. (2002) "Sequential ozonation and biological oxidation of wastewaters: a model including biomass inhibition by residual oxidant", *Ozone Sci. & Eng.* (in press)

- ESPLUGAS, S.; CONTRERAS, S. and OLLIS, D. (2001) "Simple kinetic models for the evaluation of BOD and COD in chemical oxidation treatments", *Chemie Ingenieur Technik*, **73** (6), 606.

- CONTRERAS, S.; RODRÍGUEZ, M.; CHAMARRO, E. and ESPLUGAS, S. (2001) "UV- and UV/Fe(III)-enhanced ozonation of nitrobenzene in aqueous solution", J*. Photochem. Photobiol. A: Chemistry*, **142** (1), 79-83

- CONTRERAS, S.; RODRÍGUEZ, M.; CHAMARRO, E.; ESPLUGAS, S. and CASADO, J. (2001) "Oxidation of nitrobenzene by O_3/UV: The influence of H_2O_2 and Fe(III). Experiences in a pilot plant", *Water Sci. & Technol*., **44** (5), 39-46.

9.2. Communications

- *9th Mediterranean Congress on Chemical Engineering* (Barcelona (Spain), November 26-29, 2002): "Ozonation as a pre-treatment to improve the biodegradation of aqueous 2,4-dichlorophenol solutions", poster presentation

- *8th International Conference on Advanced Oxidation Technologies for Water and Air Remediation* (Toronto (Canada), November 17-21, 2002): "Effect of ozone-based Advanced Oxidation Processes in the biodegradability of aqueous 2,4-dichlorophenol solutions", oral presentation

- *International Ozone Association 15th World Congress* (London (UK), September 10-15, 2001): "Sequential ozonation and biological oxidation of wastewaters: a model including biomass inhibition by residual oxidant", oral presentation

- *2nd European Workshop on Water, Air and Soil Treatment by Advanced Oxidation Technologies* (Poitiers (France), February 28- March 2, 2001): “Sequential ozonation and biological oxidation of wastewaters: a model including biomass inhibition by residual oxidant”, oral presentation

- *2nd International Conference on Oxidation Technologies for Water and Wastewater Treatment* (Clausthal-Zellerfeld (Germany), May 29-31, 2000): “Oxidation of nitrobenzene by O_3/UV: The influence of H_2O_2 and Fe(III). Experiences in a pilot plant”, oral presentation.

- *8th Mediterranean Congress on Chemical Engineering* (Barcelona (Spain), 10-12 November 1999): “Oxidation of nitrobenzene by ozone and its combination with H_2O_2 and Fe(III): Experiences in a pilot plant”, poster presentation.

10. Bibliography

ABE K. and TANAKA, K. (1999) "Effect of Fe^{3+} on UV-illuminated ozonation of nitrophenolic compounds", *Chemosphere*, **38** (12), 2837-2847.

ABE K. and TANAKA, K. (1997) "Fe^{3+} and UV-enhanced ozonation of chlorophenolic compounds in aqueous medium", *Chemosphere*, **35** (12), 2747-2752.

ACERO, J.L. and VON GUNTEN, U. (2000) "Influence of carbonate on the ozone/hydrogen peroxide based advanced oxidation process for drinking water treatment", *Ozone Sci. & Eng.*, **22** (3), 305-328.

ADAMS, C.D.; COZZENS, R.A. and KIM, B.J. (1997) "Effects of ozonation on the biodegradability of substituted phenols", *Wat. Res.,* **31** (10), 2655-2663.

AHLBORG U.B. and THUNBERG, T.M. (1980) "Chlorinated phenols: occurrence, toxicity, metabolism and environmental impact", *CRC Crit. Rev. Toxicol*., **7**, 1-35.

L'AIR LIQUIDE, *French Patent*, FR. 1,246,273.

ALONSO Y DEL PINO, M.A. (1996) "Aspectos fundamentales y prácticos de la aplicación de sistemas de ozonación en la eliminación de contaminantes nitroaromáticos del agua", *Doctoral Thesis*, Departamento de Ingeniería Química, Universidad de Extremadura.

ATSDR (1999), www.atsdr.cdc.gov/toxfaq.html.

ANDREOZZI, R.; CAPRIO, V.; INSOLA, A. and MAROTTA, R. (1999) "Advanced Oxidation Processes (AOP) for water purification and recovery", *Catalysis Today*, **53**, 51-59.

BADER, H. and HOIGNÉ, J. (1982) "Determination of ozone in water by the Indigo method: a submitted standard method", *Ozone Sci. & Eng.*, **4** (4), 169-176.

BADER, H. and HOIGNÉ, J. (1981) "Determination of ozone in water by the Indigo method", *Wat. Res.*, **15**, 449-456.

BAIG, S. and LIECHTI, P.A. (2001) "Ozone treatment for biorefractory COD removal", *Water Sci. & Technol*., **43** (2), 197-204.

BAILEY, P.S. (1972) "Ozone in water and wastewater treatment", Ann Arbor Science Publishers, Michigan.

BAILEY, J.B. and OLLIS, D.F. (1986), "Biochemical Engineering Fundamentals", 2nd ed., McGraw-Hill, NY (USA)

BALDRY, M.G.C. (1983) “The bactericidal, fungicidal and spericidal properties of hydrogen peroxide and peracetic acid”, *J. Appl. Bacteriol.*, **54**, 417.

BAOZHEN, W. and JUN, Y. (1988) “Removal of aromatic nitrocompounds from water by ozonation”, *Ozone Sci. & Eng*., **10**, 1-23.

BAUM, G. and OPPENLAENDER, T. (1995) “Vacuum-UV-oxidation of chloroorganic compounds in an excimer flow through photoreactor”, *Chemosphere*, **30** (9), 1781-1790.

BAUMAN, L.C. and STENSTROM, M.K. (1990) “Removal of organohalogens and organohalogens precursors in reclaimed wastewater – II”, *Wat. Res.*, **24**, 957-964.

BELTRÁN, F.J.; GONZÁLEZ, M.; RIVAS, J. and MARÍN, M. (1994) “Oxidation of mecoprop in water with ozone and ozone combined with hydrogen peroxide”, *Ind. Eng. Chem. Res.*, **33**, 125-136.

BELTRÁN, F.J.; GONZÁLEZ, M. and ÁLVAREZ, P. (1997a) “Tratamiento de aguas mediante oxidación avanzada (I): Procesos con ozono, radiación ultravioleta y combinación ozono/radiación ultravioleta”, *Ingeniería Química*, **331**, 161-168.

BELTRÁN, F.J.; GONZÁLEZ, M. and ÁLVAREZ, P. (1997b) “Tratamiento de aguas mediante oxidación avanzada (II): Procesos con peróxido de hidrógeno”, *Ingeniería Química*, **332**, 165-169.

BELTRÁN, F.J., ENCINAR, J.M. and ALONSO, M. (1998a) “Nitroaromatic hydrocarbon ozonation in water. 1. Single ozonation”, *Ind. Eng. Chem. Res.*, **37**, 25-31.

BELTRÁN, F.J., ENCINAR, J.M. and ALONSO, M. (1998b) “Nitroaromatic hydrocarbon ozonation in water. 2. Combined ozonation with hydrogen peroxide or UV radiation”, *Ind. Eng. Chem. Res.*, **37**, 32-40.

BELTRÁN, F.J.; RIVAS, J.; ÁLVAREZ, P.M.; ALONSO, M.A. and ACEDO, B. (1999a) “A kinetic model for advanced oxidation processes of aromatic hydrocarbons in water: Appplication to phenanthrene and nitrobenzene”, *Ind. Eng. Chem. Res*., **38** (11), 4189-4199.

BELTRÁN, F.J.; GARCÍA-ARAYA, J.F.; FRADES, J.; ÁLVAREZ, P. and GIMENO, O. (1999b) “Effects of single and combined ozonation with hydrogen peroxide or UV radiation on the chemical degradation and biodegradability of debittering table olive industrial wastewater”, *Wat. Res*., **33** (3), 723-732.

BELTRAN, F.J.; GARCIA-ARAYA, J.F. and ALVAREZ, P.M. (2000a), “Estimation of biological kinetic parameters from a continuous integrated ozonation–activated sludge system treating domestic wastewater”, *Biotechnol. Prog.*, **16** (6), 1018-1024.

BELTRAN, J.B.; GARCIA, J.F. and ALVAREZ, P.M. (2000b) “Continuous flow integrated chemical (ozone)–activated sludge system treating combined agroindustrial-domestic wastewater”, *Environmental Progress*, **19** (1), 28-35.

BELTRAN, F.J.; GARCIA-ARAYA, J.F. and ALVAREZ, P.M. (2000c), “Sodium dodecylbenzenesulfonate removal from water and waste water. 2. Kinetics of the integrated ozone-activated sludge”, *Ind. Eng. Chem. Res.*, **39** , 2221-2227.

BELTRÁN-HEREDIA, J.;TORREGROSA, J.; DOMÍNGUEZ, J.R. and GARCÍA, J. (2000) “Treatment of black-olive waste water by ozonation and aerobic biological degradation”, *Wat. Res*., **34** (14), 3515-3522.

BEN ABDERRAZIK, N.; AL MOMANI, F.; RODRÍGUEZ, M.; AZMANI, A.; SANS, C. and ESPLUGAS, S. (2002) “Biodegradability improvement by Photo Fenton reaction”, *Afinidad* (in press).

BENÍTEZ, F.J.; BELTRÁN-HEREDIA, J.; ACERO, J.L. and RUBIO, F.J. (2000) “Rate constants for the reactions of ozone with chlorophenols in aqueous solutions”, *J. Hazard. Mater.*, **B79**, 271-285.

BENÍTEZ, F.J.; BELTRÁN-HEREDIA, J.; ACERO, J.L. and RUBIO, F.J. (2000b) “Contribution of free radicals to chlorophenols decomposition by several advanced oxidation processes”, *Chemosphere*, **41** (8), 1271-1277.

BIGDA, R.J. (1995) “Consider Fenton’s Chemistry for Wastewater Treatment”, *Chem. Eng. Progr.*, **91** (12), 62-66.

BLANCH, H.W. and CLARK, D.S. (1996), “Biochemical Engineering”, Marcel Dekker, Inc., NY (USA)

BÖHME, A. (1999) “Ozone technology of German industrial enterprises”, *Ozone Sci. & Eng.*, **21**, 163-176.

BRILLAS, E.; MUR, E.; SAULEDA, R.; SÁNCHEZ, L.; PERAL, J.; DOMÉNECH, X. and CASADO, J. (1998a) “Aniline mineralization by AOPs: anodic oxidation, photocatalysis, electro-Fenton and photoelectro-Fenton processes”, *Appl. Catal. B: Environ*., **16**, 31-42.

BRILLAS, E.; SAULEDA, R and CASADO, J. (1998b) “Degradation of 4-chlorophenol by anodic oxidation, electro-Fenton, photoelectro-Fenton and peroxicoagulation processes”, *J. Electrochem. Soc.*., **145** (3), 759-765.

BRILLAS, E.; CALPE, J.C. and CASADO, J. (2000) “Mineralization of 2,4-D by advanced electrochemical oxidation processes”, *Wat. Res*., **34** (8), 2253-2262.

CAMEL, V. and BERMOND, A. (1998) “The use of ozone and associated oxidation processes in drinking water treatment”, *Wat. Res*., **32**, 3208-3222.

CAPRIO, V.; INSOLA, A. and VOLPICELLI, G. (1984) “Ozonation of aqueous solutions of nitrobenzene”, *Ozone Sci. & Eng*., **6**, 115-121.

CERVERA, S. and ESPLUGAS, S. (1983) “ Obtención de hidrógeno mediante fotólisis del agua”, *Energía*, **Marzo**, 103-107.

CHAMARRO, E.; MARCO, A.; PRADO, J. and ESPLUGAS, S. (1996) “Tratamiento de aguas y aguas residuales mediante utilización de procesos de oxidación avanzada”, *Química & Industria*, **½**, Sociedad Chilena de Química, 28-32.

CHAMARRO, E.; MARCO, A. and ESPLUGAS, S. (2001) “Use of Fenton reagent to improve organic chemical biodegradability”, *Wat. Res*., **35** (4), 1047-1051.

CHEN, R. and PIGNATELLO, J.J. (1997) “Role of quinone intermediates as electron shuttles in Fenton and photoassisted Fenton oxidation or aromatic compounds”, *Environ. Sci. Technol.*, **31** (8), 2399-2406.

CHEN, F.; WU, S.; CHEN, J. and RONG, S. (2001) “COD removal efficiencies of some aromatic compounds in supercritical water oxidation”, *Chinese Journal of Chemical Engineering*, **9** (2), 137-140.

CHUDOBA, J. (1990) “Comment on: The effect of reactor hydraulics on the performance of activated sludge systems. I. The traditional modelling approach”, *Wat. Res*., **24** (11), 1431.

COLUCCI, J.; MONTALVO, V.; HERNÁNDEZ, R. and POULLET, C. (1999) “Electrochemical oxidation potential of photocatalyst reducing agents”, *Electrochimica Acta*, **44** (15), 2507-2514.

COMNINELLIS, O. (1994) “Electrochemical oxidation of organic pollutants for waste water treatment”, *Studies on Environmental Science*, **59**, 77-102.

DAVIS, E.M.; TURLEY, J.E.; CASSERLY, D.M. and GUTHRIE, R.K. (1983) "Partitioning of selected organic pollutants in aquatic ecosystems", Biodeterioration 5 Oxley Ta & Barry S. Eds., 176-184.

DECISSION 2455/2001/EC of the European Parliament and of the Council of 20 November 2001 establishing the list of priority substances in the field of water policy and amending Directive 2000/60/EC (L 331 of 15.12.2001)

DIRECTIVE 2000/60/EC of the Euripean Parliament and of the Council of 23 October 2000 establishing a framework for Community action in the field of water policy (L 327 of 22.12.2000)

DOHAN, J.M. and MASSCHELEIN, W.J. (1987), "The photochemical generation of ozone: present state of art and technology", *Ozone Sci. & Eng.*, **9**, 315.

DUGUET, J.P.; ANSELME, C.; MAZOUNIE, P. and MALLEVIALLE, J. (1989) "Application of combined ozone-hydrogen peroxide for the removal of aromatic compounds from a ground water", *Ozone Sci. & Eng.*, **12**, 281-294.

DUGUET, J.P.; DUSSERT, B.; MALLEVIALLE, J. and FIESSINGER, F. (1987) "Polymerization effects of ozone: applications to the removal of phenolic compounds from industrial wastewaters", *Water Sci. Technol.*, **19**, 919-930.

DU RON, B. (1982) "Ozone generation with ultraviolet radiation" In *Handbook of ozone technology and applications*, Edited by R.G. Rice and A. Netzer, Ann Arbor Science Publishers, Ann Arbor, Mich.

EPA site, www.scorecard.org, visited on July 2002.

ESPLUGAS, S.; CONTRERAS, S. and OLLIS, D. (2001), "Simple Kinetic Models for the Evolution of BOD and COD in Chemical Oxidation Treatments", *Chemie Ingenieur Technik*, **73** (6), 606.

ESPLUGAS, S. and OLLIS, D.F. (1996), "Sequential chemical and biological treatment of water pollutants: a mathematical model", *Proc. 6th Mediterranean Congress on Chemical Engineering*, Barcelona (Spain)

ESPLUGAS, S. and VICENTE, M. (1983) "Calibrado del fotorreactor anular", *Afinidad*, **40**, 453-457.

ESPLUGAS, S.; YU, P.L. and PERVEZ, M.I. (1994) “Degradation of 4-chlorophenol by photolytic Oxidation”, *Wat. Res*., **28**, 1323-1328.

FENTON, H.J.H. (1884), “Oxidation of tartaric acid in presence of iron”, *J. Chem. Soc*., **65** 889.

GILBERT, E. (1987) “Biodegradability of ozonation products as a function of COD and DOC elimination by example of substituted aromatic substances”, *Wat. Res*., **21** (10), 1273-1278.

GILBERT, G. and ZINEDNER, H. (1980) “Ozonation of aromatic amines in water”, *Wat. Res.*, **25** (7), 1563-1570.

GIMÉNEZ, J.; CURCÓ, D. and QUERAL, M.A. (1999) “Photocatalytic treatment of phenol and 2,4-dichlorophenol in a solar plant in the way to scaling-up”, *Catalysis Today*, **54**, 229-243.

GLAZE, W.H. and KANG, J.W. (1989) “Advanced oxidation processes. Test of a kinetic model for the oxidation of organic compounds with ozone and hydrogen peroxide in a semibatch reactor”, *Ind. Eng. Chem. Res.*, **28** (11), 1580-1587.

GLAZE, W.H.; KANG. J.W. and CHAPIN, D.H. (1987) “The chemistry of water treatment processes involving ozone, hydrogen peroxide and ultraviolet radiation”, *Ozone Sci. & Eng.*, **9** (4), 335-342.

GOTTSCHALK, C.; LIBRA, J.A. and SAUPE, A. (2000) “Ozonation of water and waste water. A practical guide to understanding ozone and its application”, Wiley-VCH, Weinheim, Germany.

GRADY, C.P.L.Jr.; DAIGGER, G.T. and LIM, H.C. (1999) “Biological wastewater treatment”, Marcel Dekker, NY (USA)

GUITTONNEAU, S.; DE LAAT, J.; DUGUET, J.P.; BONNEL, C. and DORÉ, M. (1990) “Oxidation of Parachloronitrobenzene in dilute aqueous solution by O_3+UV: a comparative study”, *Ozone Sci. & Eng.,* **12**, 73-94.

GUITTONNEAU, S.; GLAZE, W.H.; DUGUET, J.P. and WABLE, O. (1991) “Characterization of natural waters for potential to oxidize organic pollutants with ozone”, *Proc. 10th Ozone World Congress*, Zürich, Switzerland.

GUROL, M.O. and VATISTAS, R. (1987) “Oxidation of phenolic compounds by ozone and ozone + UV radiation: a comparative study”, *Wat. Res.*, **21** (8), 895-900.

HA, S.R.; QISHAN, L. and VINITNANTHARAT, S. (2000) “COD removal of phenolic wastewater by biological activated carbon-sequencing batch reactor in the presence of 2,4-DCP, *Water Sci. & Technol*., **42** (5-6), 171-178.

HA, S.R.; VINITNANTHARAT, S. and ISHIBESHI, Y. (2001) “A modelling approach to bioregeneration of granular activated carbon loaded with phenol and 2,4-dichlorophenol”, *Journal of Environmental Science and Health, Part A: Toxic/Hazardous Substances & Environmental Engineering*, **A36** (3), 275-292.

HAMELIN, C. and CHUNG, Y.S. (1974) “Optimal conditions for mutagenesis by ozone in *Escherichia coli* K12”, *Mutation Research*, **24**, 271-279.

HAMELIN, C., SARHAN, F. and CHUNG, Y.S. (1977) “Ozone-induced DNA degradation in different DNA polymerase I mutants of *Escherichia coli* K12”, *Biochemical and biophysical research communications,* **77** (1), 220-224.

HAMELIN, C., SARHAN, F. and CHUNG, Y.S. (1978) “Induction of deoxyribonucleic acid degradation in *Escherichia coli* by ozone”, *Experientia,* **34**, 1578-1579.

HARRISON, R.M. (1992) “Pollution: Causes, effects and control” 2ª ed., The Royal Society of Chemistry, Cambridge.

HAUTANIEMI, M.; KALLAS, J.; MUNTER, R. and TRAPIDO, M. (1998) “Modelling of chlorophenol treatment in aqueous solutions. 1. Ozonation and ozonation combined with UV radiation under acidic conditions”, *Ozone Sci. & Eng.,* **20** (4), 259-282.

HAYWARD, K (1999), “Drinking water contaminant hit-list for US EPA”, *Water 21*, **September-October**, 4.

HEIDT, L.J.; TREGAY, G.W. and MIDDLETON, F.A. (1979) “Influence of the pH upon the photolysis of the uranyl oxalate actinometer system”, *J. Phys. Chem.*, **74**, 1876-1882.

HEINZLE, E.; STOCKINGER, H.; STERN, M.; FAHMY M. and KUT, O.M. (1995) “Combined biological-chemical (ozone) treatment of wastewaters containing chloroguaiacols”, *J. Chem. Tech. Biotechnol*., **62**, 241-252.

HIRVONEN, A.; TRAPIDO, M.; HENTUNEN, J. and TAKHAREN, J. (2000) “Formation of hydroxylated and dimeric intermediates during oxidation of chlorinated phenols in aqueous solution”, *Chemosphere*, **41** (8), 1211-1218.

HOIGNÉ, J. (1988) “The chemistry of ozone in water”, In *Process technologies for water treatment*. Edited by S. Stucki. Plenum Press, New York.

HOIGNÉ, J. and BADER, H. (1977a), “Ozonation of water: selectivity and rate of oxidation of solutes”, *Proc. 3rd IOA Congress*, Paris, France.

HOIGNÉ, J. and BADER, H. (1977b), “Rate constants for reactions of ozone with organic pollutants and ammonia in water. *IOA Symp*., Toronto, Canada.

HOIGNÉ, J. and BADER, H. (1978), “Ozone initiated oxidations of solutes in wastewater: a reaction kinetic approach”, *Prog. Wat. Technol*., **10**, 657.

HOIGNÉ, J. and BADER, H. (1979), “Ozonation of water: selectivity and rate of oxidation of solutes”, *Ozone Sci. & Eng*., **1** (1), 73-85.

HOIGNÉ, J. and BADER, H. (1983a) “Rate constants of reaction of ozone with organic and inorganic compounds in water. Part I. Non-Dissociating organic compounds” *Wat. Res.*, **17**, 173-183.

HOIGNÉ, J. and BADER, H. (1983b) “Rate constants of reaction of ozone with organic and inorganic compounds in water. Part II. Dissociating organic compounds” *Wat. Res.*, **17**, 185-194.

HOIGNÉ, J.; BADER, H.; HAAG, W.R. and STAEHELIN, J. (1985) “Rate constants of reactions of ozone with organic and inorganic compounds in water – III. Inorganic compounds and radicals, *Wat. Res*., **19**, 173-183.

HOWARD, P.H. (1989) “Handbook of environmental fate and exposure data for organic chemical. Volume I Large production and priority pollutants”, Lewis Publishers, Chelsea, Michigan (USA)

HU, S.T. and YU, Y.H. (1994) “Preozonation of chlorophenolic wastewater for subsequent biological treatment”, *Ozone Sci. & Eng*., **16**, 13-28.

HUANG, C.P. and CHU, C.S. (1992) “Electrochemical oxidation of phenolic compounds from dilute aqueous solutions”, *Chem. Oxid. Proc. Int. Symp. 1st*, 239-253.

HUNT, N.K. and MARIÑAS, B.J. (1997), "*Escherichia coli* inactivation with ozone", *Wat. Res.*, **31**, 1355-1362.

HUNT, N.K. and MARIÑAS, B.J. (1999), "Inactivation of *Escherichia coli* with ozone: chemical and inactivation kinetics", *Wat. Res.*, **33** (11), 2633-2641.

KAMEYA, T.; MURAYAMA, T.; KITANO, M. and URANO, K. (1995) "Testing and classification methods for the biodegradabilities of organic compounds under anaerobic conditions", *The Science of the Total Environment*, **170**, 31-41.

KOMANAPALI, I.R. and LAU, B.H.S. (1996) " Ozone-induced damage of *Escherichia coli* K12", *Appl. Microbiol. Biotechnol.*, **46**, 610-614.

KOO, C. and LEE, D.S. (1994) "Supercritical water oxidation of nitrogen containing aromatic compounds", *Hwahak Kongshak*, **32** (3), 385-392.

KU, Y. and HSIEH, C.B. (1992) "Photocatalytic decomposition of 2,4-dichlorophenol in aqueous TiO_2 suspensions", *Wat. Res*., **26** (11), 1451-1456.

KU, Y.; SU, W.J. and SHEN, Y.S. (1996) "Decomposition of phenols in aqueous solution by a UV/O_3 process", *Ozone Sci. & Eng.*, **18** (5), 443-460.

KUO, W.S. (1999) "Synergistic effects of combination of photolysis and ozonation on destruction of chlorophenols in water", *Chemosphere*, **39** (11), 1853-1860.

LANGLAIS, B.; RECKHOW, D.A. and BRINK, D.R. (1991), "Ozone in Water Treatment. Application and Engineering", Lewis Publishers, Chelsea (Michigan).

LEDAKOWICZ, S. (1998) "Integrated processes of chemical and biological oxidation of wastewaters", *Environment Protection Engineering*, **24** (1-2), 35-47.

LEDAKOWICZ, S. and GONERA, M. (1999) "Optimisation of oxidant dose for combined chemical and biological treatment of textile wastewater", *Wat. Res.*, **33** (11), 2511-2516.

LEE, D.S.; GLOYNE, E.F. and LI, L. (1990) "Efficiency of hydrogen peroxide and oxygen in supercritical water oxidation of 2,4-dichlorophenol and acetic acid", *J. of Supercritical Fluids*, **3** (4), 249-255.

LEGRINI, O.; OLIVEROS, E. and BRAUN, A.M. (1983) "Photochemical processes for water treatment", *Chem. Rev.*, **93**, 671-698.

LEZCANO, I.; PEREZ-REY, R.; BALUJA, CH. and SANCHEZ, E. (1999), "Ozone inactivation of *Pseudomonas aeruginosa*, *Escherichia coli*, *Shigella sonnei* and *Salmonella typhimurium* in Water", *Ozone Sci. & Eng.*, **21**, 293-300.

LI, L.; CRAIN, N.; KANTHASAMY, A.; MATTHEWS, C.P.; ROLLANS, S.W. and GLOYNE, E.F. (1994) "Supercritical water oxidation model development for selected EPA priority pollutants", *Proc. Annual Meeting - Air & Waste Management Association 87th*, **13**, 94.

LI, L.; PEISHI, C. and EARNEST, F.G. (1991) "Generalized kinetic model for wet oxidation of organic compounds", *AIChE J.*, **37** (11), 1687-1697.

LIN, K.S.; WANG, H.P. and LI, M.C. (1998) "Oxidation of 2,4-dichlorophenol in supercritical water", *Chemosphere*, **36** (9), 2075-2083.

LIPCZYNSKA-KOCHANY, E. (1991) "Degradation of aqueous nitrophenols and nitrobenzene by means of the Fenton reaction", *Chemosphere*, **22** (5-6), 529-536.

LIPCZYNSKA-KOCHANY, E. (1992) "Degradation of nitrobenzene and nitrophenols by means of advanced oxidation processes in a homogeneous phase: photolysis in the presence of hydrogen peroxide versus the Fenton reaction", *Chemosphere*, **24** (9), 1369-1380.

MALATO, S.; BLANCO, J.; FERNÁNDEZ-IBÁÑEZ, P. and CÁCERES, J. (2001) "Treatment of 2,4-dicholorophenol by solar photocatalysis: comparison of coupled photocatalytic-active carbon vs. active carbon", *Journal of Solar Energy Engineering*, **123** (2), 138-142.

MALETZKY, P. and BAUER, R. (1998) "The photo-Fenton method – Degradation of nitrogen containing organic compounds", *Chemosphere*, **24** (9), 1369-1380.

MALLEVIALLE, J. et al. (1975) "Détermination Expérimentale des Coefficients de Transfert de l'Ozone dans l'Eau", *Cebedeau*, **28**, 377.

MARCO, A.; ESPLUGAS, S. and SAUM, G. (1997) "How and why to combine chemical and biological processes for wastewater treatment", *Wat. Sci. Technol.*, **35** (4), 321-327.

MARK, H.F.; OTHMER, D.F.; OVERBERGER, C.G. and SEABURG, G.T. (1992) "Kirk-Othmer Encyclopedia of Chemical Technology", 4ª ed., Wiley-Interscience Publication, New York (USA).

MASSCHELEIN, W. (1982) “Contacting of ozone with water and contactor off-gas treatment. In *Handbook of ozone technology and applications*, edited by R.G. Rice and A. Netzer, Ann Arbor Science Publishers, Ann Arbor, Mich.

MASSCHELEIN, W.; LANGLAIS, B.; THIELSEN, E.; BLAICH, L.; BELL, J. and READING, A. (1998) “Colorimetric method for manual determination of ozone concentrations in water”, *Ozone Sci. & Eng.*, **20** (6), 443-445.

MATTHEWS, R.W. (1990) “Purification of water with near-UV illuminated suspensions of titanium dioxide”, *Wat. Res*., **24** (5), 653-660.

MAZELLIER, R.; MAILHOT, G. and BOLTE, M. (1997) “Photochemical behaviour of the Iron(III)/2,6-dimethylphenol system”, *New J. Chem.*, **21** (3), 389-397.

METCALF & EDDY, INC (1995) “Wastewater engineering: treatment, disposal and reuse (Spanish version)”, 3rd ed., McGraw-Hill, New York, USA.

MINERO, C.; PELIZZETTI, C.; PICCINI, P. and VINCETI, M. (1994) “Photocatalyzed transformation of nitrobenzene on TiO_2 and ZnO”, *Chemosphere*, **28** (6), 1229-1244.

MISHRA, V.S.; MAHAJANI, V.V. and JOSHI, J.B. (1995) “Wet air oxidation”, *Ind. Eng. Chem. Res*., **34**, 2-48.

MOKRINI, A. (1998) “Degradación de fenol mediante tratamientos de oxidación avanzada” *Doctoral Thesis*, Dpto. Ingeniería Química y Metalurgia, Universitat de Barcelona.

MOKRINI, A.; OUSSI, D. and ESPLUGAS, S. (1997) “Oxidation of aromatic compounds with UV radiation/ozone/hydrogen peroxide” *Wat. Sci. Technol.*, **35**, 95-102.

MONOD, J. (1950), Ann. Inst. Pasteur, Paris, **79**, 390.

MORRIS, J.C. (1975), “Aspects of the quantitative assessment of germicidal efficiency”, in *Disinfection: Water & Wastewater* edited by J.D. Johnson. Ann Arbor Science Publishers, Inc., Ann Arbor, MI, Chapter 1:1.

MUNTER, R.; PREIS, S.; KALLAS, J.; TRAPIDO, M. and VERESSININA, Y. (2001) “Advanced oxidation processes (AOPs): Water treatment technology for the twenty-first century”, *Kemia-Kemi*, **28** (5), 354-362.

NIELSEN, J. and VILLADSEN, J. (1994) “Bioreaction Engineering Principles”, Plenum Press, NY (USA)

OPPT Chemical Fact Sheets (1995), www.epa.gov/chemfact.

ORMAD, M.P.; OVELLEIRO, J.L. and KIWI, J. (2001) “Photocatalytic degradation of concentrated solutions of 2,4-dichlorophenol using low energy light. Identification of intermediates”, *Applied Catalysis B: Environmental*., **32**, 157-166.

PAILLARD, H.; BRUNET, R. and DORÉ, M. (1988) “ Conditions optimals d’application du systeme oxydant ozone-peroxide d’hydrogene”, *Wat. Res.*, **22**, 91-103.

PALAU, R. (1998) “Contribución al estudio de la eliminación de contaminantes acuosos mediante reacciones electroquímicas – Degradación del herbicida MCPA”, *Experimental master in Chemistry*, Dpto. Ingeniería Química y Metalurgia, Universitat de Barcelona.

PERRICH, J.R.; MCCAMMON, J.R.; CRONHOLM, L.S.; FLEISCHMAN, M.; PAVONI, J.L. and RIESSER, V. (1975) “Inactivation kinetics of viruses and bacteria in a model ozone contacting reactor system”, in *Proceedings of the 2nd International Symposium on Ozone Technology, Montreal, Canada*, eds. R.G. Rice, P.Pichet and M.Vincent, p.486, International Ozone Institute, New York

PEYTON, G.R. and GLAZE, W.H. (1988) “Destruction of pollutants in water with ozone in combination with ultraviolet radiation. 3. Photolysis of aqueous ozone”, *Environ. Sci. Technol.*, **22**, 761-767.

PIGNATELLO, J.J. (1992) “Dark and photoassisted ion (3+)-catalyzed degradation of chlorophenoxy herbicides by hydrogen peroxide”, *Environ. Sci. Technol*., **26** (5), 944-951.

PRADO, J.; CHAMARRO, E. and ESPLUGAS, S. (1992) “Tratamiento de aguas residuales con ozono y radiación UV”, *Tecnología del agua*, **93**, 26-32.

QIU, Y.; KUO, C-H. and ZAPPI, M.E. (2002) “Ozonation kinetics of six dichlorophenol isomers”, *Ozone Sci. & Eng*., **24** (2), 123-131.

RAMALHO, R.S. (1991) “Tratamiento de aguas residuales”, Ed. Reverté, S.A., Barcelona (España).

REDDY, T.V.; WIECHEMAN, B.E.; LIN, E.L.; CHANG, L.W.; SMITH, M.K. and DANIEL, F.B. (1993) “Separation and quantitation of nitrobenzenes and their reduction products

nitroanilines and phenylenediamines by reversed HPLC", *Journal of Chromatography A*, **655**, 331-335.

RENNECKER, J.L.; MARIÑAS, B.J.; OWENS, J.H. and RICE, E.W. (1999) "Inactivation of *Cryptosporidium parvum* oocysts with ozone", *Wat. Res.*, **33** (11), 2481-2488.

RICE, R.G. (1997) "Application of ozone for industrial wastewater treatment: a review", *Ozone Sci. & Eng.*, **18** (6), 477-515.

RODGERS, J.D.; JEDRAL, W. and BUNCE, N.J. (1999) "Electrochemical oxidation of chlorinated phenols", *Environ. Sci. Technol.*, **33** (9), 1453-1457.

RODRÍGUEZ, M.; KIRCHNER, A.; CONTRERAS, S.; CHAMARRO, E. and ESPLUGAS, S. (2000) "Influence of H_2O_2 and Fe(III) in the photodegradation of nitrobenzene", *J. Photochem. Photobiol. A: Chemistry*, **133**, 123-127.

RODRÍGUEZ, M.; TIMOKHIN, V.; MICHL, F.; CONTRERAS, S.; GIMÉNEZ, J. and ESPLUGAS, S. (2002a) "The influence of different irradiation sources on the treatment of nitrobenzene", *Catalysis Today*, **76** (2-4), 291-300.

RODRÍGUEZ, M.; TIMOKHIN, V.; CONTRERAS, S., CHAMARRO, E. and ESPLUGAS, S. (2002b) "Rate equation for the degradation of nitrobenzene by Fenton-like reagent", *Adv. Environ. Res*. (in press).

RUPPERT, G.; BAUER, R. and HEISLER, G. (1994) "UV-O_3, UV-H_2O_2, UV-TiO_2 and the photo-Fenton reaction. Comparison of advanced oxidation processes for waste water treatment", *Chemosphere*, **28** (8), 1447-1454.

SACHER, F; KARRENBROCK, F.; KNEPPER, T and LINDNER, K. (2001) "Adsorption studies of organic compounds for the assessment of their relevancies for drinking water production", *Vom Wasser*, **96**, 173-191.

SAFARZADEH-AMIRI, A.; BOLTON, J.R. and CATER, S.R. (1996a) "The use of iron in Advanced Oxidation Processes", *J. Adv. Oxid. Technol.*, **1** (1), 18-26.

SAFARZADEH-AMIRI, A.; BOLTON, J.R. and CATER, S.R. (1996b) "Ferrioxalate-mediated solar degradation of organic contaminants in water", Solar Energy, 56 (5), 439-443.

SCOTT, G.P. (1997) "Design, characterization and performance of a bench-scale continuous wet oxidation system", *Chem. Oxidation. Technol. Nineties*, **6**, 156-186.

SCOTT, D.B.M. and LESHER, E.C. (1963) “Effect of ozone on survival and permeability of *Escherichia coli*”, *Journal of Bacteriology*, **85**, 567-576.

SCOTT, J.P. and OLLIS, D.F. (1995) “Integration of chemical and biological oxidation processes for water treatment: review and recommendations”, *Environ. Prog.*, **14** (2), 88-103.

SCOTT, J.P. and OLLIS, D.F. (1996) “Engineering model of combined chemical and biological processes”, *Journal of Environmental Engineering*, **122**, 1110-1114.

SCOTT, J. and OLLIS, D.F. (1997), “Integration of Chemical and Biological Oxidation Processes for Water Treatment: II. Recent Illustrations and Experiences”, *J. Adv. Oxidation Technology*, **2**, 374-381.

SHEN, Y.S.; KU, Y. and LEE, K.C. (1995) “The effect of light absorbance on the decomposition of chlorophenols by ultraviolet radiation and UV/H_2O_2 process”, *Wat. Res*., **29** (3), 907-914.

SONTHEIMER, H.; HEILKER, E.; JEKEL, M.R.; NOLTE, H. and VOLLMER, F.H. (1978), “The Mülheim process”, *J. Am. Wat. Wks. Assoc*., **60** (7), 393-396.

SPETH, T.F.; MAGNUSON, M.L.; KELTY, C.A. and PARRETT, C.J. (2001) “Treatment studies of CCL (Contaminant Candidate List) contaminants*”, Proceeding – Water Quality Technology Conference*, Cincinatti, OH, US, 1048-1059.

STANDARD METHODS for the examination of water and wastewater (1985), *American Public Health Association*.

STAEHELIN, S. and HOIGNÉ, J. (1985) “Decomposition of ozone in water in the presence of organic solutes acting as promoters and inhibitors of radical chain reactions”, *Environ. Sci. Technol.*, **19**, 1209-1212.

STAEHELIN, S. et al. (1984) “Ozone decomposition in water studied by pulse radiolysis. 2. OH and HO_4 as chain intermediates”, *Jour. Phys. Chem*., **88**, 5999.

STAEHELIN, S. and HOIGNÉ, J. (1982) “Decomposition of ozone in water: Rate of initiation by hydroxide ions and hydrogen peroxide”, *Environ. Sci. Technol.*, **16**, 676-681.

STAEHELIN, S. and HOIGNÉ, J. (1983) “Mechanism and kinetics of decomposition of ozone in water in the presence of organic solutes”, *Vom Wasser*, **61**, 337.

STEINBERG, M. and BELLER, M. (1970) “Ozone synthesis for water treatment by high energy radiation”, *Chem. Engrg. Progress* (Symp. Series), **66**, 205.

STOCKINGER, H.E. (1959) “Factors modifying toxicity of ozone”, *Ozone chemistry and technology*, American Chemical Society, Washington DC, USA, 360-369.

STUMM, W. and MORGAN, J.J. (1991) “Aquatic chemistry”, 2nd edition, Wiley, New York.

SUI, M. and MA, J. (2001) “Study on NB removal by ozone/GAC process”, *Zhongguo Jishui Paishui*, **17** (10), 70-73.

SULZER, F.; RAMADAN, F. and WUHRMANN, K. (1959), “Germicidal action of ozone”, *Schweiz Z. Hidrol.*, **21**, 112-122.

TAKAHASHI, N.; NAKAI, T.;SATOH, Y. and KATOH, Y. (1994) “Variation of biodegradability of nitrogenous organic compounds by ozonation”, *Wat. Res.*, **28** (7), 1563-1570.

TOMIYASU, H.; FUKUTOMI, H. and GORDON, G. (1985) “Kinetics and mechanisms of ozone decomposition in basic aqueous solution”, *Inorg. Chem.*, **24** (19), 2962-2966.

TRAPIDO, M.; HIRVONEN, A.; VERESSINA, Y.; HENTUNEN, J. and MUNTER, R. (1997) “Ozonation, Ozone/UV and UV/H_2O_2 degradation of chlorophenols”, *Ozone Sci. & Eng.*, **19** (1), 75-96.

TRAPIDO, M.; VERESSININA, Y. and KALLAS, J. (2001) “Degradation of aqueous nitrophenols by ozone combined with UV-radiation and hydrogen peroxide”, *Ozone Sci. & Eng*., **23**, 333-342.

ULLMANN’S (1991) “Encyclopedia of Industrial Chemistry”, 5ª ed., 415-419, VCH Verlagsgesellschaft (Germany).

URANO, K. and KATO, Z. (1986) “Evaluation of biodegradation ranks of priority organic compounds”, *Journal of Hazardous Materials*, **13**, 147-159.

VOLMAN, D.H. and SEED, J.R. (1964) “The photochemistry of uranyl oxalate”, *J. Am. Chem. Soc.*, **86**, 5095-5098.

WALLING, C. (1975) “Fenton’s reagent revisited”, *Acc. Chem. Res*., **8**, 125-131.

WALLING, C. and GOOSEN, A. (1973) “Mechanism of ferric ion catalysed decomposition of hydrogen peroxide. Effect of organic substrates”, *J. Am. Chem. Soc*., **95** (9), 2987-2991.

YAMAUCHI, S. (1955) “Nitrobenzenes in reversed-phase liquid chromatography. New candidates for internal standards”, *Journal of Chromatography A*, **704**, 323-328.

YAO, C.C.D. and HAAG, W.R. (1991), “Rate constants for direct reactions of ozone with several drinking water contaminants”, *Wat. Res.*, **25** (7), 761-773.

YU, Y.H. and HU, S.T. (1994) “Preoxidation of chlorophenolic wastewaters for their subsequent biological treatment”, *Wat. Sci. & Technol*., **29**, 313-320.

YU, C.P. and YU Y.H. (2000) “Identifying useful real-time control parameters in ozonation process”, *Wat. Sci. & Technol*., **42** (3-4), 435-440.

ZEFF, J.D. and BARICH, J.T. (1990), *Symposium on Advanced Oxidation Processes and Treatment of Contaminated Water and Air: Wastewater Technologies*, Center, Ontario (Canadá).

ZEPP, L.; FAUST, B. and HOIGNÉ, J. (1992) “Hydroxyl radical formation in aqueous reactions (pH 3-8) of iron(II) with hydrogen peroxide: the photo-Fenton reaction”, *Environ. Sci. Technol.*, **26** (2), 313-319.

ZOETEMAN, B.C.; HARMSEN, K.; LINDERS, J.B.; MORRA, C.F.H. and SLOOFF, W. (1980) “Persistent organic pollutants in river water and ground water of the Netherlands”, *Chemosphere*, **9**, 231-249.

ZHOU, H. and SMITH, D.W. (1994) “Kinetics of Ozone Disinfection in Completely Mixed system”, *J. Environ. Eng. Div. ASCE*, **120**, 841-858.